Molecular regulation of circuit assembly in the cerebral cortex

Exposito-Alonso, David

Awarding institution:
King's College London

Molecular Regulation of Circuit Assembly in the Cerebral Cortex

David Exposito-Alonso

A thesis for the degree of Doctor of Philosophy

November 2020

Centre for Developmental Neurobiology

King’s College London

ABSTRACT

The cerebral cortex harbours an intricate network of interconnected cell types that is essential for sensory perception and cognitive function. The assembly of specific synaptic connections in neuronal circuits requires the expression of complementary molecular programs in pre and postsynaptic neurons. The tyrosine kinase receptor ErbB4 is critical for the wiring of specific types of GABAergic interneurons, in which it paradoxically regulates both the formation of perisomatic inhibitory synapses as well as the development of excitatory synapses received by these cells. Neuregulins, the ligands of ErbB4 receptor, play essential roles during brain development and synapse formation, yet their precise function in the wiring of cortical circuits during postnatal development remains unclear. Here we investigated the logic whereby Nrg1 and Nrg3 expression in pyramidal cells mediates ErbB4-dependent functions in cortical synaptic assembly. We found that Nrg1 and Nrg3 have segregated functions in the formation of inhibitory and excitatory synapses that pyramidal cells receive from or establish onto different types of interneurons, respectively. The differential role of Nrg1 and Nrg3 in this process is not due to a differential trans-synaptic interaction with ErbB4 through their EGF-like domain, but rather to their distinctive subcellular distribution within pyramidal cells. Nrg1 is restricted to the perisomatic region of pyramidal cells, whereas Nrg3 is precisely targeted to the presynaptic glutamatergic boutons that these cells make onto cortical interneurons. Our experiments reveal how the regulation of subcellular localisation underlies the function of the neuregulin/ErbB4 signalling pathway in specific synaptic connections. These findings uncover a novel strategy for the assembly of cortical circuits during postnatal development that involves the differential subcellular sorting of family-related synaptic proteins.

ACKNOWLEDGEMENTS

It has been an absolute pleasure to work in the Rico Lab and Marín Lab during my PhD project for the past four years, and I would like to sincerely thank all the people that made this adventure unique and unforgettable.

I am entirely thankful to my advisors Beatriz Rico and Oscar Marín. It is very hard to describe how much I have learned and enjoyed working together with these two amazing scientists. Beatriz has inspired me with her absolute passion for research and tireless motivation to achieve her goals, and we have enjoyed wonderful discussions about neuronal circuits and synapses. Oscar has taught me to have vision, resilience and drive, and it has been a thrilled experience to listen to his advice. I can't thank them enough for the constant trust, support, and patience that they have had in me, for sharing their wisdom and experience with me, and for helping me to grow as a scientist and as person. They have been role models to learn for my scientific career as well as for my personal life, and I just hope to carry with me the many memories and lessons that I have had with them for my future.

The members of the lab have made the journey throughout my doctoral research a delightful experience. Clem has been one of the most influential people during my PhD, and I would always be grateful for how much she has taught me. Especially since my beginnings, she has been a great support in my growth as a scientist. I have enjoyed so much our scientific discussions as well as the time outside the lab travelling together and going to concerts. Special thanks to Alfredo and Antonio, who have always been there to answer any of my questions and doubts, who taught me a lot about biology, and for the fun times together. I am really thankful to Martijn, for teaching me so much about neuroscience and for his uplifting support; to Monika and Fong, for always being there with a smile to comfort me; to Fernando, for the great times that we enjoyed together; and to Julie, for the inspiring lessons and values. I am very grateful to Elena and Alicia for all their support and care in the lab and for being such good friends. I am very thankful to Noe, who I have been extremely lucky to work alongside during my PhD. It has been a pleasure to be in the lab together and learn so much from her.

A very special mention goes to Ian. I can't thank him enough for all his dedicated work with the mouse colonies, for his diligence and patience with any questions or doubts to solve. For all of that, he has been a great model for me during my PhD, always being available to help anyone. I also wish to thank Laura

for her help during my PhD, and to Catarina for training when I started the research project. Special thanks to Emilia, whose advice and guidance has always been tremendously important in my progress. Last but not least, I am truly grateful to Patri and Marian, for all their support since the beginning of my PhD and throughout my stay in the lab. Not only they have been key in my training in the lab, but also have been by my side in the toughest moments to help me keep going. They are incredibly generous and deserve all my most sincere gratitude.

I would like to thank the other past and present members of the Rico and Marín labs: Rubén, Beppe, Tim, Madda, Ele, Da, Alfonso, Laura, Risto, Varun, Joe, Veronique, Alberto, Adrián, Charlotte, Kinga, Lynette, Sunny, Nancy, Claudia, Irene, Laurel, and Carmen. (Apologies if I forgot to mention someone.) I will never forget all my friends from the PhD lab, their constant support, and the amazing moments that we spent together. They have created a superb environment to work and have fun that I will most certainly miss.

During the past years, I have had the great opportunity to discuss my PhD progress with brilliant scientists that provided guidance and advice. So, I would like to especially thank Juan Burrone, Robert Hindges, and Patricia Salinas for their contribution in my career. I would also like to thank Stefania, Lauren, Emma and Enrico for their incredible administrative support during my PhD work. Lastly, special thanks to Carles and André, who I was so fortunate to have as extraordinary supervisors during my master's studies.

I would also like to remember my friends from Spain: Pau, Raul, Pablo, Antonio, Manu, Yaiza, Diego, Ada… Despite the distance, I have felt very close to all of them, and made me enjoy this adventure in London even more. And to my family, because I couldn't be luckier and happier to have them with me: Marina, Esperanza, Mayte, Make, Alonso, Paco, Adri, Carlos, Lucía, Laura, Montsé, José María, Sagra, Dan, Ana, Irene, Nicolás…

To my grandma, who has always taken care of me and worked effortlessly to give the best to her children and grandchildren. None of this would have been possible without you. To my brother, who has always been my biggest inspiration. Thank you for your love, care, and guidance. You have simply shaped my life. To the two kindest, most caring people I know, my parents. You have made me feel loved and important – I am who I am thanks to you – I am amazed how much you teach me every day. I have tried to share every step of my PhD research with you, I hope you feel this Thesis is also yours.

TABLE OF CONTENTS

LIST OF FIGURES

LIST OF ABBREVIATIONS

AIS	Axon initial segment
AP	Adaptor protein
BSA	Bovine serum albumin
CB1R	Cannabinoid receptor 1
CCK	Cholecystokinin
Cbln	Cerebellin
CBuPN	Corticobulbar projection neuron
Cdh	Cadherin
CFuPN	Corticofugal projection neuron
CGE	Caudal ganglionic eminence
Chodl	Chondrolectin
CPM	Counts per million mapped reads
CPN	Callosal projection neuron
CNV	Copy number variation
CR	Calretinin
CRD	Cysteine-rich domain
CSMN	Corticospinal motor neuron
CThPN	Corticothalamic projection neuron
DAPI	4’,6-diamidino-2-phenylindole
DSI	Depolarisation-induced suppression of inhibition
EGF/EGFR	Epidermal growth factor/epidermal growth factor receptor
ErbB	Erb-B2 receptor tyrosine kinase
Fgf	Fibroblast growth factor
FLRT	Fibronectin leucine-rich transmembrane protein
GABA	Gamma amino-butyric acid

GAD65/67	Glutamate decarboxylase 65/67
G/C	Guanine/cytosine
Geph	Gephyrin
GFP	Green fluorescent protein
GPCR	G protein-coupled receptor
GPR158	G protein-coupled receptor 158
GWAS	Genome-wide association study
HA	Hemagglutinin
HDR	Homolog-directed repair
HSPG	Heparan sulphate proteoglycan
HS	Heparan sulphate
Htr3a	Serotonin receptor 3A
icKO	Inducible conditional knock-out
IPSP	Inhibitory postsynaptic potential
IHC	Immunohistochemistry
IN	Interneuron
ITN	Intratelencephalic neuron
IUE	*In utero* electroporation
L1CAM	L1 cell adhesion molecule
L1, L2/3, L4, L5, L6	Layer 1, Layers 2/3, Layer 4, Layer 5, Layer 6
Lgi	Leucine-rich repeat LGI family member
Lphn	Latrophilin
Lrrtm	Leucine-rich repeat transmembrane neuronal
LTP	Long-term potentiation
mEPSC	Miniature excitatory postsynaptic current
MF	Mossy fibre

MGE	Medial ganglionic eminence
mIPSC	Miniature inhibitory postsynaptic current
NDNF	Neuron-derived neurotrophic factor
Nek	NIMA related kinase
Nlgn	Neuroligin
NOS	Nitric oxide synthase
NPY	Neuropeptide Y
Nrg	Neuregulin
Nrxn	Neurexin
PC	Pyramidal cell
PBS	Phosphate-buffered saline
PFA	Paraformaldehyde
POA	Preoptic area
POH	Preopto-hypothalamic area
PSD95	Postsynaptic density protein 95
pSyn	Synapsin promoter
PTPR	Protein tyrosine phosphatase receptor
PV	Parvalbumin
ROI	Region of interest
scRNA-seq	Single-cell RNA-sequencing
sgRNA	Single-guide RNA
SNAP25	Synaptosomal nerve-associated protein 25
SNARE	Soluble N-ethylmaleimide-sensitive factor attachment protein receptor
SNP	Single nucleotide polymorphism
ssODN	Single-stranded oligodeoxynucleotide

SS	Splice site
SST	Somatostatin
SVZ	Subventricular zone
Syt2	Synaptotagmin 2
tdT	tdTomato
TGN	Trans-Golgi network
TM	Tamoxifen
TMD	Transmembrane domain
TPM	Transcripts per million
UTR	Untranslated region
VGlut1/3	Vesicular glutamate transporter 1/3
VIP	Vasoactive intestinal peptide
VZ	Ventricular zone

And men (and women) ought to know that from nothing else but from the brain come joys, delights, laughter and sports, and sorrows, griefs, despondency, and lamentations. And by this, in an especial manner, we acquire wisdom and knowledge, and see and hear, and know what are foul and what are fair, what are bad and what are good, what are sweet, and what unsavory; some we discriminate by habit, and some we perceive by their utility.(…) And by the same organ we become mad and delirious, and fears and terrors assail us. (…) All these things we endure from the brain, when it is not healthy.

Hippocrates (~400 BCE)

INTRODUCTION

Preface

Mental health is a pressing matter that occupies an important position in the media and political agenda nowadays. The increased incidence of mental disorders and the awareness of their impact in our professional and social lives have not been accompanied by advances in the diagnosis nor preventive or therapeutic strategies in the health service (Arango et al., 2018). Understanding the biological underpinnings of brain disorders will have a tremendous impact on our society during this century.

The cerebral cortex plays a privileged role in our sensory perception, decision making, social communication, and emotional state. The architecture of the cortex, which conforms the outer covering of the brain, is organized by layers and columns that support a stereotypical flow of information. The cerebral cortex is composed of two main classes of neurons: pyramidal cells—neurons that abundantly populate cortical regions, and carry and integrate sensory and cognitive information—and interneurons—a minor, but diverse, group of neurons that display a high degree of specialisation in connectivity and physiology—(Harris and Mrsic-Flogel, 2013). Although the general cellular composition has remained relatively constant throughout evolution, the cerebral cortex has experienced an outstanding growth in size as well as diversified its genetic programs (Krienen et al., 2019; Tosches et al., 2018). As a result, these two neuronal classes show an outstanding cellular diversity, which is accompanied by an unparalleled specificity in the synaptic connectivity of cortical cell types.

The high level of sophistication in the wiring of cortical circuits, and the emergent network activity implicated in higher cognitive functions, have spurred the study of cortical assembly on a field of active research in the past decades (Buzsáki, 2010; Fishell and Kepecs, 2019). Furthermore, genetic variants associated with psychiatric disorders have been shown to map onto transcriptional signatures of developing cortical cell types, suggesting that the development of cortical circuits could represent a spatiotemporal window of vulnerability to these disorders (Willsey et al., 2013; Satterstrom et al., 2020). The aim of this PhD Thesis is to investigate molecular mechanisms regulating the synaptic assembly and specificity in the cerebral cortex, using the mouse as a model. The motivation of this research is to contribute to our understanding of how cortical cell types employ genetic and cellular processes to synaptically integrate into neuronal circuits during postnatal brain development. The complex genetic variations that compose the genomic architecture of neurodevelopmental disorders such as autism and schizophrenia are an additional inspiration in my research.

1. Cortical cell types

"The Butterflies of the Soul"

The first descriptions of cortical neurons date back to the late 19th century, from the pioneering work of Santiago Ramón y Cajal where he used a tracing method developed by Camilo Golgi. His neuroanatomical studies yielded detailed catalogues of neuronal diversity in the cerebral cortex.

The nervous system is a highly dense network of several billions of neurons. Despite more than a century of neuroscience research since Cajal's work, the question of how many cell types exist in distinct regions of the mammalian nervous system is still far from answered. The combination of anatomical, biochemical, and electrophysiological approaches in the late 20th century arguably increased our knowledge on the classification of major classes of neurons (Somogyi, 1977). Different types of neurons with distinct forms and functions could be classified based on the expression of biochemical markers. However, the advent of sequencing and computational technologies has triggered a rapid rate of discovery of new subtypes of neurons based on transcriptomic signatures (Saunders et al., 2018; Tasic et al., 2018; Zeisel et al., 2015, 2018). Much effort will be needed to characterize the anatomical and functional identities of these molecularly distinct clusters, and to establish the definition and limits of a cell type. Especially in the light of the remarkable plasticity of the brain, neurons can adapt their properties in a context-dependent manner (Dehorter et al., 2015), and different cell states could be a confounding factor in the quest on cell type taxonomy (Cembrowski and Spruston, 2019; Stanley et al., 2019). Altogether, the challenge ahead is to be able to provide a definition of a cell type, to understand their plasticity in different circumstances, and to establish a limit between cell type and cell state (Zeng and Sanes, 2017).

In this section, I will describe the general properties and main types of principal cells and interneurons in the mammalian cerebral cortex, a thin layer that covers the outer region of the brain composed of a highly interconnected network of intricate and diverse neuronal circuits. The cerebral cortex plays a key role in cognitive functions such as attention, perception, and consciousness. Recent

genomic advances have suggested that genetic alterations associated with an increased risk of psychiatric disorders may perturb the development of cortical circuits, and proposed the convergence of diverse genetic factors on common molecular and cellular processes (Dias and Walsh, 2020; Satterstrom et al., 2020). Thus, genetic susceptibility to neurodevelopmental disorders underscores the importance of understanding the cellular composition of the cerebral cortex. I will pay especial attention to connectivity patterns within the cortical circuitry and their function in the processing of information.

1.1. Principal cells

Principal cells abundantly populate the cerebral cortex across layers and areas, comprising approximately 80% of cortical neurons. Also known as projection neurons, they function as glutamatergic, excitatory cells that transmit neural activity to downstream targets by releasing the neurotransmitter glutamate, which acts through ionotropic and metabotropic receptors and generally depolarizes the postsynaptic cell. Most principal cells extend a dendritic shaft up to cortical layer 1, where it ramifies into an extensive dendritic arbour, as well as prominent basal dendrites; due to this characteristic morphology, they are also named pyramidal cells. Their elaborate axonal arborizations enable pyramidal cells to synapse onto local and distal targets throughout the cortex and subcortical regions (Han et al., 2018b). Pyramidal cells divide into two major classes based on their long-range projections: intracortical cells and corticofugal cells (Molyneaux et al., 2007). Intracortical cells are predominantly located in layers 2/3, and can be divided in associative or callosal neurons depending on whether they contact the same or the opposite hemisphere, respectively. Corticofugal cells are primarily present in lower layers, and can be classified in corticothalamic cells or subcerebral cells. Among the latter population, distinct subtypes project their axons to different targets below the brain, including the pons nuclei and other nuclei in the brainstem, the superior colliculus and the spinal cord.

How does the cortex integrate information from our senses to guide behaviour? Once sensory information arrives to the cerebral cortex, pyramidal cells play a central role in information processing by receiving and transmitting electrical activity across and within layers (Harris and Mrsic-Flogel, 2013) (Figure 1). Layer (L) 4 neurons are the primary input of thalamic sensory information, whereas

association inputs from higher-order cortical areas mainly arrive to L1, L5 and L6 (Fame et al., 2011; Meyer et al., 2010). L4 neurons, which comprise two distinct morphological classes, pyramidal cells and spiny stellate cells, innervate all layers of the cortex, although their major efferent output of the sensory information is L2/3 (Feldmeyer et al., 2002; Feldmeyer et al., 2005; Lübke et al., 2000; Lübke et al., 2003; Staiger et al., 2004). These superficial layers neurons send their axon terminals to L5 locally as well as to contralateral and higher-order cortices, and have an important role in lateral inhibition (Adesnik and Scanziani, 2010; Feldmeyer et al., 2006). Being the main output layer of the cortex, L5 contains two broad populations of pyramidal cells with distinct molecular and physiological determinants (Economo et al., 2018). Intratelencephalic neurons, typically found in superficial L5, project to L2/3 as well as distal regions of the contralateral cortex and striatum. Subcerebral neurons, with larger dendritic arborizations and present in deep L5, send projections to subcerebral motor centres, higher-order thalamus, and striatum (Markram et al., 1997; Sohur et al., 2014). Finally, L6 pyramidal cells include corticocortical cells and corticothalamic cells, which also send collaterals to L4 and can have a modulatory, hyperpolarizing effect mediated by metabotropic glutamate receptors (Lee and Sherman, 2009), hence a function in gain control (Olsen et al., 2012).

Specific features of the environment and internal brain states are encoded in the firing patterns of cortical cells. A hierarchical, spatial organization in the cortex endows this feature selectivity of pyramidal cells to be restricted to distinct areas, and the coding strategies can differ between layers (Sakata and Harris, 2009). For instance, in the visual cortex, direction- and orientation-selective cells were discovered when electrophysiological recordings showed that certain neurons fire best when presented with a visual stimuli moving in a particular direction or orientation, respectively (Hubel and Wiesel, 1962). In the entorhinal cortex, a component of the medial temporal lobe memory system and the main gateway between hippocampus and neocortex, a wide diversity of neurons have been found to encode information such as space, speed, and time (Hafting et al., 2005; Kropff et al., 2015; Solstad et al., 2008). In the prefrontal cortex, molecularly and anatomically distinct cell types of pyramidal neurons are activated by appetitive or aversive experiences (Ye et al., 2016). Thus, pyramidal cell types arranged in different cortical areas of different sensory and association modalities are devoted to encoding specific information.

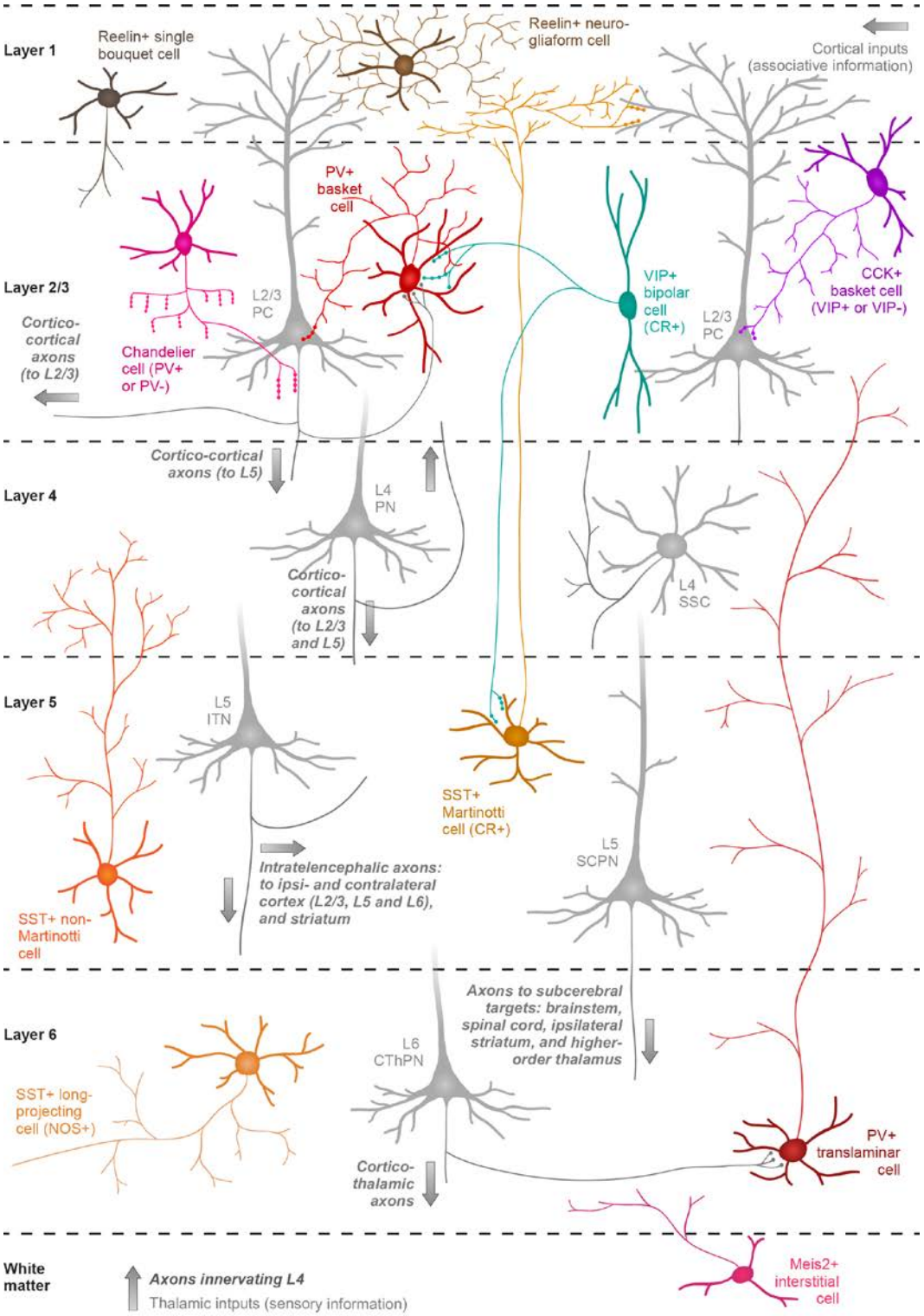

Figure 1 | **Cellular composition and organisation of the cerebral cortex**. Diagram illustrating the connectivity and distribution of distinct types of pyramidal cells and interneurons in the mammalian cerebral cortex. Abbreviations: CCK, cholecystokinin; CR, calretinin; CThPN, corticothalamic projection neuron; ITN, intratelencephalic neuron; PC, pyramidal cell; PV, parvalbumin; SSC, spiny stellate cells; SST, somatostatin; VIP, vasoactive intestinal peptide.

Although single neurons encode specific information, cortical activity is dominated by groups of neurons that are simultaneously active to create a coherent picture of the world (Cossart et al., 2003; Miller et al., 2014; Yuste et al., 1992). These groups of neurons that are coactive in a synchronous manner have been termed neuronal ensembles, and represent an emergent property of cortical circuits for the implementation of neural computations and the execution of behaviour. Interestingly, the organization of connectivity in the cortex follows a rather simple rule: neurons that are co-active *in vivo* to process similar information are more likely to be synaptically connected together (Cossell et al., 2015; Ko et al., 2011, 2013). Therefore, although single neurons can participate in multiple ensembles, these findings argue against a promiscuous connectivity of the cortex at the cellular level. Indeed, the precise stimulation of specific neurons within an ensemble via holographic optical methods has been shown to reproduce the behaviour in which that particular ensemble is active naturally (Carrillo-Reid et al., 2019; Jennings et al., 2019). However, we are still far from fully understanding how the cortex computes information to instruct behaviour. In this context, brain-wide optical and electrophysiological approaches promise to provide a better picture of how cortical activity dynamics relates with other brain regions to guide behaviour (Allen et al., 2017, 2019).

Transcriptomic studies have revealed an unprecedented diversity among pyramidal cell types, providing a vast catalogue of subtypes that expands the general types classified according to long-range connectivity and laminar allocation (Zeng and Sanes, 2017). Up to 56 molecularly distinct clusters of pyramidal cells were identified in a comparative study between two cortical areas, primary visual cortex and anterior lateral motor cortex, where most of these cell types were exclusive to one of the two areas (Tasic et al., 2018). Altogether, compared to their counterparts in the cortex (i.e., interneurons), pyramidal cells seem to have diversified to a greater extent during evolution and across cortical areas. Furthermore, new tracing methodologies have started to unravel the logic of the vast diversity of axonal projections of cortical pyramidal cells, indicating that neurons often target multiple cortical areas and, consequently, intracortical information transfer might concurrently follow distinct functional pathways (Han et al., 2018b). In the local circuitry, the innervation of pyramidal cells by interneurons is subject of an exquisite degree of specificity through precise connectivity patterns (Anastasiades et al., 2018; Hilscher et al., 2017; Lee et al., 2014; Lu et al., 2017), which suggests that pyramidal cell diversity might also be coupled to a differential modulatory control.

1.2. Interneurons

Interneurons comprise a relatively small population of cortical cells, accounting for approximately 20% of cortical neurons. Interneurons normally establish synaptic connections in their vicinity forming local circuits, hence their name, and use gamma-aminobutyric acid (GABA) as main neurotransmitter, which acts through ionotropic receptor channels that are permeable to anions, namely chloride (Cl-). Usually inhibitory in nature, interneurons shunt the firing of action potentials in the postsynaptic cell by means of GABAergic neurotransmission that evokes hyperpolarizing currents. Therefore, the major role of these cells lies in exerting an extremely accurate spatial and temporal control over the activity of pyramidal cells (Kepecs and Fishell, 2014; Klausberger and Somogyi, 2008). As an exemption to this rule, and under certain circumstances, particular subtypes of interneurons can produce depolarizing, excitatory postsynaptic responses, which is believed to be important during developmental windows for the homeostasis of cortical circuits (Ben-Ari, 2002; Pan-Vazquez et al., 2018). Indeed, the developmental assembly of pyramidal cells and interneurons relies on a tight relationship to maintain the proper relative numbers of these cortical neurons that is crucial for the correct balance of excitatory-inhibitory networks in the developing cortex (Lodato et al., 2011; Wong et al., 2018).

The diversity of cortical interneurons is astonishing. The first thorough characterizations of interneuron types date back to the 1980's and 90's (Parra et al., 1998). Despite representing a small population of cells in the brain, much effort has been required to define their anatomical and physiological properties and to reach an agreement for their nomenclature by the expert community (Ascoli et al., 2008; DeFelipe et al., 2013). Transcriptomic studies are transforming our understanding of interneuron diversity. A recent report has identified 61 interneuron subtypes, and, contrary to pyramidal cells, most of these molecularly-defined cell clusters are shared between different cortical areas (Tasic et al., 2018). These data could suggest that interneuron subtypes function as invariable elements in circuit motifs. Moreover, the conservation of transcriptomic signatures of GABAergic interneurons across species indicates that the main cortical interneuron types already existed in the common ancestor of all amniotes (Tosches et al., 2018). This appears to be strikingly different to the evolution of striatum, where a new striatal interneuron type not present in the mouse brain is found in

primates, including humans (Krienen et al., 2019). But, why is this huge diversity of cell types necessary since interneurons represent such a small proportion of cortical neurons? A plausible explanation could lie on the division of labour of interneurons at spatial and temporal scales (Kepecs and Fishell, 2014). First, interneuron types are able to selectively make synaptic contacts onto specific cellular targets and subcellular compartments. Second, different types of interneurons appear to be active at distinct behavioural timescales, and by coordinating pyramidal cell firing at different oscillation frequencies, may enable rich and rapid dynamics in cortical network activity (Buzsáki, 2002; Buzsáki and Wang, 2012; Kvitsiani et al., 2013). Overall, these findings have led to the notion that interneurons form a diversified team of specialists for orchestrating cortical activity (Fishell and Kepecs, 2019; Klausberger and Somogyi, 2008).

The combination of biochemical, anatomical, physiological and behavioural studies has proved instrumental to identify the properties of interneuron types. Currently, the majority of cortical interneurons can be reliably labelled and classified into three major classes based on the expression of biochemical markers: parvalbumin, somatostatin, and the serotonin receptor 3A (Lim et al., 2018a). Importantly, these interneuron populations have distinct developmental origins, and their molecular differences reflect the physiological and wiring characteristics that can be found in the adult cortex (Batista-Brito and Fishell, 2009; Butt et al., 2005; Jiang et al., 2015; Pfeffer et al., 2013) (Figure 2).

The most abundant interneuron population (40%) is characterised by the expression of parvalbumin (PV), exert a powerful control over the firing rate of pyramidal cells due to their perisomatic targeting, and can be broadly grouped into three cell classes according to their morphology. First, PV-expressing (PV+) basket cells form large and dense axonal arbours to specifically innervate the soma and proximal dendrites of pyramidal cells and, to a lesser extent, of other interneuron populations, thus creating the characteristic basket-like structures of their axon terminals observed in immunohistochemical experiments (Buhl et al., 1995; Hu et al., 2014; Kisvarday et al., 1987). In L4, PV+ basket cells are the main interneuron target of thalamocortical axons (Bagnall et al., 2011; Lien and Scanziani, 2018), and engage in feedforward inhibition motifs, contributing to important circuit computations such as temporal coincidence detection (Gabernet et al., 2005). In L2/3, they receive most excitatory inputs from neighbouring pyramidal cells as well as glutamatergic axons from L4, and play key roles in lateral competition and cortical gain modulation (Adesnik and Scanziani, 2010; Atallah et al., 2012).

Importantly, PV+ cells appear to be highly plastic at the molecular and cellular levels, a property that endows this interneuron population with the ability to regulate learning (Dehorter et al., 2015; Donato et al., 2013, 2015; Favuzzi et al., 2017). Second, perhaps the most emblematic morphological type of interneurons is the axo-axonic cell, which makes synaptic contacts onto the axon initial segment (AIS) of pyramidal cells, and, given its extensive axonal arbours in the form of cartridges with presynaptic boutons, it is also known as chandelier cell (Somogyi, 1977; Somogyi et al., 1985). Chandelier cells are particularly abundant at the border of L1 and L2 as well as in L6 (Taniguchi et al., 2013; Tasic et al., 2018). A fraction of chandelier cells express PV and, together with PV+ basket cells, constitute the population of fast-spiking interneurons given their non-accomodating firing pattern. The fast dynamics of PV+ cell spiking activity and the perisomatic innervation that they exert onto pyramidal neurons allow them to rapidly coordinate and synchronise the activity of neuronal ensembles, therefore supporting gamma-band (25-100 Hz) oscillations in cortical networks (Cardin et al., 2009; Sohal et al., 2009). The strong effect of PV+ interneurons on cortical activity seems to be crucial for gain control of sensory processing (Lee et al., 2012; Wilson et al., 2012). Although the behavioural correlates of chandelier cells remain enigmatic to date, recent studies have shown that they can selectively innervate distinct pyramidal cell types, arguing for a role in information processing in specific cortical circuits (Lu et al., 2017; Viney et al., 2013). Moreover, chandelier cells may play essential roles in the homeostasis of neuronal networks during postnatal development (Pan-Vazquez et al., 2018). A third morphologically distinct class of PV+ fast-spiking cells are translaminar PV+ interneurons that are particularly abundant in deeper layers of the cerebral cortex. Importantly, translaminar fast-spiking interneurons located in L6 and recruited by corticothalamic L6 pyramidal cells, are able to modulate sensory responses throughout all cortical layers (Bortone et al., 2014).

A second subclass of interneurons is characterised by the expression of the neuropeptide somatostatin (SST). It represents 30% of all cortical inhibitory neurons, and stereotypically target the distal dendrites of pyramidal cells to gate the dendritic integration of synaptic inputs (Kisvarday et al., 1987; Murayama et al., 2009; Somogyi et al., 1984). A great diversity of physiological and anatomical properties has been reported for SST+ interneuron types (Ma et al., 2006; McGarry et al., 2010), which can be generally divided into two classes based on their axonal morphology: Martinotti cells and non-Martinotti cells. Martinotti cells send ascending axonal branches that extensively ramify in L1 to target pyramidal cell

dendrites, and display diverse discharge responses, including accommodating (regular) spiking firing as well as non-accomodating (quasi-fast spiking) and irregular spiking responses (Ma et al., 2006; Wang et al., 2004). Martinotti cells are particularly enriched in L5 where they mediate disynaptic inhibition, and several subtypes with distinct connectivity and physiological characteristics have been described (Nigro et al., 2018; Silberberg and Markram, 2007). L1-targeting Martinotti cells can also be found in L2/3 of the cortex, where they frequently co-express the calcium-binding protein calretinin (CR) (Xu et al., 2006). On the other hand, non-Martinotti cells lack ascending axon branches reaching L1, are abundant in L4 and L5, and extensively spread their axonal arbours within L4, suggesting a powerful control over thalamic sensory information (Nigro et al., 2018). Indeed, non-Martinotti cells located in L4 preferentially target neighbouring fast-spiking interneurons and, consequently, disinhibit L4 thalamorecipient pyramidal cells, increasing their firing rate in active cortical networks (Xu et al., 2013). In sensory processing, SST+ interneurons, whose recruitment increases in a supralinear fashion in response to pyramidal cell activity, are preferentially excited by horizontal cortical axons and, thus, contribute to a circuit computation for surround suppression of pyramidal cells (Adesnik et al., 2012; Kapfer et al., 2007). Interestingly, PV+ soma-targeting cells and SST+ dendrite-targeting cells exhibit distinct behavioural correlates, as they are active with temporal specificity in different epochs of a reward-related decision-making task (Kvitsiani et al., 2013). This suggests that interneuron diversity in the cerebral cortex might underlie a specialised regulation of the flow of information in cortical circuits. Finally, long-range GABAergic projection neurons constitute a relatively rare and poorly characterised class of SST-expressing cells in the cerebral cortex, seem to be more abundant in deeper cortical layers, and frequently co-express nitric oxide synthase (NOS), neuropeptide Y (NPY), and chondrolectin (Chodl) (He et al., 2016; Tasic et al., 2018). NOS+ cells projecting to a wide variety of brain regions are active during sleep, and their activation is modulated by both substance P and cholinergic inputs (Dittrich et al., 2012; Gerashchenko et al., 2008; Kilduff et al., 2011; Williams et al., 2018). Moreover, long-range projection SST+ neurons in the auditory cortex have a direct inhibitory effect on amygdala pyramidal cells, and might play a role in fear behaviour driven by auditory cues (Bertero et al., 2019).

The serotonin receptor 3A (Htr3a)-expressing interneurons account for 30% of the total GABAergic population, and in superficial layers of the cortex (L1-3), they are the predominant interneuron population (Lee et al., 2010a; Vucurovic

et al., 2010). Importantly, a great heterogeneity of electrophysiological and morphological cell types has been reported among Htr3a+ interneurons (Lee et al., 2010a; Miyoshi et al., 2010). Vasoactive intestinal peptide (VIP)-expressing cells represent approximately a third of Htr3a+ interneurons. VIP+ interneurons with bipolar or double-bouquet morphology that frequently show irregular spiking pattern and co-express CR (He et al., 2016; Lee et al., 2010a). Conversely to other interneuron populations, VIP+/CR+ cells are the prototypical type of interneuron-selective interneurons because they synapse onto other interneurons (Acsády et al., 1996). They are primarily found in L2/3 of the cortex, and normally target SST+ cells or, to a lesser extent, PV+ cells (Dávid et al., 2007; Prönneke et al., 2015; Walker et al., 2016). Due to their inhibitory nature, this peculiar connectivity results in disinhibitory circuits, causing a reduction in the firing rate of pyramidal cells upon activation of VIP+ interneurons and playing important roles in learning and plasticity (Donato et al., 2013; Fu et al., 2015; Garcia-Junco-Clemente et al., 2017; Lee et al., 2013; Pi et al., 2013). A distinct group of VIP+ interneurons co-expresses cholecystokinin (CCK), have multipolar morphology, and represent a soma-targeting basket cell population that is particularly enriched in superficial locations of L2, close to the border with L1 (He et al., 2016). In addition, a related type of CCK+ basket cells with larger soma sizes lacks the expression of VIP, and are preferentially found in L5 and L6 (He et al., 2016). Importantly, the somatic boutons that CCK+ basket cells make onto pyramidal cells and other interneurons can be specifically labelled with synaptic markers such as the endocannabinoid receptor CB1R or the vesicular glutamate transporter VGlut3 (Freund et al., 1986; Nunzi et al., 1985; Omiya et al., 2015; Somogyi et al., 2004; Zhou et al., 2017). CCK+ multipolar, basket cells exhibit diverse electrophysiological patterns, from irregular spiking to bursting non-adapting and late spiking (He et al., 2016; Lee et al., 2010a). The temporal activation and potential role of CCK+ cells in network function and behaviour has remained obscure, although new genetic labelling strategies are certainly paving the way to address these questions (Del Pino et al., 2017; Dimidschstein et al., 2016; Whissell et al., 2015). A second group of Htr3a+ interneurons, almost non-overlapping with VIP+ cells, is mainly found in superficial layers of the cortex and is characterised by the expression of Reelin (Lee et al., 2010a; Rudy et al., 2011; Schuman et al., 2018). The most abundant Reelin+ interneuron type in L1 is composed by neurogliaform cells, which also co-express the neuron-derived neurotrophic factor (NDNF), poses dense and elongated axonal arborizations confined to L1 and exhibit late firing patterns (Jiang et al., 2015; Schuman et al., 2018). Some neurogliaform cells can also be identified by

the expression of NPY (Lee et al., 2010a). A unique feature of neurogliaform cells is that they can elicit long-lasting inhibitory postsynaptic potentials (IPSPs) on pyramidal cells and other interneurons through the combined activation of slow GABAA and GABAB receptors (Oláh et al., 2007; Tamás et al., 2003). In addition, neurogliaform cells do not require to form classical synaptic contacts in their axonal terminals; they release enough GABA by volume transmission to produce hyperpolarizing responses in a large proportion of nearby neurons (Oláh et al., 2009). A transcriptionally-related, Reelin+ interneuron type abundant in L1 are single-bouquet cells, which often send axon terminals to deeper layers of the cortex (Jiang et al., 2015; Tasic et al., 2018). Two other Htr3a+ cell types comprise multipolar cells particularly abundant in the border between L1 and L2, and Meis2+ interstitial cells that reside in the white matter and send axons to deeper layers of the cortex and the striatum (von Engelhardt et al., 2011; Frazer et al., 2017). Although the functional significance of the multiple types of Htr3a+ interneurons is still enigmatic, several studies have suggested key roles in sensory processing and learning during postnatal development in spite of their relatively low abundance compared to other neuronal cell populations (Batista-Brito et al., 2017; Che et al., 2018; Del Pino et al., 2017).

In conclusion, the recent years have witnessed an explosion in the development of high-throughput technologies that have allowed the rapid characterisation of new cortical cell types. These exciting findings have led to a deeper knowledge on the cellular composition of the cerebral cortex. As a consequence, it has now become evident that our mechanistic understanding of the cerebral cortex has experienced less progress in two other research avenues: how and when cortical cell types are specified during brain development, and what molecular principles govern the specific connectivity of cortical circuits.

2. Developmental specification of cortical circuits

"The epigenetic landscape"

The ideas proposed by Conrad Hal Waddington have had a major impact in developmental biology. His influential model named the 'epigenetic landscape' describes the choices that cells make along developmental pathways and how genes would influence this decision-making process.

Conrad Hal Waddington trained in a multitude of disciplines, including palaeontology, philosophy, embryology, developmental biology, and genetics, which had a great contribution in the originality of his theories on development. His master work was inspirational for embryologists and developmental biologists in the second half of the 20th century. His conceptualization of development is best captured in his book 'The strategy of the Genes': "In a canalysed system [...], trajectories starting from any point within a certain volume will converge to a single end point which is the corresponding steady state, while trajectories starting within some other volume will converge on a different point." (Waddington, 1957). Not surprisingly, modern models of cortical development have been inspired by Waddington's ideas. Recently, an "attractor" model has been proposed for the specification of interneuron types in the cerebral cortex (Fishell and Kepecs, 2019). Fishell and Kepecs argue that gene regulatory networks are shaped by codes of transcription factors to produce attractor states that will specify the developmental trajectory followed by different cell types. On top of genetic mechanisms specifying the cardinal classes of interneurons, a variety of external cues will define and adjust the neuronal properties acquired towards the stage of integration into cortical circuits.

In the next section, I will describe the mechanisms that guide the course by which cortical cell types acquire their cardinal and definitive state during embryonic and postnatal development. I will divide these processes in genetic and extrinsic strategies utilised for the specification and refinement of the neuronal properties that characterise both pyramidal cells and interneurons.

2.1. Genetic specification

At embryonic stages, the expression of distinct sets of genes pattern the developing brain into a highly organised structure. The spatially defined expression of morphogens contributes to subdividing functionally distinct domains in the forebrain across the rostro-caudal, medio-lateral and dorso-ventral axes (Rogers and Schier, 2011; Rubenstein et al., 1994; Marín and Rubenstein, 2001). Segmentation of cell lineage-restricted compartments is regulated by the expression of transcription factors such as *Hox* genes (Kiecker and Lumsden, 2005). Later, over the course of embryonic development, combinatorial and sequential action of transcription factors—including genes from the families *Dlx*, *Nkx*, and *Sox*—determines the developmental pathways that progenitors and early postmitotic neurons take to acquire their fate (Figure 2) (Custo Greig et al., 2013; Lodato and Arlotta, 2015). Thus, gene regulatory networks play crucial roles in cortical cell type specification (Fishell and Kepecs, 2019; Molyneaux et al., 2007).

Pyramidal cell progenitors are located in the ventricular and subventricular zones (VZ and SVZ, respectively) of the embryonic pallium and, after cell cycle exit, undergo radial migration to populate the cerebral cortex in an inside-out manner. Several transcriptomic studies have identified specific master regulators necessary for the specification of distinct projection neuron subtypes (Arlotta et al., 2005; Molyneaux et al., 2009). For instance, Sox5 regulates the differentiation of corticofugal neuron subtypes (Lai et al., 2008), Fezf2 is required for the regulation of genetic programs that define corticospinal motor neurons (Lodato et al., 2014; Molyneaux et al., 2005), and Ctip1 controls the specification of callosal and corticothalamic projection neurons (Woodworth et al., 2016). These findings indicate that the specification of projection neuron subtypes is determined by transcription factors during embryonic development. Notably, the fact that a single cell type can express multiple transcription factors and that the same transcription factor can be expressed by several cell types strongly supports that a combinatorial transcriptional code is required for the specification of pyramidal cells (Molyneaux et al., 2007) (Figure 2). Interestingly, the different codes of transcription factors are thought to be instrumental for the cell type-specific transcriptional dynamics during later embryonic stages and early postnatal development, in which specific projection neuron subtypes display distinct programs of axon guidance and cell adhesion molecules (Molyneaux et al., 2015). Remarkably, recent studies have shown that the fate of pyramidal neuron subtypes can be reprogrammed *in vivo* by

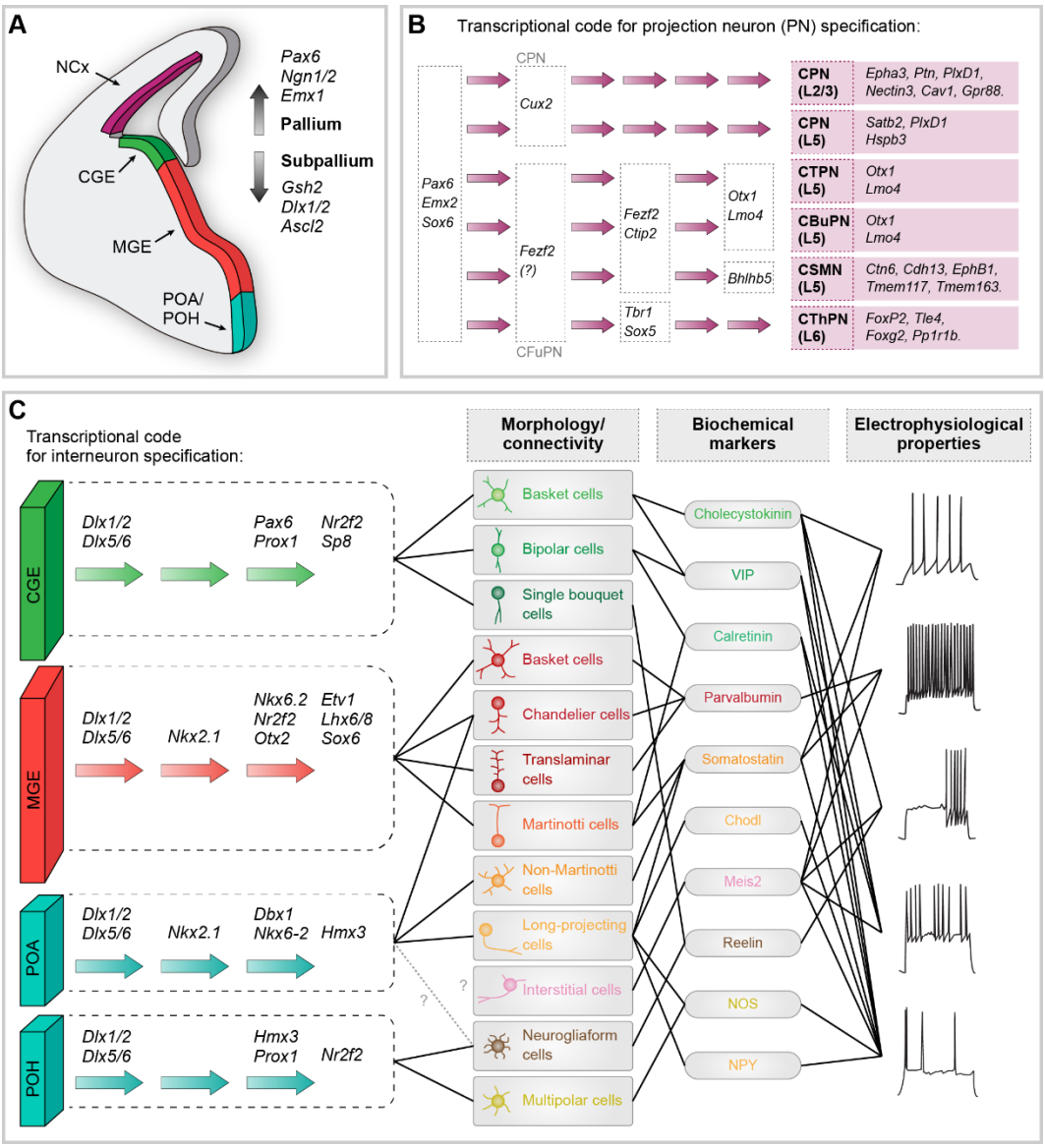

Figure 2 | **Developmental specification of cortical cell types**.
(**A**) Drawing of the embryonic brain showing neurogenic regions of pyramidal cell and interneuron progenitor: ventricular and subventricular zones in the pallium (purple), caudal ganglionic eminence (CGE) (green), medial ganglionic eminence (MGE) (red), and preoptic area (POA) and preopto-hypothalamic area (POH) (light blue). (**B**) Schematics of the combinatorial code of transcription factors that direct the fate specification of pyramidal neurons during embryonic development. (**C**) Schematics of the transcriptional logic for interneuron subtype specification in different regions of the subpallium, and how distinct developmental origins determine the morphological, biochemical, and electrophysiological properties of mature interneurons. The question marks indicate a yet unclear developmental origin for those interneuron types. Other abbreviations: NCx, neocortex; CPN, callosal projection neuron; CFuPN, corticofugal projection neuron; CBuPN, corticobulbar projection neuron; CSMN, corticospinal motor neuron; CThPN, corticothalamic projection neuron; VIP, vasoactive intestinal peptide, NOS, nitric oxide synthase; NPY, neuropeptide Y.

the expression of specific transcription factors (Lodato et al., 2015; Rouaux and Arlotta, 2010, 2013). Altogether, these findings suggest that different gene

regulatory networks involved in subtype specification are orchestrated by transcription factors and are cell type-specific in cortical pyramidal cells.

In the adult mammalian cerebral cortex, the diversity of pyramidal cell types across layers and regions seems to reflect a profound heterogeneity in cellular and molecular properties. For instance, a recent study has reported distinct anatomical, physiological and molecular properties of L3 pyramidal cells in primate association cortices (González-Burgos et al., 2019), and recent transcriptomic analysis have captured a great divergence of pyramidal cell types in motor and visual cortices of the mouse brain (Tasic et al., 2018). How the cellular heterogeneity of pyramidal cells emerges during development, and whether the mechanisms of genetic specification described above shape their properties in the adult cerebral cortex remain fundamental, unanswered questions in neuroscience. Future research addressing these questions will undoubtedly pave the way to understand the specificity in wiring and function of pyramidal cells in cortical circuits.

As opposed to pyramidal cells, cortical interneurons are born in the subpallium, in the medial, and caudal ganglionic eminences (MGE and CGE, respectively) as well as in the embryonic anlage of the preoptic region, and migrate tangentially to arrive to the cortex (Anderson et al., 1997, 2001; Corbin et al., 2001; Marín and Rubenstein, 2001). More than a decade ago, initial gene expression analysis in the ganglionic eminences and the preoptic region showed that interneuron progenitors are organised in distinct spatial domains according to the expression of combinatorial codes of transcription factors (Batista-Brito et al., 2008; Flames et al., 2007). The recent development of single-cell RNA sequencing technologies has allowed to analyse the genome-wide transcriptional profiles of cortical developing interneurons, and, surprisingly, these studies showed that, to some degree, cortical interneuron diversity is already apparent during early embryonic development (Mayer et al., 2018; Mi et al., 2018). Therefore, it has been hypothesised that transcription factors dictate the nature and dynamics of gene regulatory networks that specify interneuron cardinal classes. *Nkx2.1*, a gene that is essential to pattern the MGE, is the best example of a transcription factor involved in the fate of interneuron types; its deletion from progenitor cells prevents the generation of PV+ and SST+ interneurons (Anderson et al., 1997; Butt et al., 2008; Sussel et al., 1999). Other transcription factors expressed postmitotically are required for the specification of specific interneuron types: *Lhx6*, *Sox6* and *Satb1* regulate the normal development of PV+ and SST+ interneurons (Azim et al., 2009; Close et al., 2012; Liodis et al., 2007), and the homeodomain transcription factor

Prox1, which is expressed by postmitotic CGE-derived cortical interneurons, controls the migration, differentiation, and integration of VIP+ and Reelin+ interneurons (Miyoshi et al., 2015). Interestingly, late removal of these transcription factors tends to have a less severe impact on the differentiation and/or maturation of the cells, suggesting that the developmental trajectories, and their underlying gene regulatory networks, are more susceptible to perturbations in early embryonic stages (Batista-Brito et al., 2009; Miyoshi et al., 2015). For example, postnatal deletion of Prox1 affects the proper synaptic integration and local connectivity of VIP+ cell types while it has a mild impact on cell density and laminar allocation of these interneurons (Stachniak et al., 2020; Vagnoni et al., 2020). Again, this supports the hypothesis that cardinal class specification is a result of a coordinated, sequential regulation of gene networks directed by transcription factors in progenitor and postmitotic neurons.

2.2. Extrinsic refinement

After birth, a long journey awaits postmitotic neurons before arriving and settling to their final destination in the cerebral cortex. At this point, it is believed that, to some extent, neurons have already committed to a certain cell type, but recent studies have shown that these immature neurons, while integrating into the nascent cortical circuit, progressively unfold cellular and molecular programmes through specific interactions with the environment to develop all their characteristics and acquire their definitive state (Fishell and Kepecs, 2019; Lim et al., 2018a).

Migration entails a long process in which neurons take specific routes while are exposed to multiple external cues. A recent study showed that specific populations of migrating interneurons preferentially choose the superficial marginal zone (MZ) over the subventricular zone, and the choice of migratory route is crucial for the definitive acquisition of their axonal morphology and the tuning of adult cortical circuit (Lim et al., 2018b). Specifically, Martinotti cells migrate through the MZ and, when entering the cortex, leave their nascent trailing processes in MZ, which eventually become their translaminar axonal arborisations that innervate L1 (Lim et al., 2018b). Importantly, Martinotti cells in L2/3 and L5 as well as PV+ translaminar cells were seen to preferentially migrate through the MZ, suggesting that the coupling of cell migration and axonal targeting might be a general mechanism in developing interneurons (Lim et al., 2018b). These migrating cells

already show unique transcriptional programmes during embryonic stages, which might empower them with molecular complexes needed to undergo such developmental trajectory (Lim et al., 2018b). Besides, region-specific cues could presumably be an additional source of external cues to influence the subtype specification in different cortical areas (Scala et al., 2019).

Upon arrival to the cortex, pyramidal neurons and interneurons undergo a process of programmed cell death during a defined time window of postnatal development (Southwell et al., 2012; Wong et al., 2018). This refinement process follows temporally precise and activity-dependent waves of cell death, which seem to coordinate the final numbers of neuronal cells in the adult cerebral cortex (Denaxa et al., 2018; Priya et al., 2018; Wong et al., 2018). It has been suggested that pyramidal cells and interneurons have adopted and evolved this mechanism to match their numbers with the neighbouring cellular partners, thus maintaining the proper balance of excitation and inhibition in the cortex (Wong et al., 2018).

Several lines of evidence have demonstrated that neuronal activity and sensory experience also has a profound effect on the developmental assembly of cortical circuits. First, modulation of pyramidal cell activity remarkably affects the survival of MGE-derived interneurons during the second week of postnatal development (Wong et al., 2018). Second, neuronal activity selectively regulates the morphological development of specific types of interneurons (Babij and De Marco Garcia, 2016; De Marco García et al., 2011). Third, perturbation of the activity from thalamocortical inputs results in morphological defects in Reelin+ neurogliaform interneurons (De Marco García et al., 2015). Furthermore, SST+ interneurons in L5 integrate into early transient thalamocortical circuits that disappear after the sensory critical period, which plays a crucial role in the maturation of cortical circuits during postnatal development and is sensitive to sensory perturbation (Marques-Smith et al., 2016; Tuncdemir et al., 2016). Lastly, in adult stages, neuronal activity can also modulate the plasticity and intrinsic properties of specific subtypes of interneurons in the cortex (Dehorter et al., 2015; Favuzzi et al., 2017).

Altogether, genetic and extrinsic mechanisms during embryonic and postnatal brain development play pivotal roles on the ability of cortical cell types to wire selectively with the correct neuronal targets and establish the mature neural circuitry.

3. Mechanisms of cortical synaptic assembly

"Neurons that fire together, wire together"

Carla Shatz is recognised for her work on developmental mechanisms that generate precise patterns of connections in the nervous system. While breaking barriers for women in science, her research postulated the paradigmatic idea that the wiring of neural circuits is controlled by the intersection between genes and neural activity.

The ground-breaking discoveries from Carla Shatz's laboratory have shaped our mechanistic understanding on the development of brain circuits. Neural activity is required in the developing visual system for target selection of retinogeniculate and thalamocortical axons (Catalano and Shatz, 1998; Shatz and Stryker, 1988; Sretavan and Shatz, 1984;). Transient neuronal populations such as subplate cells play a key role in instructing the initial formation of axonal connections in the cerebral cortex (McConnell et al., 1989; Ghosh et al., 1990). The major histo-compatibility complex regulates synaptic connectivity in an activity-dependent manner (Corriveau et al., 1998; Syken et al., 2006). Altogether, these discoveries represented milestones in the investigation on the mechanisms of brain wiring.

Neurons are endowed with the ability to receive, compute, and transmit information. On average, a neuron receives over 10,000 synaptic inputs. How do neurons establish specific connections with other neurons? Given the remarkable cellular diversity in the cerebral cortex, this remains a challenging and fundamental question in neuroscience. Our knowledge on molecular and cellular mechanisms underlying synaptic assembly has exponentially increased over the past decades. This field has been nurtured by technological developments, first from the revolution of molecular biology in the 1990's and then from the post-genomics era in the 2000's. Besides, the tools provided by developmental genetics have helped to label and identify cortical circuits, thus fostering the study of specific connections (He et al., 2016; Taniguchi et al., 2011). In this section, I will review the molecular and cellular mechanisms that instruct synaptic assembly of cortical cell types, and I will highlight the emergence of these mechanisms during postnatal development. Ultimately, the interplay of distinct mechanisms at specific temporal windows is necessary for the attainment of a biological process as precisely regulated and dynamic as synaptogenesis.

3.1. Transcriptional mechanisms

As discussed above, the diversity of cortical cell types can be interrogated based on their gene expression patterns, not only in adult neural networks but also during the developmental specification in the embryo (Mayer et al., 2018; Mi et al., 2018; Tasic et al., 2018). Noticeably, the transcriptional signatures of cortical cell types are enriched in molecular components of the synaptic architecture and communication, as revealed by transcriptome-wide studies (Paul et al., 2017). These findings point out to cell type-specific expression patterns of key cell surface synaptic organizers, suggesting that they could play an important role in synapse assembly and specificity in cortical circuits (de Wit and Ghosh, 2016).

Early studies on the neurexin-neuroligin families, arguably the most emblematic molecules with roles in synapse form and function (Scheiffele et al., 2000), indicated that their members show specific patterns of expression in the brain (Ullrich et al., 1995). Recently, sophisticated conditional genetic models have demonstrated cell type-specific functions of neurexins (Nrxn) in defined circuits (Chen et al., 2017). For instance, conditional deletion of neurexins in PV+ interneuron leads to a substantial decrease in presynaptic GABAergic bouton density, while neurexin expression in SST+ interneurons is crucial for synaptic transmission with pyramidal cells. In cerebellar circuits, neuroligins (Nlgn), a family of postsynaptic neurexin ligands, have segregated functions in specific connections (Zhang et al., 2015). Conditional deletion of Nlgn-1 and Nlgn-3 from Purkinje cells specifically affected synapse formation from climbing fibres while leaving unaltered parallel fibre synapses, and Purkinje cell-specific Nlgn-2 and Nlgn-3 double knockout impairs both climbing-fibre and basket/stellate cell synaptic transmission. Cerebellins (Cbln) are a family of adaptor proteins to neurexins in the synaptic cleft with synaptogenic functions (Ito-Ishida et al., 2012; Matsuda et al., 2010; Uemura et al., 2010). Interestingly, members of the Cbln family display a striking segregation of expression patterns throughout brain circuits (Seigneur and Südhof, 2017), and genetic deletion of Cbln1, Cbln2 and Cbln4 causes a dramatic and late loss of synapses in adult cortical, cerebellar and striatal circuits, but not during postnatal development, suggesting a role for cerebellins in synapse maturation and/or stabilisation rather than synapse formation (Seigneur and Südhof, 2018).

Secreted proteins of the C1ql family are endowed with the ability to establish trans-synaptic interactions involved in synaptic assembly (Matsuda et al., 2016). The expression of several members of this protein family, namely C1ql1-3, has been mapped to different brain regions and cell types (Yuzaki, 2017). In the cerebellum, C1ql1 selectively functions in the assembly of climbing fibres onto Purkinje cells (Kakegawa et al., 2015; Sigoillot et al., 2015). C1ql2 and C1ql3 expressed in dentate gyrus granule cells are released at the mossy fibre synapse and control the postsynaptic localisation of kainate receptors (Matsuda et al., 2016). In addition, conditional Cq1l3 knockout in the basolateral amygdala decreases the formation of synaptic connections projecting to the prefrontal cortex and impairs fear memory (Martinelli et al., 2016). On the other hand, cadherins (Cdh) are transmembrane proteins localised in pre- and postsynaptic membranes that regulate synapse formation and maintenance through interactions with other synaptic organisers and intracellular signal transduction via catenin complexes (Brigidi and Bamji, 2011; Yamagata and Sanes, 2018). Importantly, the specific logic of expression patterns in the Cdh family appears to play a key role in the connectivity of hippocampal circuits (Basu et al., 2017; Williams et al., 2011), similar to the central role of cadherins in retinal connectivity (Duan et al., 2014, 2018).

In local cortical circuits, different types of inhibitory interneurons precisely target distinct subcellular compartments in the postsynaptic pyramidal cell. A recent transcriptomic study of SST+ dendrite-targeting cells, PV+ basket cells and chandelier cells identified unique molecular codes during the postnatal period of synaptogenesis (Favuzzi et al., 2019) (Figure 3). Multiple protein families implicated in axon guidance and cell adhesion, such as semaphorins, cerebellins, and protocadherins, display a remarkable cellular specificity in their expression patterns. In fact, conditional knock-down experiments for Cbln4, leucine-rich repeat LGI family member 2 (Lgi2), and fibroblast growth factor 13 (Fgf13), resulted in specific losses of dendritic, somatic and axo-axonic input synapses in pyramidal cells, respectively (Favuzzi et al., 2019). At the postsynaptic membrane, GluD1 trans-synaptically interact with Cbln4 to mediate inhibitory synapse formation onto cortical pyramidal cell dendrites (Fossati et al., 2019).

Further evidence supports the role of cell type-specific expression of synaptic proteins in the wiring of cortical interneurons (Figure 3). Selective expression of NIMA related kinase 7 (Nek7), a regulator of microtubules, in PV+ basket cells is required for normal axonal growth and synapse formation onto the

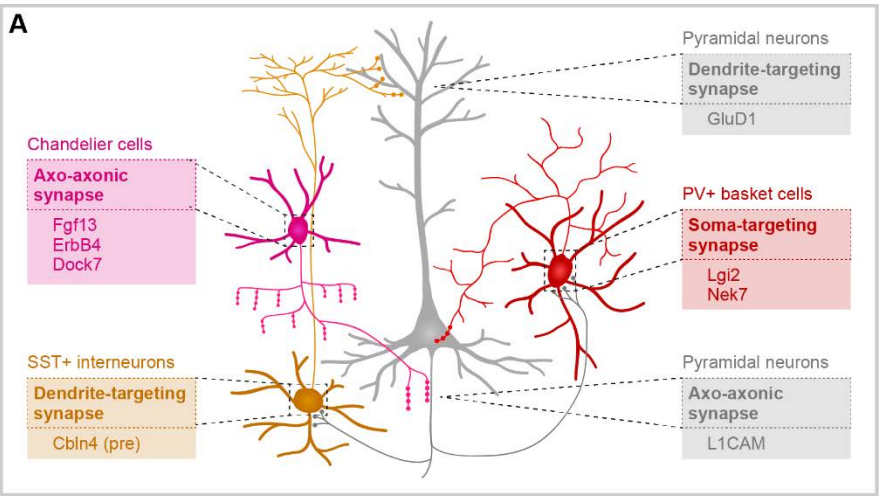

Figure 3 | **Cell type-specific molecular programs instruct the formation of distinct classes of synaptic connections in pyramidal cell-interneuron circuits of the cerebral cortex**.
(**A**) Diagram representing the differential expression of various molecules in distinct inhibitory cell types in the mouse cerebral cortex. These cell type-specific expression patterns are essential to instruct synapse specificity in local cortical circuits during postnatal development.

soma of cortical pyramidal cells (Hinojosa et al., 2018). Erb-B2 receptor tyrosine kinase 4 (ErbB4), a member of the epidermal growth factor receptor subfamily that is expressed in specific interneuron subtypes, controls the development of excitatory inputs and inhibitory outputs of CCK+ and PV+ interneurons, including basket and chandelier cells (Del Pino et al., 2013, 2017; Fazzari et al., 2010). Although little is known about the molecular strategies utilized by pyramidal cells to mediate these processes, a recent study determined that L1 cell adhesion molecule (L1CAM), a transmembrane protein targeted to the AIS, plays a fundamental role in the formation and maintenance of the synaptic innervation from chandelier cells (Tai et al., 2019).

How are these synapse-related genetic programs activated in different cell types? A prevalent model of neocortical development supports a molecular logic in which each sequential developmental decision is gated by the coordinated activity of highly interconnected networks of transcriptional regulators which direct the specification and differentiation of glutamatergic and GABAergic cell types (Custo Greig et al., 2013; Fishell and Kepecs, 2019). As a critical step in cortical assembly, the cell type-specific expression of cell-surface molecules with roles in synaptogenesis would be embedded in a downstream regulation through combinatorial transcriptional codes that drive specific developmental trajectories. Strikingly, in Drosophila, the cooperation of intrinsic and extrinsic mechanisms

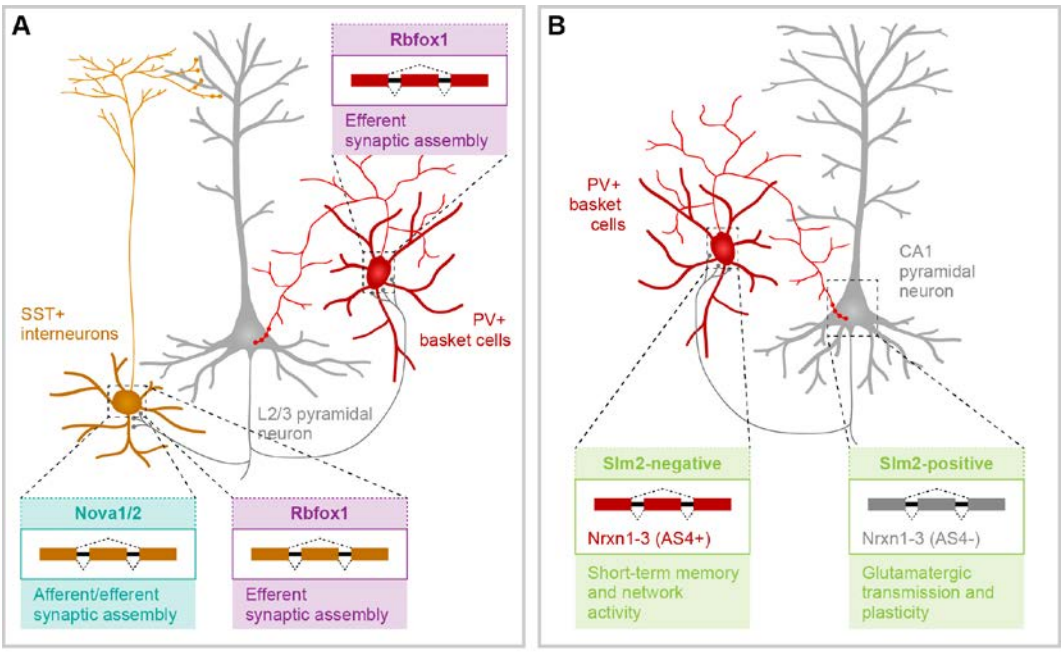

Figure 4 | **Cell type-specific regulation of alternative mRNA splicing shapes the formation and plasticity of excitatory and inhibitory circuits in the neocortex**. (**A**) Schematics illustrating the different roles of the RNA binding proteins Nova1/2 and Rbfox1 in the synaptic assembly of soma-targeting PV+ interneurons and dendrite-targeting SST+ interneurons in the cerebral cortex. (**B**) Schematics showing that the RNA-binding protein Slm2 is differentially expressed by GABAergic and glutamatergic cells in the hippocampus to regulate different cellular and circuit functions.

through succeeding waves of genetic programs has been elegantly shown to regulate the specificity of neural connectivity in the visual system (Peng et al., 2018). In this conceptual framework, future efforts will be needed to understand how transcriptional regulators might potentially contribute to unfold the selective expression of synaptic proteins in distinct cell types of the mammalian cerebral cortex.

From a regulatory genetic perspective, the molecular repertoire of cortical cell types can be further articulated by two additional strategies. First, alternative splicing can expand diversity of protein isoforms expressed by neurons, expanding the capability of synaptic proteins to trigger distinct synaptic functions (Aoto et al., 2013; Dai et al., 2019). This post-transcriptional regulation has been recently shown to function, at least in some cases, in a cell type-specific manner (Fuccillo et al., 2015; Nguyen et al., 2016b; Schreiner et al., 2014; Treutlein et al., 2014). Importantly, splicing regulators show cell type-specific patterns of expression in the brain (Iijima et al., 2011, 2014). In hippocampal circuits, the KH-domain RNA-binding protein SLM2 is differentially expressed by glutamatergic and GABAergic cells and controls the specification of synaptic transmission and short-term

plasticity properties (Nguyen et al., 2016b; Traunmüller et al., 2016) (Figure 4). In local inhibitory circuits, paradoxically, the splicing factor Rbfox1 differentially regulates alternative splicing programs in PV+ and SST+ interneurons, which empowers these two cell types with distinct abilities to control their efferent connectivity (Wamsley et al., 2018) (Figure 4). Second, high-throughput analyses are also starting to identify that the epigenetic landscape such as methylome signatures is neuronal subtype specific (Gabitto et al., 2019; Luo et al., 2017). To what extent this epigenetic regulation could influence the synaptic assembly and function in a cell type-specific manner is still unclear.

Altogether, recent efforts from transcriptome-wide studies have elucidated the importance of cell type-specific genetic programs in instructing the wiring of cortical cell types. However, the complex morphological structures of neurons and the high organization of cortical connections raise the question whether molecular complexes follow a higher-order organization at the subcellular level (Schreiner et al., 2017).

3.2. Sorting mechanisms

Emerging evidence demonstrates that synaptic cell surface proteins are differentially distributed along the cell bodies of cortical neurons (Apóstolo and de Wit, 2019). The functional relevance of this process is starting to be identified, since this subcellular restriction endows neurons with the ability to spatially segregate signalling pathways that control the architecture and function of specific synaptic connections. However, as discussed below, the sorting mechanisms underlying the subcellular compartment-dependent function of synaptic proteins are still poorly understood.

Subcellular compartmentalisation has been best documented in hippocampal pyramidal neurons due to the spatially organized logic of afferent and efferent connections (Figure 5). In CA1 pyramidal cells, the leucine-rich repeat (LRR)-containing protein NGL-2 (*Lrrc4*) is precisely located at the dendritic fragments in the stratum radiatum and specifically regulates the development of synaptic inputs from Schaffer collaterals (DeNardo et al., 2012). Similarly, the postsynaptic localisation of the LRR adhesion molecules FLRT2, LRRTM1 and Slitrk1 is finely defined to control diverse synaptic properties in an input-dependent

manner (Schroeder et al., 2018). Through a hitherto unknown mechanism, two members of the latrophilin (Lphn) family, Lphn2 and Lphn3, are differentially localised to dendritic fragments in the stratum radiatum and stratum lacunosum-moleculare, respectively, thereby instructing synapse specificity to organize hippocampal connectivity (Anderson et al., 2017; Sando et al., 2019).

The CA3 pyramidal neuron has also implemented specialised subcellular distributions of molecular components to orchestrate input-specific properties (Figure 5). The synaptic expression of the orphan G protein-coupled receptor GPR158 is enriched in the stratum lucidum, requires the heparan sulfate glypican 4 at the presynaptic surface, and selectively controls the formation and function of mossy fibre (MF)-CA3 synaptic connections (Condomitti et al., 2018). Interestingly, MF filopodia, the synaptic contacts that dentate gyrus granule cell axons make onto GABAergic CA3 interneurons, have been shown to be specifically regulated by Kirrel3 and Ablim3 (Guo et al., 2018; Martin et al., 2015), suggesting a subcellular restriction for these molecular mechanisms.

Although the intricate pattern of connections in the cortex have made the exploration of this question more challenging in cortical circuits, some observations indicate that this process is also apparent in cortical cell types. Through conditional knock-down and exogenous expression approaches *in vivo*, Cbln4 was recently shown to selectively regulate the formation of dendrite-targeting synapses that SST+ interneurons establish onto pyramidal cells, whereas it is incapable of specifying somatic and axo-axonic synaptic contacts onto the same postsynaptic neurons (Favuzzi et al., 2019). One possibility is that the differential distribution of the potential receptors for Cbln4 function in particular cellular compartments of pyramidal neurons is required to drive the formation of synapses by specific interneuron populations (Fossati et al., 2019). In this context, the selective sorting of L1CAM to the AIS of cortical pyramidal cells controls is required for axo-axonic innervation by chandelier cells (Tai et al., 2019). Interestingly, Nlgn4 has recently been found to be targeted to excitatory synapses in human cortical neurons (Marro et al., 2019). Since this expression pattern differs from findings in the mouse, this species-specific control of synapse specificity might suggest that subcellular segregation of synaptic molecules represents an evolutionary adaptation to expand the capacity of cortical circuit assembly.

Despite the previous findings, the sorting mechanisms responsible for the subcellular distribution of synaptic proteins in cortical cell types remain largely

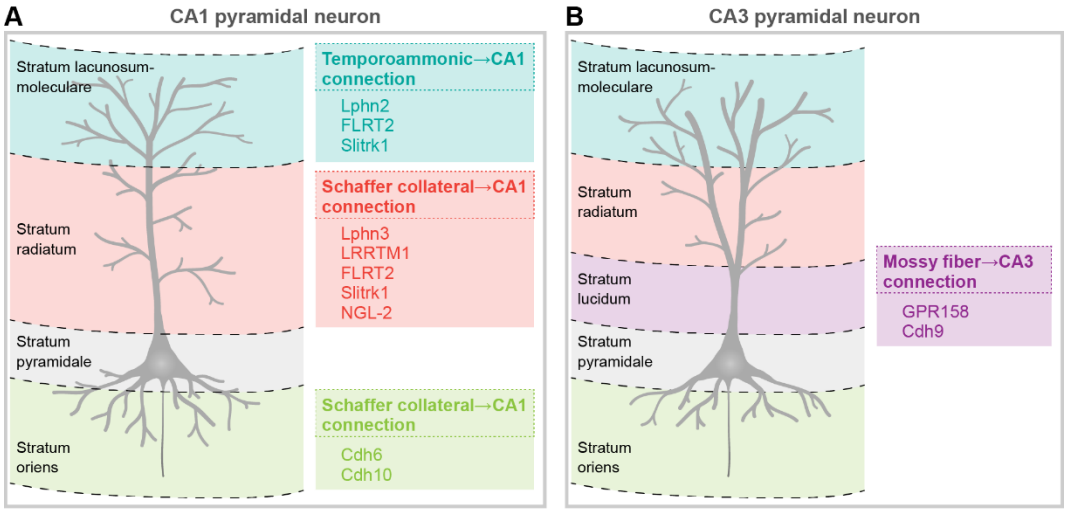

Figure 5 | **Subcellular distribution of synaptic proteins along dendritic arbours of hippocampal pyramidal cells**.
(**A-B**) Diagram of the subcellular patterns of expression in hippocampal pyramidal cells. In CA1 pyramidal cells, a large diversity of cell adhesion molecules and other synaptic proteins are specifically localised in restricted fragments of the dendritic arbours (**A**). The differential subcellular distribution allow these molecules to be targeted to specific synaptic contacts received by CA1 pyramidal cells. In the CA3 region, pyramidal cells also show restricted expression of some synaptic proteins in specific dendritic fragments, particularly those found in the stratum lucidum that receive synaptic connections from the Mossy fibres arriving from the dentate gyrus (**B**).

unknown. This is in marked contrast to the progress made in understanding the molecular mechanisms underlying the sorting and subcellular localisation of ion channels along the neuronal cell body (Gu et al., 2003; Rivera et al., 2003, 2005). From a mechanistic perspective, neurons can use two alternative, not necessarily exclusive, pathways for selective sorting of synaptic molecules to different compartments. First, it has been recently shown that messenger RNA (mRNA) molecules can be transported and compartmentalised in both dendrites and axons, and local mRNA regulation mediated by translation and degradation processes supports varied neuronal functions (Biever et al., 2019; Glock et al., 2017). Deep sequencing technologies and live imaging approaches have elucidated that mRNA composition strikingly differs in somatic and neuropil compartments (Cajigas et al., 2012). These studies revealed that the mRNA signatures found in neurites are enriched in dendritic, axonal and synaptic genes. mRNA stability, localisation and translation is largely determined by cis-acting elements present in the 3' untranslated region (UTR) (Andreassi and Riccio, 2009; Glock et al., 2017). The generation of transcript isoforms with different localisations is orchestrated by alternative cleavage and polyadenylation of mRNA, and the transport is mediated by the interaction with RNA-binding proteins (Tian and Manley, 2017; Ule and

Darnell, 2006). The localised mRNAs in the neuropil of cortical neurons usually represent isoforms with longer 3' UTRs (Miura et al., 2013; Tushev et al., 2018), intriguingly suggesting the presence of sequence motifs necessary for the sorting of axonal and dendritic transcripts (Urwyler et al., 2019).

Local mRNA translation participates in multiple steps of neurite organisation and function. Not only local translation plays an important role in dendrites and synaptic plasticity (Steward and Schuman, 2001; Sutton and Schuman, 2006), but also regulates the formation and maturation of presynaptic structures in the axon (Biever et al., 2019; Cioni et al., 2018). Two intriguing studies elucidated a role for local translation of axonal beta-actin and the active zone protein SNAP25 in remodelling axonal arborisation and in presynaptic terminal development and synaptic release, respectively (Batista et al., 2017; Wong et al., 2017). More recently, it has been shown that late endosomes provide stations for local translation of mRNA in axons (Cioni et al., 2019). However, to what extent this molecular process could modulate the function of cell adhesion molecules in synapse specification and cortical connectivity remains unknown.

A second mechanism by which cell surface molecules can be targeted to different neuronal compartments is protein sorting. Trafficking pathways for polarized proteins ensure the accurate localisation of these proteins to their appropriate subcellular domain, maintaining neuronal polarity necessary for neural signalling and plasticity, and entails membrane budding, transport and fusion events of carrier vesicles (Bentley and Banker, 2016; Ribeiro et al., 2018). Protein trafficking is a sequential process that follows multiple events: post-translational maturation and exit of the endoplasmic reticulum (ER) mediated by folding factors such as classical chaperons (Braakman and Hebert, 2013), sorting and loading into specific transport vesicles by adaptor proteins at the trans-Golgi network (TGN) station (Bonifacino, 2014; Guardia et al., 2018), selective transport of vesicles mediated by different motor proteins (Gumy and Hoogenraad, 2018; Namba et al., 2011), and selective fusion to the plasma membrane by tethering factors and soluble N-ethylmaleimide-sensitive factor attachment protein receptor (SNARE) proteins (Harris et al., 2016; Soo Hoo et al., 2016). Of note, the clathrin-binding adaptor proteins AP-1 and AP-3 at the TGN act as regulators to recognise, sort and load transmembrane proteins into somatodendritic and axonal transport vesicles, respectively (Farías et al., 2012; Li et al., 2016). Besides, several motor proteins, such as dynein, kinesin-1/KIF5, kinesin-2/KIF17 and kinesin-3/KIF1, are involved in the bidirectional, regulated transport and delivery of vesicles through

the cytoskeleton in dendrites and axons (Guedes-Dias et al., 2019; Kapitein et al., 2010). In this process, the AIS constitutes a dense cytoplasmic structure enriched in AnkyrinG and F-actin that selectively allows the transport of KIF5-driven carriers to the axon (Song et al., 2009). Similarly, the pre-axonal exclusion zone, a more proximal region to the axonal hillock, is able to exclude the entry of somatodendritic vesicles to the axon through a mechanism dependent on the coordinated actions of motor proteins KIF1 and KIF5 (Farías et al., 2015; Gumy et al., 2017). These selective filters largely shape the polarized behaviour of vesicle transport in neurons; however, a variety of additional mechanisms can contribute to the final allocation of proteins.

The endocytic system has also been involved in selective sorting of synaptic proteins. Sorting receptors play a crucial role in recycling transmembrane proteins. Strikingly, the deletion of SorCS1 leads to differential composition of synaptic organizers and receptors in synapses (Savas et al., 2015). In particular, endosomal SorCS1 interacts with Rab11 family-interacting proteins to mediate the sorting of dendritic internalised Nrxn1α to the axonal surface compartment (Ribeiro et al., 2019). Moreover, post-translational mechanisms that comprise activity-dependent events, including phosphorylation and proteolytic cleavage, control the surface levels of cell-adhesion molecules (Bemben et al., 2014; Peixoto et al., 2012; Suzuki et al., 2012). Lastly, cell surface transmembrane proteins can be redistributed between synaptic sites and perisynaptic locations via lateral diffusion, a dynamic mechanism that might depend in part on the interaction with receptor/ligand partners at the other side of the synapse (Biermann et al., 2014; Chamma et al., 2016; Neupert et al., 2015).

In conclusion, transmembrane proteins involved in the development of specific synaptic connections in the brain show restricted subcellular localisation in their expression patterns, and a variety of molecular mechanisms have been implicated in RNA and protein sorting. While some reports have already shed light on how sorting mechanisms influence the architecture and function of neuronal circuits (Ribeiro et al., 2019), I anticipate a large number of studies in the coming years to functionally link the basis of subcellular sorting (e.g. structural determinants and molecular interacting partners) to the precise synaptic assembly of cortical cell types.

3.3. Trans-synaptic mechanisms

The synapse can be seen as a highly complex, modular, and dynamic structure, composed by a multitude of nodes—proteins present within the synaptic membrane, cytoplasm and extracellular matrix—connected through an organised and iterative network of internodes—protein-protein interactions mediated by binding through specific protein domains. Proteomic analyses have identified more than 2,400 proteins in synaptosome fractions prepared from cultured cortical neurons, which indicate that a high molecular diversity make up the architecture of cortical synapses (Loh et al., 2016). Importantly, structural biology has informed neurobiologists about the molecular foundations of trans-synaptic interactions that mediate synapse formation (Elegheert et al., 2016; Li et al., 2018).

In the hippocampus, a dedicated, and unexpected, logic of interactions between latrophilins, fibronectin leucine-rich repeat transmembrane proteins (FLRTs) and teneurins is necessary to properly develop excitatory synapses targeting the proximal region of dendrites in CA1 pyramidal cells (Sando et al., 2019) (Figure 6). Latrophilin G protein-coupled receptors (GPCRs) are expressed postsynaptically (Anderson et al., 2017; Sando et al., 2019), and, at the structural level, Lphn3 utilises its olfactomedin-like domain to interact with FLRTs, on the one hand, and its lectin domain to interact with teneurins, on the other hand (Li et al., 2018; Lu et al., 2015). When Lphn3 is deleted postsynaptically, CA1 pyramidal neurons show a specific reduction in dendritic spines in the stratum radiatum, and receive fewer and weaker evoked excitatory synaptic inputs (Sando et al., 2019). Remarkably, the observed synaptic deficits could be rescued by expression of wild-type Lphn3 but not mutant forms in the interacting domains for FLRTs and teneurins. Altogether, these results uncovered a mechanism by which the coincident binding of two transcellular ligands, FLRT3 and teneurin-2, to Lphn3 in the postsynaptic membrane is required to regulate synaptogenesis in specific hippocampal connections.

At the presynaptic membrane, protein tyrosine phosphatase receptors (PTPRs) mediate synaptogenic functions via the interaction with a diverse amalgam of postsynaptic adhesion ligands (Takahashi and Craig, 2013). Trans-synaptic interactions between the leukocyte activated receptor LAR-PTPR (also named PTPRF) with the netrin-G ligand NGL-3 (Woo et al., 2009), and the binding of PTPRS with the neurotrophin receptor TrkC (Takahashi et al., 2011), control the

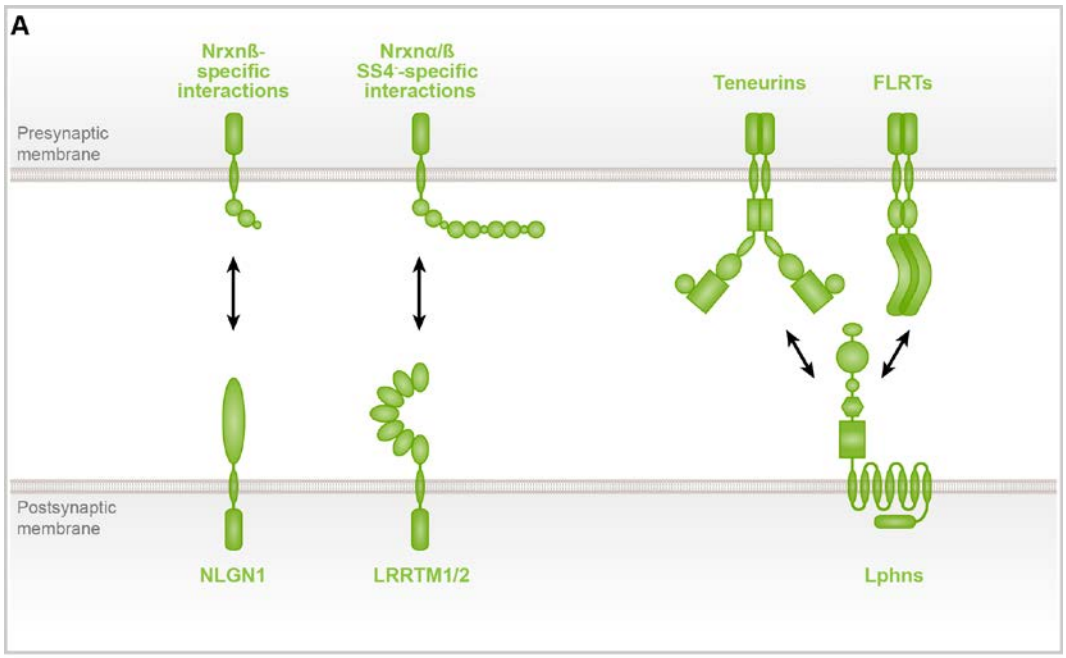

Figure 6 | **Context-specific interactions of cell adhesion molecules at the synapse**. (**A**) Examples of trans-synaptic interactions between pre- and postsynaptic molecules involved in synapse formation. Abbreviations: FLRT, fibronectin leucine-rich transmembrane protein; Lphns, latrophilins; LRRTM, leucine-rich repeat transmembrane neuronal; NLGN, neuroligin; Nrxn, neurexin.

formation of excitatory synapses. Furthermore, the specific binding of PTPRD to the interleukin-1 receptor family proteins IL1RAP1L or IL1RAcP regulates excitatory synapse development (Yoshida et al., 2011, 2012), whereas its interaction with the Slit and NTRK-like family member-3 (Slitrk3) selectively promotes inhibitory synapse formation (Takahashi et al., 2012). Importantly, a variety of extracellular domains and alternative splicing events in the PTPR family govern these specific protein-protein interactions (Kwon et al., 2010; Yamagata et al., 2015a, 2015b). Intracellular domain-mediated functions of PTPRS, likely due to interaction and signalling through distinct cytoplasmic presynaptic proteins, have also been shown to participate in synapse assembly (Han et al., 2018a). Thus, a complex network of interactions between presynaptic PTPRs and postsynaptic ligands orchestrate the formation of various classes of synaptic connections.

Heparan sulfate proteoglycans (HSPGs) are membrane-bound or secreted proteins to which long heparan sulfate (HS) glycosaminoglycan chains are covalently attached (Condomitti and de Wit, 2018). A presynaptic HSPG, GPC4, binds to the postsynaptic ligands LRRTM4 and GPR158 to induce the development of excitatory synapses in hippocampal neuronal circuits (Condomitti et al., 2018; de Wit et al., 2013). Nonetheless, these trans-cellular interactions, which require

HS, depend on distinct presynaptic co-receptors: whereas LRRTM4-induced presynaptic differentiation requires PTPRS but not LAR-PTPR, GPR158's synaptogenic activity depends in part on LAR-PTPR and, surprisingly, is inhibited by PTPRS (Condomitti et al., 2018; Ko et al., 2015; Siddiqui et al., 2013; de Wit et al., 2013). These results highlight a difference in co-receptor requirement for GPR158 and LRRTM4-mediated presynaptic differentiation, suggesting a high level of sophistication in protein-protein interacting networks at the synapse that is likely mediated, at least in part, through HS-dependent regulation. Furthermore, glycan modifications observed in Nrxn1 mediate binding to postsynaptic ligands and are directly involved in synaptic functions (Zhang et al., 2018). This striking finding suggests that the interactome of synaptic organisers might be potentially expanded to novel binding partners due to the presence of HS chains. Altogether, these results reinforce the idea that synaptic specificity, at least to some extent, might be dependent on a higher-order level of complexity encoded by trans-synaptic interactions.

The alternative splicing code of presynaptic neurexins specifies their synaptic properties by controlling the differential binding to manifold postsynaptic ligands, including neuroligins, LRRTMs, calsyntenins, cerebellins and C1qls, among others (reviewed in (Südhof, 2017)). Six alternative splice sites (SS1-SS6) generate a high diversity of isoforms from three neurexin genes, each encoding a longer α-protein or a shorter β-protein transcribed from distinct promoters (Tabuchi and Südhof, 2002; Ullrich et al., 1995). Neuroligins (Nlgn), the first neurexin ligands to be discovered, were shown to selectively bind to beta-neurexins lacking an insert at the splice site SS4 (SS4-); however, subsequent studies identified a wider network of Nlgn interaction with alpha- and beta-neurexins that is regulated by the splice site B in Nlgn1 in addition to the SS4 in neurexins (Boucard et al., 2005; Comoletti et al., 2006) (Figure 6). The leucine-rich repeat transmembrane proteins LRRTM1 and LRRTM2 exclusively bind SS4- Nrxnα/β, which represents a complementary, cooperative pathway to Nrxn-Nlgn interactions required for synaptogenesis (Ko et al., 2009; Linhoff et al., 2009; Siddiqui et al., 2010; de Wit et al., 2009) (Figure 6). In contrast, calsyntenin-3 is a selective Nrxnα binding partner that induces presynaptic differentiation (Pettem et al., 2013). Intriguingly, small secreted proteins, such as cerebellins and C1qls, can bridge neurexins to postsynaptic glutamate receptors to exert synaptogenic functions. Cbln1 binds to the N-terminal domain of GluRD2, postsynaptically, and to all neurexin isoforms containing an insert in the SS4, presynaptically, and this peculiar trans-synaptic

interaction is capable of mediating synapse formation (Elegheert et al., 2016; Matsuda et al., 2010; Uemura et al., 2010). Similarly, C1ql2 and C1ql3 selectively bridges presynaptic Nrxn3 containing a specific sequence at SS5 to postsynaptic receptors GluK2 and GluK4 (Matsuda et al., 2016), and C1ql3 plays a role in synapse formation in specific brain circuits (Martinelli et al., 2016), although a direct link between this selective trans-synaptic interaction and a synaptogenic function has not been probed yet. As a modulatory mechanism, the anchor proteins MDGA1 and MDGA2 are able to bind all Nlgn isoforms via two interface sites to block their interaction with presynaptic neurexins (Elegheert et al., 2017). Besides protein domain binding, an alternative mode of heparan sulfate-dependent interactions is required for the synaptic organising functions of neurexins through the postsynaptic Nlgn and Lrrtm partners, and could potentially expand the Nrxn interactome (Zhang et al., 2018). Finally, recent studies have identified unique roles for intracellular domains of neuroligins in implementing specific synaptic functions (Gokce and Südhof, 2013; Nguyen et al., 2016a; Wu et al., 2019). In inhibitory synapses, Nlgn2 and IgSF9b are coupled together to assemble synaptic clusters via intracellular interactions with the multi-PDZ protein S-SCAM (Woo et al., 2013), and trans-synaptic interactions between Nrxn2α and IgSF21 promote presynaptic differentiation (Tanabe et al., 2017). Altogether, these findings illustrate how extra- and intracellular mechanisms regulate the development of synapses in cortical circuits, and how cell-surface molecules expand their functional repertoire by acquiring different context-dependent, higher-order binding properties with specific partners in defined compartments. Complex protein interactions at the synapse—both in *cis* and *trans*—form building modules that instruct the formation of defined synaptic connections, and alternative splicing and postsynaptic modifications have emerged as key mechanisms that increase the ability to build diverse synaptic networks.

In conclusion, a wide diversity of cellular strategies has been implicated in the control of cortical wiring. Increasing evidence shows that specific cell types express distinct genetic programmes of cell-surface molecules. In addition, sorting mechanisms and trans-synaptic molecular interactions allow neurons to specify the development and properties of synapses in distinct subcellular compartments. Although significant progress has been made in our understanding of cortical circuit connectivity, much work will be required to decode the molecular foundations that regulate and specify synaptic assembly.

4. Neuregulin/ErbB4 signalling pathway

> *"The nerve growth-promoting factor is a protein or is bound to a protein."*
>
> Rita Levi-Montalcini observed for the first time the ability of proteins to promote nerve growth. Her outstanding work would precede the explosion of molecular neurobiology to identify proteins with roles in the establishment of synaptic connections between neurons.

This exciting field set off in quest of a map of proteins in the synaptic domain. The early work in the 1980's and 90's led by biochemists, including Pietro De Camilli, Paul Greengard, Eric Kandel, Reinhard Jahn, Thomas Südhof and many others, systematically identified proteins involved in the formation and function of synaptic connections, extending our knowledge on the molecular organisation of the nervous system similar to the detailed anatomical descriptions that Cajal and his disciples reported a century ago.

Neuregulins (Nrg) are a large family of proteins that were first identified for their potent effects in organogenesis, oncogenesis and cellular differentiation, including cardiac development, mammary gland morphogenesis, Schwann cell and oligodendrocyte differentiation, and acetylcholine receptor inducing activity in the neuromuscular junction (Carraway et al., 1997; Chang et al., 1997; Falls et al., 1993; Holmes et al., 1992; Marchionni et al., 1993; Meyer and Birchmeier, 1995; Peles et al., 1992; Wen et al., 1992; Zhang et al., 1997). They activate proteins of the ErbB family of receptors via trans-cellular binding through the EGF-like domain, and both ligands and receptors have high homology with the epidermal growth factor (EGF) and EGF receptor (EGFR) (Burden and Yarden, 1997; Lemke, 1996). Later, a role for neuregulin signalling was discovered at central and peripheral synapses (Huang et al., 2000; Wolpowitz et al., 2000), which spurred further investigations into the intricate functions of neuregulins in synaptogenesis, synaptic plasticity, and neuronal connectivity (Chen et al., 2010; Fazzari et al., 2010; Krivosheya et al., 2008; Li et al., 2007; Ting et al., 2011). In my PhD Thesis, I have studied the role of neuregulins, and underlying molecular mechanisms, in the synaptic integration of neuronal cell types in the cerebral cortex.

4.1. ErbB4 receptor

Molecular and cellular studies first identified the specialized functions of the ErbB4 receptor in cortical development and plasticity, and recent investigations have established its importance for behavioural performance and cognitive function, thus revealing the privileged position that this protein holds in the organisation and function of the cerebral cortex (Mei and Nave, 2014; Rico and Marín, 2011).

The ErbB family of tyrosine kinase receptors is composed of four members of Type I transmembrane proteins (ErbB1-ErbB4) that contain a large extracellular region responsible for ligand binding, a single transmembrane domain, and an intracellular region with kinase activity (Mei and Xiong, 2008) (Figure 7). The extracellular region includes four domains with cysteine-rich sequences, and the intracellular region contains two asymmetric tyrosine kinase domains. Upon neuregulin binding, the extracellular domains undergo major conformational changes that lead to receptor dimerization and, through an allosteric mechanism, activation of the kinase domains by auto- and trans-phosphorylation, which triggers the downstream signalling pathway (Citri and Yarden, 2006; Zhang et al., 2006). This involves cascades of phosphorylation events via, among others, the ERK, PI3K/Akt, and mTOR pathways (Mei and Nave, 2014; Mei and Xiong, 2008). While this represents the canonical pathway of ErbB receptor activation, it has also been shown that ErbB4 can be proteolytically cleaved to release its intracellular domain that is translocated to the nucleus and regulates transcription, establishing a non-canonical forward signalling (Sardi et al., 2006).

Among the four members of the ErbB family, ErbB4 receptor is highly expressed in the brain across developmental and adult stages in a characteristic pattern. First, ErbB4 is selectively expressed by MGE-derived fast-spiking cells and a few other types of interneurons, but not in excitatory pyramidal cells in all mammals studied so far (Fazzari et al., 2010; Vullhorst et al., 2009). More recent studies have also characterised the specific expression of ErbB4 in certain CGE-derived interneurons that express markers such as CCK, VGlut3 and VIP (Batista-Brito et al., 2017; Del Pino et al., 2017). Overall, expression of ErbB4 in cortical circuits is restricted to GABAergic interneurons and follows a cell type-specific pattern.

ErbB4 is precisely targeted to defined synaptic connections in cortical circuits. Electron microscopy proved that ErbB4 is found in both the excitatory

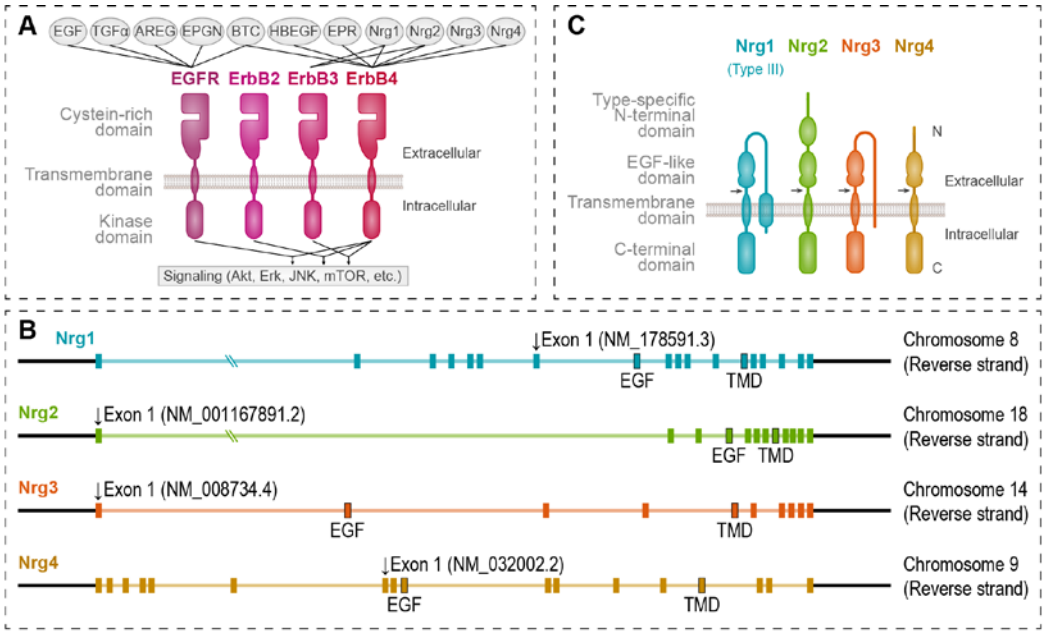

Figure 7 | **Genomic and protein structure of neuregulins and ErbB receptors**.
(**A**) Protein structure of the four members of the ErbB family of tyrosine kinase receptors. (**B**) Genomic sequences of *Nrg1-Nrg4* genes indicating the number of exons of each loci as well as the specific location of the exons encoding for EGF-like domain (EGF) and transmembrane domain (TMD). (**C**) Protein structure of neuregulin proteins.

synaptic inputs that interneurons receive from pyramidal cells as well as the inhibitory boutons that interneurons make onto pyramidal cell bodies, in particular in axo-axonic and somatic boutons from chandelier and CCK basket interneurons (Fazzari et al., 2010; Vullhorst et al., 2009). In the excitatory synapse, ErbB4 is present at the postsynaptic membrane and colocalises with the excitatory synaptic marker PSD95 (Fazzari et al., 2010; Krivosheya et al., 2008; Vullhorst et al., 2009). In the inhibitory synapse, ErbB4 is present at the presynaptic membrane of boutons and colocalises with the inhibitory synaptic markers GAD65 and VGAT, and with CCK in basket terminals (Fazzari et al., 2010; Vullhorst et al., 2009; Woo et al., 2007). Therefore, this paradoxical subcellular targeting of ErbB4 to the pre- and postsynaptic membranes of interneurons suggests a central role for ErbB4 in the afferent/efferent connectivity of these cells.

Genetic manipulations of *ErbB4* in specific interneuron populations result in specific synaptic deficits. It was first identified that genetic deletion of *ErbB4* from interneurons, using the *Dlx5/6-Cre* mouse line, leads to specific inhibitory and excitatory synaptic losses (Fazzari et al., 2010). Subsequent experiments conditionally deleted ErbB4 from MGE-derived interneurons, causing heterogenous deficits in the inhibitory boutons that innervate pyramidal cells (Del

Pino et al., 2013). In addition, both chandelier and basket cells lacking ErbB4 receive fewer excitatory inputs (Del Pino et al., 2013). In a follow-up study, ErbB4 was deleted from CCK+ cells, which represent a population of interneurons that are mainly generated in the CGE and express CB1R in their axon terminals (Eggan et al., 2010; López-Bendito et al., 2004; Morozov et al., 2009; Tricoire et al., 2011); in these conditional mutant mice, CCK+ basket cells form less somatic GABAergic boutons onto pyramidal cells, and receive reduced synapse numbers and weaker excitation (Del Pino et al., 2017). Of note, ErbB4 is abundantly expressed in developing interneurons in the embryo, when it has an important role in controlling migration and final allocation into the nascent cortical circuit (Bartolini et al., 2017; Flames et al., 2004; Marín, 2013). Importantly, the synaptic phenotypes that characterise conditional ErbB4 mutant mice were observed in the hippocampus, where no alteration of interneuron migration or lamination was detected (Del Pino et al., 2013, 2017).

Recent advances in the genetics of neuropsychiatric disorders have suggested an association between *ERBB4* mutations and schizophrenia and intellectual disability (Kasnauskiene et al., 2013; Mei and Nave, 2014; Walsh et al., 2008). Remarkably, further studies in animal models have shed light on the significance of this genetic association to behavioural dysfunction in disease. On the one hand, mice lacking *ErbB4* from fast-spiking interneurons show altered gamma-band oscillations and synchrony between hippocampus and prefrontal cortex, and heterogenous defects in locomotion, social and cognitive behaviours (Del Pino et al., 2013). On the other hand, mice lacking *ErbB4* from CCK+ interneurons show reduced oscillatory activity in the theta-band, disrupted place cell firing, and altered spatial representation (Del Pino et al., 2017). In conclusion, these results demonstrate that ErbB4 plays a central role in cortical development and function.

4.2. Neuregulin family

Neuregulins are encoded in four different genes (*Nrg1-Nrg4*) that generate a diverse range of protein isoforms through alternative splicing. Despite this diversity, all neuregulin proteins are type I transmembrane proteins that contain an amino (N-) terminal domain, an EGF-like domain, a single transmembrane, and a carboxy (C-) terminal domain (Mei and Nave, 2014; Mei and Xiong, 2008) (Figure 7). The

N-terminal domain is probably the most diverse region among neuregulins, and varies the most in the different isoforms of Nrg1, which can be subclassified in six isoform classes (type I-type VI). Types I, II, IV, and V isoforms contain an immunoglobulin (Ig)-like domain upstream of the EGF-like domain, with varying type-specific sequences in the N-terminal; type III isoforms contain a cysteine-rich domain (CRD); and type IV lacks Ig-like domain and CRD. The EGF-like domain, which interacts with the receptor trans-synaptically, constitutes a relatively short amino acid region with high sequence homology between neuregulin members. Most neuregulins are synthesized as precursor proteins (called pro-Nrg) and require proteolytic processing in cleavage sites located at the juxtamembrane region upstream of the transmembrane domain to acquire the mature stage. This allows the EGF-like domain to become available for receptor binding. In the case of both Nrg1 CRD (type III) isoform and Nrg3, their N-terminal domains harbour a stretch of hydrophobic amino acids conforming a second transmembrane domain that anchors the EGF-like domain to the membrane after cleavage of the unprocessed forms of the proteins (Vullhorst et al., 2017). On the other hand, the C-terminal domain represents a large portion of the mature neuregulin protein, but little is known about its physiological roles. In the case of Nrg1, some studies have reported essential roles for the C-terminal domain in the processing of the mature protein (Hartmann et al., 2015; Liu et al., 1998; Parra et al., 2015), as well as functioning in backward signalling to the nucleus after cleavage in the membrane (Bao et al., 2003, 2004).

Since their discovery, neuregulin expression was found to be enriched in the nervous system, both during development and in the adult (Carraway et al., 1997; Chang et al., 1997; Zhang et al., 1997). Of note, Nrg1 (type III isoform) and Nrg3 mRNA transcripts are abundantly expressed in the cerebral cortex during postnatal development, the period in which synaptogenesis begins (Fazzari et al., 2010; Rahman et al., 2018). In contrast, Nrg2 shows higher levels of expression at later adult stages and is enriched in the cerebellum (Carraway et al., 1997; Chang et al., 1997; Longart et al., 2004), whereas Nrg4 appears to be scarcely expressed in the cortex (Paramo et al., 2018).

During neocortical development, Nrg1 and Nrg3 play important roles in the formation of the architecture of neuronal circuits. First, Nrg1 functions as an attractor factor for the migration of cortical GABAergic interneurons from the ganglionic eminences (Flames et al., 2004). Second, Nrg3 controls the correct lamination of GABAergic interneurons in the cortex (Bartolini et al., 2017).

Therefore, interneuron-pyramidal cell circuits rely on Nrg1 and Nrg3 signalling during embryonic and early postnatal development to generate the appropriate cytoarchitecture in the cerebral cortex. Based on their still abundant expression at later developmental and adult stages, Nrg1 and Nrg3 could function in cortical synaptic assembly.

Developmental and activity-dependent regulation of gene expression unfolds molecular mechanisms that guide the assembly of neuronal circuits (Bloodgood et al., 2013; Favuzzi et al., 2019; Hrvatin et al., 2018; Stroud et al., 2020). Notably, Nrg3 expression has been shown to undergo a developmental increase from prenatal to adult stages (Grieco et al., 2020; Rahman et al., 2018), and Nrg1 expression peaks at 4 weeks of postnatal development specifically in PV+ cells, followed by low expression levels in the adult cortex (Grieco et al., 2020; Sun et al., 2016). In the mouse visual cortex, it has been shown that monocular deprivation during a developmental critical period downregulates Nrg1 expression in PV+ interneurons and leads to impaired excitatory inputs, indicating that sensory experience has a dramatic effect on how Nrg1 signalling modulates the wiring of cortical circuits (Sun et al., 2016). In addition, the secreted Nrg1 type I isoform shapes cortical connectivity during the first two weeks of postnatal development, a temporal window in which local GABAergic, transient circuits play a major role in the maturation of thalamocortical circuits (Anastasiades et al., 2016; Marques-Smith et al., 2016). Specifically, Nrg1 overexpression has a detrimental impact on transient connections from L5b SST+ interneurons onto stellate spiny neurons, which results in a delay in the formation of thalamic inputs onto recipient cortical neurons (Marques-Smith et al., 2016). Altogether, neuregulin expression is finely regulated at developmental stages and during critical periods of plasticity by sensory experience. These findings highlight the relevance of neuregulin signalling in ensuring the normal development of cortical connectivity in a timely coordinated manner, and suggests that activity-dependent mechanisms could contribute to these processes. It is yet unclear whether cortical activity might influence the function, targeting, and processing of distinct neuregulin isoforms at the synapse, and how this regulation could impact the formation and plasticity of circuits.

In the adult, constitutive *Nrg3* knock-out mice have a loss of excitatory synapses targeting PV+ interneurons in the hippocampus (Müller et al., 2018). Nrg3 is found in excitatory synapses at the presynaptic membrane *in vitro* and *in vivo* (Müller et al., 2018; Vullhorst et al., 2017). Nrg1 appears to colocalise with excitatory synapses *in vitro* in a similar pattern (Ting et al., 2011; Vullhorst et al.,

2017), and gain- and loss-of-function models of Nrg1 disrupt synaptic plasticity in the hippocampus (Agarwal et al., 2014). *In vitro*, treatment of neuronal cultures with recombinant peptide containing the EGF-like domain of Nrg1 induces excitatory synapse development (Ting et al., 2011). Moreover, infusion of exogenous polypeptide containing the EGF-like domain of Nrg1 intracerebrally in mice represses epileptogenic activity by regulating PV+ interneuron excitability (Li et al., 2011; Tan et al., 2011). Due to their structural similarities and overlapping expression patterns *in vitro*, it has been hypothesized that Nrg1 and Nrg3 cooperate in the regulation of synaptic connectivity (Müller et al., 2018). However, how Nrg1 and Nrg3 could mediate ErbB4-dependent synaptic functions in cortical circuits during postnatal development remains unclear.

The general importance of neuregulins in synapse development is well established. Current data suggest that different neuregulin proteins similarly control synaptic connections in central neurons, a perplexing idea given the great diversity of neuregulin genes and isoforms. Do neuregulins redundantly regulate pyramidal cell-interneuron assembly in the cerebral cortex *in vivo*? How is neuregulin expression in pyramidal cells organised to ensure the interaction through ErbB4 receptor in distinct interneuron types? Do specific neuregulin members establish a specific pattern of subcellular distribution in cortical developing circuits? Despite the general homology of protein domains between neuregulin members, large structural differences at the amino acid level suggest specific functions for distinct domains or motifs. Indeed, a large evolutionary divergence of neuregulin genes is apparent in vertebrate lineages (Chou and Ozaki, 2010). At present, apart from the transcellular binding of the EGF-like domain to ErbB receptors, there is no evidence for physiological functions attributed to extracellular or cytoplasmic domains of neuregulins. Uncovering these unsolved questions will not only provide novel insight into fundamental mechanisms of neuregulin/ErbB4 function in circuit assembly, but also shed light into the molecular determinants that instruct the formation and specificity of synaptic connectivity in the cerebral cortex. Despite two decades of research in Nrg/ErbB4 signalling in synaptogenesis, much remains to be learned.

OBJECTIVES

In my PhD project, I have researched the organisation and mechanisms of neuregulin function in cortical circuit assembly during postnatal development. The objectives of this thesis are outlined here, and constitute the three chapters of results:

Aim 1. To study the function of Nrg1 and Nrg3 in the synaptic assembly of pyramidal cell-interneuron circuits in the mouse cerebral cortex.

Aim 2. To analyse the subcellular distribution of Nrg1 and Nrg3 in cortical pyramidal cells *in vivo*.

Aim 3. To investigate the underlying mechanisms of synaptic sorting and function of Nrg1 and Nrg3 by exploring the structural determinants that mediate and specify neuregulin function in cortical pyramidal cells.

MATERIALS & METHODS

1. Generation of inducible conditional knock-out mice for *Nrg1* and *Nrg3*

To generate mouse models for inducible conditional deletion of *Nrg1* or *Nrg3* specifically in pyramidal cells during postnatal development, we designed the following breeding strategy (Figure 8). Our knock-out strategy targeted pyramidal cells in superficial and deep cortical layers, and synaptic analysis were focused in L2/3 to be consistent with the targeted population in gain-of-function experiments via *in utero* electroporation. To generate inducible conditional (icKO) mice, we crossed the following mouse lines: *Nex-Cre*^{ERT2} (*Neurod6*$^{tm2.1(cre/ERT2)Kan}$) (Agarwal et al., 2012), *Nrg1*^{floxed} (*Nrg1*^{tm3Cbm}) (Yang et al., 2001), *Nrg3*^{floxed} (*Nrg3*$^{tm1a(KOMP)Mbp}$) (Bartolini et al., 2017), and *RCL*^{tdT} (*Gt(ROSA)26Sor*$^{tm9(CAG-tdTomato)Hze}$) (Madisen et al., 2010), to generate mice carrying three alleles. Initially, we crossed mice carrying floxed alleles for *Nrg1* (*Nrg1*^{floxed}) or *Nrg3* (*Nrg3*^{floxed}) with either pyramidal cell-specific Cre-driver mice (*Nex-Cre*^{ERT2}) or tdT-reporter mice (*RCL*^{tdT}). After the generation of mice heterozygous for neuregulin-floxed alleles (*Nrg1*^{floxed} or *Nrg3*^{floxed}) and homozygous for either the Cre-driver allele (*Nex-Cre*^{ERT2}) or the reporter allele (*RCL*^{tdT}), we crossed these mouse lines carrying two alleles in order to generate wild-type (*Nrg*$^{+/+}$, 1/4 ratio), heterozygous (*Nrg*$^{F/+}$, 2/4 ratio) and homozygous (*Nrg*$^{F/F}$, 1/4 ratio) mice for *Nrg1* or *Nrg3* that are also heterozygous for both the Cre-driver allele (*Nex-Cre*^{ERT2}) and the reporter allele (*RCL*^{tdT}) (Figure 8). Quantification of the density of tdTomato+ cells was conducted to analyse the pattern of recombination across animals and genotypes. We included mice from at least three different litters, and the cell counting was performed in the same anatomical regions in L2/3 of the somatosensory cortex to be able to compare across mice and litters; notably, tamoxifen injection (see below) in pups at P0 resulted in a recombination pattern at P30 that was consistent across genotypes (Figure 8D). Mice were ear-tagged with identifier codes; downstream analysis of synapse and cell density were performed blind to genotype, and identifier codes were used to annotate brain samples to the corresponding genotype. All animals were maintained in a C57BL/6J background (Jackson Laboratories, #000664).

Mice were maintained under standard, temperature controlled, laboratory conditions, and were housed in groups of up to five littermates per cage after weaning. Genotyping of the litter was performed prior to the experiment procedure to cull off mice of unwanted genotype. Mice were kept on a 12:12 light/dark cycle

and received food and water ad libitum. All animal procedures were approved by the ethical committee (King's College London) and conducted in accordance with European regulations, and Home Office personal and project licenses under UK Animals (Scientific Procedures) 1986 Act.

The following primer sequences were used for routine genotyping: *Nex-Cre^{ERT2}* (5' - GAGTCCTGGAATCAGTGTTTTTC - 3'; 5' - AGAATGTGGAGTAGGGTGAC - 3'; 5' - CCGCATAACCAGTGAAACAG - 3'), *Nrg1^{floxed}* (5' - TCCTTTTGTGTGTTCAGCACCGG - 3'; 5' - GCACCAAGTGGTTGCGATTGTTGCT - 3'), *Nrg3^{floxed}* (5' - AGAGGGAGAATGGAAAACAATGAGC - 3'; 5' - AGATGCCAGTGTCTCTTGTTTAGGG - 3'), and *RCL^{tdT}* (5' - AAGGGAGCTGCAGTGGAGTA - 3'; 5' - CCGAAAATCTGTGGGAAGTC - 3'; 5' - GGCATTAAAGCAGCGTATCC - 3'; 5' - CTGTTCCTGTACGGCATGG - 3').

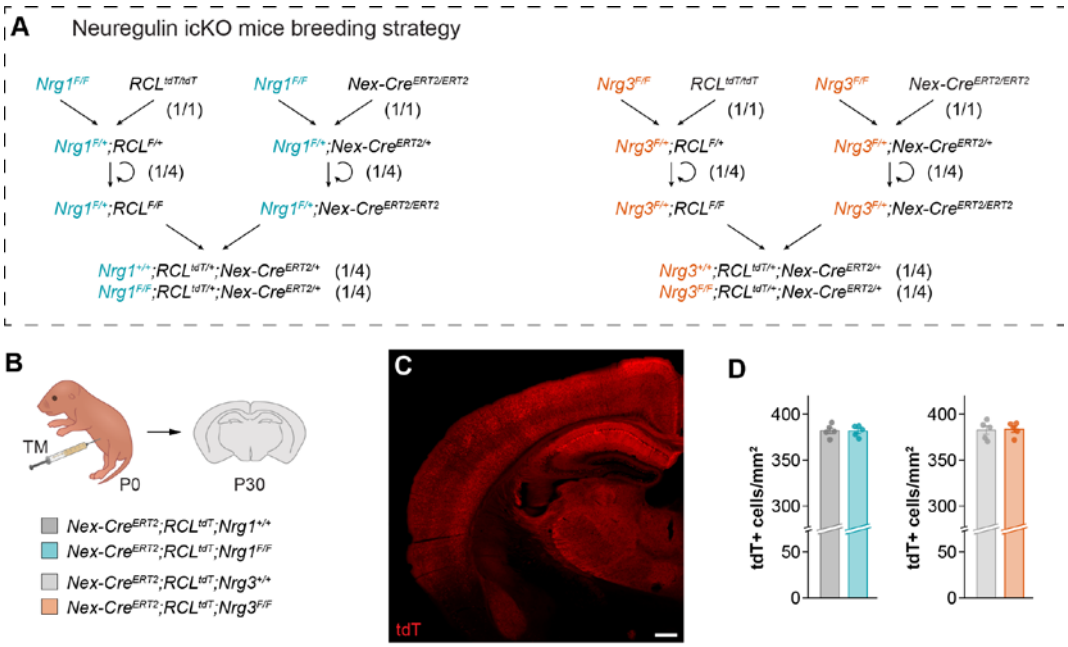

Figure 8 | **Generation of inducible conditional knock-out mice for *Nrg1* and *Nrg3*.** (**A**) Schematics of breeding scheme to generate inducible conditional knock-out (icKO) mice carrying three alleles. (**B**) Conditional deletion of *Nrg1* and *Nrg3* was achieved by tamoxifen (TM) injection in newly born pups at P0. (**C**) Expression of tdTomato in the cerebral cortex of *Nex-Cre^{ERT2};RCL^{tdT}* mice at P30 following tamoxifen injection at P0 illustrates the extent of genetic recombination. (**D**) Quantification of the density of tdTomato+ pyramidal cells at P30. Two-tailed Student's t-tests. For *Nex-Cre^{ERT2};RCL^{tdT};Nrg1^{F}*, $P = 0.929$; n = 5 mice (18 regions of interest, ROIs) for controls and 5 mice (18 ROIs) for mutants. For *Nex-Cre^{ERT2};RCL^{tdT};Nrg3^{F}*, $P = 0.869$; n = 5 mice (18 ROIs) for controls and 5 mice (18 ROIs) for mutants.
Data are shown as mean ± s.e.m. Scale, 400 µm.

2. Tamoxifen injection

Tamoxifen (Sigma-Aldrich, Cat# 85256) was dissolved in corn oil (Sigma-Aldrich, Cat# C8267) (10 mg/ml) at 37°C with constant agitation. Tamoxifen at a dose of 1 mg/10 g of body weight was administered via intragastric injection into P0 postnatal *Nex-Cre*$^{ERT2/+}$*;RCL*$^{tdT/+}$*;Nrg1*$^{F/F}$ or *Nex-Cre*$^{ERT2/+}$*;RCL*$^{tdT/+}$*;Nrg3*$^{F/F}$ mouse pups, and the control littermates (*Nex-Cre*$^{ERT2/+}$*;RCL*$^{tdT/+}$*;Nrg1*$^{+/+}$ or *Nex-Cre*$^{ERT2/+}$*;RCL*$^{tdT/+}$*;Nrg3*$^{+/+}$, respectively), to conditionally knock-out the corresponding Nrg gene in cortical pyramidal cells during postnatal development.

3. Generation of DNA constructs

Neuregulin constructs (Nrg) were generated by standard molecular biology procedures (Figure 9). Due to the high guanine/cytosine (G/C) content and a very low efficiency in PCR amplification of Nrg sequences, plasmids that contain inserts encoding for wild-type and mutant proteins of Nrg1 and Nrg3 harbouring an HA tag epitope were designed and produced using the Invitrogen GeneArt Gene Synthesis platform (Thermo Fisher Scientific). We used the DNA sequences of the predominant isoforms for *Nrg1* (GenBank: 178591, Ensembl Transcript ID: ENSMUST00000073884.5) and *Nrg3* (GenBank: NM_008734, Ensembl Transcript ID: ENSMUST00000166968.8). The Nrg sequences lacked the 5'- and 3'-untranslated regions (UTR) and were preceded by the Kozak consensus sequence. The different Nrg inserts were cloned into an expression vector plasmid containing the synapsin promoter (*pSyn*) using standard molecular biology procedures; namely, restriction digestion with restriction enzymes, DNA band purification from agarose gel, ligation of digested plasmids of sticky ends, transformation into competent *E. coli* bacterial cells, and plasmid production and purification (QIAGEN Plasmid Mini Kit, Cat# 12123; and QIAGEN Plasmid Midi Kit, Cat# 12143). The restriction sites NotI/EcoRI were used to clone the different Nrg inserts into the expression vector plasmids. These vector plasmids contained an additional *pSyn* promoter followed by a green fluorescent protein (GFP) as a reporter to label the electroporated cells (Gascón et al., 2008). For control experiments, we used the *pSyn-Gfp* plasmid lacking any Nrg insert.

To identify the subcellular localisation of neuregulins, constructs harboured a human influenza hemagglutinin (HA) epitope tag upstream of the EGF-like domain (exon 2). It has been previously reported that this tag insertion site in Nrg loci does not alter their function (Wang et al., 2001). The HA tag was inserted between amino acids 222 (Leucine, L) and 223 (Serine, S) for Nrg1 protein, and between amino acids 277 (Histidine, H) and 278 (Threonine, T) for Nrg3 protein. In a separate set of experiments aiming to identify the subcellular localisation of the intracellular domain of Nrg1, the HA tag was inserted after amino acid 700 (Valine, V) of Nrg1 protein, right upstream of the STOP codon.

For EGF-like domain replacement experiments, the chimeric neuregulins were generated by swapping the EGF-like domain of a neuregulin member by the corresponding domain from its homologous gene. First, the EGF-like domain of Nrg1 (amino acids 223 to 286, corresponding to exons 2 and 3) was replaced by

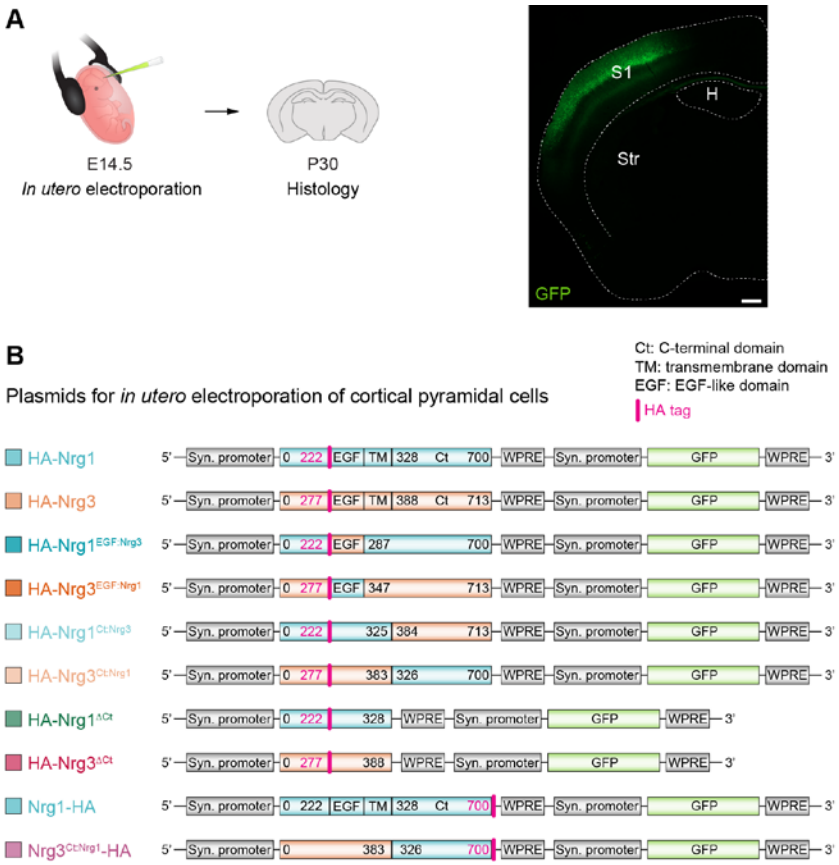

Figure 9 | **Plasmids encoding for wild-type and mutant neuregulin proteins used for *in utero* electroporation experiments of cortical pyramidal cells.**
(**A**) Schematics of experimental design (left), and coronal section of mouse brain that illustrates the expression of GFP in a typical experiment (right). (**B**) Diagrams of the structure of plasmids used in these experiments; numbers indicate the amino acid positions. Scale, 400 µm.

the EGF-like domain of Nrg3 (amino acids 278 to 346, corresponding to exons 2 and 3); this chimeric protein was named Nrg1$^{EGF:Nrg3}$. Second, the EGF-like domain of Nrg3 (amino acids 278 to 346) was replaced by the EGF-like domain of Nrg1 (amino acids 223 to 286); this chimeric protein was named Nrg3$^{EGF:Nrg1}$.

For C-terminal domain replacement experiments, the chimeric neuregulins were generated by swapping the C-terminal domain of a neuregulin member by the corresponding domain from its homologous gene. First, the C-terminal domain of Nrg1 (amino acids 326 to 700, corresponding to exons 6-9) was replaced by the C-terminal domain of Nrg3 (amino acids 384 to 713, corresponding to exons 6-10); this chimeric protein was named Nrg1$^{Ct:Nrg3}$. Second, the C-terminal domain of Nrg3 (amino acids 384 to 713) was replaced by the C-terminal domain of Nrg1 (amino acids 326 to 700); this chimeric protein was named Nrg3$^{Ct:Nrg1}$.

For C-terminal domain lacking experiments, the mutant neuregulins were generated by deleting the C-terminal domain of each neuregulin member. First, the C-terminal domain of Nrg1 (amino acids 326 to 700) was deleted, and a stop codon was inserted after amino acid 325 (Valine, V); this mutant protein was named Nrg1ΔCt. Second, the C-terminal domain of Nrg3 (amino acids 384 to 713) was deleted, and a stop codon was inserted after amino acid 383 (Valine, V); this mutant protein was named Nrg3ΔCt.

4. CRISPR/Cas9-mediated endogenous protein tagging

CRISPR/Cas9-mediated homology-directed repair (HDR) was used for single-cell labelling of endogenous proteins *in vivo* (Mikuni et al., 2016) (Figure 10). For custom single-guide RNA (sgRNA) design, we used the following web-based tools: WTSI Genome Editing (https://wge.stemcell.sanger.ac.uk/) and Zhang's lab website (https://zlab.bio/guide-design-resources). The 20-base sequences which precede a 5'-NGG protospacer-adjacent motif (PAM) sequence were selected to induce DNA double-stranded breaks within 10 bp from the tag insertion sites. The N- and C-terminus regions of Nrg1 and Nrg3 loci were selected as insertion sites for a single HA tag sequence (TACCCCTACGACGTGCCCGACTACGCC), as recommended previously (Mikuni et al., 2016). The sgRNAs were cloned into the human codon-optimised *S. pyogenes* Cas9 (*SpCas9*) and EGFP expression plasmid (*pSpCas9(BB)-2A-GFP*, pX458, Addgene Plasmid #48138) (Ran et al.,

2013). For each sgRNA, a pair of complementary oligos (20 nucleotides, nt) encoding for the target genomic locus were annealed and ligated into the sgRNA scaffold of the pX458 plasmid using the BbsI restriction site. We generated between 2-4 sgRNAs per insertion site for testing of gene editing efficiency. For homologous recombination-dependent knock-in, we designed single-stranded oligodeoxynucleotides (ssODNs) containing the HA tag (27 base pairs, bp) sequence flanked by sequences of ~80-90 bp on each side that were homologous to the target genomic region. To design the homologous arms to the genomic loci, We used the following reference DNA sequences: *Nrg1* (GenBank: 178591, Ensembl Transcript ID: ENSMUST00000073884.5) and *Nrg3* (GenBank: NM_008734, Ensembl Transcript ID: ENSMUST00000166968.8).

The following sgRNAs were used for gene editing:

Nrg1 (N-terminal): CCTTCTGGAGGTGATCCGGA TGG (Fw)

Nrg1 (N-terminal): CCATCCGGATCACCTCCAGA AGG (Rv)

Nrg1 (N-terminal): CGGGCCTTCTGGAGGTGATC CGG (Fw)

Nrg1 (N-terminal): CTGGGGGATAAATCTCCATC CGG (Rv)

Nrg1 (C-terminal): TTTATACAGCAATAGGGTCT TGG (Rv)

Nrg1 (C-terminal): TTAGGTTTTATACAGCAATA GGG (Rv)

Nrg1 (C-terminal): TTTAGGTTTTATACAGCAAT AGG (Rv)

Nrg3 (N-terminal): GAAGGTGAAGATCGGCTCCT TGG (Fw)

Nrg3 (N-terminal): CGGCTCCTAGGATGAGTGAA GGG (Fw)

Nrg3 (N-terminal): AGGATGAGTGAAGGGGCGGC CGG (Fw)

Nrg3 (C-terminal): GAAGGTGAAGATCGGCTCCT TGG (Fw)

Nrg3 (C-terminal): CGGCTCCTAGGATGAGTGAA GGG (Fw)

(Note that ‘Fw’ (forward) and ‘Rv’ (reverse) indicate the strand of the genomic region targeted by each sgRNA.)

The ssODN sequences used for HDR were as follows (5’-3’; HA tag sequence in lower case):

Template for HA tag integration in N-terminal of Nrg1 locus:

CCTTCAAGATGCTGTATCATTTGGTTGGGGGGAGCTCTGCATGGTAATGCA
CTGTGAGAGAGGCCGGGCCTTCTGGAGGTGATCCGGATGtacccatacgatgttcc
agattacgctGAGATTTATCCCCCAGACATGTCTGAGGGAGCTGGCGGGAGGTC
CTCCAGCCCCTCCACTCAGCTGAGTGCAGACCCATCTCTCGATGGGC

Template for HA tag integration in C-terminal of Nrg1 locus:

GCAGGACTAACCCAGCAGGCCGCTTCTCCACACAGGAAGAATTACAGGCCA
GGCTGTCTAGTGTAATCGCTAACCAAGACCCTATTGCTGTAtacccatacgatgttcc
agattacgctTAAAACCTAAATAAACACATAGATTCACCTGTAAAACTTTATTTTAT
ATAATAAAGTATTTCACCTTAAATTAAACAATTTATTTTATTTTAGC

Template for HA tag integration in N-terminal of Nrg3 locus:

CGCCCGCGCCCGGCCCGCGCGGCCCCATGCCTCTGGCGCGGCCCTCGGG
GGGGCGAAGGTGAAGATCGGCTCCTAGGATGtacccatacgatgttccagattacgctAG
TGAAGGGGCGGCCGGTGCCTCGCCACCTGGTGCCGCTTCGGCAGCCGCC
GCCTCAGCCGAGGAGGGCACCGCGGCGGCTGCGGC

Template for HA tag integration in C-terminal of Nrg3 locus:

CTTTCTCCCCCTGAGTCCCACGGCCAAATCAGAACGAGAGGCACAATTTGT
CTTAAGAAATGAAATACAAAGAGACTCTGTGCTAACCAAGtacccatacgatgttcca
gattacgctTGACTGGAAATGTAGGAATCTGTGCATTCTATGCTTTGCTCAACAG
GAAGGAGAGGAAATTAAATACAAATTATTTATATGC

5. Cell culture, transfection, and functional validation

N2a cells were cultured in D10 medium supplemented with 10% (vol/vol) FBS at 37°C and 5% CO2. Prior to sgRNA and ssODN design, the genomic DNA of N2a cells was harvested and sequenced (Sanger Sequencing Service, Source BioScience) to validate the absence of any nucleotide change in the target insertion region.

To detect insertion/deletion (indel) mutations in cells transfected with plasmid containing sgRNA and Cas9, T7 endonuclease-based mutation detection protocol was used. First, genomic DNA was harvested from transfected cells using GeneJET Genomic DNA Purification Kit (Thermo Fisher Scientific, Cat# K0721). Custom designed primers were used to amplify the region of interest from the

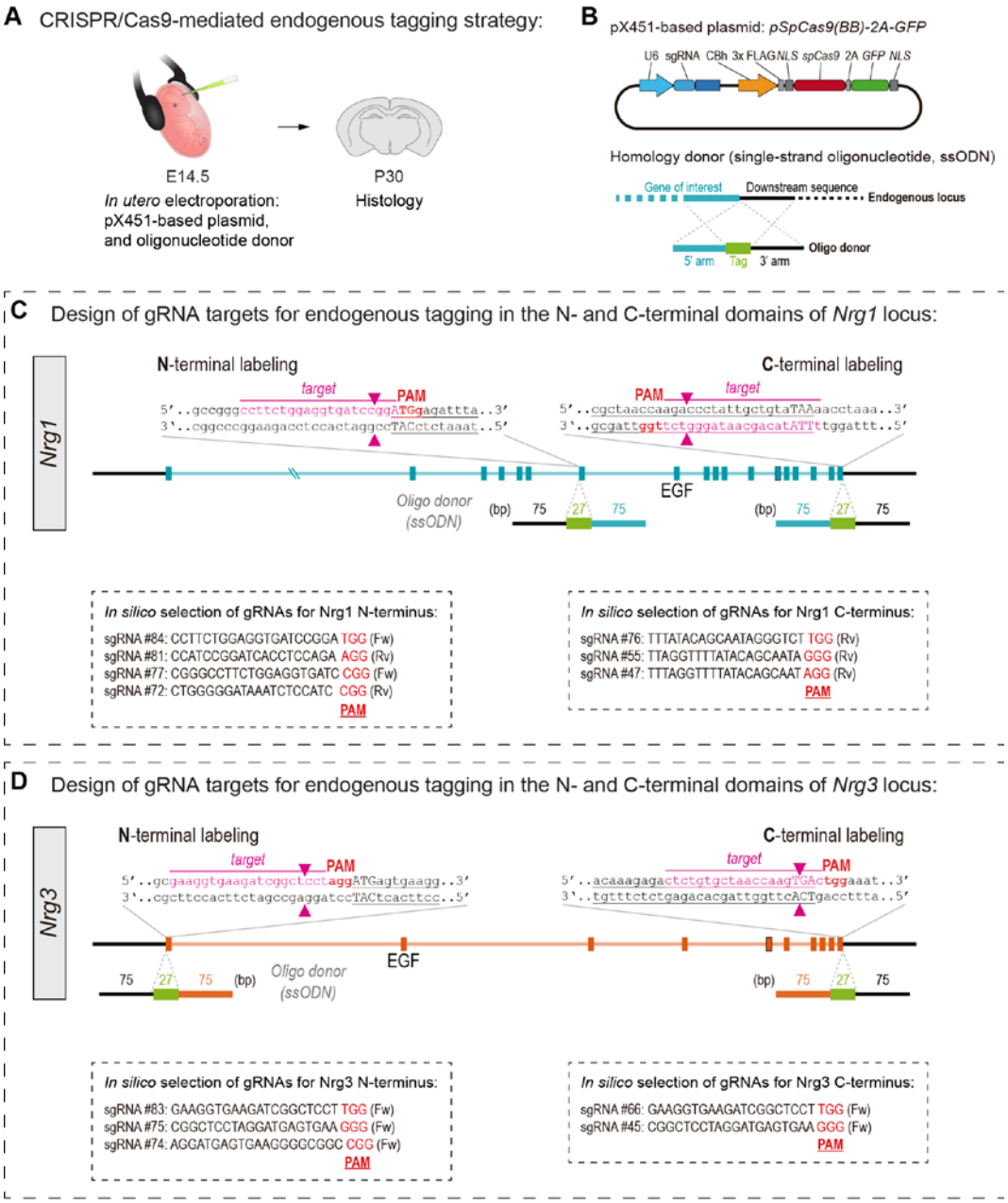

Figure 10 | **Design of a CRISPR/Cas9, homology recombination-based strategy for tagging the endogenous *Nrg1* and *Nrg3* loci in the mouse brain *in vivo*.**
(**A**) Schematics of experimental design. CRISPR/Cas9 constructs were electroporated into pyramidal cell progenitors in the mouse embryo at E14.5, and histology was performed at P30 to detect for GFP and HA labelling. (**B**) Constructs used for CRISPR/Cas9-mediated gene editing. (**C-D**) Representation of genomic loci of *Nrg1* and *Nrg3* to indicate the regions in the N- and C-terminal of both genes targeted by the designed sgRNA. The numbers indicated for each sgRNA represent the relative DNA cutting efficiencies as determined in a web-based sgRNA design tool (https://zlab.bio/guide-design-resources).

harvested genomic DNA. After gel purification of the band with proper size (Nrg1-Nt: 703 bp, Nrg1-Ct: 685 bp, Nrg3-Nt: 644 bp, Nrg3-Ct: 736 bp) (QIAQuick

purification kit, Cat# 28706), DNA heteroduplex formation was achieved by an annealing reaction with gradually decreasing temperatures (95°C to 20°C, in a gradient of -2°C/s). The heteroduplex products were subjected to T7 endonuclease digestion (New England Biolab, Cat# E3321), and the result was visualised on a 2% (wt/vol) agarose gel.

6. *In utero* electroporation

CD-1 (Crl:CD1(ICR)) mice (Charles River, #022) were used for *in utero* electroporation (IUE) experiments. Animals were housed and maintained in the same conditions as described for icKO mice. Timed-pregnant females were deeply anesthetized with isoflurane (Piramal Critical Care Limited). Buprenorphine (Vetergesic, Ceva Animal Health Ltd) was administered for analgesia via subcutaneous injection, and ritodrine hydrochloride (Sigma-Aldrich, Cat# R0758) was applied to the exposed uterine horns to relax the myometrium. DNA solution was mixed with Fast Green (Roche, Cat# 06402712001), and 1-2 µl of solution was injected into the lateral ventricle of embryos at E14.5. Forceps-shaped electrodes (CUY650P3, Nepa Gene) connected to an electroporator (NEPA21 Super Electroporator, Nepa Gene) were used to deliver five electric pulses (45 V for 50 ms, with 950 ms intervals). The electrodes were positioned to target cortical pyramidal cell progenitors in the subventricular zone.

For IUE in exogenous expression experiments, Nrg expression plasmids or control plasmids were used at a concentration of 1 µg/µl. For IUE in endogenous tagging experiments, the plasmid encoding for Cas9 and sgRNA (pX458-derivatives) and ssODN for HDR were used at a final concentration of 1 µg/µl and 20 µM, respectively.

7. Histology and immunohistochemistry

Mice were deeply anesthetized with pentobarbital sodium (Euthatal, Merial Animal Health Ltd) by intraperitoneal injection, and transcardially perfused with sodium chloride solution (Sigma-Aldrich, Cat# S76530) followed by 4% paraformaldehyde (PFA) (Sigma-Aldrich, Cat# 441244) in phosphate-buffered saline (PBS).

Dissected brains were post-fixed for 2h in 4% PFA at 4°C, cryoprotected first in 15% sucrose (Sigma-Aldrich, Cat# S0389) in PBS overnight and then in 30% sucrose in PBS, and cut frozen on a sliding microtome (Leica SM2010 R) at 40 µm. Free-floating brain slices were permeabilized with 0.2% Triton X-100 (Sigma-Aldrich, Cat# T8787) in PBS for 1h, and blocked for 2h in a solution containing 0.3% Triton X-100, 1% serum, and 5% bovine serum albumin (BSA) (Sigma-Aldrich, Cat# A8806). Then, brain slices were incubated overnight at 4°C with primary antibodies. The next day, the tissue was repeatedly rinsed in PBS and incubated with secondary antibodies for 2h at room temperature. When required, brain slices were counterstained with 5 µM 4',6-diamidine-2'-phenylindole dihydrochloride (DAPI) (Sigma-Aldrich, Cat# D9542) in PBS. All primary and secondary antibodies were diluted in 0.3% Triton X-100, 1% serum, and 2% BSA. The following primary antibodies were used at the indicated concentrations: chicken anti-parvalbumin (1:500, Synaptic Systems, #195 006), goat anti-CB1 (1:400, Frontier Institute, #CB1-Go-Af450), goat anti-Nrg3 (1:500, Neuromics, #GT15220), guinea pig anti-VGlut1 (1:2000, Merck Millipore, #AB5905), mouse IgG2a anti-GAD65 (1:500, Merck Millipore, #MAB351R), mouse IgG2a anti-GAD67 (1:5,000, Merck Millipore, #MAB5406), mouse IgG1 anti-gephyrin (1:500, Synaptic Systems, #147 011), mouse anti-HA (1:500, BioLegend, #901502), mouse anti-PSD95 (1:500, NeuroMab, #70-028), mouse IgG2a anti-Synaptotagmin-2 (1:250, ZFIN, #ZDB-ATB-081002-25), rabbit anti-DsRed (1:500, Clontech, #632496), rabbit anti-HA (1:500, Cell Signaling Technology, #3724), rabbit anti-Nrg1 (1:500, Abcam, #ab23248), rabbit anti-parvalbumin (1:2,000, Swant, #PV27), and rabbit anti-pIκBα (1:200, Cell Signaling Technology, #2859). The following secondary antibodies were used at the indicated concentrations: donkey anti-chicken-DyLight 405 (1:200, Jackson ImmunoResearch Europe Ltd., #703-475-155), donkey anti-guinea pig-Alexa 647 (1:250, Jackson Immuno-Research Europe Ltd., #706-605-148), donkey anti-goat-Alexa 647 (1:400, Molecular Probes, #A-21447), donkey anti-mouse-Alexa 488 (1:200, Molecular Probes, #A-21202), donkey anti-rabbit-Alexa 647 (1:500, Molecular Probes, #A-31573), donkey anti-rabbit-Cy3 (1:500, Jackson ImmunoResearch Europe Ltd., #711-165-152), goat anti-chicken-Alexa 488 (1:600, Molecular Probes, #A-11039), goat anti-mouse IgG1-Alexa 488 (1:500, Molecular Probes, #A-21127), goat anti-mouse IgG1-Alexa 555 (1:500, Molecular Probes, #A-21240), goat anti-mouse IgG2a-Alexa 647 (1:500, Molecular Probes, #A-21241), biotinylated goat anti-rabbit (1:200, Vector Laboratories, #BA-1000), biotinylated goat anti-rat (1:200, Vector Laboratories, #BA-9400), biotinylated horse anti-mouse (1:200, Vector

Laboratories, #BA-2000), biotinylated rat anti-mouse IgG1 (1:200, BioLegend, #406603), streptavidin-Alexa 488 (1:400, Thermo FIsher Scientific, #S11223), streptavidin-Alexa 555 (1:400, Thermo Fisher Scientific, #S32355), streptavidin-Alexa 647 (1:200, Jackson ImmunoResearch Europe Ltd., #016-600-084), and streptavidin-DyLight 405 (1:400, Jackson ImmunoResearch Europe Ltd., #016-470-084).

8. Single-molecule fluorescent *in situ* hybridisation

Mice were perfused as described above, and brains were postfixed overnight in 4% PFA in PBS followed by cryoprotection, first in 15% sucrose-RNase free PBS overnight, and then in 15% sucrose-RNase free PBS. Brains were sectioned frozen on sliding microtome at 30 µm. Fluorescent *in situ* hybridization on brain slices was performed according to manufacturer's protocol (ACDBio, RNAscope Multiplex Fluorescent Assay v2, Cat# 323110). The following probes from the RNAscope catalogue were used: Nrg1-C3 (ACDBio, Cat# 418181), and Nrg3-C1 (ACDBio, Cat# 441831).

9. Image acquisition and image analysis

Images were acquired at 1,024 x 1,024 pixel resolution in an inverted Leica TCS-SP8 confocal microscope. Imaging for cell density and synapse density analyses was performed at 8-bit depth, and imaging for subcellular compartment analysis was performed at 12-bit depth. Tile scan images of brain slices were acquired in a ZEISS Apotome.2. Samples from the same experiment were imaged and analysed in parallel, using the same laser power, photomultiplier gain and detection filter settings.

For subcellular compartment analysis, images were acquired with 20X/0.50 (Magnification/Numerical Aperture) objective, and 0.75 digital zoom at 200 Hz acquisition speed. Analysis of HA-tagged neuregulin localisation in somas and neuropil was performed in Matlab (MathWorks), using a script written by Elisa F. Maraver, a former Erasmus student in our group. First, single-channel images positive for GFP, corresponding to pyramidal cell bodies, were normalised to a

reference image by using a histogram matching function to allow the detection of soma and neuropil across samples using intensity-based thresholding with the same parameters. Images from the same experiment were normalised to the same reference image. For somatic compartment analysis, pyramidal cell somas—that show higher intensity of GFP+ signal compared to neuropil—were masked using a low threshold. Masks of neuregulin expression in somas were generated by thresholding of single-channel images positive for HA. The GFP+ and HA+ masks were merged, and the number of GFP-masked somas containing HA+ signal was automatically quantified. Somatic neuregulin expression was represented as the percentage of HA/GFP double-positive somas per region of interest (ROI). For neuropil compartment analysis, the neuropil of pyramidal cells was masked from the single-channel images positive for GFP using a high threshold and an additional subtraction of the area of the soma identified with a low threshold. The image thresholding method 'IsoData' was used to detect and generate masks of HA expression in the neuropil. After merging the GFP+ mask and the HA+ mask, the quantification of the percentage of HA+/GFP+ colocalisation was used to estimate neuregulin expression in the neuropil of a given ROI. Imaging was performed in 3-4 slices of the somatosensory cortex, and 4-10 ROIs were quantified and averaged per animal.

For cell density analysis, images were acquired with 10X/0.30 objective, and 0.75 digital zoom at 200 Hz acquisition speed. Analysis of PV+ interneuron density was performed in FIJI (ImageJ) software. The number of PV+ cells was manually counted across layers in the somatosensory cortex. This number was then divided by area (μm^2) of cortex to estimate the density of cells. A minimum of 6 brain slices were quantified and averaged per animal. For quantification of tdTomato-labelled pyramidal cells, the cell density analyses were performed in upper layers of the somatosensory cortex of 3-4 slices that contain the ROIs used in synaptic analyses.

For synapse density analysis, images were acquired with 100X/1.44 objective and 2.20 digital zoom at 200 Hz acquisition speed. To estimate the relative position of each neuron within the L2/3 of the cortex, we then took images of the same cells with 40X/1.40 objective and 0.75 digital zoom to measure the relative depth from the border between L1 and L2. analysis of bouton or synapse densities was performed using a custom macro in FIJI (ImageJ) software (Favuzzi et al., 2017). Processing of surface and synaptic single-channel images included background subtraction, Gaussian blurred, smoothing, and contrast enhancement.

For quantification of somatic synaptic contacts, the PV+, tdTomato (tdT)+ or GFP+ soma was detected based on intensity levels and automatically drawn to create a mask representing the surface of the cell body and to measure its perimeter. PV+ cell bodies were identified using immunohistochemistry, and stained and imaged in 405 nm wavelength range because synaptic markers co-labelled in these experiments were imaged in the rest of the wavelength spectrum; although staining intensity in the 405 nm wavelength results in weaker signal, it is sufficient to detect, reconstruct, and analyse the soma of PV+ cells. Differences in PV+ intensity levels were not taken into account; however, the large number of cells analysed likely helped to overcome some of this biological variation by including many cells with various degrees of intensity. Selection of PV+ cell somas was performed in a random manner, not targeted to any specific feature and/or location of the cells. Image acquisition followed the same procedure systematically across genotypes, to reduce biological and/or technical variability related to PV+ levels across different brain samples. For quantification of axo-axonic synaptic contacts, a mask of the axon initial segment (AIS) was created from pIκBα+ structure, and its length was measured. For presynaptic boutons and postsynaptic clusters, a threshold of intensity was used to automatically detect putative synaptic puncta while excluding any background. The thresholds for the different synaptic markers were unbiasedly selected in a set of random images prior to quantification, and the same threshold was applied to all images from the same experiment. The 'Analyze Particles' (circularity 0.00-1.00) and 'Watershed' tools were applied to the synaptic channels, and a mask was generated. The minimum sizes for particles were defined as follows: 0.06 for GAD67+, GAD65+ and CB1R+ boutons; and 0.05 for Syt2+ and VGlut1+ boutons and Geph+ and PSD95+ clusters. Finally, a merged image of the surface and synaptic masks was created to automatically quantify the number of contacts opposed to the soma or AIS structures. The criterion to identify presynaptic boutons (GAD67+, GAD65+, CB1R+, Syt2+, or VGlut1+) contacting the surface border of a soma or AIS was that ≥ 0.04 μm^2 of the puncta area in the synaptic mask was colocalising with the mask of the soma or AIS. The criterion to identify postsynaptic clusters (Geph+, or PSD95+) contained within a defined soma was that ≥ 0.04 μm^2 of the puncta area in the synaptic mask was colocalising with the mask of the soma. Putative synapses (Syt2+/Geph+, or VGlut1+/PSD95+) were identified when a presynaptic bouton and a postsynaptic cluster were contacting each other, with a colocalisation area of ≥ 0.03 μm^2 of their corresponding masks. VGlut1+/PSD95+ synaptic contacts were considered to

originate from tdT- or GFP-labelled axon terminals when ≥ 0.025 μm^2 of their area was colocalising with the mask of the tdT+ or GFP+ processes.

For the analysis of endogenous Nrg expression in interneurons, images were acquired with 100X/1.44 objective and 0.75 digital zoom at 200 Hz acquisition speed. ROIs were imaged in a non-targeted manner in hippocampal CA1 region, PV+ intensity levels were not taken into account, and a minimum of 10 ROIs were imaged per brain slice (including > 30 cells per sample). PV+ cells were manually counted as positive or negative for the expression of Nrg1 or Nrg3; given that high-magnification images provided high resolution in these analyses, the expression of Nrg1 or Nrg3 in PV+ cells was reliably detected.

For the analysis of the density of endogenous Nrg puncta, images were acquired with 100X/1.44 objective and 0.75 digital zoom at 200 Hz acquisition speed, and quantitative analyses were performed using a custom macro in FIJI (ImageJ) software. For Nrg1 puncta density, ROIs (2,000 μm^2) were analysed in both the stratum pyramidale and stratum radiatum, distinguished by the localisation of neuronal somas labelled with NeuN. Intensity-based threshold for Nrg1 signal was unbiasedly selected in a set of random images to detect putative puncta, and the same threshold was applied to all images from the same experiment. For Nrg3 puncta density, images were processed similarly to Nrg1 density analysis, using the same criteria to detect and analyse the number of Nrg3+ clusters per ROI (24,025 μm^2). In addition, to quantitatively estimate and distinguish between Nrg3+ clusters that are in close apposition to PV+ cells—putatively representing Nrg3-labelled presynaptic excitatory inputs onto interneurons—and Nrg3+ clusters that are not in contact with PV+ cells, we used PV immunostaining to generate masks representing the cell bodies of PV+ interneurons. ROIs with similar proportion of PV+ cell body masks across genotypes were used (average, 8,561.4 μm^2). ROIs included several PV+ cells (> 20) per cortical region and brain sample analysed, and PV intensity levels were not taken into account in these analyses.

10. Quantification and statistical analysis

All statistical analyses were performed using R Project for Statistical Computing (https://www.r-project.org/). For data analysis and visualisation, we used the 'ggplot2' package in RStudio (https://rstudio.com/). Shapiro-Wilk test was used as

a normality test to compare the empirical distribution function of the data sets with a normal probability distribution. To test the null hypothesis that the difference between two independent and parametric data samples measured in control and experimental conditions has a mean value of zero, we used two-tailed Student's *t*-test. Mann-Whitney *U*-test was used as the non-parametric alternative. To analyse the differences among multiple experimental groups, we used one-or two-way analysis of variance (ANOVA) test followed by Tukey's range test as a post hoc comparison test. Kruskal-Wallis test was used as the non-parametric alternative. Statistical significance was considered at p-values < 0.05. Data are presented as mean ± s.e.m (standard error of the mean). Number of cells or ROIs analysed and number of animals for each experiment are described in each figure legend.

RESULTS

CHAPTER 1. Study of neuregulin function in cortical synaptic assembly

In Chapter 1, we studied the function of Nrg1 and Nrg3 in the assembly of inhibitory-excitatory cortical circuits. The generation of inducible conditional knock-out (icKO) mice for *Nrg1* and *Nrg3* enabled us to specifically examine the role of Nrg1 and Nrg3 in the formation of synaptic connections that pyramidal cells establish with or receive from distinct classes of interneurons. These experiments aimed to determine whether neuregulin function in synaptic assembly is redundant or specific.

1.1. Cellular expression of *Nrg1* and *Nrg3* in the cerebral cortex

Previous reports have determined that, among neuregulin family members, *Nrg1* and *Nrg3* are most abundantly expressed in the brain, and indicated that their expression is particularly enriched in the cerebral cortex (Longart et al., 2004; Rahman et al., 2018). Consequently, we first examined the gene expression patterns of *Nrg1* and *Nrg3* in the mouse cerebral cortex at postnatal day 30 (P30), an age when developing cortical circuits have largely been established. We used RNAscope, a recently developed *in situ* hybridisation assay that allows highly sensitive detection of RNA molecules in intact brain tissue, and found that a large proportion of cortical cells express *Nrg1* and *Nrg3* across layers 2 to 6 of the somatosensory cortex (Figure 11A-B). Interestingly, we observed some cortical cells co-expressing RNA molecules of both *Nrg1* and *Nrg3* as well as some cells expressing only one neuregulin gene (Figure 11C). To quantify the relative proportions of specific neuronal types that express either neuregulin gene or both, RNAscope can be combined with *post hoc* immunostaining for markers of cell subtypes, a methodology that is still not established in our lab and we are currently optimising. To overcome this limitation and gain further insight into the cell-type specificity pattern of neuregulin expression, I performed bioinformatic analysis of publicly available datasets from single-cell RNA sequencing (scRNA-seq) (Tasic et al., 2018) (Cell Types Database from the Allen Brain Map: https://portal.brain-map.org/atlases-and-data/rnaseq). These analyses confirmed the broad and

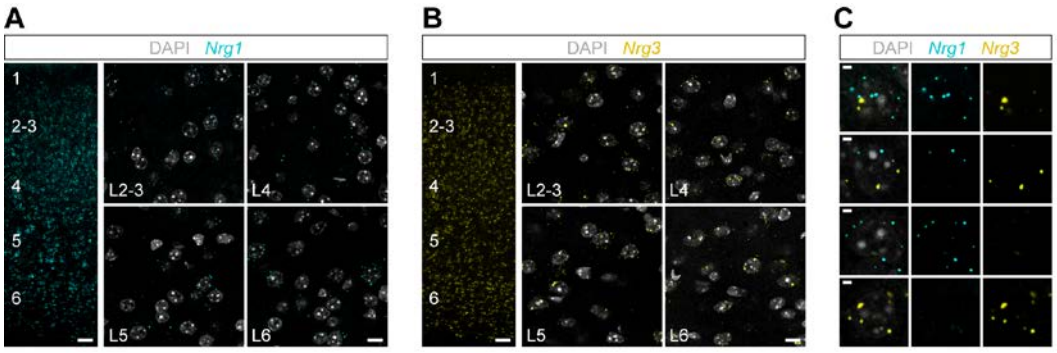

Figure 11 | **Cellular expression of *Nrg1* and *Nrg3* mRNA in the mouse cerebral cortex assessed by RNAscope *in situ* hybridisation.**
(**A-B**) Single-molecule fluorescent *in situ* hybridisation with *Nrg1* (**A**) and *Nrg3* (**B**) RNAscope probes in coronal sections through somatosensory cortex at P30. *Nrg1* and *Nrg3* mRNA expression is abundantly detected across layers 2-6 in the mouse cerebral cortex. (**C**) Examples of double-colocalisation of *Nrg1* (cyan) and *Nrg3* (yellow) mRNA in nuclei counterstained with DAPI (gray) in superficial layers of the somatosensory cortex at P30. Scale bars, 50 µm (A-B) and 10 µm (high magnification), and 2 µm (C).

abundant expression of *Nrg1* and *Nrg3* in pyramidal cells across layers 2-6 of the cerebral cortex at adult stages (Figure 12A). Intriguingly, *Nrg1* and *Nrg3* are expressed by diverse subtypes of glutamatergic projection neurons, although at different expression levels (Figure 12B). Additional analysis of publicly available RNA-seq datasets from the developing cerebral cortex showed *Nrg1* and *Nrg3* expression in pyramidal cells at P28 and P10 (Figure 12C-D) (Favuzzi et al., 2019; Furlanis et al., 2019). Altogether, these data ascertain that both neuregulin genes are expressed by pyramidal cells in the cerebral cortex throughout postnatal development and into adulthood. To explore whether other neuronal classes and subtypes express *Nrg1* and *Nrg3*, I first explored the scRNA-seq database (Tasic et al., 2018), and found that a wide diversity of interneurons—including the major populations of PV+ basket cells, SST+ dendrite-targeting interneurons, and VIP+ cells—express *Nrg1* and *Nrg3* mRNA (Figure 13A). Notably, *Nrg3* appears to consistently show higher levels of gene expression than *Nrg1* across interneuron subtypes (Figure 13A). Developing PV+ interneurons also express *Nrg1* and *Nrg3* mRNA, as evidenced in the RNA-seq datasets at P28 and P10 (Figure 13B-C) (Favuzzi et al., 2019; Furlanis et al., 2019). These data show higher *Nrg3* expression levels than *Nrg1* during development in a similar manner to the adult cortex, a finding that reinforces the idea of a differential pattern of neuregulin expression in interneurons. To confirm whether neuregulins are expressed by interneurons at the protein level, I performed immunostaining using commercial antibodies against Nrg1 and Nrg3 in conditional mutant mice, where *Nrg1* or *Nrg3*

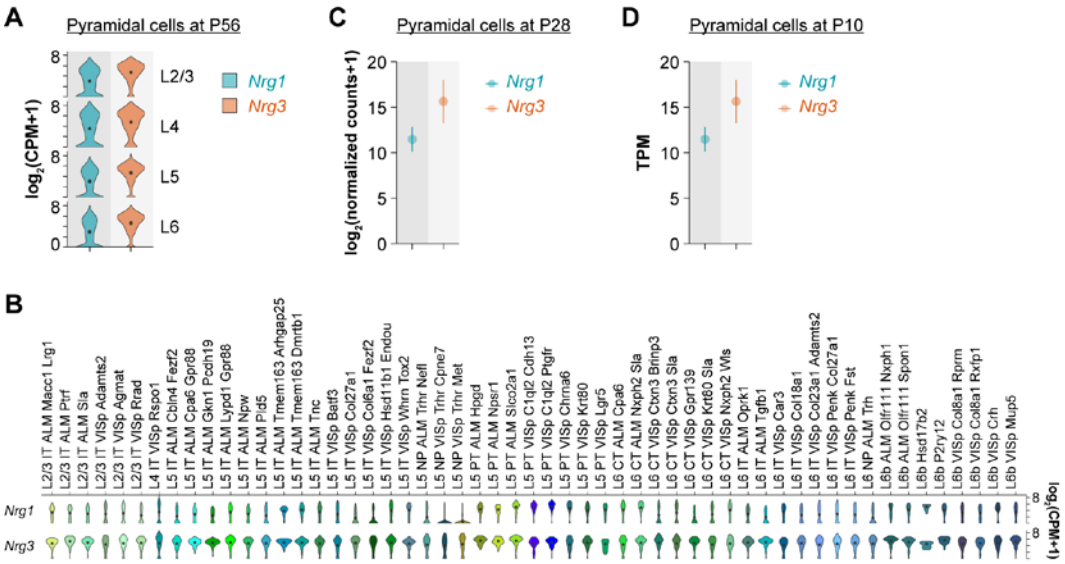

Figure 12 | **Gene expression profiles of *Nrg1* and *Nrg3* in pyramidal cells in the developing and adult cerebral cortex.**
(**A-B**) mRNA expression of *Nrg1* and *Nrg3* in pyramidal cells across cortical layers at P56. The violin plots depict single-cell RNA-sequencing data from the Cell Types Database of the Allen Brain Map (http://celltypes.brain-map.org/rnaseq/mouse). Gene expression is averaged for all pyramidal cells per layer (A), and represented by individual violin plots for each cell subtype cluster (B). (**C**) mRNA expression of *Nrg1* and *Nrg3* in pyramidal cells at P28 from bulk RNA-seq dataset of the Scheiffele lab (https://scheiffele-splice.scicore.unibas.ch/). Expression data are shown as normalized counts. (**D**) mRNA expression of *Nrg1* and *Nrg3* in pyramidal cells at P10 from bulk RNA-seq dataset of the Rico lab (https://devneuro.org/cdn/synapdomain.php). Expression data are shown as transcripts per kilobase million (TPM).

genes are specifically deleted from cortical pyramidal cells using a transgenic mouse line that expresses Cre recombinase under the control of the pyramidal cell-specific *Neurod6* promoter (Goebbels et al., 2006) (Figure 13D-G). In these conditional mutant mice, interneurons are the only remaining source of neuronal expression of either *Nrg1* or *Nrg3* in the cerebral cortex. By performing co-localisation analysis, we found that the majority of PV+ interneurons at P30 express Nrg1 and Nrg3 protein (Figure 13D-G). Intriguingly, Nrg1 protein was detected to be present in the cytoplasm as well as the cell surface of PV+ interneurons (Figure 13D), whereas Nrg3 protein was mainly located at the surface of PV+ cell bodies in a punctate manner (Figure 13F). Altogether, these results indicate that Nrg1 and Nrg3 are expressed by both pyramidal cells and interneurons in the cerebral cortex during postnatal development. Given the important role of ErbB4 in regulating the wiring of cortical interneurons and the abundant expression of neuregulins in pyramidal cells, we aimed to study the

function of Nrg1 and Nrg3 in the synaptic assembly of excitatory pyramidal cells with specific classes of GABAergic interneurons in the cerebral cortex.

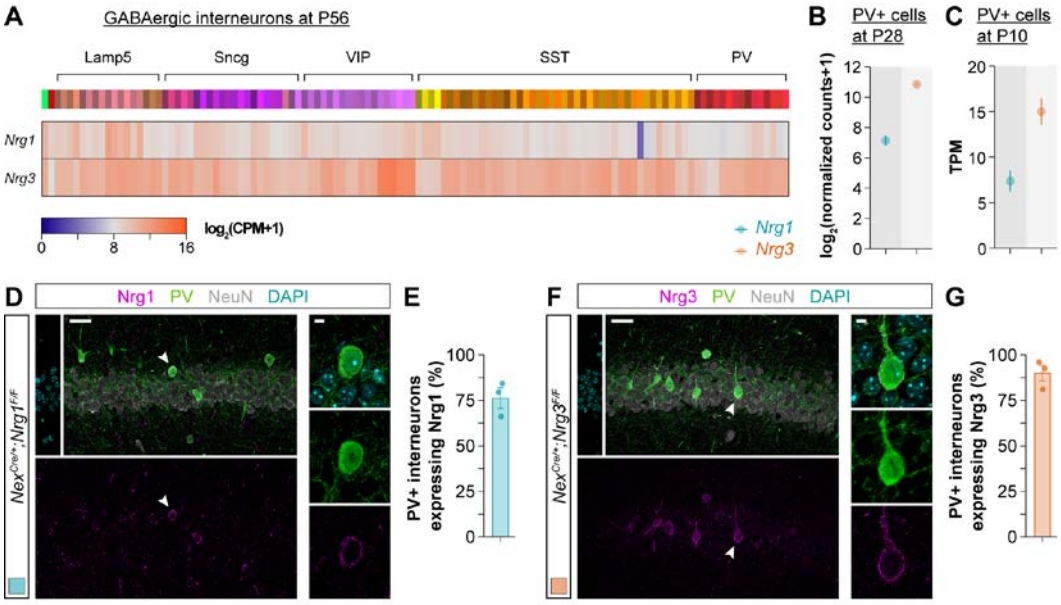

Figure 13 | **Gene expression profiles of *Nrg1* and *Nrg3* in interneurons in the developing and adult cerebral cortex.**
(**A-B**) mRNA expression of *Nrg1* and *Nrg3* in cortical interneurons at P56. Heatmap representing median expression values (counts per million mapped reads, CPM) for each interneuron subtype clusters in the single-cell RNA-sequencing dataset from the Cell Types Database of the Allen Brain Map (http://celltypes.brain-map.org/rnaseq/mouse). (**B**) mRNA expression of Nrg1 and Nrg3 in PV+ interneurons at P28 from bulk RNA-seq dataset of the Scheiffele lab (https://scheiffele-splice.scicore.unibas.ch/). Expression data are shown as normalized counts. (**C**) mRNA expression of Nrg1 and Nrg3 in PV+ interneurons at P10 from bulk RNA-seq dataset of the Rico lab (https://devneuro.org/cdn/synapdomain.php). Expression data are shown as transcripts per kilobase million (TPM). (**D**) Coronal sections through the hippocampus processed for immunohistochemistry against Nrg1 (magenta), parvalbumin (PV) (green), and the neuronal marker NeuN (gray), and counterstained with DAPI (cyan), in conditional mutant mice in which *Nrg1* is specifically deleted from pyramidal cells (*Nex$^{Cre/+}$;Nrg1$^{F/F}$*). Note the expression of Nrg1 protein in both the cytoplasm and the cellular surface of a PV+ interneuron in the high-magnification panel (right). (**E**) Quantification of the proportion of PV+ interneurons that co-express Nrg1 protein in the hippocampal CA1 region. N = 3 mice (142 cells). (**F**) Coronal section through the hippocampus processed for immunohistochemistry against Nrg3 (magenta), parvalbumin (PV) (green), and NeuN (gray), and counterstained with DAPI (cyan), in conditional mutant mice in which *Nrg3* is specifically deleted from pyramidal cells (*Nex$^{Cre/+}$;Nrg3$^{F/F}$*). Note the membrane localisation of Nrg3 protein in the cellular surface of a PV+ interneuron in the high-magnification panel (right). (**G**) Quantification of the proportion of PV+ interneurons that co-express Nrg3 protein in the hippocampal CA1 region. N = 3 mice (146 cells).
Data in bar graphs are shown as mean ± s.e.m. Scale bars, 30 µm (D, F) and 5 µm (high magnification).

1.2. Generation of inducible conditional knock-out mice for *Nrg1* and *Nrg3*

Since Nrg1 and Nrg3 are widely expressed by diverse subtypes of pyramidal cells during postnatal development (Figure 12A-B), we hypothesised that these two homologous members of the neuregulin family may play redundant functions in the connectivity of these cells. To test this hypothesis, we performed genetic loss-of-function experiments using conditional alleles for both genes. Since neuregulin signalling in pyramidal cells plays a role in the migration and laminar allocation of neocortical interneurons (Bartolini et al., 2017; Flames et al., 2004), we deleted *Nrg1* and *Nrg3* from pyramidal cells postnatally to avoid interfering with the function of neuregulins during embryonic stages. To this end, we bred *Nex-Cre*^{ERT2} mice, in which a tamoxifen-inducible version of Cre recombinase is under the control of the endogenous regulatory sequences of the pyramidal cell-specific *Neurod6* locus (Agarwal et al., 2012), with mice carrying loxP-flanked *Nrg1* or *Nrg3* alleles (Bartolini et al., 2017; Yang et al., 2001) (Figure 8). By introducing the allele *Ai9* in our mouse models, we were able to label pyramidal cells after recombination of this conditional floxed allele, which encodes the tdTomato reporter, after induction with tamoxifen injection in newborn pups at P0 (Figure 8B). This would allow us to quantify the reduction of neuregulin mRNA expression in recombined (putative knock-out) pyramidal cells by performing RNAscope with *Nrg1* and *Nrg3* probes followed by immunofluorescence staining against tdTomato. The latter step is necessary to amplify the fluorescence signal since the harsh conditions of the RNAscope protocol result in decreased endogenous signal of the reporter. As noted above, we are actively optimising the combined staining protocol with RNAscope probes and antibodies in order to obtain successful co-labelling of RNA and protein; at present, to improve labelling and image quality, better preservation of the tissue and improved signal-to-noise ratio is needed. This optimisation will allow us to quantitatively estimate the loss of neuregulin mRNA expression in the inducible knock-out mouse models. In a complementary control experiment, to determine the efficacy of recombination of floxed alleles, and therefore the deletion of neuregulin genes *in vivo*, we performed immunostaining against Nrg1 and Nrg3 proteins in conditional mutants and control littermates using a heat-induced antigen retrieval protocol that enhances the signal of the labelled proteins. We found a marked reduction in the expression of Nrg1 and Nrg3 in conditional mutant mice as compared to wild-type littermates (Figure 14). Notably, expression of

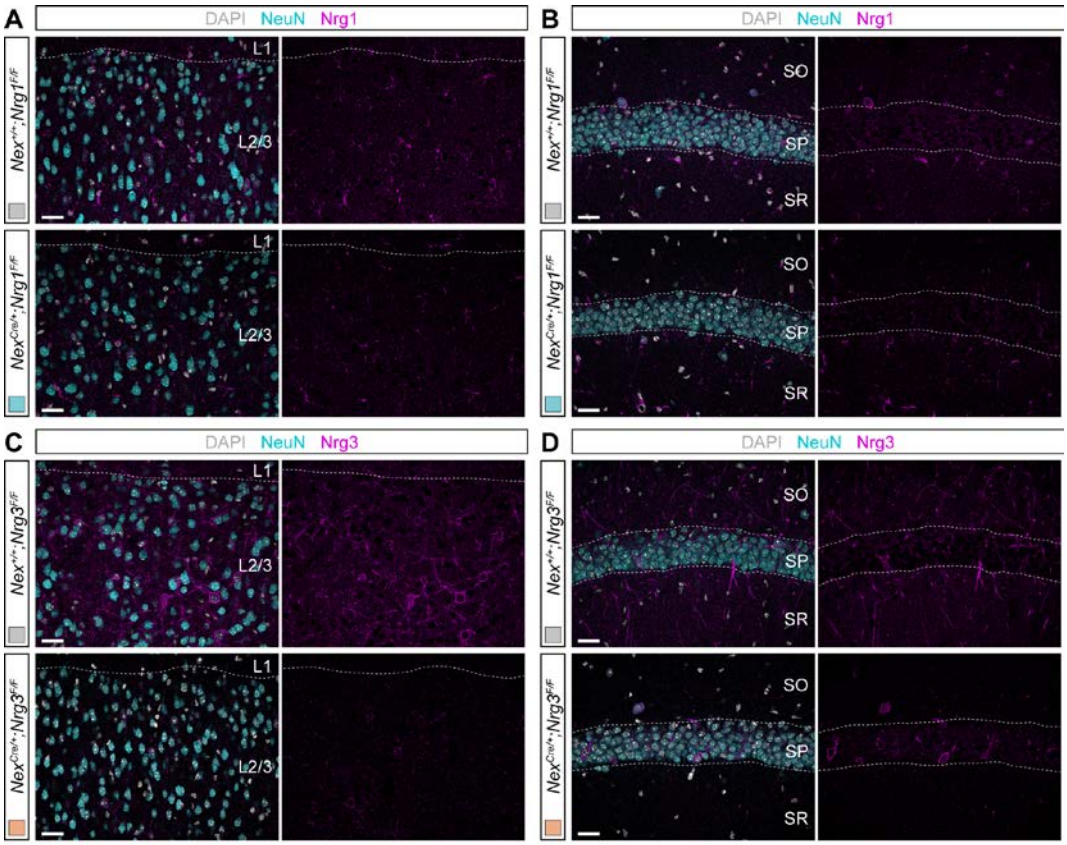

Figure 14 | **Conditional deletion of *Nrg1* or *Nrg3* in cortical pyramidal cells.** (**A-B**) Coronal sections through the somatosensory cortex (A) and hippocampus (B) processed for immunohistochemistry against Nrg1 (magenta) and NeuN (cyan), and counterstained with DAPI (gray) in control and conditional neuregulin mutant mice. (**C-D**) Coronal sections through the somatosensory cortex (C) and hippocampus (D) processed for immunohistochemistry against Nrg3 (magenta) and NeuN (cyan), and counterstained with DAPI (gray) in control and conditional neuregulin mutant mice. Abbreviations: SO, stratum oriens; SP, stratum pyramidale; SR, stratum radiatum. Scale bars, 30 (A-D).

neuregulins was still evident in some cells (Figure 14). Because the deletion of neuregulins is specific to pyramidal cells as mice carrying *Nrg1* or *Nrg3* floxed alleles were crossed with *Nex-Cre* transgenic mice, this observation is consistent with the notion that neuregulins are expressed by other neuronal and glial cell types (Figure 13) (Liu et al., 2011; Stassar et al., 2013; Rahman et al., 2018; Grieco et al., 2020). We performed this initial test in our conditional mutant models (*Nex-Cre*) because we previously validated the specificity of neuregulin antibodies and optimised the antigen retrieval immunostaining protocol using tissue samples from these mice; it is worth noting that the neuregulin antibodies are very sensitive to the histological procedure and the quality of the tissue. It will be important to further corroborate these tests in samples from inducible mutant mice (*Nex-Cre*^{ERT2}), in which it was not possible to further optimise this protocol at the time of this

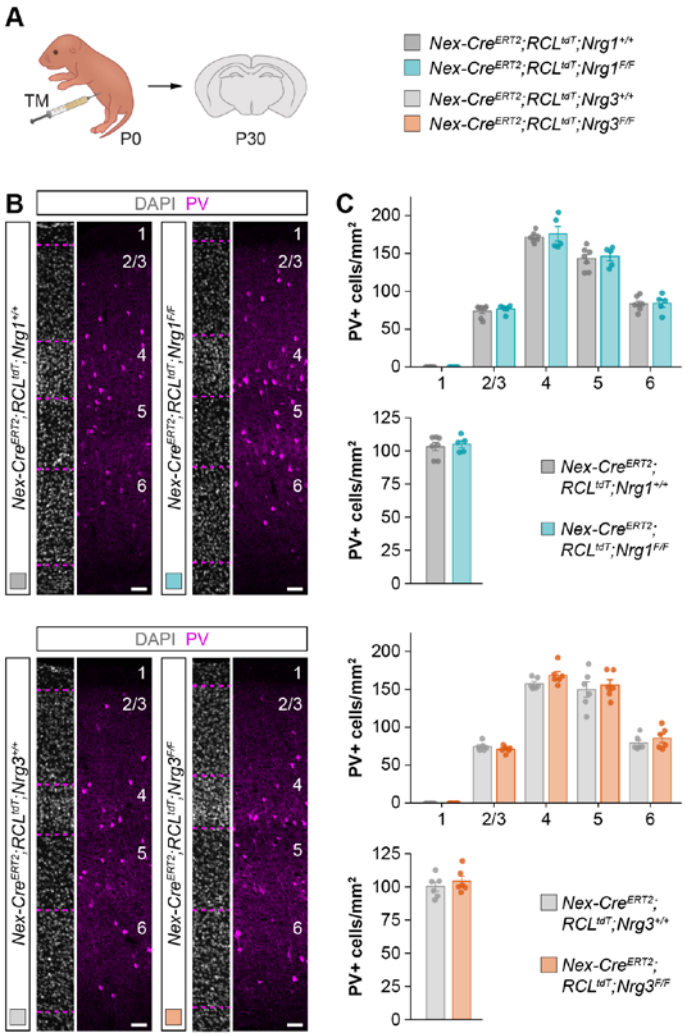

Figure 15 | **Postnatal deletion of *Nrg1* or *Nrg3* in cortical pyramidal cells does not affect the density and distribution of cortical PV+ interneurons.**
(**A**) Schematic of experimental design. Conditional deletion of *Nrg1* or *Nrg3* in cortical pyramidal cells was achieved by tamoxifen (TM) injection in newly born pups at P0. (**B**) Coronal sections through the somatosensory cortex processed for immunohistochemistry against parvalbumin (PV) (magenta) and counterstained with DAPI (gray) in control and conditional neuregulin mutant mice. (**C**) Quantification of the distribution and density of PV+ cells in pyramidal cell-specific *Nrg1* and *Nrg3* mutant mice and control littermates at P30. Distribution in *Nrg1* mutants: Kruskal-Wallis rank sum test, $F = 0.018$, $P = 0.894$; n = 7 mice (63 regions of interest, ROIs) for controls and 5 mice (45 ROIs) for mutants. Density in *Nrg1* mutants: Mann-Whitney *U*-test, $P = 0.876$; n = 7 mice (63 ROIs) for controls and 5 mice (45 ROIs) for mutants. Distribution in *Nrg3* mutants: Kruskal-Wallis rank sum test, $F = 0.059$, $P = 0.824$; n = 6 mice (50 ROIs) for controls and 6 mice (51 ROIs) for mutants. Density in *Nrg3* mutants: Two-tailed Student's *t*-test, $P = 0.425$; n = 6 mice (50 ROIs) for controls and 6 mice (51 ROIs) for mutants.
Data are shown as mean ± s.e.m. Scale bars, 50 µm (B).

validation because of the time required for the breeding strategy to generate these animals (Figure 8). Overall, our initial results show the effective deletion of Nrg1 and Nrg3 proteins in conditional mutant mice, and our current efforts aim to

optimise two complementary methods—RNAscope and antibody staining—to corroborate and quantify the reduction in Nrg1 and Nrg3 expression in samples from inducible conditional knock-out mice.

Next, we asked whether postnatal deletion of *Nrg1* or *Nrg3* affects cortical interneuron migration and laminar allocation. Since the precise time of full protein depletion from the neuron and therefore any impact in layer migration is difficult to predict, we assessed the total density and layer distribution of PV+ interneurons in the cortex of control and neuregulin icKO mice. We observed that postnatal induction of Cre recombinase in pyramidal cells does not disrupt the density and distribution of PV+ interneurons in *Nrg1* and *Nrg3* conditional mutant mice at P30 (Figure 15). These data suggest that the general organisation and cellular architecture of cortical interneuron circuits develops normally in icKO mice. Therefore, these mice represent ideal models to investigate the precise role of *Nrg1* and *Nrg3* in pyramidal cells during the postnatal assembly of cortical circuits.

1.3. Specific inhibitory synaptic deficits in *Nrg1* icKO mice

We first examined the function of Nrg1 and Nrg3 in the development of inhibitory synapses onto pyramidal cells. We analysed the two types of inhibitory synapses made onto pyramidal cells that are known to be altered in the absence of ErbB4 from interneurons: synapses made by cholecystokinin (CCK+) basket cells onto the soma and synapses made by chandelier cells on the axon initial segment (AIS) (Del Pino et al., 2013, 2017). We used GAD65 and CB1R to label somatic boutons of CCK+ interneurons, and GAD67 to identify chandelier cell boutons on the AIS of pyramidal cells as labelled by pIκBα (Fish et al., 2011; Katona et al., 1999). To identify Cre-expressing pyramidal cells, we included the conditional reporter allele *Ai9* (tdTomato) in the breeding scheme (Madisen et al., 2010) (Figure 8) (see Methods for selection of tdTomato+ cells). To assess CCK+ synaptic deficits, we focused our analysis on L2 pyramidal cells since they receive higher innervation compared to L3 cells (Figure 16). We observed a significant decrease in the density of GAD65+/CB1R+ presynaptic boutons contacting the soma of L2 pyramidal cells in conditional *Nrg1* mutants compared to controls (Figure 17B-C). In contrast, deletion of *Nrg3* from pyramidal cells did not affect the formation of somatic boutons by CCK+ basket cells (Figure 17B-C). Importantly, we did not observe significant changes in the density of GABAergic boutons that were not labelled with

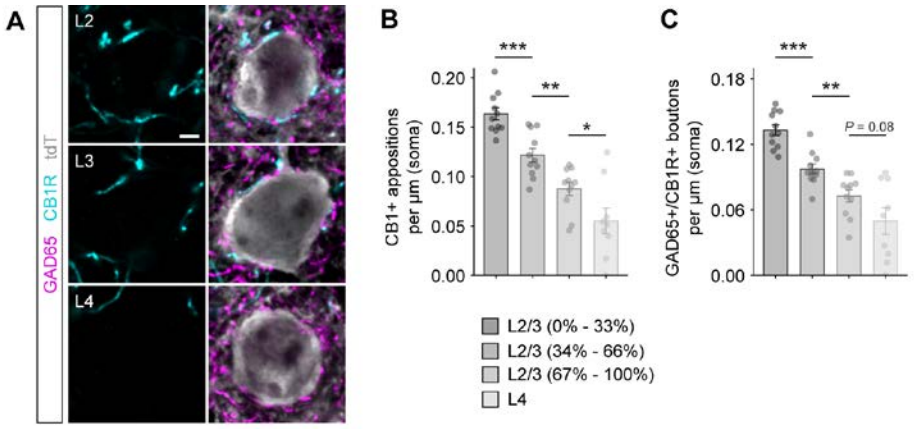

Figure 16 | **CCK+ synaptic innervation of pyramidal cells across layers 2 to 4 in the somatosensory cortex.**
(**A**) Confocal images showing CB1R+ (cyan) and GAD65+ (magenta) boutons contacting the soma of tdTomato+ pyramidal cells (gray) in the somatosensory cortex at P30. Note the differential innervation of pyramidal cells located in different cortical layers. Layers were identified by DAPI counterstaining, and pyramidal cells within L2/3 were grouped based on their position in the upper, middle, and lower portions across the radial axis of the cerebral cortex. (**B-C**) Quantification of the density of CB1R appositions (B) and GAD65+/CB1R+ boutons (C) contacting pyramidal cells across layers. Two-tailed Student's *t*-test: ****P* < 0.001, ***P* < 0.01, **P* = 0.05; n = 11 mice (149 cells) for L2/3 (upper portion), 11 mice (111 cells) for L2/3 (middle portion), 11 mice (74 cells) for L2/3 (lower portion), 9 mice (38 cells) for L4.
Data are shown as mean ± s.e.m. Scale bar, 2 µm.

CB1R (Figure 17D), suggesting that the deficits in somatic inhibitory inputs observed in *Nrg1*-lacking pyramidal cells are specific to a CCK+ presynaptic population. Differences in bouton sizes were not estimated due to lack of resolution in the microscopy approach used (the same limitation applies for the rest of the analyses in this study). Altogether, these results indicated that Nrg1, and not Nrg3, is required for the development of CCK+ basket cell synapses on pyramidal cells.

We next examined the function of Nrg1 and Nrg3 in the formation of inhibitory axo-axonic boutons made by chandelier cells. We observed that the AIS of cortical L2/3 pyramidal cells lacking *Nrg1* received significantly fewer GAD67+ boutons than in controls (Figure 18). In contrast, we found that the density of axo-axonic boutons is unaltered following deletion of *Nrg3* from L2/3 pyramidal cells (Figure 18). These results reinforced the idea that Nrg3 function is dispensable for the development of inhibitory synaptic inputs on pyramidal cells, a function that is mediated by Nrg1.

To establish whether Nrg1 functions in specific inhibitory circuits that are dependent on ErbB4 function (chandelier and CCK+ basket cell synapses) or is generally required for GABAergic synaptogenesis, we analysed the number of PV+

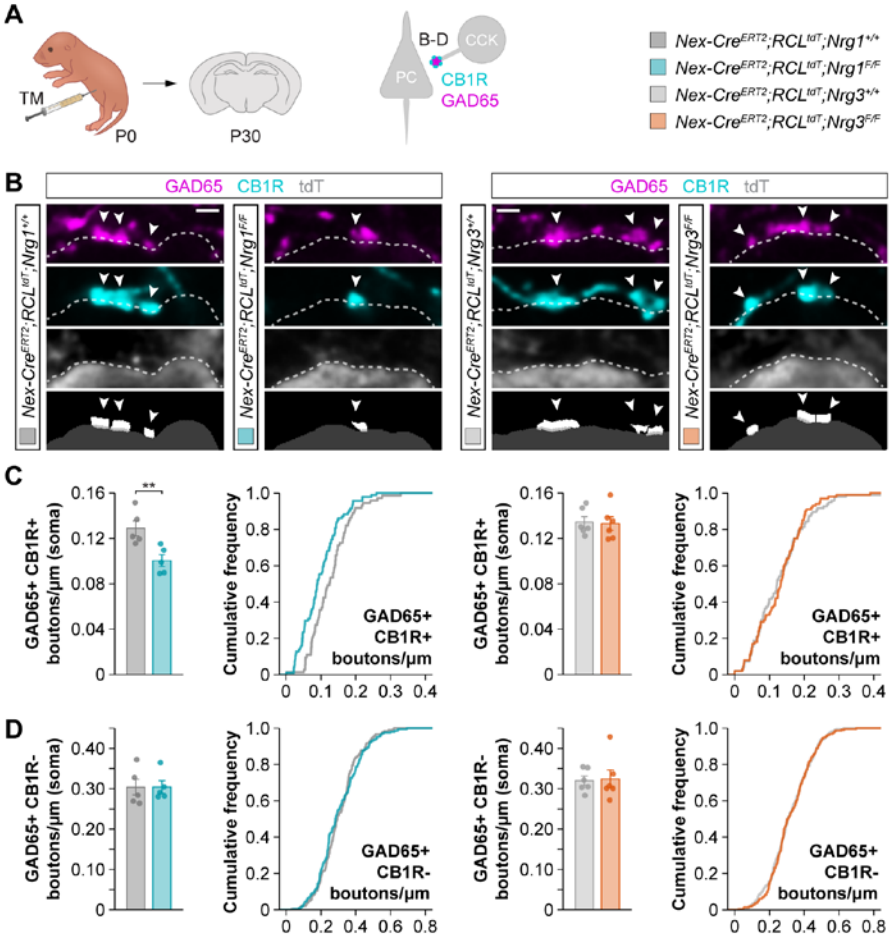

Figure 17 | **Synaptic deficit of CB1R+ inhibitory boutons contacting the soma of pyramidal cells lacking *Nrg1*, but not *Nrg3*.**
(**A**) Schematic of experimental design. Conditional deletion of *Nrg1* or *Nrg3* in pyramidal cells (PC) was achieved by tamoxifen (TM) injection in newly born pups at P0. Inhibitory presynaptic boutons made by cholecystokinin (CCK)+ basket cells onto the soma of pyramidal cells (GAD65/CB1R) were analysed in these experiments. (**B**) Confocal images (top three panels) and binary images (bottom panel) illustrating presynaptic GABAergic boutons (arrowheads) labelled with GAD65 (magenta) and CB1R (cyan) contacting the soma of tdTomato+ pyramidal cells (gray) in controls, *Nrg1* and *Nrg3* conditional mutant mice. (**C**) Quantification of the density of GAD65+/CB1R+ boutons formed onto pyramidal cell somas in *Nrg1* and *Nrg3* conditional mutant mice. Two-tailed Student's *t*-tests: for *Nex-Cre^{ERT2};RCL^{tdT};Nrg1^{F}*, $^{**}P < 0.01$; n = 5 mice (73 cells) for controls and 5 mice (94 cells) for mutants; for *Nex-Cre^{ERT2};RCL^{tdT};Nrg3^{F}*, $P = 0.867$; n = 6 mice (96 cells) for controls and 6 mice (100 cells) for mutants. (**D**) Quantification of the density of GAD65+/CB1R- boutons formed onto pyramidal cell somas in *Nrg1* and *Nrg3* conditional mutant mice. Two-tailed Student's *t*-tests: for *Nex-Cre^{ERT2};RCL^{tdT};Nrg1^{F}*, $P = 0.963$; n = 5 mice for controls and 5 mice for mutants; for *Nex-Cre^{ERT2};RCL^{tdT};Nrg3^{F}*, $P = 0.828$; n = 6 mice for controls and 6 mice for mutants. Data are shown as mean ± s.e.m. The averages per animal and genotype are represented in bar graphs, and the distributions of values per cell are shown in cumulative frequency plots. Scale bars, 1 µm.

basket cell synapses contacting pyramidal cells lacking specific neuregulins. We used synaptotagmin-2 (Syt2) to specifically identify the presynaptic compartment of these synapses (Sommeijer and Levelt, 2012). We found no differences in the

density of Syt2+ boutons or Syt2+/Gephyrin+ synaptic puncta contacting the soma of L2/3 pyramidal cells between *Nrg1* icKO and control mice (Figure 19). In addition, as expected from our previous results which suggest that Nrg3 is not involved in inhibitory synapse formation, we observed that pyramidal cells lacking *Nrg3* receive a normal complement of PV+ basket cell synapses (Figure 19). Altogether, these results are consistent with the hypothesis that Nrg1 plays a predominant role in the formation of specific inhibitory connections (i.e., those made by chandelier cells and CCK+ basket cells).

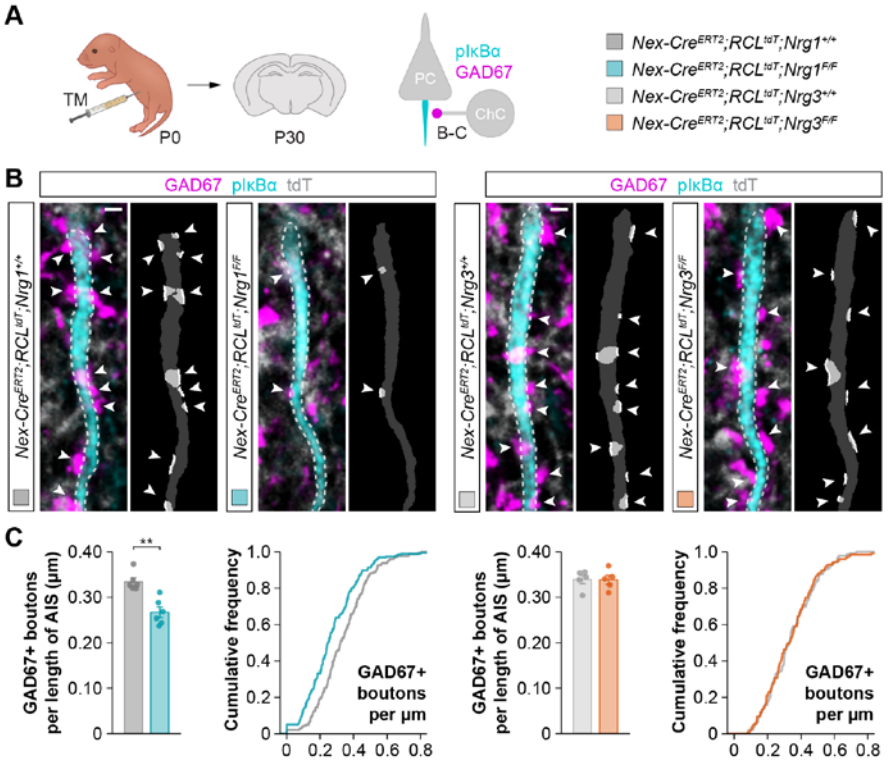

Figure 18 | **Loss of axo-axonic boutons innervating cortical pyramidal cells lacking *Nrg1*, but not *Nrg3*.**
(**A**) Schematic of experimental design. Conditional deletion of *Nrg1* or *Nrg3* in pyramidal cells (PC) was achieved by tamoxifen (TM) injection in newly born pups at P0. GABAergic presynaptic boutons made by chandelier cells (ChC) onto the axon initial segment (AIS) of pyramidal cells (GAD67/pIκBα) were analysed in these experiments. (**B**) Confocal images (left panels) and binary images (right panel) showing GAD67+ boutons (magenta, arrowheads) contacting the AIS (pIκBα, cyan) of tdTomato+ pyramidal cells (gray) in controls, *Nrg1* and *Nrg3* conditional mutant mice. (**C**) Quantification of the density of axo-axonic inhibitory boutons formed onto pyramidal cells in *Nrg1* and *Nrg3* conditional mutant mice. Mann-Whitney *U*-test: for *Nex-Cre^{ERT2};RCL^{tdT};Nrg1^{F}*, $^{**}P < 0.01$; n = 6 mice (178 cells) for controls and 6 mice (196 cells) for mutants. Two-tailed Student's *t*-test: for *Nex-Cre^{ERT2};RCL^{tdT};Nrg3^{F}*, $P = 0.959$; n = 5 mice (139 cells) for controls and 5 mice (127 cells) for mutants.
Data are shown as mean ± s.e.m. The averages per animal and genotype are represented in bar graphs, and the distributions of values per cell are shown in cumulative frequency plots. Scale bars, 1 µm.

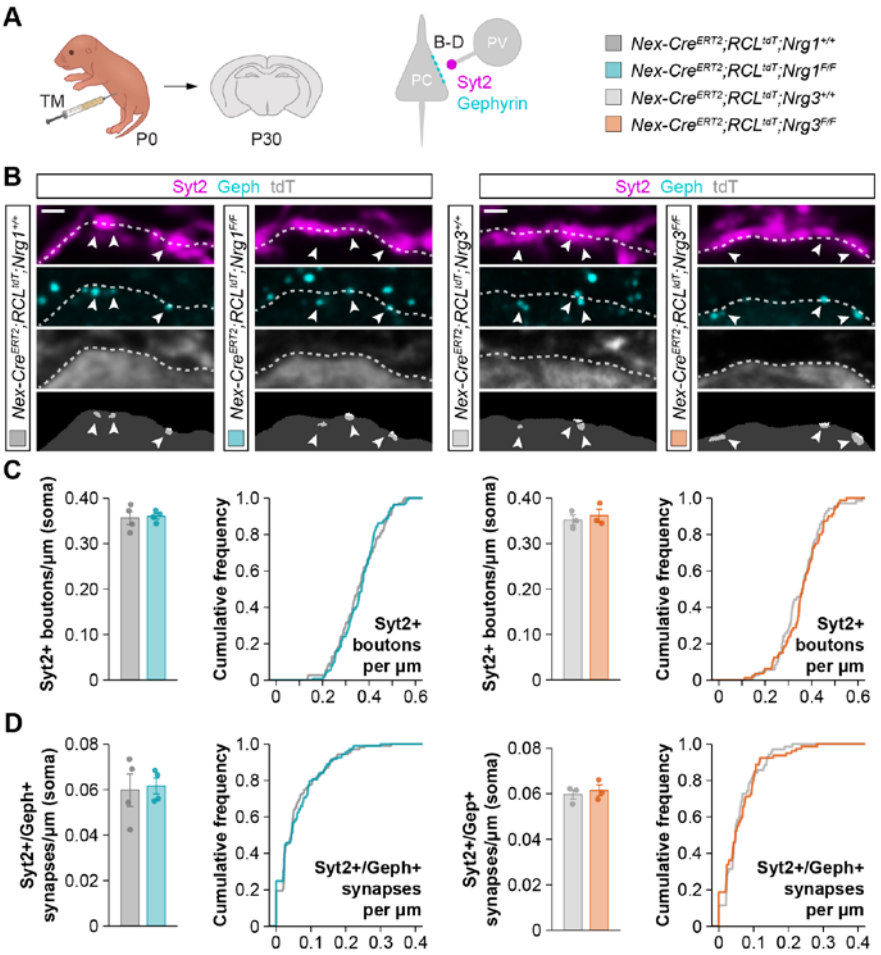

Figure 19 | **Density of inhibitory somatic synapses formed by PV+ basket cells onto pyramidal cells in conditional mutant mice for *Nrg1* or *Nrg3*.**
(**A**) Schematic of experimental design. Conditional deletion of *Nrg1* or *Nrg3* in pyramidal cells (PC) was achieved by tamoxifen (TM) injection in newly born pups at P0. Inhibitory synapses made by PV+ basket cells onto the soma of pyramidal cells (Syt2/Gephyrin) were analysed in these experiments. (**B**) Confocal images (top three panels) and binary images (bottom panel) illustrating inhibitory synapses labelled with Syt2+ boutons (magenta) in close apposition to gephyrin+ clusters (cyan) on the surface of tdTomato+ pyramidal cell somas (gray) in controls, *Nrg1* and *Nrg3* conditional mutant mice. (**C**) Quantification of the density of Syt2+ somatic boutons contacting pyramidal cells in controls and *Nrg1* and *Nrg3* conditional mutant mice. Two-tailed Student's *t*-tests: for *Nex-Cre^{ERT2};RCL^{tdT};Nrg1^{F}*, $P = 0.803$; n = 4 mice (108 cells) for controls and 4 mice (109 cells) for mutants; for *Nex-Cre^{ERT2};RCL^{tdT};Nrg3^{F}*, $P = 0.618$; n = 3 mice (70 cells) for controls and 3 mice (80 cells) for mutants. (**D**) Quantification of the density of Syt2+/Gephyrin+ synapses formed onto contacting pyramidal cells in controls and *Nrg1* and *Nrg3* conditional mutant mice. Two-tailed Student's *t*-tests: for *Nex-Cre^{ERT2};RCL^{tdT};Nrg1^{F}*, $P = 0.828$; n = 4 mice (108 cells) for controls and 4 mice (109 cells) for mutants; for *Nex-Cre^{ERT2};RCL^{tdT};Nrg3^{F}*, $P = 0.609$; n = 3 mice (139 cells) for controls and 5 mice (127 cells) for mutants.
Data are shown as mean ± s.e.m. The averages per animal and genotype are represented in bar graphs, and the distributions of values per cell are shown in cumulative frequency plots. Scale bars, 1 µm.

1.4. Selective excitatory synaptic alteration in *Nrg3* icKO mice

We next investigated the role of neuregulins in the assembly of excitatory synapses onto PV+ interneurons, since ErbB4 is located at these synapses and is essential for their formation (Del Pino et al., 2013, 2017; Fazzari et al., 2010; Ting et al., 2011). We quantified the density of VGlut1+/PSD95+ synapses within the population of tdTomato-expressing axonal terminals contacting PV+ interneurons of the somatosensory cortex of control and icKO mutant mice at P30. PV+ cells

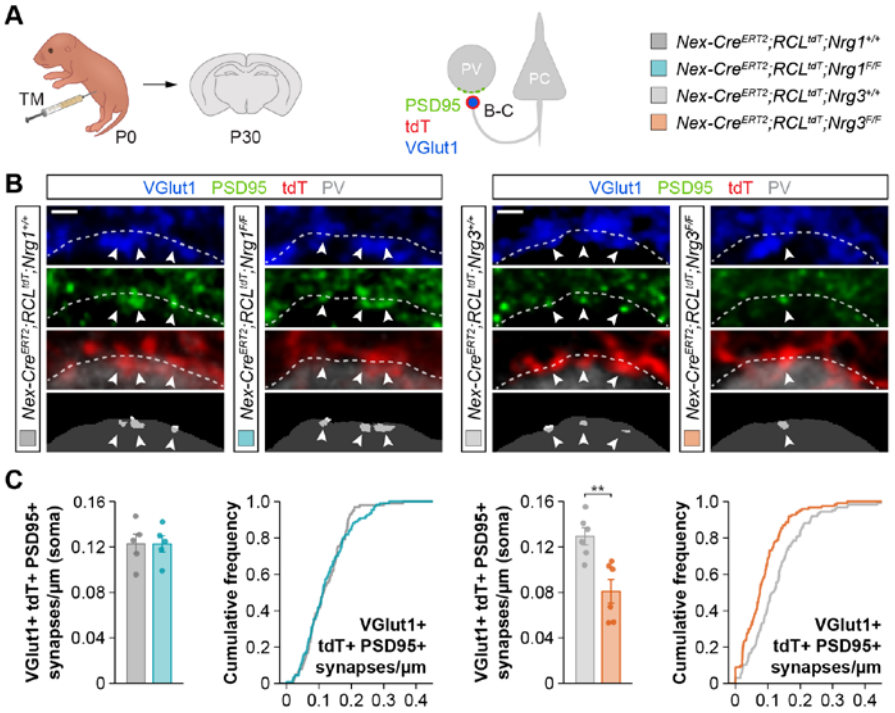

Figure 20 | **Excitatory synaptic deficit in cortical pyramidal cells lacking *Nrg3*, but not *Nrg1*.**
(**A**) Schematic of experimental design. Conditional deletion of *Nrg1* or *Nrg3* in pyramidal cells (PC) was achieved by tamoxifen (TM) injection in newly born pups at P0. Excitatory synapses (VGlut1/PSD95) made by tdTomato+ pyramidal cell axons onto the soma of PV+ interneurons were analysed in these experiments. (**B**) Confocal images (top three panels) and binary images (bottom panel) illustrating presynaptic VGlut1+ puncta (blue) within tdTomato+ axons (red) of pyramidal cells located in close apposition to PSD95+ clusters (green) in PV+ interneurons (gray) in controls, *Nrg1* and *Nrg3* conditional mutant mice. (**C**) Quantification of the density of VGlut1+/PSD95+/tdTomato+ synapses contacting PV+ interneurons in *Nrg1* and *Nrg3* conditional mutant mice. Two-tailed Student's *t*-tests: for *Nex-Cre^{ERT2};RCL^{tdT};Nrg1^{F}*, $P = 0.993$; n = 5 mice (101 cells) for controls and 5 mice (110 cells) for mutants; for *Nex-Cre^{ERT2};RCL^{tdT};Nrg3^{F}*, $^{**}P < 0.01$; n = 6 mice (126 cells) for controls and 6 mice (123 cells) for mutants.
Data are shown as mean ± s.e.m. The averages per animal and genotype are represented in bar graphs, and the distributions of values per cell are shown in cumulative frequency plots. Scale bars, 1 µm.

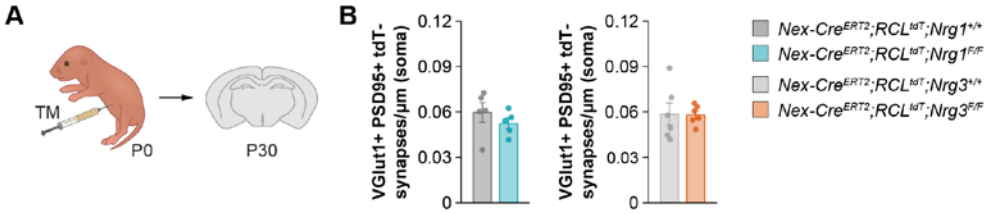

Figure 21 | **Cell-autonomous requirement of Nrg3 in excitatory synapse development.**
(**A**) Schematic of experimental design. Conditional deletion of *Nrg1* or *Nrg3* in pyramidal cells (PC) was achieved by tamoxifen (TM) injection in newly born pups at P0. (**B**) Quantification of the density of VGlut1+/PSD95+ synapses that do not arise from tdTomato+ pyramidal cell axons at P30 in *Nrg1* and *Nrg3* conditional mutant mice. Two-tailed Student's *t*-tests: for *Nex-Cre^{ERT2};RCL^{tdT};Nrg1^{F}*, *P* = 0.360; n = 5 mice (101 cells) for controls and 5 mice (110 cells) for mutants; for *Nex-Cre^{ERT2};RCL^{tdT};Nrg3^{F}*, *P* = 0.940; n = 6 mice (126 cells) for controls and 6 mice (123 cells) for mutants.
Data are shown as mean ± s.e.m. The averages per animal and genotype are represented in bar graphs.

were selected within L2/3, prior to imaging of the other synaptic markers, and independent on PV intensity levels (see Methods for further description of PV+ cell selection). We found that conditional deletion of *Nrg1* from pyramidal cells does not alter the density of excitatory synapses that these neurons make onto PV+ interneurons (Figure 20). In contrast, we observed a significant reduction in the density of excitatory synapses targeting PV+ interneurons when pyramidal cells lacked *Nrg3* (Figure 20). Of note, quantification of VGlut1+/PSD95+ synapses that did not contain tdTomato (i.e., arising from non-recombined, wild-type pyramidal neurons) revealed comparable values between control and icKO mutant mice (Figure 21). These results reinforced the notion that synaptic deficits in neuregulin icKO mutant mice are cell autonomous.

1.5. Specificity of neuregulin synaptic function revealed by gain-of-function experiments

To further demonstrate the specificity of the synaptic deficits observed in *Nrg1* and *Nrg3* icKO mice, we performed gain-of-function experiments by electroporating plasmids encoding for Nrg1 or Nrg3 into pyramidal cell progenitors of the mouse brain embryo at E14.5. Electroporated pyramidal neurons were labelled by the expression of GFP, which was contained in the same plasmids. Then, we quantified the densities of inhibitory and excitatory synapses made onto or by

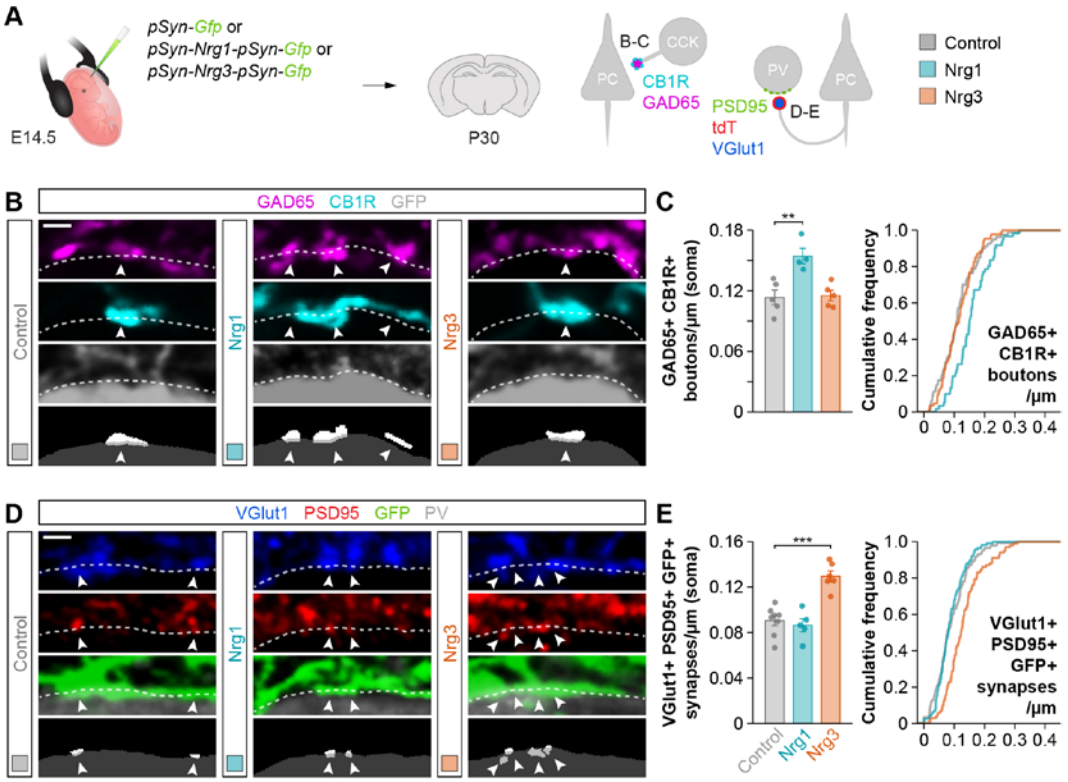

Figure 22 | **Gain-of-function experiments show the specificity of Nrg1 and Nrg3 in inhibitory and excitatory synapse formation.**

(**A**) Schematic of experimental design. Plasmids encoding for Nrg1 or Nrg3 and GFP were electroporated in pyramidal cell progenitors at E14.5, and the density of inhibitory and excitatory synapses that pyramidal cells receive or make onto interneurons was analysed at P30. (**B**) Confocal images (top three panels) and binary images (bottom panel) illustrating presynaptic boutons co-labelled with GAD65 (magenta) and CB1R (cyan) innervating the soma of GFP+ pyramidal cells (grey) in electroporation experiments. (**C**) Quantification of the density of GAD65+/CB1R+ boutons contacting GFP+ pyramidal cells in gain-of-function experiments. One-way ANOVA: $F = 11.100$, $P < 0.01$. Tukey's range test for post hoc comparison between control and experimental groups: for *pSyn-Nrg1-pSyn-Gfp*, $^{**}P < 0.01$; for *pSyn-Nrg3-pSyn-Gfp*, $P = 0.976$; n = 5 mice (80 cells) for *pSyn-Gfp* (control), 4 mice (61 cells) for *pSyn-Nrg1-pSyn-Gfp*, 5 mice (87 cells) for *pSyn-Nrg3-pSyn-Gfp*. (**E**) Confocal images (top three panels) and binary images (bottom panel) illustrating presynaptic VGlut1+ puncta (blue) in GFP+ axons (red) of pyramidal cells located in close apposition to PSD95+ clusters (green) in PV+ interneurons (gray) in electroporation experiments. (**F**) Quantification of the density of VGlut1+/PSD95+/GFP+ synapses contacting PV+ interneurons in gain-of-function experiments. One-way ANOVA: $F = 22.120$, $P < 0.001$. Tukey's range test for post hoc comparison between control and experimental groups: for *pSyn-Nrg1-pSyn-Gfp*, $P = 0.999$; for *pSyn-Nrg3-pSyn-Gfp*, $^{***}P < 0.001$; n = 8 mice (147 cells) for *pSyn-Gfp* (control), 5 mice (116 cells) for *pSyn-Nrg1-pSyn-Gfp*, 6 mice (101 cells) for *pSyn-Nrg3-pSyn-Gfp*.

Data represent mean s.e.m. The averages per animal and genotype are represented in bar graphs, and the distributions of values per cell are shown in cumulative frequency plots. Scale bars, 1 µm (B, D).

GFP+ pyramidal cells at P30. We observed that overexpression of Nrg1 resulted in a significant increase of somatic GAD65+/CB1R+ boutons innervating pyramidal cells, while Nrg3 overexpression did not change the density of these synaptic inputs (Figure 22B-C). In contrast, axonal excitatory synapses that pyramidal cells form onto PV+ interneurons were specifically augmented by overexpression of Nrg3, but not Nrg1 (Figure 22D-E). Altogether, these data add further support to the notion that Nrg1 and Nrg3 function in cortical pyramidal cells to induce the formation of inhibitory and excitatory synapses, respectively.

In conclusion, in chapter 1 we used a mouse genetic strategy and a gain-of-function approach to test the idea that two members of the gene family of ErbB4 ligands, neuregulins, act either in combination or in a non-redundant manner to specify the intricate connectivity required for cortical circuit function. Results presented here show that Nrg1 specifically control the development of inhibitory boutons that basket and chandelier cells make onto pyramidal cells, whereas Nrg3 selectively regulate the formation of excitatory synapses in pyramidal cell axons innervating cortical interneurons. Thus, two family-related synaptic proteins have segregated functions in the assembly of pyramidal cell-interneuron circuits during postnatal development.

CHAPTER 2. Subcellular distribution of Nrg1 and Nrg3 in cortical pyramidal cells

In Chapter 2, we asked whether the segregated functions of Nrg1 and Nrg3 in inhibitory and excitatory synapse formation could be due to their differential subcellular localisation in pyramidal cells in the cerebral cortex. To this end, I tested various techniques including standard immunohistochemical procedures, CRISPR/Cas9-based knock-in methodologies, and *in vivo* exogenous expression experiments through *in utero* electroporation in the mouse brain embryo.

Surface cell-adhesion proteins can specifically regulate brain connections according to their subcellular localisation, as shown in recent studies (Condomitti et al., 2018; Sando et al., 2019). Likewise, the precise targeting of neuregulins to specific subcellular compartments in cortical neurons could determine their differential function in the assembly of cortical circuits. We hypothesised that Nrg1 and Nrg3 differentially control the development of inhibitory and excitatory synapses in cortical circuits because they are targeted to different subcellular compartments in pyramidal cells. To test this hypothesis, we investigated whether Nrg1 and Nrg3 proteins are heterogeneously distributed in pyramidal cells. As a first approach, we performed a heat-induced antigen retrieval immuno-histochemistry protocol in coronal sections of the mouse brain at P30 using antibodies against Nrg1 and Nrg3. Antigen specificity of these antibodies was validated in a previous test where we stained samples from wild-type littermates and conditional mutant mice in which *Nrg1* and *Nrg3* have been conditionally deleted from cortical pyramidal cells ($Nex^{Cre/+};Nrg1^{F/F}$ and $Nex^{Cre/+};Nrg3^{F/F}$ mice, respectively) (Figure 14). To explore the subcellular distribution of Nrg1 and Nrg3 *in vivo*, endogenous protein expression was analysed in the hippocampus, a cortical region with segregated location of somas and neurites. On the one hand, a high density of Nrg1-labelled puncta was specifically decreased within the stratum pyramidale in CA1, a typical targeting area of inhibitory somatic synapses where the cell bodies of pyramidal cells are located (Figure 23A-D). The density of Nrg1+ puncta in the stratum radiatum, an area where neurites from pyramidal cells are predominantly found, was much lower and did not differ between mutant mice and control littermates (Figure 23A-D). Our results indicate that Nrg1 expression is concentrated in the hippocampal layer where pyramidal cell somas reside. Moreover, we observed Nrg1+ clusters within NeuN+ somas in close apposition to

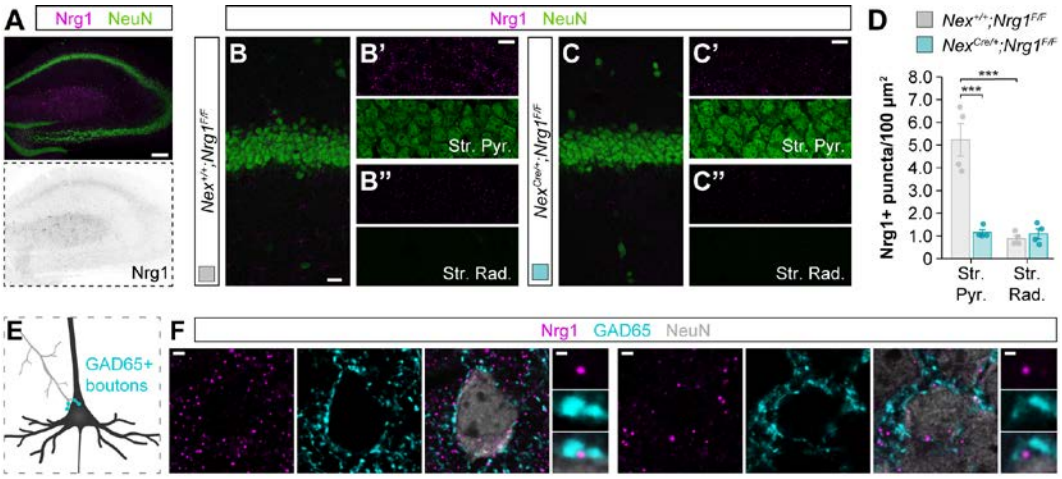

Figure 23 | **Localisation of endogenous Nrg1 in somas of cortical neurons, and specific targeting to inhibitory GABAergic clusters.**
(**A**) Expression of endogenous Nrg1 protein (magenta) in the hippocampus of wild-type mice at P30, co-stained with NeuN marker (green) to label the cell bodies of neurons. The bottom panel depicts Nrg1 staining in a color-inverted image. Note the intense expression of Nrg1 along the Stratum Pyramidale in CA1 region, where the somas of pyramidal cells reside. (**B-C**) Coronal sections through CA1 region of *Nex*$^{+/+}$*;Nrg1*$^{F/F}$ (B) and *Nex*$^{Cre/+}$*;Nrg1*$^{F/F}$ (C) mice at P30. Sections were processed for immunohistochemistry against Nrg1 (magenta) and NeuN (green). The high-magnification images illustrate Nrg1+ puncta expression within the stratum pyramidale and stratum radiatum. Note that endogenous Nrg1 protein is abundantly expressed in the stratum pyramidale, where the somas of pyramidal cells are located. (**D**) Quantification of the density of Nrg1+ clusters in regions of interest (ROIs) in both the stratum pyramidale and stratum radiatum of conditional mutant mice and wild-type littermates. Stratum pyramidale: Two-tailed Student's *t*-test, ***P < 0.001, n = 4 mice (40 ROIs) for *Nex*$^{+/+}$*;Nrg1*$^{F/F}$, n = 4 mice (40 ROIs) for *Nex*$^{Cre/+}$*;Nrg1*$^{F/F}$. Stratum radiatum: Two-tailed Student's *t*-test, P = 0.980, n = 4 mice (40 ROIs) for *Nex*$^{+/+}$*;Nrg1*$^{F/F}$, n = 4 mice (40 ROIs) for *Nex*$^{+/+}$*;Nrg1*$^{F/F}$. Two-tailed Student's *t*-test between stratum pyramidale and stratum radiatum in wild-type mice, ***P < 0.001. (**E**) Schematic illustrating the synaptic innervation of GABAergic boutons (labelled with the presynaptic marker GAD65) onto the somatic compartment of cortical pyramidal cells. (**F**) Colocalisation of endogenous Nrg1 (magenta) with GAD65 (cyan) in the soma of NeuN+ cells in both the cerebral cortex (left) and the hippocampus (right). Data are shown as mean ± s.e.m. Scale bar, 100 µm (A), 20 µm (B-C) and 10 µm (high magnifications), and 2 µm (F) and 0.5 µm (high magnifications).

GAD65+ inhibitory boutons (Figure 23E-F). On the other hand, Nrg3+ clusters were found to be highly enriched in contact to the somatodendritic compartment of PV+ interneurons, both in the hippocampus and neocortex (Figure 24). Nrg3 expression around PV+ interneurons was dramatically reduced in *Nrg3* conditional mutant mice (Figure 24A-C). Notably, Nrg3+ clusters were found to be precisely located within VGlut1+ presynaptic boutons contacting PV+ interneurons (Figure 24D-E). This remarkable expression of Nrg3 in excitatory inputs innervating cortical PV+ interneurons is in agreement with previous findings (Muller et al., 2018).

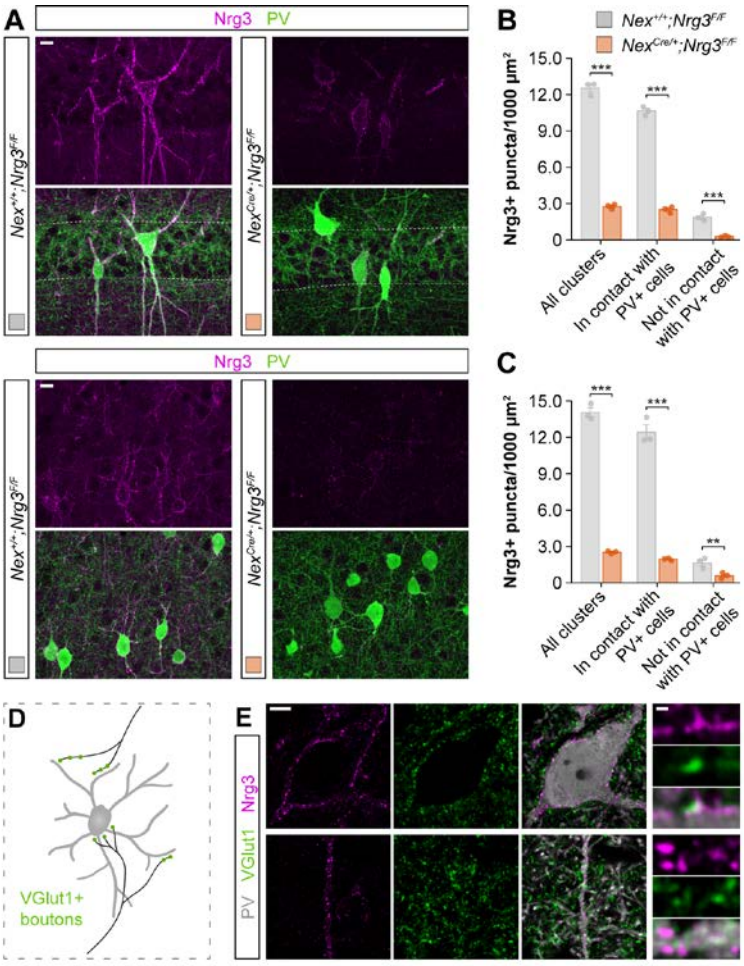

Figure 24 | **Localisation of endogenous Nrg3 in the neuropil of the neocortex, and specific targeting to excitatory presynaptic boutons innervating PV+ interneurons.** (**A**) Coronal sections through CA1 region (top) and cerebral cortex (bottom) of *Nex*$^{+/+}$*;Nrg3*$^{F/F}$ and *Nex*$^{Cre/+}$*;Nrg3*$^{F/F}$ mice at P30. Sections were processed for immunohistochemistry against Nrg3 (magenta) and PV (green). Endogenous Nrg3 protein is primarily found as a punctate pattern in close apposition to PV+ cell bodies. Note that the conditional deletion of *Nrg3* is driven by the transgenic line *Nex*^{Cre}, which only recombines the LoxP site-flanked *Nrg3* allele in pyramidal cells. Therefore, Nrg3 expression by PV+ cells can still be appreciated in the neocortex of this conditional KO model. (**B**) Quantification of the total density of Nrg3+ clusters in regions of interest (ROIs) in the CA1 region of conditional mutant mice and wild-type littermates, and quantification of the density of Nrg3+ clusters in apposition to, or not in contact with, PV+ cell bodies. All clusters: Two-tailed Student's *t*-test, ***$P < 0.001$, n = 3 mice (36 ROIs) for *Nex*$^{+/+}$*;Nrg3*$^{F/F}$, n = 3 mice (36 ROIs) for *Nex6*$^{Cre/+}$*;Nrg3*$^{F/F}$. In contact with PV+ cells: Two-tailed Student's *t*-test, ***$P < 0.001$, n = 3 mice (44 ROIs) for *Nex*$^{+/+}$*;Nrg3*$^{F/F}$, n = 3 mice (36 ROIs) for *Nex*$^{Cre/+}$*;Nrg3*$^{F/F}$. Not in contact with PV+ cells: Two-tailed Student's *t*-test, ***$P < 0.001$, n = 3 mice (36 ROIs) for *Nex*$^{+/+}$*;Nrg3*$^{F/F}$, n = 3 mice (36 ROIs) for *Nex*$^{Cre/+}$*;Nrg3*$^{F/F}$. (**C**) Quantification of the total density of Nrg3+ clusters in regions of interest (ROIs) in the cerebral cortex of conditional mutant mice and wild-type littermates, and quantification of the density of Nrg3+ clusters in apposition to, or not in contact with, PV+ cell bodies. All clusters: Two-tailed Student's *t*-test, ***$P < 0.001$, n = 3 mice (36 ROIs) for *Nex*$^{+/+}$*;Nrg3*$^{F/F}$, n = 3 mice (36 ROIs) for *Nex*$^{Cre/+}$*;Nrg3*$^{F/F}$. In contact with PV+ cells: Two-tailed Student's t-test, ***$P < 0.001$, n = 3 mice (36 ROIs) for *Nex*$^{+/+}$*;Nrg3*$^{F/F}$, n = 3 mice (36 ROIs) for *Nex*$^{Cre/+}$*;Nrg3*$^{F/F}$. Not in contact with PV+ cells: Two-tailed
(*Figure legend continues in next page.*)

Student's *t*-test, ***P* = 0.01, n = 3 mice (36 ROIs) for *Nex*$^{+/+}$;*Nrg3*$^{F/F}$, n = 3 mice (36 ROIs) for *Nex*$^{Cre/+}$;*Nrg3*$^{F/F}$. (**D**) Schematic illustrating the synaptic innervation of glutamatergic boutons (labelled with the presynaptic marker VGlut1) onto cortical PV+ interneurons. (**E**) Colocalisation of endogenous Nrg3 (magenta) with VGlut1 (green) within excitatory inputs innervating PV+ interneurons in the neocortex.
Data are shown as mean ± s.e.m. Scale bar, 10 µm (A), 5 µm (E) and 0.5 µm (high magnifications).

Altogether, these data indicate that the endogenous expression patterns of Nrg1 and Nrg3 are strikingly different in the cerebral cortex and suggest that they might be differentially distributed in specific compartments of pyramidal cells. Therefore, we then decided to develop techniques to study the subcellular localisation of neuregulins in single pyramidal cells.

We devised a CRISPR/Cas9-mediated endogenous protein tagging strategy, based on a published technique named SLENDR (Mikuni et al., 2016), to tag neuregulins with an HA tag epitope *in vivo* and monitor the resulting tagged proteins in single pyramidal cells in cortical circuits. We generated plasmids encoding for gRNAs and Cas9 protein in order to edit the specific N- and C-terminal regions of *Nrg1* and *Nrg3* loci after *in utero* electroporation of pyramidal cell progenitors at E14.5. We co-electroporated single-strand oligonucleotides that contain an HA tag epitope flanked by 70-90 base pair arms homologous to the targeted region of the genome. An initial test of this strategy resulted in

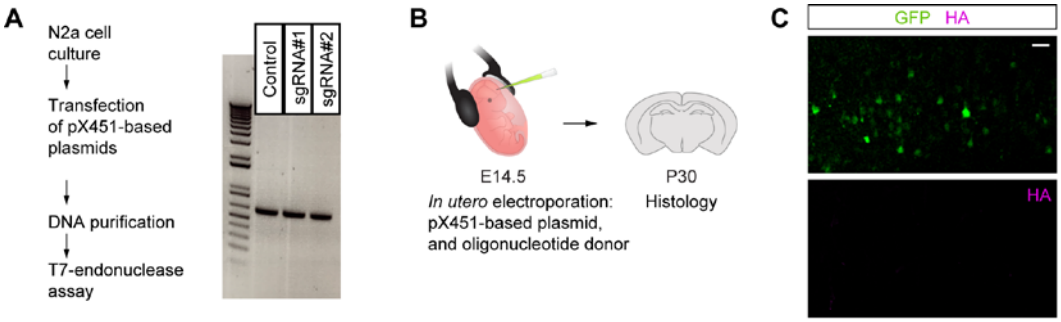

Figure 25 | **Validation of CRISPR/Cas9-mediated endogenous tagging of *Nrg1* and *Nrg3* in cortical pyramidal cells *in vivo*.**
(**A**) *In vitro* test to evaluate the efficiency in DNA cutting of sgRNA constructs in cultured N2a cells by the T7-endonuclease assay (left). The gel shows the absence of DNA cutting in transfected conditions similar to the control experiment (right). (**B**) *In vivo* validation of the CRISPR/Cas9 constructs (sgRNA#1 in (A)) together with single-stranded oligonucleotides for HA integration in the *Nrg3* loci. (**C**) Electroporated brain section stained with anti-GFP (green) and anti-HA (magenta).
Scale bar, 40 µm (C).

unsuccessful labelling of the endogenous protein in cortical pyramidal cells (Figure 25A-B). When we tested the editing efficiency of the designed gRNAs *in vitro* after transfection of the plasmids into N2a cells, we detected absence of DNA cutting (Figure 25C). It has been noticed that gRNAs targeting distinct regions of the same gene might show different efficiencies of DNA editing (Mikuni et al., 2016; Nishiyama et al., 2017), which implies that further testing of various gRNAs targeting different genomic regions within *Nrg1* and *Nrg3* loci will be required. Besides, it has been previously reported that this method yields a low percentage of tagging efficiency (Mikuni et al., 2016). Since novel CRISPR-based knock-in methodologies have been recently developed that could potentially overcome current technical limitations (Gao et al., 2019; Willems et al., 2019), future work will be required to successfully tag neuregulin proteins in the mouse brain *in vivo*.

In order to characterise pyramidal cell-specific subcellular distribution of neuregulins, we generated new molecular tools to be specifically delivered and expressed into pyramidal cells *in vivo*. We cloned plasmids encoding for Nrg1 or Nrg3 with a single HA tag epitope inserted into the extracellular region of the protein. These plasmids also contained a GFP gene to label the cell bodies of the electroporated neurons. We used *in utero* electroporation to express these constructs in cortical pyramidal cell progenitors at E14.5 and monitor the localisation of both proteins at specific subcellular compartments (Figure 26A). When examining the expression patterns of HA-tagged neuregulin proteins in upper layers of the somatosensory cortex at P21, we found that Nrg1 and Nrg3 exhibit differential subcellular localisation in pyramidal cells: Nrg1 is spatially restricted to the perisomatic compartment of pyramidal cells, whereas Nrg3 is highly enriched in the neuropil (Figure 26B). Quantification of the percentage of HA+/GFP+ somas shows that the vast majority of pyramidal cells target Nrg1 protein to their somatic compartment, whereas Nrg3 is rarely found in somas (Figure 26C). Analysis of the overlapping area of HA+ signal in GFP+ neuronal processes shows that Nrg3, but not Nrg1, is abundantly expressed in the neuropil of the electroporated pyramidal cells (Figure 26C). These results revealed a segregated targeting of Nrg1 and Nrg3 to distinct subcellular compartments within cortical pyramidal cells.

We next explored the synaptic localisation of Nrg1 and Nrg3 with markers of inhibitory and excitatory synapses. We observed that Nrg1+ puncta colocalise in synaptic clusters with gephyrin, a scaffolding protein present in the postsynaptic membrane of inhibitory synapses (Figure 27B). In addition, Nrg1+ puncta were

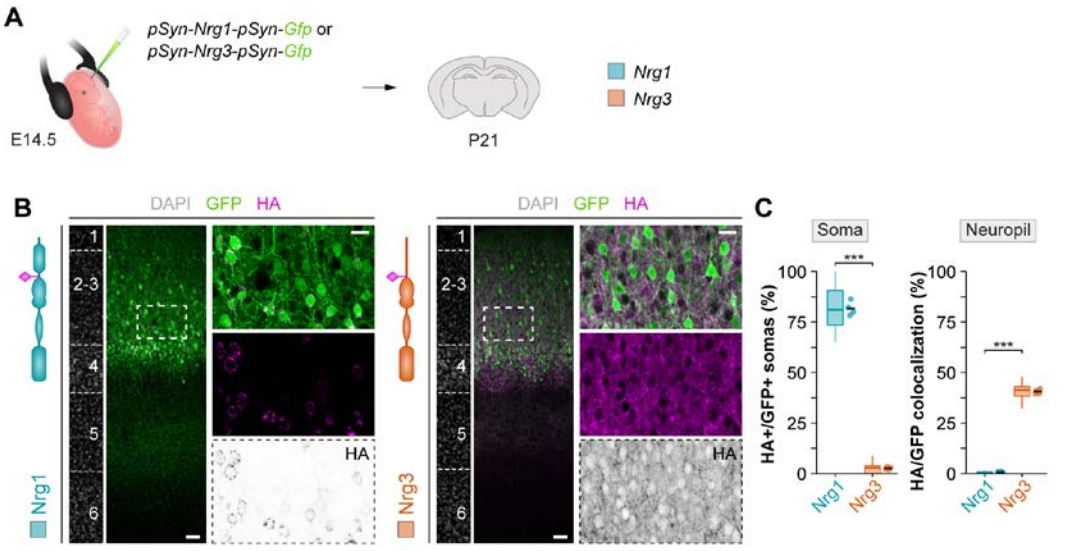

Figure 26 | **Distinct subcellular distribution of Nrg1 and Nrg3 in cortical pyramidal cells during postnatal development**.
(**A**) Schematic of experimental design. Plasmids encoding HA-tagged neuregulins and GFP were electroporated in pyramidal cell progenitors at E14.5, and the subcellular localisation of neuregulins was analysed at P21. (**B**) Coronal sections through somatosensory cortex of P21 mice following *in utero* electroporation of *pSyn-Nrg1-pSyn-Gfp* or *pSyn-Nrg3-pSyn-Gfp* plasmids at E14.5. Sections were processed for immunohistochemistry against GFP (green) and HA (magenta) and counterstained with DAPI (gray). The high-magnification images illustrate the localisation of HA-tagged neuregulins in GFP+ pyramidal cells. The bottom panel depicts HA staining in a colour-inverted image. Dotted squares indicate the localisation of the cells shown in the high magnification images. (**C**) Quantification of the localisation of HA+ neuregulin in the soma and neuropil of GFP+ pyramidal cells. Soma: Two-tailed Student's *t*-test, ***$P < 0.001$; n = 4 mice (32 regions of interest, ROIs) for *pSyn-Nrg1-pSyn-Gfp*, n = 4 mice (32 ROIs) for *pSyn-Nrg3-pSyn-Gfp*. Neuropil: Two-tailed Student's *t*-test, ***$P < 0.001$; n = 4 mice (32 ROIs) for *pSyn-Nrg1-pSyn-Gfp*, n = 4 mice (32 ROIs) for *pSyn-Nrg3-pSyn-Gfp*.
Data from the distributions of ROIs are shown as box plots, and the adjacent data points and lines represent the averages per animal and averaged mean per group, respectively. Scale bars, 50 µm (A) and 20 µm (high magnification).

often opposed to presynaptic markers of inhibitory cells, such as CB1R, GAD65, and GAD67, targeting the soma and AIS of pyramidal cells (Figure 27C-H). Colocalisation of HA-tagged Nrg1 with Syt2, a marker for PV+ basket cell synapses, was not tested since we did not observe any changes in the density of these synaptic inputs onto pyramidal cell somas in Nrg1 icKO mice (Figure 19). In contrast, we found that HA-tagged Nrg3 colocalises to boutons expressing VGlut1, a characteristic presynaptic protein of excitatory glutamatergic synapses, that contact neighbouring parvalbumin-expressing (PV+) interneurons (Figure 28C-D). GFP+ axon terminals from electroporated L2/3 pyramidal cells also expressed HA-tagged Nrg3 in their presynaptic boutons innervating L5 PV+ interneurons,

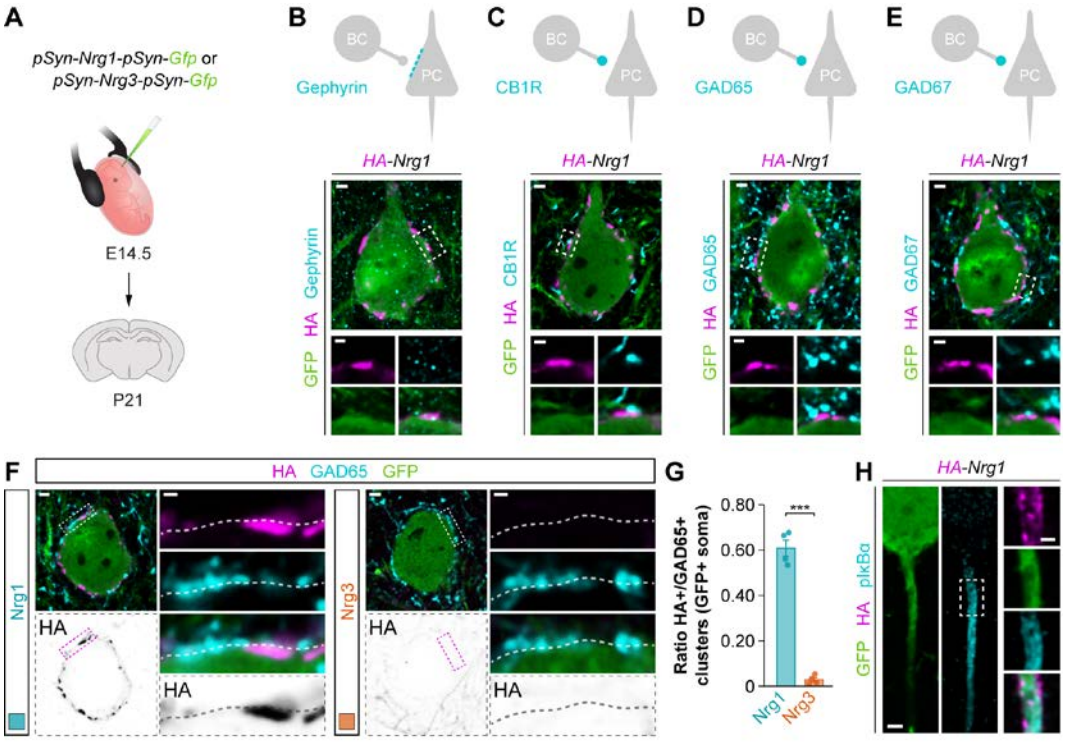

Figure 27 | **Synaptic targeting of Nrg1 to inhibitory postsynaptic clusters in the perisomatic compartment of pyramidal cells.**
(**A**) Schematic of experimental design. Plasmids encoding HA-tagged neuregulins and GFP were electroporated in pyramidal cell progenitors at E14.5, and the synaptic colocalisation of neuregulins with different synaptic markers was analysed at P21. (**B-E**) Somatic Nrg1+ clusters (magenta) colocalise with the postsynaptic marker gephyrin (cyan) (B), and are found in close proximity to presynaptic GABAergic boutons (cyan) labelled by CB1R (C), GAD65 (D), and GAD67 (E). (**F**) Colocalisation of HA-tagged Nrg1 (left) and HA-tagged Nrg3 (right) (magenta) with soma-targeting GAD65+ boutons (cyan) in electroporated GFP+ pyramidal cells (green). The bottom panel depicts HA staining in a color-inverted image. The high-magnification images illustrate the localization of HA-tagged neuregulins contacted by presynaptic GAD65+ boutons. (**G**) Quantification of the proportion of GAD65+ boutons that colocalise with HA-tagged Nrg clusters within the soma of electroporated GFP+ pyramidal cells. Two-tailed Student's *t*-test: ***$P < 0.001$; n = 4 mice (34 cells) for *pSyn-Nrg1-pSyn-Gfp*, n = 4 mice (32 cells) for *pSyn-Nrg3-pSyn-Gfp*. (**H**) Nrg1+ clusters (magenta) are also found in the axon initial segment (cyan) of pyramidal cells. Abbreviations: BC, basket cell; ChC, chandelier cell; PC, pyramidal cell. Data represent mean ± s.e.m. The average per animal and electroporation condition are shown in bar graphs. Scale bars, 2 µm (B, C, D, E, F, H), and 0.5 µm (high magnifications).

a natural target of superficial pyramidal cells in the cerebral cortex (Figure 28E-F). Notably, Nrg3+ puncta innervating PV+ interneurons were opposed to postsynaptic clusters expressing PSD95, the major scaffolding protein in the excitatory postsynaptic density (Figure 28H). We also detected that most postsynaptic densities labelled by ErbB4 in PV+ interneurons were contacted by Nrg3+ boutons from GFP+ axon terminals (Figure 27I-J). Importantly, these findings are

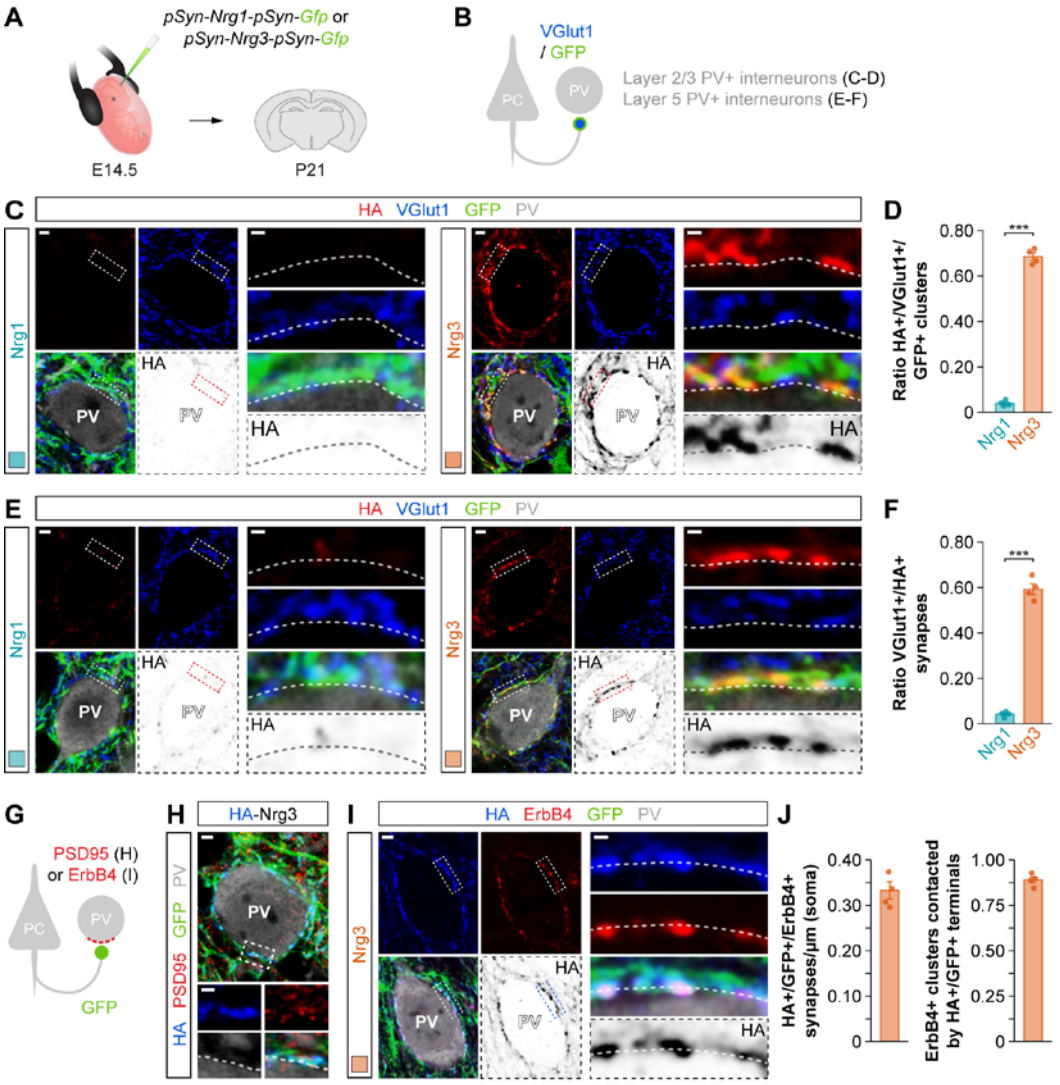

Figure 28 | **Synaptic targeting of Nrg3 to presynaptic boutons in pyramidal cell axons in the cerebral cortex.**

(**A-B**) Schematic of experimental design. Plasmids encoding HA-tagged neuregulins and GFP were electroporated in pyramidal cell progenitors at E14.5 (A), and the synaptic colocalisation of neuregulins with glutamatergic presynaptic boutons within GFP+ axon terminals was analysed at P21 (B). (**C**) Colocalisation of HA-tagged Nrg1 (left) and HA-tagged Nrg3 (right) (red) with presynaptic VGlut1+ boutons (blue) in GFP+ pyramidal cell axons (green) contacting PV+ interneurons. The color-inverted images correspond to HA staining and illustrate the localisation of HA-tagged Nrg clusters opposed to PV+ cell bodies. The high-magnification images illustrate the colocalisation of HA-tagged neuregulins with excitatory VGlut1+ boutons. (**D**) Quantification of the proportion of VGlut1+ boutons that colocalise with HA-tagged Nrg clusters in axon terminals of electroporated GFP+ pyramidal cells. Two-tailed Student's *t*-test: ***$P < 0.001$; n = 4 mice (40 cells) for *pSyn-Nrg1-pSyn-Gfp*, n = 4 mice (50 cells) for *pSyn-Nrg3-pSyn-Gfp*. (**E**) Colocalisation of HA-tagged Nrg1 (left) and HA-tagged Nrg3 (right) (red) with presynaptic VGlut1+ boutons (blue) in GFP+ pyramidal cell axons (green) contacting PV+ interneurons (gray) in L5. (**F**) Quantification of the proportion of VGlut1+ boutons that colocalise with HA-tagged neuregulin clusters in axons of electroporated pyramidal cells contacting L5 PV+ cells. Two-tailed Student's *t*-test: ***$P < 0.001$; n = 4 mice (42 cells) for *pSyn-Nrg1-pSyn-Gfp*, n = 4 mice (34 cells) for *pSyn-Nrg3-pSyn-Gfp*. (**G**) Synaptic

(*Figure legend continues in next page.*)

colocalisation of neuregulins with markers of the postsynaptic density was analysed in PV+ cell somas at P21. (**H-I**) Axonal Nrg3+ clusters (blue) are found in close apposition to postsynaptic densities (red) labelled by PSD95 (**H**) and ErbB4 (**I**). (**J**) . Quantification of the density of synapses, co-labelled with HA-tagged Nrg3 and GFP at the presynaptic site and ErbB4 at the postsynaptic site, innervating PV+ cell somas (left), and the proportion of ErbB4+ postsynaptic densities within PV+ interneurons that are contacted by HA+/GFP+ presynaptic boutons (right).
Data represent mean ± s.e.m. The average per animal and electroporation condition are shown in bar graphs. Scale bars, 2 µm (C, E, H, I), and 0.5 µm (high magnifications).

are consistent with the analysis of endogenous neuregulin expression (Figures 23-24), and further support the notion that neuregulins exhibit specific subcellular distributions in the mouse neocortex *in vivo*. In conclusion, our data demonstrate that Nrg1 and Nrg3 are differentially targeted to inhibitory and excitatory synapses, respectively, in cortical pyramidal cells (Figure 29).

In conclusion, the results from Chapter 2 show the subcellular logic of Nrg1 and Nrg3 beyond their abundant cellular expression in cortical pyramidal neurons. These experiments reveal a striking segregation in the subcellular distribution of neuregulins in cortical pyramidal cells: Nrg1 is enriched in the postsynaptic specialisation of inhibitory synapses targeting the soma of pyramidal cells, whereas Nrg3 is mostly restricted to excitatory presynaptic terminals contacting interneurons. The differential subcellular localisation of Nrg1 and Nrg3 in the somatic and axonal compartments of pyramidal cells, respectively, is consistent with the specific inhibitory and excitatory synaptic deficits reported in Chapter 1. Altogether, these data suggest the hypothesis that the subcellular targeting of both neuregulins to the cell surface is regulated by a differential sorting.

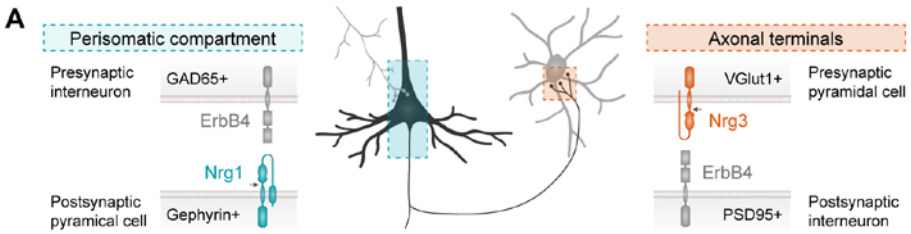

Figure 29 | **Differential subcellular compartmentalisation and synaptic targeting of Nrg1 and Nrg3 in cortical pyramidal cells.**
(**A**) Schematic drawing illustrates the subcellular localisation of Nrg1, Nrg3, and ErbB4 in cortical circuits.

CHAPTER 3. Mechanisms of synaptic sorting and function of Nrg1 and Nrg3

In Chapter 3, we explored the mechanisms of neuregulin synaptic function within the specific subcellular compartments identified in the previous chapter. *In utero* electroporation of mutant Nrg constructs provided us with a robust gain-of-function paradigm to interrogate which protein domains of Nrg1 and Nrg3 determine the observed subcellular selectivity in synapse formation.

3.1. Compartment-specific dependence of neuregulin function in synapse formation

Despite the various important roles of Nrg/ErbB4 signalling pathway in brain development, the mechanisms of action of different neuregulins have remained largely unclear. The extracellular EGF-like domain of neuregulins binds to ErbB4 homo- or heterodimers, inducing tyrosine phosphorylation of its kinase domains and triggering several intracellular signalling cascades. Hence, the signalling capacity of neuregulins depends on their extracellular EGF-like domain. Nrg1 and Nrg3 are targeted to distinct compartments in cortical pyramidal cells to presumably interact with pre- or postsynaptic ErbB4 receptors expressed in interneurons, respectively. Therefore, it is plausible that synaptogenic signalling in inhibitory and excitatory cortical synapses might differ characteristically based on Nrg/ErbB4 binding properties. Interestingly, the EGF-like domain of Nrg1 activates ErbB4 tyrosine kinase signalling with nanomolar affinity in an *in vitro* assay, whereas the EGF-like domain of Nrg3 appears to be a poor signalling molecule (Müller et al., 2018). Are the differential binding properties of these two ligands physiologically relevant *in vivo*, and are differences in Nrg/ErbB4 signalling necessary to specify inhibitory and excitatory synaptogenesis?

To address these questions, we generated HA-tagged constructs of Nrg1 and Nrg3 in which we swapped their EGF-like domains and performed *in utero* electroporation to express them in pyramidal cells. We observed that both chimeric constructs were efficiently expressed and transported to the subcellular compartments characteristic of wild-type Nrg1 and Nrg3 proteins: Nrg1 carrying

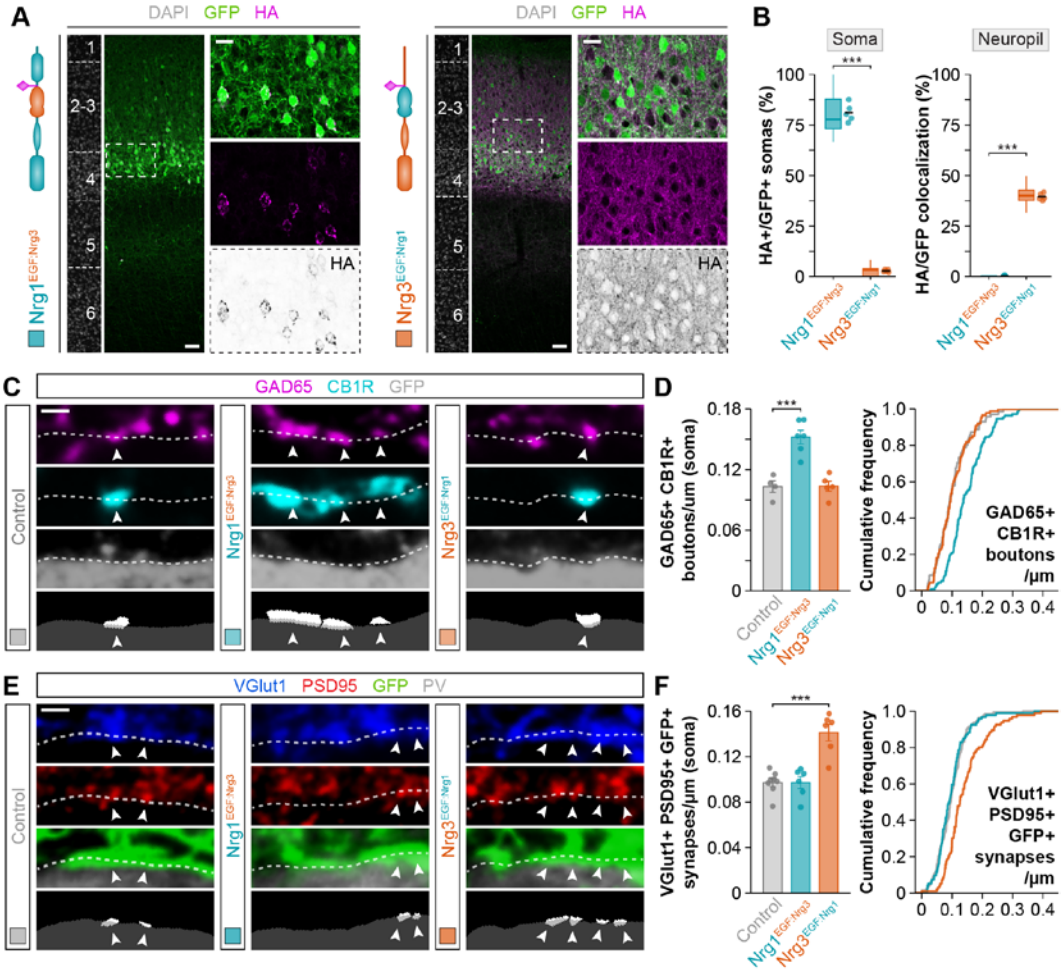

Figure 30 | **Neuregulin-dependent synapse formation requires compartment-specific localisation but not receptor binding differences in the EGF-like domain.** (**A**) Coronal sections through somatosensory cortex of P30 mice following *in utero* electroporation of *pSyn-Nrg1$^{EGF:Nrg3}$-pSyn-Gfp* or *pSyn-Nrg3$^{EGF:Nrg1}$-pSyn-Gfp* plasmids at E14.5. Sections were processed for immunohistochemistry against GFP (green) and HA (magenta) and counterstained with DAPI (grey). The high-magnification images illustrate the localisation of HA-tagged neuregulins in GFP+ pyramidal cells. The bottom panel depicts HA staining in a colour-inverted image. Dotted squares indicate the localisation of the cells shown in the high-magnification images. The schematics illustrate the structure of the chimeric neuregulins in which the EGF-like domain was swapped between Nrg1 and Nrg3. (**B**) Quantification of the localisation of HA+ neuregulin in the soma and neuropil of GFP+ pyramidal cells. Soma: Two-tailed Student's *t*-test: ***$P < 0.001$; n = 5 mice (40 regions of interest, ROIs) for *pSyn-Nrg1$^{EGF:Nrg3}$-pSyn-Gfp*, n = 5 mice (40 ROIs) for *pSyn-Nrg3$^{EGF:Nrg1}$-pSyn-Gfp*. Neuropil: Two-tailed Student's *t*-test, ***$P < 0.001$, n = 5 mice (40 ROIs) for *pSyn-Nrg1$^{EGF:Nrg3}$-pSyn-Gfp*, n = 5 mice (40 ROIs) for *pSyn-Nrg3$^{EGF:Nrg1}$-pSyn-Gfp*. (**C**) Confocal images (top three panels) and binary images (bottom panel) illustrating presynaptic boutons co-labelled with GAD65 (magenta) and CB1R (cyan) innervating the soma of GFP+ pyramidal cells (grey) in EGF-like domain swapping experiments. (**D**) Quantification of the density of GAD65+/CB1R+ boutons contacting GFP+ pyramidal cells in chimeric gain-of-function experiments. One-way ANOVA: $F = 23.260$, $P < 0.001$. Tukey's range test for post hoc comparison between control and experimental groups: for *pSyn-Nrg1$^{EGF:Nrg3}$-pSyn-Gfp*, $P = 0.997$; for *pSyn-Nrg3$^{EGF:Nrg1}$-pSyn-Gfp*, , ***$P < 0.001$; n = 4 mice (71 cells) for *pSyn-Gfp* (control), 6
(*Figure legends continues in next page.*)

mice (110 cells) for *pSyn-Nrg1*$^{EGF:Nrg3}$*-pSyn-Gfp*, 5 mice (88 cells) for *pSyn-Nrg3*$^{EGF:Nrg1}$*-pSyn-Gfp*. (**E**) Confocal images (top three panels) and binary images (bottom panel) illustrating presynaptic VGlut1+ puncta (blue) in GFP+ axons (red) of pyramidal cells located in close apposition to PSD95+ clusters (green) in PV+ interneurons (gray) in EGF-like domain swapping experiments. (**F**) Quantification of the density of VGlut1+/PSD95+/GFP+ synapses contacting PV+ interneurons in chimeric gain-of-function experiments. One-way ANOVA: $F = 21.730$, $P < 0.001$. Tukey's range test for post hoc comparison between control and experimental groups: for *pSyn-Nrg1*$^{EGF:Nrg3}$*-pSyn-Gfp*, $P = 0.999$; for *pSyn-Nrg3*$^{EGF:Nrg1}$*-pSyn-Gfp*, ***$P < 0.001$; n = 8 mice (143 cells) for *pSyn-Gfp* (control), 6 mice (94 cells) for *pSyn-Nrg1*$^{EGF:Nrg3}$*-pSyn-Gfp*, 6 mice (96 cells) for *pSyn-Nrg3*$^{EGF:Nrg1}$*-pSyn-Gfp*.
Data from the distributions of ROIs are shown as box plots, and the adjacent data points and lines represent the averages per animal and averaged mean per group, respectively. Data in synaptic quantifications represent mean ± s.e.m. The averages per animal and genotype are represented in bar graphs, and the distributions of values per cell are shown in cumulative frequency plots. Scale bars, 50 µm (A) and 20 µm (high magnification), and 1 µm (C, E).

the ErbB4-activating EGF-like domain of Nrg3 (Nrg1$^{EGF:Nrg3}$) localised to the soma, whereas Nrg3 carrying the ErbB4-activating EGF-like domain of Nrg1 (Nrg3$^{EGF:Nrg1}$) localised to the neuropil (Figure 30A-B). In addition, synaptic targeting of Nrg1$^{EGF:Nrg3}$ to inhibitory postsynaptic sites and of Nrg3$^{EGF:Nrg1}$ to excitatory presynaptic boutons was similar to that observed with Nrg1 and Nrg3 wild-type constructs (Figures 31 and 32).

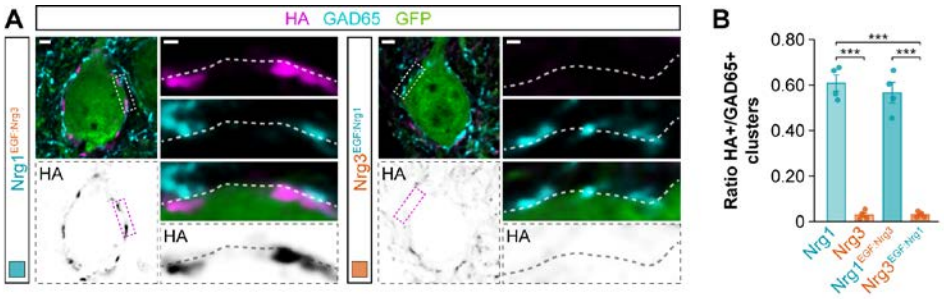

Figure 31 | **Synaptic targeting of EGF-like domain-swapping neuregulin constructs to inhibitory postsynaptic clusters in the somatic compartment of cortical pyramidal cells.**
(**A**) Colocalisation of HA-tagged chimeric Nrg1$^{EGF:Nrg3}$ (left) and Nrg3$^{EGF:Nrg1}$ (right) (magenta) with soma-targeting GAD65+ boutons (cyan) in electroporated GFP+ pyramidal cells (green). The bottom panel depicts HA staining in a color-inverted image. The high-magnification images illustrate the localisation of HA-tagged neuregulins contacted by presynaptic GAD65+ boutons. (**B**) Quantification of the proportion of GAD65+ boutons that colocalise with Nrg clusters in the soma of GFP+ pyramidal cells. Tukey's range test for *post hoc* comparison between wild-type Nrg1 construct and chimeric Nrg constructs: $P = 0.745$, n = 4 mice (32 cells) for *pSyn-Nrg1*$^{EGF:Nrg3}$*-pSyn-Gfp*; ***$P < 0.001$, n = 4 mice (32 cells) for *pSyn-Nrg3*$^{EGF:Nrg1}$*-pSyn-Gfp*; ***$P < 0.001$, for comparison between chimeric Nrg constructs. Note that data for wild-type Nrg constructs are the same data shown in Figure 27.
Data are shown as mean ± s.e.m. Scale bar, 2 µm (A) and 0.5 µm (high magnifications).

We then examined how expression of these constructs influenced inhibitory synaptic inputs and excitatory synaptic output in electroporated pyramidal cells in the somatosensory cortex at P30. Consistent with its specific somatic localisation, we found that the receptor-binding chimeric construct of Nrg1 ($Nrg1^{EGF:Nrg3}$) was able to increase the density of CCK+ presynaptic boutons innervating the soma of GFP+ pyramidal cells, as visualized by GAD65/CB1R colocalisation, in similar quantities than wild-type Nrg1 (Figure 30C-D). However, overexpression of the receptor-binding chimeric construct of Nrg3 ($Nrg3^{EGF:Nrg1}$), which is efficiently targeted to the axonal compartment, did not result in significant changes in CCK+ bouton density (Figure 30C-D).

To examine the synaptogenic properties of neuregulin chimeric constructs in the axonal compartment, we measured VGlut1+/PSD95+ synapse density within GFP+ pyramidal cell axons targeting PV+ interneurons. The receptor-binding chimeric construct of Nrg3 ($Nrg3^{EGF:Nrg1}$) significantly augmented the density of axonal excitatory synapses that electroporated pyramidal cells made onto PV+ interneurons (Figure 30E-F). In contrast, overexpression of the receptor-binding chimeric construct of Nrg1 ($Nrg1^{EGF:Nrg3}$), which is targeted to the somatic region, did not change excitatory synapse densities in axon terminals (Figure 30E-F). Thus, chimeric neuregulins containing the EGF-like domain of the homologous

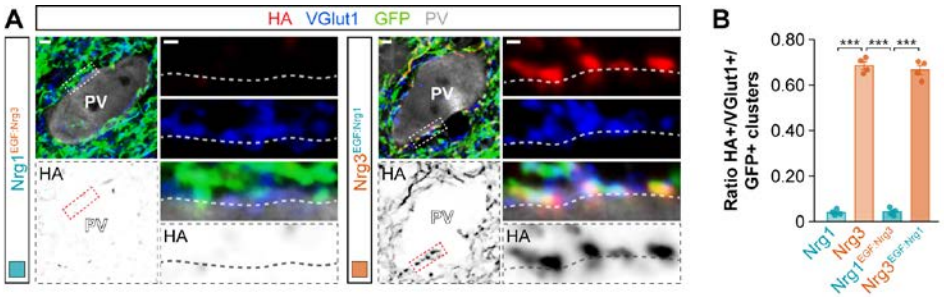

Figure 32 | **Synaptic targeting of EGF-like domain-swapping neuregulin constructs to excitatory presynaptic boutons innervating PV+ interneurons.**
(**A**) Colocalisation of HA-tagged chimeric $Nrg1^{EGF:Nrg3}$ (left) and $Nrg3^{EGF:Nrg1}$ (red) with presynaptic VGlut1+ boutons (blue) in GFP+ pyramidal cell axons (green) contacting PV+ interneurons (gray). The bottom panel depicts HA staining in a color-inverted image. The high magnification images illustrate the colocalisation of HA-tagged neuregulins with excitatory VGlut1+ boutons. (**B**) Quantification of the proportion of VGlut1+ boutons that colocalise with HA-tagged Nrg clusters in axon terminals of electroporated GFP+ pyramidal cells. Tukey's range test for *post hoc* comparison between wild-type Nrg3 construct and chimeric Nrg constructs: ***$P < 0.001$, n = 4 mice (42 cells) for *pSyn-*$Nrg1^{EGF:Nrg3}$*-pSyn-Gfp*; $P = 0.775$, n = 4 mice (39 cells) for *pSyn-*$Nrg3^{EGF:Nrg1}$*-pSyn-Gfp*; ***$P < 0.001$, for comparison between chimeric Nrg constructs. Note that data for wild-type Nrg1 and Nrg3 constructs are the same data shown in Figure 28.
Data are shown as mean ± s.e.m. Scale bar, 2 µm (A) and 0.5 µm (high magnifications).

neuregulin member can recapitulate the specific synaptic functions of wild-type Nrg1 and Nrg3 *in vivo*, indicating a tight dependence of neuregulin subcellular localisation and synaptic function. These findings also suggest that, surprisingly, Nrg1 and Nrg3 functions in inhibitory and excitatory synapse formation do not depend on differential binding properties with the trans-synaptic ErbB4 receptor, but on their selective sorting to the somatic and axonal compartment, respectively.

3.2. Role of the C-terminal domain of Nrg1 and Nrg3 in subcellular sorting and synaptic function

Since the extracellular EGF-like domain of Nrg1 and Nrg3 is not responsible for the differential functions of these two family-related synaptic molecules, we hypothesised that the intracellular region (C-terminal) of these proteins might be important for their localisation and, therefore, differential physiological roles. To test this idea, we engineered HA-tagged constructs in which the C-terminal domains were swapped between both neuregulins, and used *in utero* electroporation to express them in cortical pyramidal cells. We observed that the C-terminal domain of Nrg3 was sufficient to re-route some Nrg1 from the soma to the neuropil ($Nrg1^{Ct:Nrg3}$; Figure 33A-B), although with limited efficiency compared to wild-type Nrg3 (Figure 26B-C). Accordingly, the proportion of VGlut1+/GFP+ boutons innervating PV+ interneurons that express the chimeric $Nrg1^{Ct:Nrg3}$ protein was significantly reduced compared to Nrg3 wild-type protein, which suggested that this chimeric protein is less efficiently expressed and/or targeted to axonal excitatory synapses than the wild-type form (Figure 34). We also found that the C-terminal domain of Nrg1 is sufficient to sequester a large fraction of Nrg3 in the soma, dramatically decreasing its normal targeting to the neuropil ($Nrg3^{Ct:Nrg1}$; Figure 33A-B, and Figure 34). Remarkably, the chimeric $Nrg3^{Ct:Nrg1}$ proteins found in the soma of electroporated GFP+ pyramidal cells were precisely located in postsynaptic clusters adjacent to inhibitory inputs (Figure 35). Because it has been previously noticed that the C-terminal domain of Nrg1 display backward signalling from the cell surface (Bao et al., 2003, 2004), we generated a Nrg1 construct where an HA tag was inserted upstream of its stop codon to monitor the subcellular localisation of its intracellular region when expressed in cortical pyramidal cells *in vivo*. These experiments showed that the C-terminal domain of Nrg1 was precisely targeted to the somatic compartment in a similar fashion than the HA-tagged

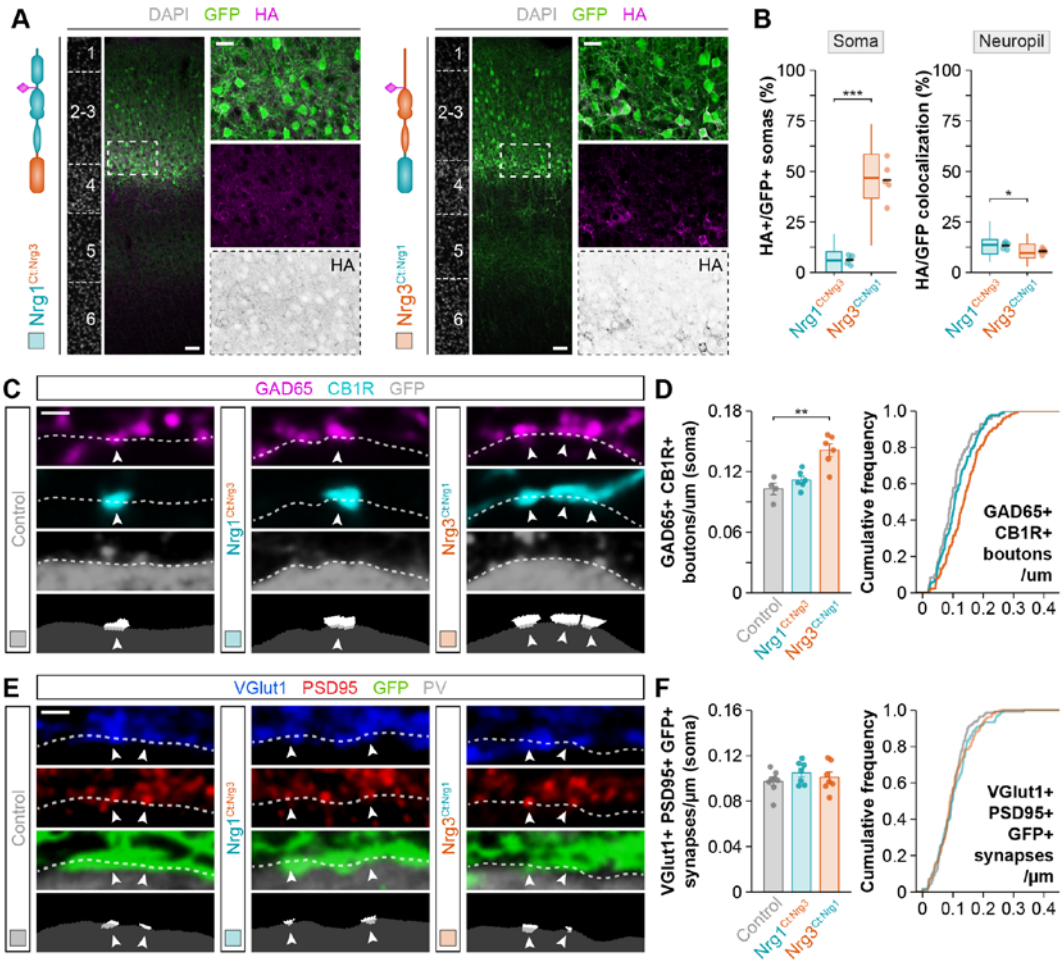

Figure 33 | **Neuregulin C-terminal domain specifies subcellular sorting to input and output synapses in pyramidal cells**.
(**A**) Coronal sections through somatosensory cortex of P30 mice following *in utero* electroporation of *pSyn-Nrg1$^{Ct:Nrg3}$-pSyn-Gfp* or *pSyn-Nrg3$^{Ct:Nrg1}$-pSyn-Gfp* plasmids at E14.5. Sections were processed for immunohistochemistry against GFP (green) and HA (magenta) and counterstained with DAPI (grey). The high-magnification images illustrate the localisation of HA-tagged neuregulins in GFP+ pyramidal cells. The bottom panel depicts HA staining in a colour-inverted image. Dotted squares indicate the localisation of the cells shown in the high-magnification images. The schematics illustrate the structure of the chimeric neuregulins in which the intracellular, C-terminal domain was swapped between Nrg1 and Nrg3. (**B**) Quantification of the localisation of HA+ neuregulin in the soma and neuropil of GFP+ pyramidal cells. Soma: Two-tailed Student's *t*-test: ***P < 0.001; n = 5 mice (40 regions of interest, ROIs) for *pSyn-Nrg1$^{Ct:Nrg3}$-pSyn-Gfp*, n = 5 mice (40 ROIs) for *pSyn-Nrg3$^{Ct:Nrg1}$-pSyn-Gfp*. Neuropil: Two-tailed Student's *t*-test, *P < 0.05, n = 5 mice (40 ROIs) for *pSyn-Nrg1$^{Ct:Nrg3}$-pSyn-Gfp*, n = 5 mice (40 ROIs) for *pSyn-Nrg3$^{Ct:Nrg1}$-pSyn-Gfp*. (**C**) Confocal images (top three panels) and binary images (bottom panel) illustrating presynaptic boutons co-labelled with GAD65 (magenta) and CB1R (cyan) innervating the soma of GFP+ pyramidal cells (grey) in C-terminal domain swapping experiments. (**D**) Quantification of the density of GAD65+/CB1R+ boutons contacting GFP+ pyramidal cells in chimeric gain-of-function experiments. One-way ANOVA: F = 13.740, P < 0.001. Tukey's range test for post hoc comparison between control and experimental groups: for *pSyn-Nrg1$^{Ct:Nrg3}$-pSyn-Gfp*, P = 0.534; for *pSyn-Nrg3$^{Ct:Nrg1}$-pSyn-Gfp*, , **P < 0.01; n = 4 mice (71 cells) for *pSyn-Gfp* (control), 6
(*Figure legends continues in next page.*)

mice (136 cells) for *pSyn-Nrg1*$^{Ct:Nrg3}$*-pSyn-Gfp*, 6 mice (127 cells) for *pSyn-Nrg3*$^{Ct:Nrg1}$*-pSyn-Gfp*. (**E**) Confocal images (top three panels) and binary images (bottom panel) illustrating presynaptic VGlut1+ puncta (blue) in GFP+ axons (red) of pyramidal cells located in close apposition to PSD95+ clusters (green) in PV+ interneurons (grey) in C-terminal swapping experiments. (**F**) Quantification of the density of VGlut1+/PSD95+/GFP+ synapses contacting PV+ interneurons in chimeric gain-of-function experiments. One-way ANOVA: $F = 0.929$, $P = 0.412$. Tukey's range test for post hoc comparison between control and experimental groups: for *pSyn-Nrg1*$^{Ct:Nrg3}$*-pSyn-Gfp*, $P = 0.379$; for *pSyn-Nrg3*$^{Ct:Nrg1}$*-pSyn-Gfp*, $P = 0.801$; n = 8 mice (143 cells) for *pSyn-Gfp* (control), 7 mice (121 cells) for *pSyn-Nrg1*$^{Ct:Nrg3}$*-pSyn-Gfp*, 7 mice (135 cells) for *pSyn-Nrg3*$^{Ct:Nrg1}$*-pSyn-Gfp*.
Data from the distributions of ROIs are shown as box plots, and the adjacent data points and lines represent the averages per animal and averaged mean per group, respectively. Data in synaptic quantifications represent mean s.e.m. The averages per animal and genotype are represented in bar graphs, and the distributions of values per cell are shown in cumulative frequency plots. Scale bars, 50 µm (A) and 20 µm (high magnification), and 1 µm (C, E).

extracellular domain of Nrg1 (Figure 36), which suggests that sequences in the C-terminal domain of Nrg1 contain sorting information to restrict its subcellular localisation to the soma of pyramidal cells. Altogether, these findings indicate that swapping the C-terminal domains of Nrg1 and Nrg3 is sufficient to disrupt the normal localisation of these proteins in pyramidal cells *in vivo*, and suggest that the intracellular, C-terminal domains contain unique amino acid sequences that instruct the specific subcellular trafficking of both neuregulins.

The previous experiments suggested that C-terminal domain-dependent subcellular sorting may determine the specificity of neuregulin signalling in inhibitory and excitatory synapse formation. To test this hypothesis, we first quantified the density of CCK+ somatic inputs in pyramidal cells expressing the C-terminal domain-swapping neuregulin proteins. Consistent with its inefficient retention in the soma (Figure 33A-B and Figure 35), we observed that overexpression of a chimeric Nrg1 protein containing the C-terminal domain of Nrg3 (Nrg1$^{Ct:Nrg3}$) did not increase the number of CB1R+/GAD65+ presynaptic boutons contacting electroporated pyramidal cells (Figure 33C-D). In contrast, overexpression of a chimeric Nrg3 protein carrying the C-terminal domain of Nrg1 (Nrg3$^{Ct:Nrg1}$), which is unusually retained in the soma of pyramidal cells (Figure 33A-B and Figure 35), led to a significant increase in the density of these GABAergic inputs (Figure 33C-D). Secondly, we measured the ability of these chimeric constructs to influence the formation of excitatory synapses onto PV+ interneurons. Consistent with their inefficient transport to the neuropil compared to wild-type

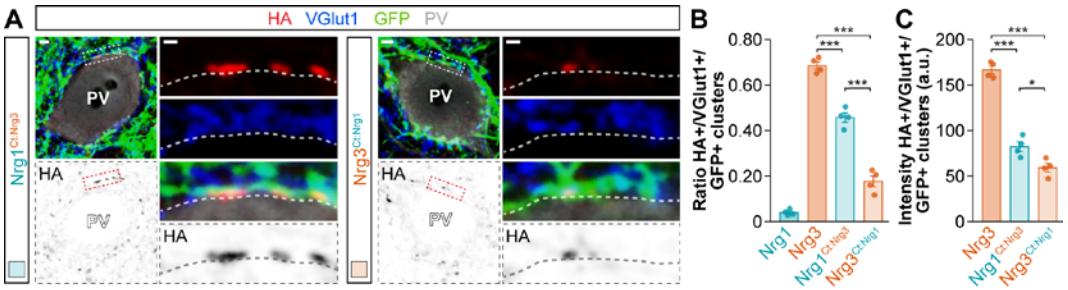

Figure 34 | **Synaptic targeting of C-terminal domain-swapping neuregulin constructs to excitatory presynaptic boutons innervating PV+ interneurons.** (**A**) Colocalisation of HA-tagged chimeric Nrg1$^{Ct:Nrg3}$ (left) and HA-tagged chimeric Nrg3$^{Ct:Nrg1}$ (right) (red) with presynaptic VGlut1+ boutons (blue) in GFP+ pyramidal cell axons (green) contacting PV+ interneurons (gray). The bottom panel depicts HA staining in a color-inverted image. The high-magnification images illustrate the colocalisation of HA-tagged neuregulins with excitatory VGlut1+ boutons. (**B**) Quantification of the proportion of VGlut1+ boutons that colocalise with HA-tagged Nrg clusters in axon terminals of electroporated GFP+ pyramidal cells. Tukey's range test for *post hoc* comparison between wild-type Nrg3 construct and chimeric Nrg constructs: ***P < 0.001, n = 4 mice (50 cells) for *pSyn-Nrg1$^{Ct:Nrg3}$-pSyn-Gfp*; ***P < 0.001, n = 4 mice (42 cells) for *pSyn-Nrg3$^{Ct:Nrg1}$-pSyn-Gfp*; ***P < 0.001, for comparison between chimeric constructs. Note that data for wild-type Nrg1 and Nrg3 constructs are the same data shown in Figure 28. (**C**) Quantification of the intensity of HA+ clusters within VGlut1+/GFP+ terminals innervating cortical PV+ interneurons. Tukey's range test for *post hoc* comparison between wild-type Nrg3 construct and chimeric constructs: ***P < 0.001, n = 4 mice (50 cells) for *pSyn-Nrg1$^{Ct:Nrg3}$-pSyn-Gfp*; ***P < 0.001, n = 4 mice (42 cells) for *pSyn-Nrg3$^{Ct:Nrg1}$-pSyn-Gfp*; *P < 0.05, for comparison between chimeric constructs.
Data are shown as mean ± s.e.m. Scale bar, 2 µm (A) and 0.5 µm (high magnifications).

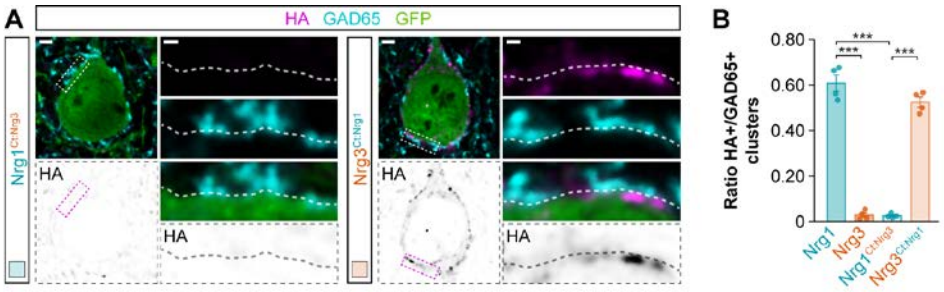

Figure 35 | **Synaptic targeting of C-terminal domain-swapping neuregulin constructs to inhibitory postsynaptic clusters in the soma of pyramidal cells.** (**A**) Colocalisation of HA-tagged chimeric Nrg1$^{Ct:Nrg3}$ (left) and HA-tagged chimeric Nrg3$^{Ct:Nrg1}$ (right) (magenta) with soma-targeting GAD65+ boutons (cyan) in electroporated GFP+ pyramidal cells (green). The bottom panel depicts HA staining in a color-inverted image. The high-magnification images illustrate the localisation of HA-tagged neuregulins contacted by presynaptic GAD65+ boutons. (**B**) Quantification of the proportion of GAD65+ boutons that colocalise with HA-tagged Nrg clusters in the soma of electroporated GFP+ pyramidal cells. Tukey's range test for *post hoc* comparison between wild-type Nrg1 construct and chimeric Nrg constructs: ***P < 0.001, n = 4 mice (32 cells) for *pSyn-Nrg1$^{Ct:Nrg3}$-pSyn-Gfp*; P = 0.077, n = 4 mice (34 cells) for *pSyn-Nrg3$^{Ct:Nrg1}$-pSyn-Gfp*; ***P < 0.001, for comparison between chimeric constructs. Note that data for wild-type Nrg1 and Nrg3 constructs is the same data shown in Figure 27.
Data are shown as mean ± s.e.m. Scale bar, 2 µm (A) and 0.5 µm (high magnifications).

Nrg3 (Figure 33A-B and Figure 34), neither Nrg1$^{Ct:Nrg3}$ nor Nrg3$^{Ct:Nrg1}$ caused a significant change in the number of VGlut1+/PSD95+ puncta within GFP+ axon terminals contacting PV+ interneurons (Figure 33E-F). Although the chimeric Nrg1$^{Ct:Nrg3}$ protein was sorted into the neuropil (Figure 33A-B), the levels of targeting were reduced compared to wild-type Nrg3 protein (Figure 26B-C). Importantly, detailed analysis of the synaptic expression of this chimeric construct showed that, although targeted to axon terminals, this protein is less efficiently localised to VGlut1+ presynaptic boutons within electroporated GFP+ pyramidal cells (Figure 34). A simple explanation for the lack of increase in excitatory synapses after Nrg1$^{Ct:Nrg3}$ overexpression is that the amount of chimeric protein reaching the presynaptic boutons is insufficient to activate the receptor trans-synaptically and, consequently, unable to trigger synaptogenic signalling. Thus, these experiments confirmed that efficient targeting of neuregulins to specific subcellular compartments in pyramidal cells mediates their function in synapse formation. They also revealed that the C-terminal domain of neuregulins is essential for the specificity of this process.

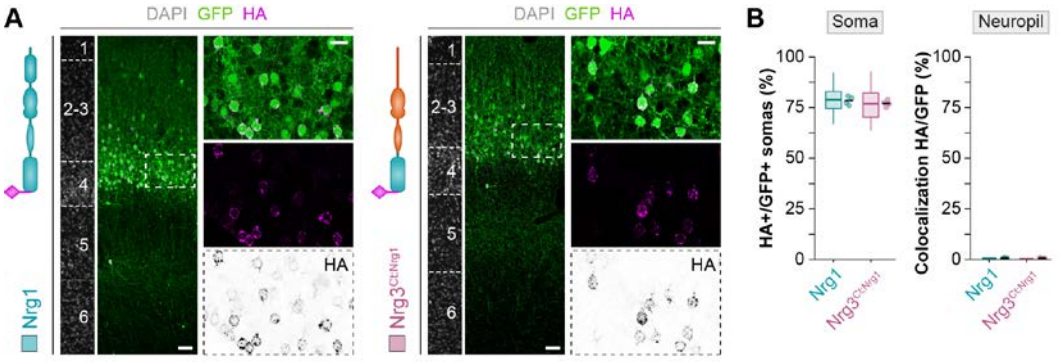

Figure 36 | **The C-terminal domain of Nrg1 encodes information for subcellular sorting to the somatic compartment of cortical pyramidal cells.**
(**A**) Coronal sections through somatosensory cortex of P30 mice following *in utero* electroporation of *pSyn-Nrg1HA-pSyn-Gfp* or *pSyn-Nrg3$^{Ct:Nrg1}$HA-pSyn-Gfp* plasmids at E14.5. Sections were processed for immunohistochemistry against GFP (green) and HA (magenta) and counterstained with DAPI (gray). The high-magnification images illustrate the localisation of HA-tagged neuregulins in GFP+ pyramidal cells. The bottom panel depicts HA staining in a colour-inverted image. Dotted squares indicate the localisation of the cells shown in the high-magnification images. (**B**) Quantification of the localisation of HA+ neuregulin in the soma and neuropil of GFP+ pyramidal cells. Soma: Two-tailed Student's *t*-test, *P* = 0.550; n = 4 mice (27 regions of interest, ROIs) for *pSyn- Nrg1HA -pSyn-Gfp*, n = 4 mice (27 ROIs) for *pSyn- Nrg3$^{Ct:Nrg1}$HA -pSyn-Gfp*. Neuropil: Two-tailed Student's t-test, *P* = 0.335; n = 4 mice (27 ROIs) for *pSyn-Nrg1HA-pSyn-Gfp*, n = 4 mice (27 ROIs) for *pSyn- Nrg3$^{Ct:Nrg1}$HA -pSyn-Gfp*.
Data from the distributions of ROIs are shown as box plots, and the adjacent data points and lines represent the averages per animal and averaged mean per group, respectively. Scale bars, 50 µm (A) and 20 µm (high magnification).

To add further support to this idea and probe whether the C-terminal domains actively segregate both neuregulin members to distinct neuronal compartments, we performed a final series of experiments in which we electroporated plasmids encoding truncated forms of Nrg1 and Nrg3 that lack the entire intracellular, C-terminal region. Interestingly, we found that both Nrg1 and Nrg3 lacking the C-terminal domain (Nrg1$^{\Delta Ct}$ and Nrg3$^{\Delta Ct}$) lose the specific subcellular segregation found in full-length Nrg1 and Nrg3, showing similar heterogeneous distributions in pyramidal cells (Figure 37A-B). Specifically, we observed that Nrg1$^{\Delta Ct}$ was no longer restricted to the somatic compartment of pyramidal cells and was in turn abundantly found throughout the neuropil (Figure 37A-B). Remarkably, truncation of Nrg1 protein results in its presence in both

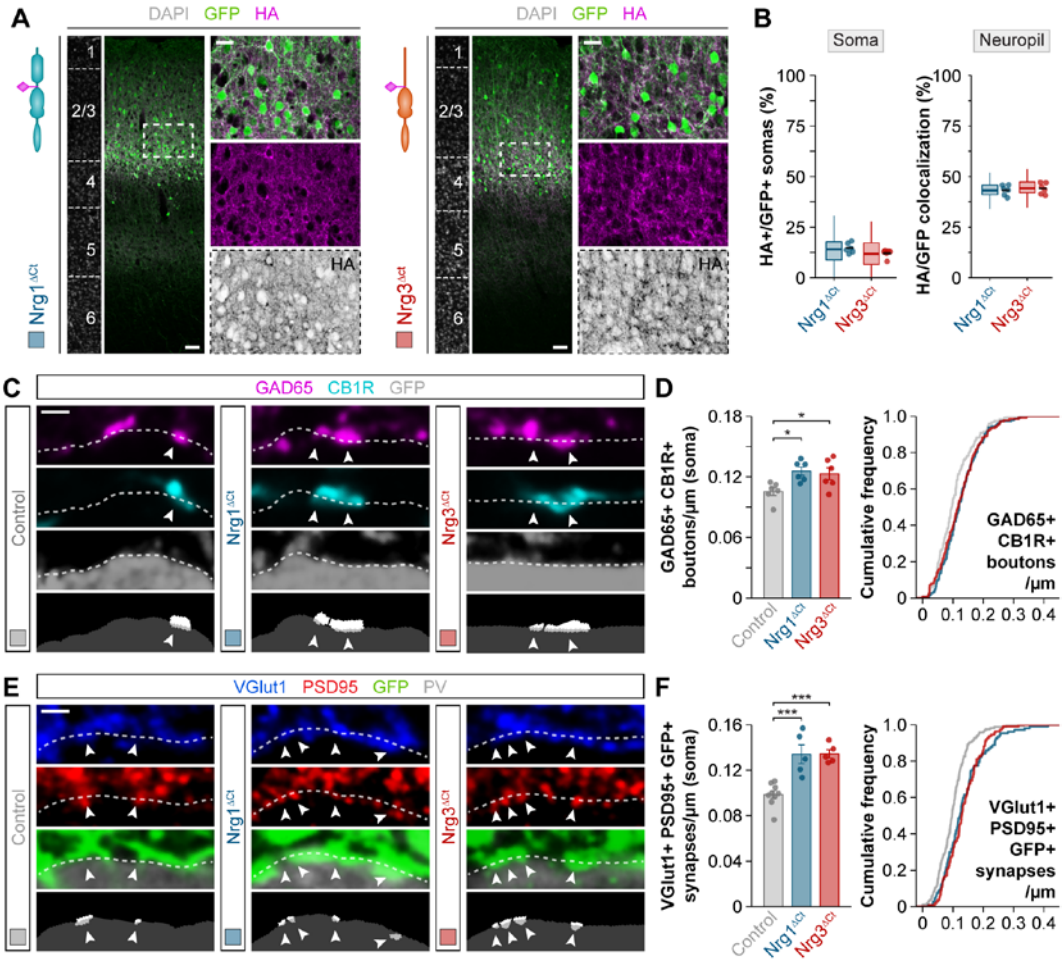

Figure 37 | **Subcellular segregation of neuregulins is encoded in the C-terminal domain**.

(**A**) Coronal sections through somatosensory cortex of P30 mice following *in utero* electroporation of *pSyn-Nrg1$^{\Delta Ct}$-pSyn-Gfp* or *pSyn-Nrg3$^{\Delta Ct}$-pSyn-Gfp* plasmids at E14.5. Sections were processed for immunohistochemistry against GFP (green) and HA (magenta) and counterstained with DAPI (grey). The high-magnification images illustrate

(*Figure legends continues in next page.*)

the localisation of HA-tagged neuregulins in GFP+ pyramidal cells. The bottom panel depicts HA staining in a color-inverted image. The schematics illustrate the structure of truncated neuregulins in which the C-terminal domain was removed. (**B**) Quantification of the localisation of HA+ neuregulin in the soma and neuropil of GFP+ pyramidal cells. Soma: Mann-Whitney *U*-test, $P = 0.093$; n = 6 mice (66 regions of interest, ROIs) for *pSyn-Nrg1$^{\Delta Ct}$-pSyn-Gfp*, n = 6 mice (66 ROIs) for *pSyn-Nrg3$^{\Delta Ct}$-pSyn-Gfp*. Neuropil: Two-tailed Student's *t*-test, $P = 0.589$; n = 6 mice (58 ROIs) for *pSyn-Nrg1$^{\Delta Ct}$-pSyn-Gfp*, n = 6 mice (58 ROIs) for *pSyn-Nrg3$^{\Delta Ct}$-pSyn-Gfp*. (**C**) Confocal images (top three panels) and binary images (bottom panel) illustrating presynaptic boutons co-labelled with GAD65 (magenta) and CB1R (cyan) innervating the soma of GFP+ pyramidal cells (gray) in C-terminal domain deletion experiments. (**D**) Quantification of the density of GAD65+/CB1R+ boutons contacting GFP+ pyramidal cells in gain-of-function truncation experiments. One-way ANOVA: $F = 5.325$, $P < 0.05$. Tukey's range test for post hoc comparison between control and experimental groups: for *pSyn-Nrg1$^{\Delta Ct}$-pSyn-Gfp*, $*P < 0.05$; for *pSyn-Nrg3$^{\Delta Ct}$-pSyn-Gfp*, $*P < 0.05$; n = 6 mice (120 cells) for *pSyn-Gfp* (control), 6 mice (145 cells) for *pSyn-Nrg1$^{\Delta Ct}$-pSyn-Gfp*, 6 mice (138 cells) for *pSyn-Nrg3$^{\Delta Ct}$-pSyn-Gfp*. (**E**) Confocal images (top three panels) and binary images (bottom panel) illustrating presynaptic VGlut1+ puncta (blue) in GFP+ axons (green) of pyramidal cells located in close apposition to PSD95+ clusters (red) in PV+ interneurons (gray) in C-terminal domain deletion experiments. (**F**) Quantification of the density of VGlut1+/PSD95+/GFP+ synapses contacting PV+ interneurons in gain-of-function truncation experiments. One-way ANOVA: $F = 19.500$, $P < 0.001$. Tukey's range test for post hoc comparison between control and experimental groups: for *pSyn-Nrg1$^{\Delta Ct}$-pSyn-Gfp*, $***P < 0.001$, for *pSyn-Nrg3$^{\Delta Ct}$-pSyn-Gfp*, $***P < 0.001$; n = 9 mice (167 cells) for *pSyn-Gfp* (control), 5 mice (107 cells) for *pSyn-Nrg1$^{\Delta Ct}$-pSyn-Gfp*, 5 mice (111 cells) for *pSyn-Nrg3$^{\Delta Ct}$-pSyn-Gfp*. Data from the distributions of ROIs are shown as box plots. Data in synaptic quantifications represent mean ± s.e.m. The averages per animal and genotype are represented in bar graphs, and the distributions of values per cell are shown in cumulative frequency plots. Scale bars, 50 µm (A) and 20 µm (high magnification), and 1 µm (C, E).

dendrites and axon terminals, indicating that somatic retention sequences are encoded in its C-terminal domain (Figure 37A-B). On the other hand, we observed that Nrg3$^{\Delta Ct}$ was no longer restricted to axons as it is the case for wild-type Nrg3: it was also abundantly expressed in the somatodendritic compartment of pyramidal cells, suggesting that this truncated form of the protein has lost its specific presynaptic localisation (Figure 37A-B). Consistently, both Nrg1$^{\Delta Ct}$ and Nrg3$^{\Delta Ct}$ were observed in somatic inhibitory synapses as well as axonal excitatory synapses in electroporated GFP+ pyramidal cells (Figures 38 and 39). These findings reinforce the idea that the specific localisation of Nrg1 and Nrg3 in the somatic and axonal compartments, respectively, requires amino acid sequences encoded in their C-terminal domain.

We examined how the lack of specificity in the distribution of neuregulins would impact the formation of inhibitory inputs and excitatory outputs in pyramidal cells. First, we assessed the effect of Nrg1 and Nrg3 proteins lacking the C-terminal

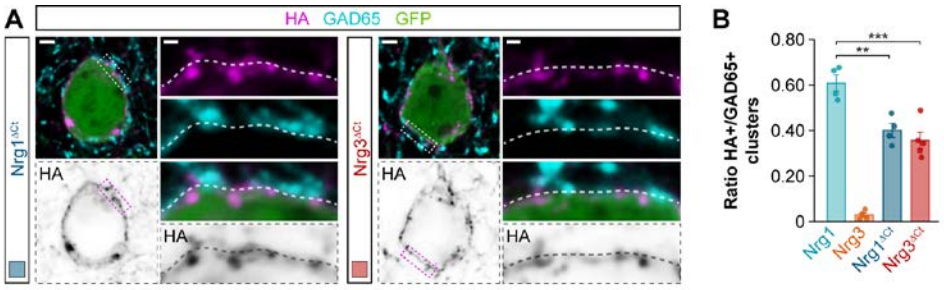

Figure 38 | **Synaptic targeting of C-terminal domain-truncated neuregulin constructs to inhibitory postsynaptic clusters in the soma of pyramidal cells.** (**A**) Colocalisation of HA-tagged chimeric Nrg1$^{\Delta Ct}$ (left) and HA-tagged chimeric Nrg3$^{\Delta Ct}$ (right) (magenta) with soma-targeting GAD65+ boutons (cyan) in electroporated GFP+ pyramidal cells (green). The bottom panel depicts HA staining in a color-inverted image. The high-magnification images illustrate the localization of HA-tagged neuregulins contacted by presynaptic GAD65+ boutons. (**B**) Quantification of the proportion of GAD65+ boutons that colocalise with HA-tagged Nrg clusters in the soma of electroporated GFP+ pyramidal cells. Tukey's range test for post hoc comparison between wild-type Nrg1 construct and truncated Nrg constructs: $^{**}P < 0.01$, n = 4 mice (34 cells) for *pSyn-Nrg1$^{\Delta Ct}$-pSyn-Gfp*; $^{***}P < 0.001$, n = 5 mice (43 cells) for *pSyn-Nrg3$^{\Delta Ct}$-pSyn-Gfp*; $P = 0.739$, for comparison between truncated constructs. Note that data for wild-type Nrg1 and Nrg3 constructs are the same data shown in Figure 27. Data are shown as mean ± s.e.m. Scale bar, 2 µm (A) and 0.5 µm (high magnifications).

domain in inducing the formation of GABAergic boutons from CCK+ basket cells onto the soma of pyramidal neurons. Strikingly, overexpression of the truncated forms of Nrg1 and Nrg3 resulted in a significant increase in the density of GAD65+/CB1R+ boutons innervating electroporated pyramidal cells (Figure 37C-D). Of note, these phenotypes appeared to be moderate as compared to overexpression experiments of wild-type Nrg1 protein (Figure 22B-C), likely due to the fact that the synaptic targeting of both neuregulins lacking the C-terminal domain to the somatic compartment is less efficient than the wild-type Nrg1 protein (Figure 38). An alternative explanation lies on the possibility that the neuregulin C-terminal domain could contribute to the development and/or stabilization of GABAergic synapses at the postsynaptic membrane. Second, we quantified excitatory synaptic contacts formed onto PV+ interneurons by pyramidal cells expressing the truncated forms of Nrg1 and Nrg3. Overexpression of these truncated proteins robustly induced the formation of VGlut1+/PSD95+ synapses within GFP+ axon terminals innervating PV+ interneurons (Figure 37E-F). Altogether, the ability of neuregulins lacking their C-terminal domains to induce synapse formation *in vivo* suggests that their synaptogenic function does not depend on intracellular signalling pathways but rather on the trans-synaptic interaction with ErbB4 receptor. These results are consistent with the hypothesis

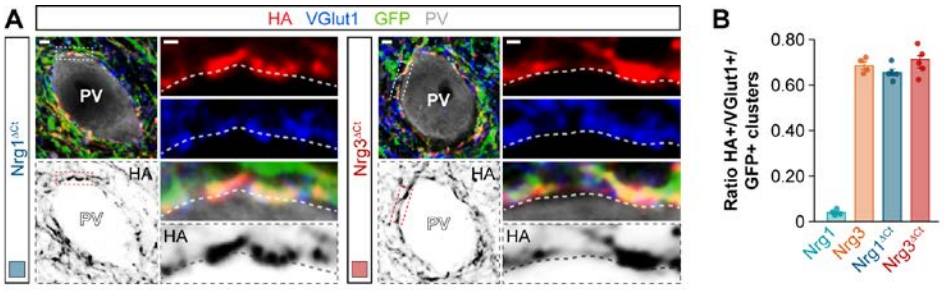

Figure 39 | **Synaptic targeting of C-terminal domain-truncated neuregulin constructs to excitatory presynaptic boutons innervating PV+ interneurons.** (**A**) Colocalisation of HA-tagged chimeric Nrg1$^{\Delta Ct}$ (left) and Nrg3$^{\Delta Ct}$ (red) with presynaptic VGlut1+ boutons (blue) in GFP+ pyramidal cell axons (green) contacting PV+ interneurons (gray). The bottom panel depicts HA staining in a color-inverted image. The high-magnification images illustrate the colocalisation of HA-tagged neuregulins with excitatory VGlut1+ boutons. (**B**) Quantification of the proportion of VGlut1+ boutons that colocalise with HA-tagged Nrg clusters in axon terminals of electroporated GFP+ pyramidal cells. Tukey's range test for post hoc comparison between wild-type Nrg3 construct and truncated Nrg constructs: $P = 0.689$, n = 5 mice (38 cells) for *pSyn-Nrg1$^{\Delta Ct}$-pSyn-Gfp*; $P = 0.928$, n = 5 mice (36 cells) for *pSyn-Nrg3$^{\Delta Ct}$-pSyn-Gfp*; $P = 0.304$, for comparison between truncated Nrg constructs. Note that data for wild-type Nrg1 and Nrg3 constructs are the same data shown in Figure 28.
Data are shown as mean ± s.e.m. Scale bar, 2 µm (A) and 0.5 µm (high magnifications).

that the selective subcellular segregation of Nrg1 and Nrg3 in cortical pyramidal cells controls their specific function in inhibitory and excitatory synapses, respectively.

In conclusion, in Chapter 3 we performed structure-function analysis in combination with a gain-of-function paradigm to examine the role of distinct protein domains of Nrg1 and Nrg3 in their specific sorting and function in pyramidal cell connectivity. Our findings suggest two major conclusions: (i) the C-terminal domains of Nrg1 and Nrg3 determine their subcellular sorting to the somatic and axonal compartments, respectively; and (ii) Nrg/ErbB4 signalling in inhibitory and excitatory synapses does not seem to depend on the ligand binding properties of the respective EGF-like domains to the receptor. Thus, Nrg1 and Nrg3 act as ligands for ErbB4 receptor in two distinct subcellular compartments of cortical pyramidal cells through a selective sorting that is mediated by signal sequences present in their C-terminal domains, to specifically regulate the formation of inhibitory and excitatory synapse formation, respectively. Altogether, these results reveal a differential sorting of cell surface molecules involved in the developmental synaptic assembly of pyramidal cells and interneurons in the cerebral cortex.

DISCUSSION

The developmental assembly of cell types in the cerebral cortex involves the establishment of spatially-defined connections with distinct properties and molecular composition. It has become evident in recent years that elucidating mechanisms underlying neuronal connectivity requires a detailed understanding of the subcellular distributions and synapse-specific functions of synaptic proteins. Here, we aimed to dissect the precise roles of two family-related cell-surface molecules, Nrg1 and Nrg3, in the cell type-specific synaptic assembly of a defined neuronal circuit, the interneuron-pyramidal cell perisomatic circuitry in the neocortex, using the superficial layers of the somatosensory cortex as a model. To approach this question, we applied a combination of molecular biology, mouse genetics, gene editing, histology, and imaging tools. Below I will discuss how the findings presented in this Thesis influence our knowledge on the molecular control of circuit connectivity and the sorting mechanisms of synaptic proteins in the cerebral cortex. I will dedicate the last section to reflect on the relevance of mechanistic insights in cortical connectivity to inform the pathophysiological basis, and ultimately therapeutic strategies, of neurodevelopmental disorders.

1. Molecular control of cortical connectivity

How neuronal circuits are formed during development and what molecular mechanisms underlie the specificity of synaptic connections in the mammalian cerebral cortex remain fundamental questions in neuroscience. Neuregulins are a family of transmembrane proteins that bind and activate the ErbB4 receptor, function as synaptogenic molecules, and are abundantly expressed in developing circuits of the cerebral cortex. Despite decades of work, the role of neuregulins in the formation of cortical connectivity is yet not well understood. Here, we provide multiple lines of evidence that reveal that subcellular partitioning of neuregulin localisation enforces their segregated roles in inhibitory and excitatory synapses. Hence, pyramidal cells have implemented a subcellular mechanism whereby neuregulins gain specific control over the development synaptic connections with distinct types of interneurons. Our study reveals a novel strategy for the assembly of cortical circuits that involves the differential subcellular sorting of family-related synaptic proteins.

1.1. Pyramidal cell-interneuron wiring controlled by neuregulin/ErbB4 signalling

Our findings show that the assembly of pyramidal cell-interneuron connections in the mammalian cerebral cortex depends on a *trans*-synaptic interaction in which the matching subcellular localisation of neuregulin ligands and their ErbB4 receptor promotes synapse formation. Conditional elimination of *Nrg1* uncovers a specific impairment of GABAergic somatic and axo-axonic innervation onto cortical pyramidal cells by CCK+ basket cells and chandelier cells, respectively. Conversely, pyramidal cells lacking *Nrg3* show a reduced capacity to form excitatory synapses onto PV+ interneurons. Overexpression of Nrg1 and Nrg3 expression in cortical pyramidal cells corroborated their highly selective involvement in inhibitory and excitatory synaptogenesis. Thus, our data supports that Nrg1 and Nrg3 differentially control the assembly of inhibitory and excitatory synapses in cortical circuits, and suggests that developing synaptic connections form with latent autonomy: Nrg1 deletion-associated loss of synapses leaves Nrg3-dependent functions intact, and *vice versa*. Since ErbB4 expression in PV+ and CCK+ interneurons plays an important role in the formation of their excitatory inputs as well as inhibitory outputs (Del Pino et al., 2013, 2017), these observations indicate that a non-redundant system of neureuglin/ErbB4 signalling underlies the development of these cortical circuits (Figure 40-41).

Our conditional genetic strategy is advantageous for two reasons. First, tamoxifen inductions were carried out in postnatal newborn pups, ensuring that neuregulin expression levels are normal during embryonic development. This is especially important due to the essential roles of Nrg1 and Nrg3 in early developmental processes in the cortex, such as migration, cortical plate invasion, and lamination (Bartolini et al., 2017; Flames et al., 2004). Disrupting the normal course of developing interneurons in the embryo has tremendous consequences for cortical network function in adult stages (Cho et al., 2015; Wang et al., 2010). Thus, alterations in the cytoarchitecture of the cortex in mouse genetic models represent a confounding factor to interpret phenotypes derived from disrupting functions in synapse formation and/or maturation during postnatal development. In contrast with previous studies (Agarwal et al., 2014; Wang et al., 2018b), we did not observed deficits in density or laminar organization of interneurons in the cortex of icKO mice, which suggests that they are ideal mouse models to specifically study

neuregulin function during synaptogenesis. Second, neuregulins play diverse neuronal and glial functions during developmental and adult stages (Agarwal et al.,

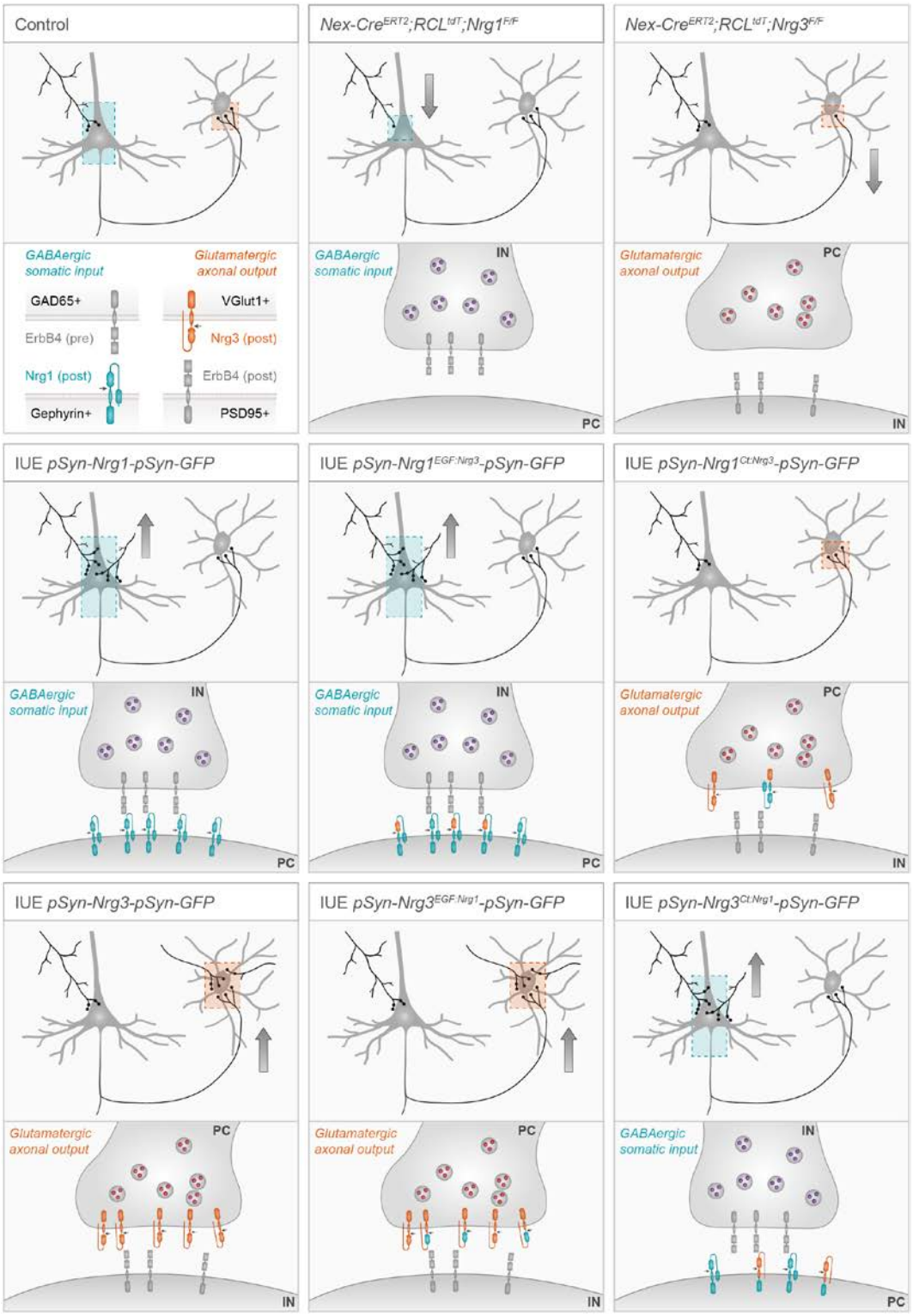

Figure 40 | **Summary diagrams of synaptic phenotypes observed upon neuregulin genetic manipulations and structural modifications.**
Diagrams that recapitulate the phenotypes observed in loss- and gain-of-function experiments. The synaptogenic capability and synaptic targeting of neuregulin proteins is represented in the top and bottom panels, respectively, for each experimental condition.

2014; Brinkmann et al., 2008; Chen et al., 2008; Kotzadimitriou et al., 2018; Rio et al., 1997; Sun et al., 2016; Taveggia et al., 2008; Wang et al., 2018b). Our pyramidal cell-specific approach avoids ambiguous effects originating from disrupted expression in other cell types that naturally express neuregulins.

The observed synaptic phenotypes in neuregulin icKO mice prominently mirror those found in *ErbB4* cKO mice, and these synaptic deficits are characteristically subtle (Del Pino et al., 2013, 2017; Yang et al., 2013). Thus, the summation of inhibitory and excitatory deficits in mice lacking *Nrg1* and *Nrg3*, respectively, recapitulates the heterogeneous alterations observed in mice lacking ErbB4 from fast-spiking interneurons (Del Pino et al., 2013) or CCK+ basket cells (Del Pino et al., 2017). Further evidence of the similarity between Nrg1, Nrg3 and ErbB4 mouse models comes from the absence of phenotypes in PV+ basket cell synapses innervating the soma of pyramidal cells (Del Pino et al., 2013; Yang et al., 2013), as analysed here by synaptotagmin-2/gephyrin co-immunostaining. This suggests that developing PV+ basket boutons—in contrast to chandelier or CCK+ boutons—depend on a distinct pool of molecules, yet to be determined. This finding also reveals a high degree of specificity in the assembly of pyramidal cell-interneuron connections through neuregulin/ErbB4 signalling. Moreover, neuregulin function in pyramidal cells seem to be cell-autonomous because the synaptic loss after inducible deletion of *Nrg3* does not involve axon terminals originating from non-recombined neurons.

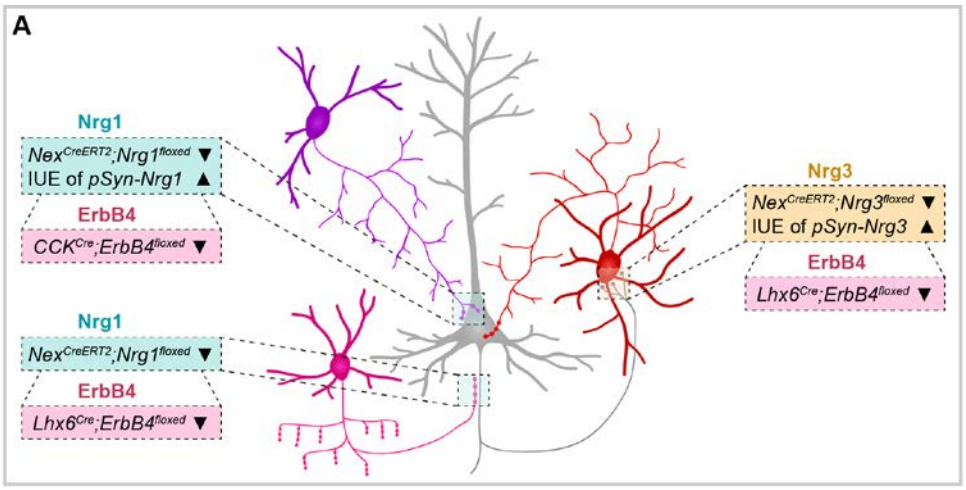

Figure 41 | **Role of neuregulin/ErbB4 signalling in cortical synaptic assembly.** (**A**) Drawing illustrating the function of the neuregulin/ErbB4 signalling pathway in the wiring of perisomatic local circuits in the mouse cerebral cortex (Del Pino et al., 2013, 2017; and this Thesis). The coloured boxes indicate the density changes in inhibitory and excitatory synapses observed in genetic manipulations of Nrg1, Nrg3 and ErbB4 receptor in neuronal circuits *in vivo*.

Of note, the synaptic analyses presented in the current work are limited to anatomical changes, as assessed via confocal imaging and quantifications of synapse densities. To determine whether these structural phenotypes have a functional correlate in synaptic transmission, it would be important to explore changes in functional synaptic events by performing electrophysiological recordings of miniature excitatory and inhibitory postsynaptic currents (mEPSCs and mIPSCS, respectively) in neuregulin icKO mice. Since Nrg3 is precisely localised to presynaptic glutamatergic boutons (Figures 24 and 28), and it has been shown to interact with members of the SNARE complex (Wang et al., 2018), it would be particularly relevant to investigate the effect of Nrg3 deletion in presynaptic release and short-term plasticity. Elucidating whether this potential role of Nrg3 requires binding with cis-interacting partners exclusively, or additionally trans-synaptic interaction with ErbB4 receptor, will shed further light on the molecular mechanisms underlying its presynaptic function. Furthermore, electron microscopy-based ultrastructural studies offer important avenues to investigate the involvement of cell-surface molecules in building the synaptic architecture (Acuna et al., 2016; Condomitti et al., 2018; Steinecke et al., 2017). This experimental approach would allow us to examine fine changes in synaptic differentiation and/or maturation in neuregulin icKO mice, including bouton size, density and positioning of synaptic vesicles, and shape and size of postsynaptic structures. Therefore, further investigation of physiological and structural properties will provide invaluable insights into the synaptic functions of Nrg1 and Nrg3 in cortical circuits.

1.2. A synapse-specific neuregulin/ErbB4 interaction code

Nrg1 and Nrg3 act in a non-redundant and cell-autonomous manner to control the density of distinct classes of synapses in pyramidal cells. In line with these findings, we observed a remarkable segregation in the subcellular localisation of Nrg1 and Nrg3 to distinct pyramidal cell compartments. Nrg1 is highly restricted to the perisomatic compartment, where it is found in postsynaptic clusters of various GABAergic inputs, whereas Nrg3 is selectively sorted into the axonal compartment and targeted to presynaptic glutamatergic boutons innervating PV+ interneurons. Noticeably, the distinctive distribution of Nrg1 and Nrg3 in pyramidal cells matches the patterns of ErbB4 targeting to specific subcellular compartments in interneuron cell types, thereby generating a coincidence matrix of ligand-receptor proteins

expressed by pre- and postsynaptic partners. On the one hand, ErbB4 is present in the presynaptic membrane of GABAergic boutons innervating both the soma and AIS of pyramidal cells (Fazzari et al., 2010). On the other hand, ErbB4 is found in the postsynaptic membrane of dendrites and somas of several classes of interneurons (Fazzari et al., 2010; Vullhorst et al., 2009). Taken together, our results suggest a mechanism by which the differential subcellular sorting of Nrg1 and Nrg3 in pyramidal cells ensures the activation of synaptogenic signalling through the same kinase receptor in distinct neuronal connections of cortical circuits (Figure 29, and Figure 41).

Our observations are consistent with *in vitro* studies of the localisation of Nrg3, but not Nrg1 (Müller et al., 2018; Vullhorst et al., 2017). Nrg1 and Nrg3 proteins appear to be similarly distributed along axons of cultured neurons *in vitro*. Indeed, we have previously tested transfection of our neuregulin-encoding plasmids in primary cultures of cortical cells and found that both proteins seem to be similarly distributed, with abundant targeting and high intensity levels in the perisomatic region (preliminary observations, data not shown). This could suggest saturation of expression *in vitro*, causing the proteins to be non-specifically targeted to distinct subcellular compartments, which has been reported in previous studies. For instance, the characteristic segregation of input-specific properties of spines from different fragments of dendrites in CA1 pyramidal cells seems to be lost when these neurons are cultured *in vitro* (Sando et al., 2019). Alternatively, the possibility that sorting mechanisms function abnormally in cultured neurons cannot be ruled out. In the case of Nrg3, our results fit with its localisation to excitatory synapses *in vivo*, as reported by antibody staining (Müller et al., 2018). Of note, since neuregulins are also expressed in other cell types in the cortex apart from glutamatergic neurons, our experimental design—that is, *in utero* electroporation of pyramidal cell progenitors—provides a cell type-specific examination of Nrg3 in pyramidal cell axon terminals that innervate PV+ interneurons.

Our work shows the precise logic of neuregulin/ErbB4 interactions in cortical circuits. There are several important questions arising from these findings regarding the nature of the downstream mechanisms involved in this process. First, the signalling mechanisms downstream of neuregulin/ErbB4 at the synapse are still poorly characterised. Do Nrg1 and Nrg3 trigger shared or distinct signalling cascades to influence the formation of inhibitory and excitatory synapses? Our results suggest that there is no specificity in the synaptic function of neuregulin EGF-like domains. However, given the paradoxically different localisation of Nrg1

and Nrg3 at the post- and presynaptic membranes, it is reasonable to hypothesise that some molecular functions and interactions might differ between Nrg1 and Nrg3 independently of the EGF-like domain (Wang et al., 2017). For instance, does the backward signalling of Nrg1 (Bao et al., 2003, 2004) play a role in the inhibitory postsynaptic membrane? On the other hand, Nrg3 has been shown to interact with proteins of the soluble N-ethylmaleimide-sensitive factor attachment protein receptor (SNARE) complex such as synaptosomal nerve-associated protein 25 (SNAP25) (Wang et al., 2018b). Do neuregulins interact with other co-receptor or auxiliary proteins at the synapse? Are these interactions synapse-specific and required for neuregulin function in synaptogenesis? As new binding partners are identified, direct manipulations of these molecular interactions will be needed to test these questions.

Given the segregation of neuregulins to distinct synapses, it is tempting to suggest that pyramidal cells may have implemented different upstream regulatory mechanisms for transcription of *Nrg1* and *Nrg3*. This could represent a mechanistic strategy utilised by pyramidal cells to independently control input and output synaptic connections by differential regulation of the expression of *Nrg1* and *Nrg3*, respectively. In this regard, a preliminary study in our laboratories using qPCR analysis in mouse cortical samples at different time points across postnatal development shows that *Nrg1* and *Nrg3* expression patterns follow distinct temporal dynamics. *Nrg1*, which is highly expressed during embryonic development (Flames et al., 2004), continues to be abundant during the first two postnatal weeks in the cerebral cortex, a period that is followed by a gradual decline in expression until 4-5 weeks of age (unpublished work). In contrast, expression levels of *Nrg3* are lower than Nrg1 during the first week after birth, and progressively increase throughout postnatal development reaching its peak at 4-5 weeks. Mapping the promoter regions of *Nrg1* and *Nrg3* and identifying their transcriptional regulators would be required to better understand the spatiotemporal windows of the role of neuregulins in the integration of pyramidal cells into developing circuits (Peng et al., 2019; Vormstein-Schneider et al., 2019).

1.3. Limitations in the study of protein localisation

The development of protein tagging methodologies has proved extremely powerful to reveal the subcellular distribution patterns of proteins in the highly complex

morphologies of neuronal bodies (Mikuni et al., 2016; Nishiyama et al., 2017; Suzuki et al., 2016), not only to replace the lack of specific antibodies but also to implement cell type-specific approaches. Using IUE of exogenous DNA constructs in the mouse brain *in vivo*, we identified the synapse-specific localisation of two members of the neuregulin family in cortical pyramidal cells. This approach has been successfully used to study subcellular distribution of several proteins in hippocampal pyramidal cells (Condomitti et al., 2018; Favuzzi et al., 2017). For the insertion of the HA tag in both neuregulin genes, we selected a previously reported insertion site that does not alter the structure nor the function of the proteins (Wang et al., 2001). Our experiments represent, to the best of our knowledge, the first description of subcellular segregation of family-related proteins in cortical circuits.

Exogenous protein expression experiments, nonetheless, are inherently problematic due to the overexpression conditions. Therefore, we initially performed two experiments for monitoring the endogenous localisation of Nrg1 and Nrg3 in cortical circuits. First, we used immunostaining against Nrg1 and Nrg3 in brain sections using commercial antibodies that have been reported in the literature to show specific labeling of these proteins (Müller et al., 2018; Vullhorst et al., 2017). However, our results showed similar labelling patterns when these antibodies were tested in wild-type and conditional knock-out tissue for *Nrg1* and *Nrg3*. This lack of antibody specificity has been well documented in other studies, and in particular for cell adhesion molecules (Anderson et al., 2017; Condomitti et al., 2018; Fazzari et al., 2010).

Gene editing technologies are quickly becoming standard approaches to knock-in tag epitopes in specific genes of interest in order to monitor the precise subcellular localisation of endogenous proteins (Ribeiro et al., 2019; Sando et al., 2019). Therefore, we next designed a CRISPR/Cas9-mediated approach to endogenously tag the neuregulin loci in the mouse brain *in vivo*. These experiments were unsuccessful since the designed sgRNA showed low efficiency of gene editing *in vitro* as tested by the T7-endonuclease assay, and IUE of the DNA constructs did not result in HA+ signal in electroporated cortical pyramidal cells. Two plausible possibilities could account for this result. First, genomic structure can be influenced by chromatin arrangement, which might differ between genes and can make some regions of the genome less amenable than others for gene editing. Second, large regions of neuregulin genes are very rich in high guanines and cytosines (G/C); high G/C content increases the stability of genomic regions, and therefore the DNA secondary structure is an important factor that

influences the accessibility and efficiency in molecular biology techniques (Duret et al., 2002; SantaLucia and Hicks, 2004; Romiguier et al., 2010). Because the strategy used here was based on plasmid delivery, which has been previously reported to yield lower efficiencies compared to other approaches such as viral delivery (Mikuni et al., 2016; Nishiyama et al., 2017), optimisation of these experiments would be necessary to determine the feasibility of endogenous tagging of neuregulin loci. Recent development of CRISPR/Cas9 technology has improved the efficiency and versatility of strategies for endogenous tagging in the mouse brain, which would represent interesting new avenues to test in the endogenous loci of neuregulins. A much higher degree of tagging efficiencies seems to be achieved using homology-independent approaches, such as the HITI method (Suzuki et al., 2016), the ORANGE system (Willems et al., 2019), and plug-and-play system (Gao et al., 2019). Thus, additional work will be required to optimise the current CRISPR/Cas9 experiments presented here.

1.4. Diverse molecular complexes shape the cortical synaptic network

A panoply of cell surface molecules composes the molecular architecture of cortical synapses (Loh et al., 2016; Paul et al., 2017). Our data provides an explanation for protein diversity in the neuregulin family at the synapse. By selective sorting to the perisomatic compartment of pyramidal cells, Nrg1 specifically controls the development of inhibitory synaptic innervation into the soma and AIS. In marked contrast, selective axonal sorting endows Nrg3 with the ability to localise to presynaptic terminals contacting PV+ interneurons to regulate excitatory synapse formation. Building on previous work from our lab and others (Del Pino et al., 2013, 2017), these findings suggest that these two ligands are able to drive synaptogenic signalling through the same receptor, ErbB4, in two different classes of synapses. In addition, our chimeric protein experiments add further information to this mechanism. By swapping the EGF-like domain of Nrg1 and Nrg3, a manipulation that does not affect their subcellular sorting, we found that their specific functions in promoting synapse development is not encoded in a differential *trans*-synaptic interaction with ErbB4 receptor (Figure 30). In this context, *in vitro* studies previously indicated that the EGF-like domain of Nrg1 is a more potent effector than Nrg3 to trigger ErbB4 activation in phosphorylation assays (Müller et al., 2018). Nonetheless, in our *in vivo* gain-of-function

experiments, chimeric neuregulin proteins where the EGF-like domain is swapped between Nrg1 and Nrg3 are similarly capable to promote synapse formation in inhibitory and excitatory connections. These results suggest that receptor activation and signalling triggered by Nrg1 and Nrg3, irrespective of the specific EGF-like domain, induce similar synaptogenic activity *in vivo*. In contrast, our modifications of the C-terminal domain of Nrg1 and Nrg3 suggest that structural determinants are found in the cytoplasmic, intracellular domain of neuregulins to instruct their sorting to different subcellular compartments. These findings are consistent with the hypothesis that the neuregulin family diversified by acquisition and/or loss of structural sequences in the C-terminal domain to specify a distinct subcellular distribution of Nrg1 and Nrg3 within pyramidal cell bodies, hence enabling a division of labour in this family of ErbB4 ligands to impose a differential control on inhibitory input and excitatory output synapses.

Our study provides further evidence to the notion that protein diversity plays an important role in synapse formation and specification (Apóstolo and de Wit, 2019; de Wit and Ghosh, 2016). Latrophillins instruct synapse development in an input-specific manner in CA1 pyramidal cell dendrites; Lphn2 promotes the development of perforant path synapses from the entorhinal cortex into distal dendrites, whereas Lphn3 controls synapse formation in proximal dendrites that are targeted by Schaffer collaterals from the CA3 (Anderson et al., 2017; Sando et al., 2019). Type II classic cadherins regulate specific synaptic properties in hippocampal circuits; presynaptic Cdh9 and postsynaptic Cdh6 and Cdh10 mediate *trans*-cellular interactions that are required for spine development and high-magnitude long-term potentiation (LTP) in stratum oriens dendrites (Basu et al., 2017). Moreover, Cdh9 specifically regulates mossy fibre bouton formation in dentate gyrus neurons (Williams et al., 2011). In inhibitory cortical circuits, a wide variety of protein families involved in cell adhesion, including semaphorins, protocadherins and contactins, are differentially expressed by distinct interneuron types (Favuzzi et al., 2019). In the retina, cadherins cooperate in promoting specificity of connectivity patterns; several Cdhs (Cdh6-10 and 18) independently or coordinately regulate the specific assembly of distinct retinal cell types (Duan et al., 2014, 2018). In the presynaptic membrane, synaptotagmins precisely control the temporal dynamics of neurotransmitter release by acting as Ca^{2+} sensors; various members (Syt1, Syt2, Syt7 and Syt9) have been implicated in synchronous and asynchronous phases of synaptic release (Bacaj et al., 2013; Luo and Südhof, 2017; Xu et al., 2007). In conclusion, these results might illustrate how evolution,

through gene duplication and divergence, has generated a great diversity of family-related synaptic proteins that specialise in specific functions, probably to gain further control in regulating fine biological processes such as synapse formation and synaptic release.

Despite the specific alterations in cortical connectivity observed, a proportion of inhibitory and excitatory synapses are still established in the absence of *Nrg1* or *Nrg3* from pyramidal cells. As shown for example for other cell adhesion molecules, conditional genetic manipulations usually result in moderate or subtle changes in synapse density, rather than dramatic or absolute loss of synapses (Chen et al., 2017; Lee et al., 2017; Schroeder et al., 2018; Zhang et al., 2015). This suggests that synaptic proteins might be cooperating for a common goal—synapse formation—instead of acting as master regulators of this complex and multifaceted process (Kurshan and Shen, 2019; Kurshan et al., 2018). Pentraxins and neuroligin 3 regulate the maturation of excitatory synapses innervating PV+ interneurons, where Nrg3 presynaptic function takes place (Pelkey et al., 2016; Polepalli et al., 2017). Similarly, DOCK7 and L1CAM control the development of axo-axonic synapses (Tai et al., 2014, 2019), and dystroglycan plays a role in CCK+ basket synapse formation (Früh et al., 2016), the two inhibitory inputs that depend on Nrg1 signalling. Whether and how the combinatorial action of cell adhesion molecules in specific connections sculpt the formation of an elaborate synaptic network remains to be determined. Given the diversity of cell surface molecules expressed by particular cell types and the moderate or subtle deficits observed in genetic models, it is tempting to hypothesise that multiple, parallel molecular pathways cooperate to guide the assembly of circuits in the mammalian cerebral cortex.

In this study, we focused our efforts on elucidating the general principles of Nrg1 and Nrg3 function in pyramidal cells. Future directions should aim to address two major outstanding questions. First, in our exploratory analysis of scRNA-seq data we noticed that *Nrg1* and *Nrg3* expression in pyramidal cells, at least in adulthood, is not homogeneous, but rather different subtypes of projection neurons seem to express *Nrg1* and *Nrg3* at different levels (Figure 12). Cellular heterogeneity has emerged as a fundamental property to understanding the organisation and function of pyramidal cell subtypes and states (Cembrowski and Spruston, 2019; Cembrowski et al., 2016, 2018; González-Burgos et al., 2019; Stanley et al., 2019). Do distinct pyramidal cell subtypes display a differential usage of neuregulins? Do spatial gradients of *Nrg1* and *Nrg3* expression in pyramidal

cells exist across cortical layers and/or brain regions? Gene expression analysis of *Nrg1* and *Nrg3* by *in situ* hybridization or RNA-seq in combination with genetic labelling strategies to identify specific subtypes of pyramidal cells will undoubtedly shed light onto this question. This potential mechanism could explain differences underlying the differential, selective wiring of pyramidal cell subtypes (Lee et al., 2014; Ye et al., 2015). Second, neuregulins are also expressed by some populations of interneurons (Rahman et al., 2018; Sun et al., 2016). For example, VIP+ cells are important circuit elements for the control of network activity through disinhibitory mechanisms of pyramidal cells (Pi et al., 2013), and ErbB4 deletion from VIP+ cells leads to dramatic changes in cortical network activity and sensory perception (Batista-Brito et al., 2017). However, the specific synaptic alterations that may exist in this mouse model are unknown. Therefore, uncovering whether and how the synaptic communication between interneuron cell types requires neuregulin/ErbB4 signalling will be an important question to solve. In this scenario, would the same pre- and postsynaptic rules governing neureuglin/ErbB4 interactions between pyramidal cells and interneurons described here apply to interneuron-selective circuits? Overall, the mechanistic examination of neureuglin function in the cortex is only beginning to be revealed, and detailed studies of the spatial logic of neuregulin expression in subtypes of cortical neurons will pave the path for future investigations.

1.5. Impact of neuregulin function in cortical activity and behaviour

This thesis work uncovers a remarkable selectivity in the subcellular distribution of Nrg1 and Nrg3 that specifies their segregated roles in the synaptic assembly of pyramidal cells. Our work raises multiple questions regarding the physiological role of such molecular specificity for circuit performance. Synapses formed by CCK+ interneurons undergo depolarisation-induced suppression of inhibition (DSI) through a mechanism mediated by presynaptic CB1R, and this form of short-term plasticity exhibits layer and postsynaptic target specificity (Bodor et al., 2005; Hill et al., 2007; Lee et al., 2010b; Wilson et al., 2001). In agreement, we observed that CB1R-expressing somatic terminals preferentially target L2 pyramidal cells over L3 pyramidal cells (Figure 16). In addition, recent efforts in the phenotypic characterisation of transcriptomic cell types in the mouse cerebral cortex have revealed a great diversity of morphologies, physiological properties, and

anatomical locations for CCK+ interneurons (Scala et al., 2020). It is tempting to hypothesise that CCK+ interneurons exert their inhibitory control of cortical circuits in a cell type-specific fashion. In this context, our initial observations showed that *Nrg1* is expressed at variable levels by different pyramidal cell subtypes (Figure 12), which raises the possibility that Nrg1 could act as a molecular cue instructing the selective connectivity of CCK+ interneurons with different postsynaptic targets, thereby guiding circuit specificity. Retrograde labelling of target-specific pyramidal cell populations could help to elucidate the patterns of Nrg1 expression in, for instance, intratelencephalic neurons that project to associational cortices as well as pyramidal tract neurons that send long-descending projections to motor structures in the brainstem and spinal cord (Economo et al., 2018; Klingler et al., 2019). Further, electrophysiological recordings in brain slices could be used to assess whether Nrg1 function in circuit assembly might impact CB1R-mediated modulation of specific projection neurons, and therefore the plasticity of cortical networks relevant for different computations. Specifically, if Nrg1 deletion in pyramidal cells results in impaired DSI of specific cell types, endocannabinoid-dependent cortical activity and related behaviours could be affected. Notably, mouse models for *Nrg1* haploinsufficiency display sensorimotor gating deficits and stress-related disorders (Boucher et al., 2007; Chohan et al., 2014; Clarke et al., 2017), which underscores the relevance of Nrg1 function in a range of behaviours. In addition, endocannabinoid system dysregulation has been reported in the brain of heterozygous *Nrg1* mice (Clarke et al., 2017). As it has been recently shown that CCK+ cells play an important role in memory retrieval and represent an abundant interneuron population in the prefrontal cortex (Nguyen et al., 2020; Whissell et al., 2015), it will be important to explore working memory-related, prefrontal-dependent behaviours in *Nrg1* icKO mice.

The activity of cortical neurons faithfully represents the temporal features of sensory stimuli (Harris and Mrsic-Flogel, 2013). The temporal resolution of neuronal integration depends on the time window within which excitatory inputs summate to reach the threshold for spiking activity (Buzsáki, 2010; Buzsáky and Tingley, 2018; Lien and Scanziani, 2013; Pouille and Scanziani, 2001). Feed-forward inhibition enables cortical neurons to report tactile information in the somatosensory cortex with highly accurate temporal fidelity (Gabernet et al., 2005), and excitatory synapses formed onto PV+ fast-spiking interneurons control their participation in feed-forward inhibitory pathways (Atallah et al., 2012; Polepalli et al., 2017; Pouille and Scanziani, 2001). These circuit mechanisms for enhanced

temporal contrast are present in L4 and L2/3 in the form of thalamocortical and intracortical projections (Atallah et al., 2012; Bagnall et al., 2011; Gabernet et al., 2005; Xue et al., 2014). In addition, PV+ interneurons, which are known to enforce strong somatic inhibition onto pyramidal cells, are recruited by the network to rapidly balance excitation with inhibition, thereby generating rhythmic activity (Atallah and Scanziani, 2009; English et al., 2017; Klausberger et al., 2003; Stark et al., 2014). As a result, high-frequency, gamma oscillations can be modulated by engaging the spiking activity of PV+ interneurons (Cardin et al., 2009; Sohal et al., 2009). The physiological relevance of Nrg3 function has been previously studied in the context of hippocampal rhythmic activity and hippocampus-related behaviours (Müller et al., 2018). Mice lacking Nrg3 display lower gamma activity, and show altered memory performance (Müller et al., 2018; Wang et al., 2018b). In the future, it will be important to examine how the excitatory synapse loss found in *Nrg3* icKO mice may impact the temporal fidelity of pyramidal cells in cortical circuits. If feed-forward inhibition is altered, one could expect a distortion in the precise coincidence detection of sensory stimuli that govern somatosensory perception. Electrophysiological recordings coupled with stimulation of thalamic and cortical pathways could be used to study the temporal accuracy with which circuits convey sensory information when PV+ interneurons are presumably less engaged by the neuronal network as a result of reduced excitatory synaptogenesis in these cells. Furthermore, sensory discrimination tasks in mice would provide an experimental paradigm to investigate the functional consequences of excitatory synaptic deficit of PV+ interneurons in somatosensory integration and perceptual learning (Chen et al., 2020; Drapeau et al., 2018; Goel et al., 2018). In conclusion, future work should aim to investigate the impact of the specific synaptic deficits observed in *Nrg1* and *Nrg3* icKO mice in sensory, social, and cognitive function. The efforts addressing these questions will shed light on our understanding of the distinct physiological roles of Nrg1 and Nrg3 in cortical computations as well as behavioural performance.

2. Sorting mechanisms of synaptic proteins

The establishment of cortical circuits entails the formation of precise connections between defined population of neurons, where the specificity seems to depend on the recruitment of pre- and postsynaptic partners to different synaptic connections. To date, the underlying mechanisms mediating the sorting of cell-surface molecules to subcellular compartments in neurons of the cerebral cortex remain largely unknown. Here, we provide multiple lines of evidence that suggest an intrinsic genetic mechanism for subcellular sorting of family-related synaptic proteins in cortical pyramidal cells.

2.1. Cytoplasmic tails function in neuregulin subcellular sorting

We have shown that mutant Nrg1 or Nrg3 proteins lacking the whole intracellular, C-terminal domain lose their characteristic subcellular segregation. This finding indicates that the C-terminal domain is necessary for subcellular sorting, and suggests that specific amino acid sequences or motifs potentially mediate this sorting. Encouragingly, when we swapped the C-terminal domain of Nrg1 or Nrg3 by the corresponding homologous domain of the other gene, we found that the resulting chimeric proteins were relocated, at least to a large extent, to the alternative subcellular compartment. This partial rerouting of the chimeric constructs is due to lower intensity levels of the detected protein, as visualized by immunofluorescence, which could be explained by two possibilities. First, although little is known about the physiological roles of neuregulin intracellular domains, it is conceivable that distinct subdomains play various roles in the final allocation of the protein (e.g., processing, trafficking, or stability at the membrane). For instance, in the case of Nrg1, particular amino acid residues in the juxtamembrane region, downstream of the transmembrane domain, have been shown to be important for processing of the precursor form of the proteins by regulating the proteolytic cleavage of the ectodomain (Hartmann et al., 2015; Parra et al., 2015). If C-terminal domains of Nrg1 and Nrg3 contained several instructive amino acid sequences, swapping the entire domain could not only be affecting the subcellular distribution, as observed in the relocation phenotype of the chimeric proteins, but also other features of the processing and/or trafficking pathway. Second, since the

C-terminal domains of neuregulins constitute a large portion of the entire protein (360 and 382 amino acids, respectively) and the degree of homology between Nrg1 and Nrg3 intracellular domains at the amino acid level is relatively low, conformational changes in the tertiary and/or quaternary structure of the chimeric proteins could account for a lower expression and/or synaptic targeting. Consistent with this idea, structural changes in the cytoplasmic domain affecting protein expression and/or trafficking to the cell surface have been previously reported in other transmembrane proteins (Comoletti et al., 2004), as well as in other chimeric protein experiments (Gu et al., 2003; Rivera et al., 2003, 2005). Importantly, EGF-like domain swapping experiments did not change the subcellular localisation or synapse targeting of the chimeric proteins, suggesting that the sorting motifs are not encoded in extracellular domains, and reinforcing the idea that cytoplasmic, intracellular domains are responsible for the observed sorting.

Our data reveal a role for the C-terminal domain of neuregulins in subcellular sorting (Figure 42). This is consistent with previous publications studying the function of intracellular domains in other transmembrane proteins, such as NgCAM, L1CAM, Nlgn1, and VAMP2 (Rosales et al., 2005; Sampo et al., 2003; Wisco et al., 2003). The involvement of the C-terminal domain has also been shown for polarized ion channels and neurotransmitter receptors, including sodium channels, voltage-gated potassium channels, and AMPA glutamate receptors (Garrido et al., 2001; Gu et al., 2003; Matsuda et al., 2008). Thus, our work expands upon these efforts by uncovering the intracellular domain-dependent functions of neuregulins in specific compartments of pyramidal cells.

Protein trafficking represents a crucial event in establishing the subcellular organisation of molecular machineries in neurons, a process that ultimately influences neuronal differentiation and function (Ribeiro et al., 2019). Proteins are synthesised in the rough endoplasmic reticulum, modified through the Golgi apparatus, and packaged into carrier vesicles for their transport to the plasma membrane. Type I transmembrane proteins travel through distinct cytoplasmic organelles in an inside-out manner, meaning that the C-terminal tails are facing the cytoplasm and the N-terminal tails are within the lumen of the organelles. In this trafficking pathway, the trans-Golgi network (TGN) plays a crucial role in sorting transmembrane proteins into distinct pools of vesicles defined by their final fate: somatodendritic vesicles and axonal vesicles (Bentley and Banker, 2016; Burack et al., 2000; Guardia et al., 2018; Gumy and Hoogenraad, 2018; Robinson and Bonifacino, 2001). Targeting to the correct subcellular destination relies on specific

protein-protein interactions as specific subunits of clathrin-associated adaptor proteins (APs) recognize particular sorting motifs in the amino acid sequence of transmembrane proteins, as revealed by crystallography and site-directed mutagenesis studies (Mardones et al., 2013; Mattera et al., 2011; Ren et al., 2013), and, as a result, polarized proteins are loaded into the proper trafficking vesicles (Li et al., 2016).

In the light of these mechanisms for selective trafficking, what are the sorting signals in somatic Nrg1 and axonal Nrg3 proteins? What is the intracellular machinery that recognises these signals to target both neureuglin members to the correct subcellular destination? In invertebrates and mammals, the specificity of somatodendritic versus axonal sorting is mediated by the differential binding efficiencies of different AP members to specific amino acid motifs (Bonifacino, 2014; Guardia et al., 2018). For instance, tyrosine-based signals (YXXΦ) in the cytoplasmic tails of various transmembrane proteins mediate somatodendritic sorting by interaction with AP-1 (Farías et al., 2012), and preferential binding of AP-3 with dileucine motifs ([D/E]XXX[L/I]) within the cytoplasmic domain direct the sorting of proteins into vesicle pools that are targeted to axons (Li et al., 2016).

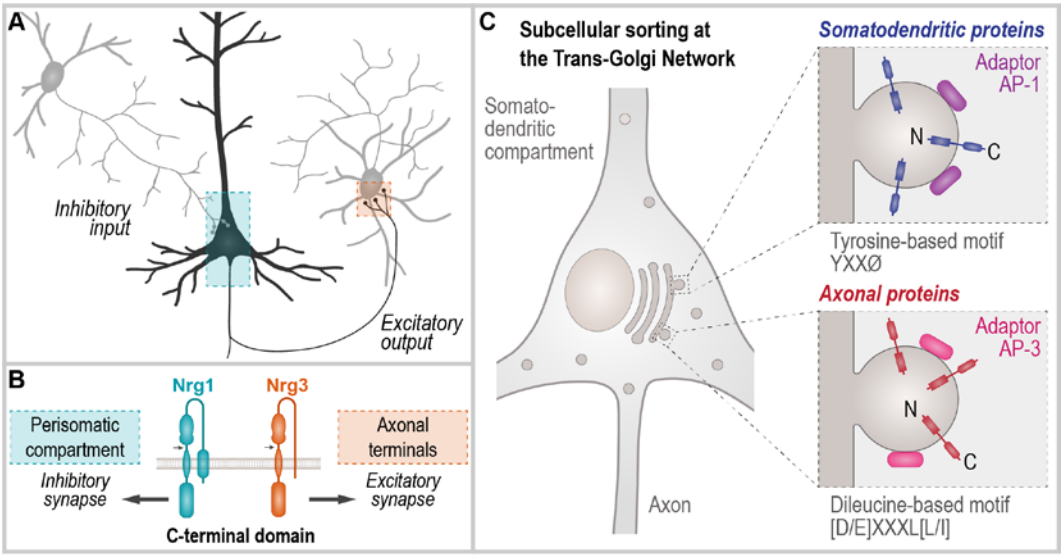

Figure 42 | **Model of C-terminal domain-dependent subcellular localisation of Nrg1 and Nrg3 in cortical pyramidal cells, and hypothesis for a molecular mechanism underlying neuregulin protein sorting.**
(**A**) Distinct subcellular distribution of Nrg1 and Nrg3 in cortical pyramidal cell bodies: somatic compartment (blue-coloured square) and axon terminals (orange-coloured square), respectively. (**B**) Representation of a differential sorting of Nrg1 and Nrg3 to inhibitory and excitatory synapses, respectively, guided by their C-terminal domain. (**C**) Proposed model of a hypothetical sorting of neuregulins at the Trans-Golgi network by the specific loading into somatodendritic and axonal vesicles through the interaction with adaptor proteins (AP-1 and AP-3).

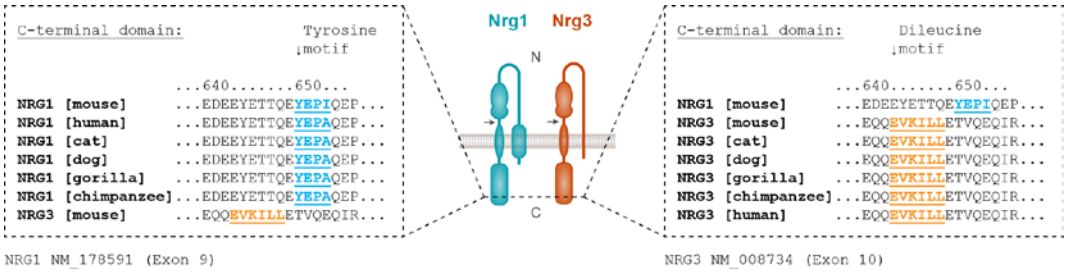

Figure 43 | **Conserved amino acid sequences related to subcellular sorting in the C-terminal domains of Nrg1 and Nrg3.**
Protein sequence analysis of the C-terminal domain of Nrg1 and Nrg3 identifies tyrosine- and dileucine-based amino acid motifs, respectively, as candidate for subcellular sorting to distinct neuronal compartments.

Interestingly, tyrosine-based and dileucine-based motifs are found in the C-terminal domains of Nrg1 and Nrg3, respectively (Figure 43). This raises the question whether these distinct amino acid motifs in the cytoplasmic tails of Nrg1 and Nrg3 play a role in a differential binding with AP-1 and AP-3, respectively, at the TGN to determine the specific loading of neuregulins into somatic and axonal vesicles. Is a tyrosine-based motif in Nrg1 C-terminal domain responsible for differential binding to AP-1 and, consequently, does it instruct somatic targeting? Does a dileucine-based motif in Nrg3 C-terminal domain preferentially binds to AP-3 to guide axonal sorting? To address this hypothetical model, we performed some initial experiments specifically introducing mutations in tyrosine- and dileucine-based motifs of Nrg1 and Nrg3, as well as swapping these amino acid motifs between both genes, and electroporating the mutation constructs into cortical pyramidal cells *in vivo*. Preliminary observations from these experiments show that modifications of the candidate motifs do not seem to alter the nature of Nrg1 and Nrg3 targeting to somatic and axonal compartment, respectively (Figure 44). However, these manipulations apparently lower the amount of Nrg1 and Nrg3 protein that reaches the cell surface, raising questions about protein synthesis, stability and/or degradation due to conformational or structural changes (Figure 44). Alternatively, we cannot rule out the possibility that subcellular sorting is dependent on multiple amino acid motifs, which could explain why modifications in a single motif do not noticeably relocate Nrg1 and/or Nrg3 proteins to different subcellular compartments within pyramidal cell bodies.

Noteworthy, a fascinating, but puzzling finding in our study is the striking restriction of Nrg1 to the perisomatic region, as opposed to a wider somatodendritic distribution. There could be additional motifs in the Nrg1 sequence that

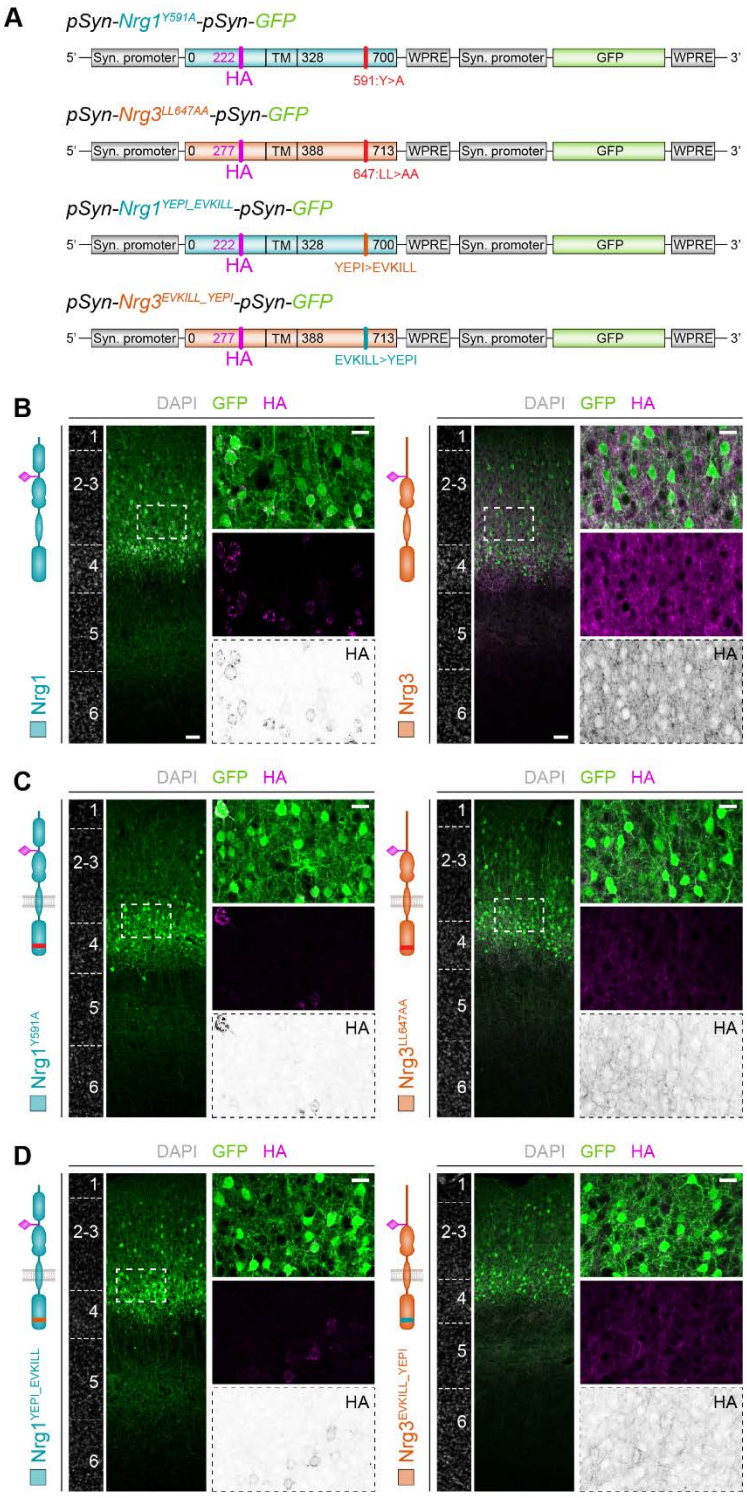

Figure 44 | **Preliminary study of the effect of mutations in candidate sorting motifs in the subcellular localisation of Nrg1 and Nrg3.** (**A**) Plasmids encoding for mutant neuregulin proteins in amino acid motifs of the C-terminal domains. (**B-D**) Coronal sections of the cerebral cortex of mice electroporated with the plasmids in shown (A). Subcellular distribution of: wild-type neuregulin proteins (**B**), Nrg1 and Nrg3 with mutations in the tyrosine- and dileucine-based motifs, respectively, within their cytoplasmic domains (**C**), and Nrg1 and Nrg3 chimeric proteins where the candidate amino acid motifs where swapped between the homologous genes.

coordinately participate in this peculiar sorting to confine the protein to pyramidal cell somas, although the nature of such motifs remains to be discovered. A potential candidate is the N-terminal region of Nrg1 containing the cysteine-rich domain (CRD), which is also located in the cytoplasmic space due to the stretch of hydrophobic amino acids that conforms a second transmembrane domain to

anchor the mature protein to the membrane (Wang et al., 2001). Regarding axonal sorting, previous studies have documented that axonal proteins can reach the axonal compartment via multiple, alternative pathways (Sampo et al., 2003; Wisco et al., 2003; Yap et al., 2008). This raises the question whether the C-terminal domain-dependent mechanism of Nrg3 axonal sorting presented here is exclusive or if alternative mechanisms may exist.

Taken together, our structure-function analysis of neuregulins uncover an essential role for the C-terminal domain in subcellular sorting (Figures 33-39). Nonetheless, clearly elucidating the mechanisms underlying Nrg1 and Nrg3 spatial segregation in cortical pyramidal cells will require further investigations, especially since our initial attempts did not yield conclusive findings on the specific recognition signals driving this process (Figure 44). One could envision systematically examining the role of other amino acid motifs as well as interacting partners, in the sorting and binding of neuregulins, although this will be technically challenging. Thus, much remains to be understood concerning the molecular mechanisms that regulate synaptic protein subcellular organisation in the mammalian cerebral cortex.

2.2. Role of subcellular sorting in cortical circuit development

Studying how the diversity of sorting mechanisms regulates trafficking of synaptic proteins to date has mostly been examined in invertebrates or *in vitro* systems (Li et al., 2016). Our study constitutes, to our knowledge, the first evidence coupling subcellular sorting mechanisms dependent on C-terminal domains to a family of cell adhesion molecules in the cerebral cortex, suggesting a fundamental role for subcellular sorting in the assembly of cortical circuits (Figure 41-42). By altering the localisations of neuregulin proteins through protein domain manipulations, we gained insight into how subcellular sorting influences afferent/efferent connectivity of pyramidal cells during postnatal development. In particular, remarkably, the sole replacement of the C-terminal domain of Nrg3 by the homologous domain of Nrg1 was sufficient to target this chimeric protein to the somatic compartment and drive synaptogenic signaling of inhibitory presynaptic inputs from CCK+ cells. In addition, overexpression of EGF-like domain swapping neuregulin constructs results in specific augmentations of inhibitory and excitatory synapses, with

comparable values to wild-type neuregulin overexpression conditions, demonstrating a direct link between neuregulin subcellular sorting and compartment-specific synaptogenesis.

While our experiments shown here focused on systematic manipulations of neuregulin domains, an alternative approach to understanding the role of subcellular sorting within cortical circuits could involve individual and/or combinatorial knock-down of the molecular machinery responsible for sorting. For instance, given AP-3 specific function in axonal sorting (Li et al., 2016), will conditional removal of AP-3 in pyramidal cells affect Nrg3 axonal transport and thus excitatory synaptogenesis in axon terminals? Encouragingly, this strategy has been proven valid in the study of endocytic system-dependent mechanism (Ribeiro et al., 2019; Savas et al., 2015). However, one could also argue that deletion of subcellular trafficking organisers could dampen clear conclusions about their specific functions in subcellular sorting of cell-adhesion molecules since this approach might likely also compromise more generally neuronal differentiation and diverse synaptic functions. Further investigation of these questions will undoubtedly help to elucidate the relationship between subcellular sorting of cell-adhesion proteins and synaptic integration of neuronal cell types into cortical circuits.

2.3. Convergence or divergence of trafficking pathways in neuronal cell types?

Our work uncovers a physiological function for the cytoplasmic tails of neuregulins in subcellular sorting as well as the molecular mechanism underlying such process. These findings raise a number of questions regarding the generalization of this mechanism. Is this sorting mechanism evolutionary conserved? Interestingly, some amino acid motifs with high homology of somatodendritic and axonal sorting sequences are evolutionary conserved across species (Figure 43), which suggests the intriguing possibility that the evolutionary acquisition of these sequence determinants could have played a role in segregating neuregulin functions to different synapses. How evolution has sculpted the assembly and connectivity of the mammalian brain remains a major question in neuroscience (Fishell and Kepecs, 2019; Krienen et al., 2019).

Whether the reported subcellular distributions and functions for Nrg1 and Nrg3 are conserved in distinct cell types and across brain regions remains a question that will require future investigation. Interestingly, expression of Nrg1 in motor neurons has been described in terminal axons, where it regulates surface targeting of nicotinic acetylcholine receptors (Hancock et al., 2008). This differential subcellular localisation of Nrg1 in central and peripheral axons might suggest a mechanism whereby its unique interaction with cell type-specific molecular repertoires provides an additional level of control to instruct the required subcellular sorting in different neuronal circuits. Neuregulins are also expressed by certain interneuron cell types in the cortex (Grieco et al., 2020; Rahman et al., 2018). What other functions Nrg1 and Nrg3 perform in different synaptic connections (e.g., in interneuron-selective interneurons) (Pfeffer et al., 2013), and how these might be mechanistically regulated, are other considerable questions that will require further attention. In this context, future experiments on the function of neuregulins in interneurons will certainly benefit from using cell type-specific approaches as shown in this work, and it will be very interesting to ascertain whether the sorting mechanisms identified in pyramidal cells is shared by GABAergic interneurons.

Several recent studies, described in the introduction, have shown the restricted subcellular distribution of cell adhesion molecules. Especially, this has been well-documented in hippocampal pyramidal cells, where NGL-2, GPR158, and two members of the latrophilin family, Lphn2 and Lphn3, are selectively targeted to different dendritic fragments (Condomitti et al., 2018; DeNardo et al., 2012; Sando et al., 2019). Are these subcellular distributions controlled by intrinsic determinants in the C-terminal domains of the proteins? And, are the underlying mechanisms dependent on the interactive network of AP proteins at the TGN? Future efforts in solving these questions will determine whether this is a general, conserved sorting mechanism, and will provide invaluable insights on the molecular regulation of cortical circuit assembly. Importantly, *in silico* surveys of amino acid motif sequences present in synaptic cell-surface proteins have been proven very informative to guide candidate-based approaches for future experimentation (Li et al., 2016).

Based on our observations and experimental approach, protein sorting acts as an important mechanism for neuregulin subcellular distribution. However, a deep RNA-sequencing study discovered the abundant presence of RNA molecules encoding for a high diversity of synapse-related proteins in the neuropil

compartment (Cajigas et al., 2012); interestingly, Nrg3 is found in this catalogue. This raises the exciting question whether *Nrg3* mRNA is locally translated in cortical axons. Given the importance of local translation in supporting synaptic function and plasticity (Biever et al., 2019), an intriguing possibility is that pyramidal cells might use two alternative mechanisms for the localized expression pattern of Nrg3 in axon terminals. From a speculative perspective, the combination of RNA and protein sorting could act in a cooperative, temporally coordinated manner to support a common goal: synaptic assembly. During cortical development, protein-based sorting might efficiently provide abundant amount of Nrg3 protein to support synapse formation, while in adult stages, RNA sorting could represent an alternative mechanism for storing an mRNA reservoir of *Nrg3* that may be rapidly accessible by the local translation machinery for synapse plasticity. A temporally regulated, activity-dependent mechanism has been similarly proposed for the concerted synaptic function of neuregulins (Müller et al., 2018), although none of these proposed mechanisms have been experimentally tested yet. New methods for direct visualization and analysis of ribosome-associated RNAs and newly synthesized proteins *in situ* (Alvarez-Castelao et al., 2019; tom Dieck et al., 2015; Sanz et al., 2009, 2019), combined with cell type-specific studies of temporal dynamics of gene expression, will be necessary to address these fascinating questions.

Our work highlights the relevance of subcellular sorting and compartment-specific targeting of synaptic proteins in the assembly of cortical circuits, a process that has escaped our attention thus far. Beyond cell type-specific control of expression patterns, it becomes now manifest the importance of elucidating the subcellular distribution of cell surface molecules, and underlying molecular mechanisms, to understanding synaptic connectivity of cell types in the cerebral cortex (Apóstolo and de Wit, 2019).

3. Implications for understanding of connectivity dysfunction in schizophrenia

The Nrg/ErbB4 signaling pathway has been associated with neuropsychiatric disorders as intensive genetic study over the last two decades has been undertaken to dissect the nature of these complex conditions. Through genome-wide association studies (GWAS) and structural variation studies, robust and replicable findings have reported a set of large-scale deletions or duplications of genomic regions (termed copy number variations, CNVs), single nucleotide variants present in high frequency in the population (referred to as single nucleotide polymorphisms, SNPs), and rare single-point mutations mapping to the *NRG1*, *NRG3* and *ERBB4* loci of patients with schizophrenia and intellectual disability (Kasnauskiene et al., 2013; Mei and Nave, 2014; Norton et al., 2006a; Walsh et al., 2008). Therefore, it was initially thought that the Nrg/ErbB4 pathway may constitute a genetic hub in mental disorders (Harrison and Law, 2006; Norton et al., 2006b).

Schizophrenia is a disabling and chronic psychiatric disorder that causes enormous personal and societal burdens, and affects about one per cent of the world's population (Collins et al., 2011). Although a basic understanding of the pathophysiology of schizophrenia is proving elusive, and therefore the lack of diagnostic and curative strategies for this condition, the hypothesis that schizophrenia could be viewed as a neurodevelopmental disorder has gained considerable attention recently (Insel, 2010; Marín, 2016; Murray and Lewis, 1988; Weinberger, 1987). Early disturbances during embryonic and postnatal brain development impact the normal course for the formation and maturation of cortical circuits, and the intervention at defined sensitive temporal windows (also called critical periods) has been proposed to be key to alter the progression to disease and even restore network and cognitive dysfunction (Millan et al., 2016; Mukherjee et al., 2019). It has also been suggested that schizophrenia, rather than being a discrete psychiatric disorder, lies on an etiological and neurodevelopmental continuum, and a complex network of gene-environment interactions is thought to underlie the susceptibility and onset of the disorder (Owen and O'Donovan, 2017). Thus, the identification of specific circuit alterations that might cause the symptoms with different degrees of severity and age of onset that characterise schizophrenia has been challenging. In this context, research on genetic mouse models has

greatly impacted our understanding of molecular and cellular processes that are closely linked to discrete behavioural abnormalities that resemble schizophrenia-like phenotypes (Del Pino et al., 2018). After a decade of progress, this approach has yielded valuable insights on the pathophysiological roles of genes associated with schizophrenia, such as *ERBB4*, *SHANK3*, and *ZDHHC8* (Del Pino et al., 2013, 2017; Mukai et al., 2015; Peixoto et al., 2016).

3.1. Synaptic dysfunction in schizophrenia — lessons from mouse models

It has been previously reported that genetic mouse models of ErbB4 dysfunction show cortical synaptic deficits similar to those seen in schizophrenia patients, and strikingly, these mutant mice display schizophrenia-like phenotypes in cognition and behaviour (Del Pino et al., 2013, 2017). Interestingly, here we have observed synaptic alterations in inhibitory-excitatory circuits in the cerebral cortex of neuregulin icKO mice that recapitulate those found in *ErbB4* cKO mice.

On the one hand, *Nrg1* icKO mice show the most characteristic synaptic alteration seen in schizophrenia patients: reduced density of axo-axonic synapses (Rocco et al., 2017; Woo et al., 1998). This synaptic deficit in schizophrenia appears to reflect a differential susceptibility of specific classes of axo-axonic boutons and their characteristic enzymes (Rocco et al., 2016, 2017). Here, we used GAD67 as a general marker to label the most chandelier cell enzymes and found a robust, selective decrease in the density of axo-axonic boutons innervating pyramidal cells in L2/3 of Nrg1 mutant mice (Fish et al., 2011). Therefore, our current findings will benefit from a further and thorough study of how Nrg1 might differentially control the development of AIS synapses in specific classes of cortical pyramidal cells and/or by distinct subpopulations of chandelier cells (Lu et al., 2017). Moreover, we found that pyramidal cells in mice lacking *Nrg1* receive reduced density of CCK+ basket cell synapses in the somatic compartment, a synaptic deficit that has also been described in schizophrenia (Eggan et al., 2008; Hashimoto et al., 2003). Due to the expression of endocannabinoid receptors in their presynaptic boutons, depolarisation-induced suppression of inhibition (DSI) plays an essential role in the spiking behaviour of CCK+ basket cells, hence the recruitment of neighboring pyramidal cells (Bodor et al., 2005; Glickfeld and

Scanziani, 2006; Trettel and Levine, 2002). Future studies should aim to address whether Nrg1 function in the inhibitory assembly of pyramidal cells contributes to this form of short-term plasticity, and ultimately, how a dysfunctional CCK+ basket cell integration into cortical circuits might be underlying abnormalities in cortical network activity in schizophrenia. In addition, studies in schizophrenia patients have also reported alterations in the expression levels of GAD67 and vesicular GABA transporter (vGAT) in basket cell synapses from PV+ interneurons, although no apparent changes in PV+ somatic bouton density have been observed (Hoftman et al., 2015; Rocco et al., 2016). Since we did not find deficits in PV+ basket synapse numbers, it would be interesting to evaluate whether GAD67 levels in these presynaptic boutons are changed after *Nrg1* conditional deletion. In this regard, electron microscopy-based ultrastructural analysis would help to explore if changes in protein levels in these synapses in *Nrg1* mutant mice may be related to fine anatomical alterations in the presynaptic nano-scale organisation. Altogether, the results presented here from neuregulin icKO mouse models appear to recapitulate the inhibitory synaptic abnormalities observed in schizophrenia patients, supporting the prevalent hypothesis of dysfunction of perisomatic inhibition in this neurodevelopmental disorder (Curley and Lewis, 2012; Lewis et al., 2011). Another consistent cellular phenotype seen in schizophrenia patients is the reduced density of dendritic spines within the dendritic domains of cortical pyramidal cells (Glantz and Lewis, 2000; Glausier and Lewis, 2013). Since this deficit could result as a compensatory change to the primary deficient inhibitory innervation of pyramidal cells, a compelling question that will draw our attention in future analyses is whether *Nrg1* icKO mice show any alterations in spine density in their apical or basal dendrites.

On the other hand, we have shown that *Nrg3* mutant mice are characterised by specific synaptic deficits in excitatory drive onto PV+ interneurons, an alteration recently associated with schizophrenia. (Chung et al., 2016). Altogether, the synaptic phenotypes found in *Nrg1* and *Nrg3* icKO mice appear to accurately match the heterogeneous synaptic deficits observed in schizophrenia patients, and thus our data further supports the hypothesis of interneuron dysfunction in this neurodevelopmental disorder (Lewis et al., 2005; Marín, 2012). Interestingly, our results point out to a striking specificity in the synaptic alterations that characterise *Nrg1* and *Nrg3* icKO mouse models, which represents a compelling evidence that certain circuit-level alterations in schizophrenia might be caused by dysfunction of selective genetic programs. Since we have not observed any evidence for

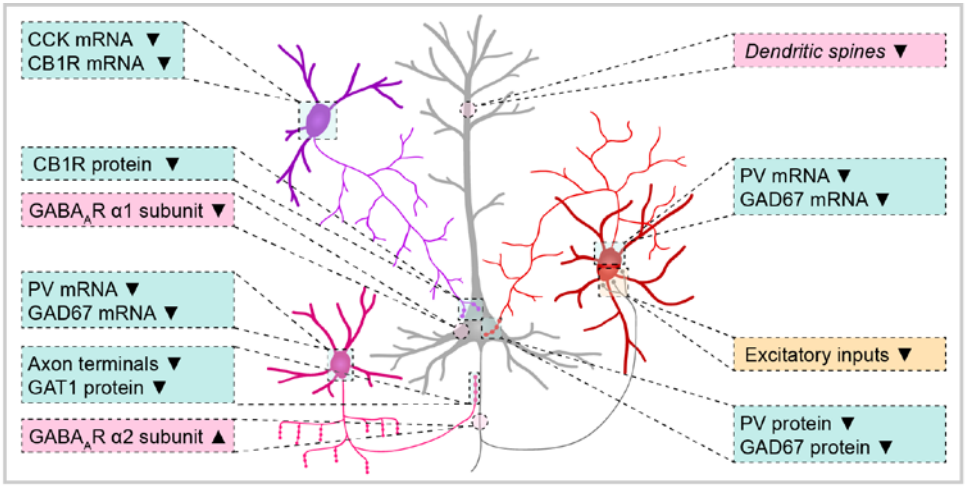

Figure 45 | **Cortical synaptic deficits in schizophrenia**.
Schematics illustrating molecular and cellular changes in the connectivity and composition of cortical circuits reported in schizophrenia patients.

compensatory synaptic changes in *Nrg1* and *Nrg3* mutant mice, these data might also suggest that, at least in superficial layers of cortical circuits involved in perisomatic inhibitory control of pyramidal neurons, the synaptic connectivity is not resilient—not able to adapt—to genetic risk factors associated with schizophrenia.

Cortical interneurons play fundamental roles in the generation of gamma-oscillations and the performance of cortical networks as well as sensory and cognitive behaviour (Cardin et al., 2009; Kim et al., 2016; Sohal et al., 2009). Multiple lines of evidence have shown a strong link between synaptic dysfunction in cortical circuits and alterations in oscillatory activity recorded in schizophrenia patients (Gonzalez-Burgos and Lewis, 2012; Gonzalez-Burgos et al., 2015; Spellman and Gordon, 2015; Uhlhaas and Singer, 2010). Remarkably, conditional deletion of *ErbB4* from specific cortical interneuron populations causes profound defects in oscillatory activity, which resembles the changes observed in schizophrenia (Del Pino et al., 2013). Therefore, it will be interesting to investigate whether *Nrg1* and *Nrg3* icKO mice display neural oscillation deficits similar to schizophrenia patients, and how they might be related to specific synaptic alterations found in cortical circuits of these mutant mice.

Overall, research on genetic animal models has rapidly transformed our ability to interrogate pathophysiological mechanisms that might affect brain development (Insel, 2010). In particular, our neuregulin conditional mutant mice have highlighted that cell type-specific connectivity dysfunction might constitute an underlying abnormality in schizophrenia (Figure 45). In addition, by combining this

loss-of-function approach with overexpression experiments *in vivo*, we have been able to corroborate that cortical synaptic assembly can be bidirectionally modulated by controlling the expression of neuregulins in pyramidal cells. This is especially important in the light that some common or structural variations linked to neurodevelopmental disorders could result in gain-of-function phenotypes rather than being deleterious. Mechanistically, to what extend our insights into the subcellular localisation and sorting of neuregulins is linked to disease will require further investigation. Undoubtedly, mechanistic and functional examination of genes associated with psychiatric disorders is paving the way to a better basic understanding of disease pathophysiology as well as brain development (Del Pino et al., 2018; Lewis, 2014).

3.2. Genetic susceptibility in neurodevelopmental disorders — lessons from psychiatry genomics

Currently, an outstanding challenge in psychiatry research is to map out the genomic architecture of psychiatric disorders in order to provide a complete catalogue of genetic variations associated with these complex traits. In the last decade, the field of human psychiatry genetics has experienced an unprecedented rate of growth, leading to fundamental insights into the biological bases of mental disorders (Sullivan et al., 2012). In fact, the development of next-generation sequencing technologies and bioinformatic tools in the current century has opened new avenues to understanding the genetic underpinnings of psychiatric disease. Through GWAS and deep exome sequencing studies of large populations—composed of thousands of patients and healthy controls—common and rare genetic variants associated with psychiatric disorders are increasingly and more rapidly documented nowadays. As a result, the emerging picture of schizophrenia at the genomic level is of a highly polygenic, heritable disorder, with pleiotropic risk genetic loci and likely complex networks of protein-protein interactions. Not only common alleles of small effect (genetic variations known as SNPs) confer a high risk for schizophrenia susceptibility (Pardiñas et al., 2018; Schizophrenia Working Group of the Psychiatric Genomics Consortium, 2014), but also this psychiatric disease shows an important burden of rare disruptive mutations (Genovese et al., 2016; Purcell et al., 2014). In addition, *de novo* mutations and CNVs have been reported to carry large effects on risk of schizophrenia (Kirov et al., 2012; Purcell

et al., 2014). Strikingly, a substantial enrichment of these genetic variations occurs in genes encoding for synaptic proteins, particularly pre- and postsynaptic signaling complexes characteristic of both inhibitory and excitatory synapses (Fromer et al., 2014; Kirov et al., 2012; Pocklington et al., 2015). Thus, consistent findings from human psychiatry genetics provide strong support to the idea that dysfunction of synapse-related processes are at the core of schizophrenia (Owen and O'Donovan, 2017).

Since the discovery of neuregulins and their cognate receptor ErbB4, multiple genetic variations found in schizophrenia patients have mapped out to their genomic loci (Kasnauskiene et al., 2013; Mei and Nave, 2014; Norton et al., 2006a; Walsh et al., 2008). Therefore, the neuregulin/ErbB4 signalling pathway represents a good example of how parallel findings in human genomics and genetic mouse models have informed each other. This has resulted in fundamental insights into the neurodevelopmental roles of these synaptic proteins and how genetic variations might affect their function in schizophrenia. Altogether, these findings suggest an underlying pathophysiological mechanism linked to cortical circuit assembly.

Of note, psychiatry genomic studies face technical limitations that challenge their current potential to reflect on the genome-wide architecture of neurodevelopmental disorders (Sullivan et al., 2012). The still limited number of patients and control samples, and the variability in the genetic background of different populations likely accounts for the still incomplete collection of genetic variations associated with schizophrenia. As the sample sizes in these studies is expected to increase, the successful characterisation of an increasing body of genetic risk factors of schizophrenia will be possible as a consequence of higher statistical power to detect association of genetic variants to phenotypes of high aetiological complexity. Despite current challenges, the recent revolution of psychiatry genomics has yielded hundreds of common and rare alleles for schizophrenia susceptibility, which has deepened our knowledge on the genetic bases of this disorder. In my opinion, nonetheless, there are two major questions regarding the impact of these findings on the biological understanding of circuit dysfunction underlying schizophrenia.

First, will the data from human genetic studies offer novel ways to screen and identify proteins with important roles for brain development? Which approaches should be developed in parallel to help fostering gene candidate studies? A current limitation of certain bioinformatics analysis lies in the

dependence on large, annotated databases of gene function that frequently lack information at the genome-wide scale due to the fact that the role of many proteins remains unexplored. Therefore, relying exclusively on data analysis of genomic patterns to infer biological mechanisms underlying the pathophysiology of schizophrenia seems an approach that would provide an incomplete understanding of this complex condition. Recent efforts to generate well-curated databases of synaptic gene functions might help to overcome these limitations (Koopmans et al., 2019). Some analytical methods have been developed to establish generalised strategies to prioritise gene candidate selection that incorporate diverse types of datasets including pathways analysis and protein-protein interaction networks (Tranchevent et al., 2016). Furthermore, the combination of omics strategies could represent a novel tool for the identification of potential gene candidates (Hall et al., 2019; Huckins et al., 2019). In this context, the development of spatial transcriptomics and human cell atlases promises to generate a coherent molecular framework to help approach these questions (Codeluppi et al., 2018; Polioudakis et al., 2019; Wang et al., 2018a).

Second, how feasible is the study of human genetic variation in animal models and with current tools? Will we be able to recapitulate and study human mutations in animal models? These questions are very relevant if one wants to understand the specific effects of genetic variants in physiological functions in intact brain circuits (Comoletti et al., 2004; Yi et al., 2016). A variety of novel methods developed in the past five years might represent new avenues to address these issues: CRISPR-mediated gene editing *in vivo*, human induced pluripotent stem cells (iPSCs), and brain organoids cultured *in vitro* (Heidenreich and Zhang, 2016; Marro et al., 2019; Quadrato et al., 2016; Yi et al., 2016; Zhang et al., 2013).

In conclusion, I believe that the convergence of human genetics and developmental neurobiology will have a major impact in our understanding of the genetic and molecular bases of neurodevelopmental disorders such as schizophrenia. The rapid development of new technological tools in biology, engineering, and computation will greatly expand the ability to systematically test the function of susceptibility genetic factors in the organisation and dynamic remodelling of cortical circuits. If basic understanding of neurodevelopmental disorders at the genetic and physiological levels is our primary goal today, our future aims must include the use of these insights to identify diagnostic markers, prevent and/or delay the development of symptoms, and restore normal cognitive functions in currently intractable, devastating mental disorders.

CONCLUSIONS

1. *Nrg1* and *Nrg3* are abundantly expressed in pyramidal cells and interneurons in the developing cerebral cortex.

2. Pyramidal cell-specific deletion of *Nrg1* and *Nrg3* during postnatal development reveals the segregated functions of these proteins in the wiring of cortical circuits.

3. Nrg1 specifically controls the development of inhibitory boutons that CCK+ basket cells and chandelier cells make onto the soma and axon initial segment of pyramidal cells, respectively.

4. Nrg3 selectively regulate the formation of excitatory synapses in pyramidal cell axons innervating PV+ interneurons.

5. Nrg1 and Nrg3 have distinct subcellular distributions in cortical pyramidal cells during postnatal development.

6. Nrg1 is restricted to the perisomatic region of pyramidal cells, and colocalises with postsynaptic clusters of inhibitory nature.

7. Nrg3 is precisely targeted to the presynaptic glutamatergic boutons that pyramidal cells make onto cortical PV+ interneurons.

8. The EGF-like domain of Nrg1 and Nrg3 does not encode the specificity in subcellular sorting nor synaptogenic function of these proteins.

9. The C-terminal domain is essential for the differential subcellular sorting of Nrg1 and Nrg3 to specific synaptic connections formed by pyramidal cells *in vivo*.

Disclosure statement

Most of the technical work presented in this thesis has been carried out by myself, and I have performed all image and data analysis. The bioinformatic analyses presented in Figures 12-13 were conducted by myself using online transcriptomic databases that are publicly available for data analysis and visualization. I have prepared all illustrations, schematics, and drawings, presented in the figures of this thesis. Nonetheless, during my PhD work, I have received some technical support in order to complete some of the experiments of my project in a time-efficient manner. In this section, I clearly state the experiments and graphs shown in this Thesis which derive from work carried out by former and current members of the lab (Laura Doglio, Catarina Osório, and Clémence Bernard):

- Staining of *Nrg1* and *Nrg3* mRNA expression in brain slices via RNAscope assay. By Laura Doglio. Corresponding to Figure 11.
- *In utero* electroporation of control *pSyn-GFP* plasmid (four brain samples) and *pSyn-Nrg3-pSyn-GFP* plasmid (six brain samples). By Catarina Osório. Corresponding to Figure 22.
- Tissue samples from control and mutant mice in Figures 13, 14, 23, and 24 were kindly provided by Clémence Bernard.
- *In utero* electroporation of *pSyn-Nrg3*$^{Ct:Nrg1}$*HA-pSyn-GFP* plasmid (four brain samples). By Catarina Osório. Corresponding to Figure 37.

REFERENCES

Acsády, L., Görcs, T.J., and Freund, T.F. (1996). Different populations of vasoactive intestinal polypeptide-immunoreactive interneurons are specialized to control pyramidal cells or interneurons in the hippocampus. Neuroscience 73, 317–334.

Acuna, C., Liu, X., and Südhof, T.C. (2016). How to Make an Active Zone: Unexpected Universal Functional Redundancy between RIMs and RIM-BPs. Neuron 91, 792–807.

Adesnik, H., and Scanziani, M. (2010). Lateral competition for cortical space by layer-specific horizontal circuits. Nature 464, 1155–1160.

Adesnik, H., Bruns, W., Taniguchi, H., Huang, Z.J., and Scanziani, M. (2012). A neural circuit for spatial summation in visual cortex. Nature 490, 226–231.

Agarwal, A., Dibaj, P., Kassmann, C.M., Goebbels, S., Nave, K.-A., and Schwab, M.H. (2012). In vivo imaging and noninvasive ablation of pyramidal neurons in adult NEX-CreERT2 mice. Cereb. Cortex 22, 1473–1486.

Agarwal, A., Zhang, M., Trembak-Duff, I., Unterbarnscheidt, T., Radyushkin, K., Dibaj, P., Martins de Souza, D., Boretius, S., Brzózka, M.M., Steffens, H., et al. (2014). Dysregulated expression of neuregulin-1 by cortical pyramidal neurons disrupts synaptic plasticity. Cell Rep. 8, 1130–1145.

Allen, W.E., Kauvar, I.V., Chen, M.Z., Richman, E.B., Yang, S.J., Chan, K., Gradinaru, V., Deverman, B.E., Luo, L., and Deisseroth, K. (2017). Global Representations of Goal-Directed Behavior in Distinct Cell Types of Mouse Neocortex. Neuron 94, 891–907.e6.

Allen, W.E., Chen, M.Z., Pichamoorthy, N., Tien, R.H., Pachitariu, M., Luo, L., and Deisseroth, K. (2019). Thirst regulates motivated behavior through modulation of brainwide neural population dynamics. Science.

Alvarez-Castelao, B., Schanzenbächer, C.T., Langer, J.D., and Schuman, E.M. (2019). Cell-type-specific metabolic labeling, detection and identification of nascent proteomes in vivo. Nat. Protoc. 14, 556–575.

Anastasiades, P.G., Marques-Smith, A., Lyngholm, D., Lickiss, T., Raffiq, S., Kätzel, D., Miesenböck, G., and Butt, S.J.B. (2016). GABAergic interneurons form transient layer-specific circuits in early postnatal neocortex. Nat. Commun. 7, 10584.

Anastasiades, P.G., Marlin, J.J., and Carter, A.G. (2018). Cell-Type Specificity of Callosally Evoked Excitation and Feedforward Inhibition in the Prefrontal Cortex. Cell Rep. 22, 679–692.

Anderson, G.R., Maxeiner, S., Sando, R., Tsetsenis, T., Malenka, R.C., and Südhof, T.C. (2017). Postsynaptic adhesion GPCR latrophilin-2 mediates target recognition in entorhinal-hippocampal synapse assembly. J. Cell Biol. 216, 3831–3846.

Anderson, S.A., Eisenstat, D.D., Shi, L., and Rubenstein, J.L. (1997). Interneuron migration from basal forebrain to neocortex: dependence on Dlx genes. Science 278, 474–476.

Anderson, S.A., Marín, O., Horn, C., Jennings, K., and Rubenstein, J.L. (2001). Distinct cortical migrations from the medial and lateral ganglionic eminences. Development 128, 353–363.

Andreassi, C., and Riccio, A. (2009). To localize or not to localize: mRNA fate is in 3'UTR ends. Trends Cell Biol. 19, 465–474.

Aoto, J., Martinelli, D.C., Malenka, R.C., Tabuchi, K., and Südhof, T.C. (2013). Presynaptic neurexin-3 alternative splicing trans-synaptically controls postsynaptic AMPA receptor trafficking. Cell 154, 75–88.

Apóstolo, N., and de Wit, J. (2019). Compartmentalized distributions of neuronal and glial cell-surface proteins pattern the synaptic network. Curr. Opin. Neurobiol. 57, 126–133.

Arango, C., Díaz-Caneja, C.M., McGorry, P.D., Rapoport, J., Sommer, I.E., Vorstman, J.A., McDaid, D., Marín, O., Serrano-Drozdowskyj, E., Freedman, R., et al. (2018). Preventive strategies for mental health. Lancet Psychiatry.

Arlotta, P., Molyneaux, B.J., Chen, J., Inoue, J., Kominami, R., and Macklis, J.D. (2005). Neuronal subtype-specific genes that control corticospinal motor neuron development in vivo. Neuron 45, 207–221.

Ascoli, G.A., Alonso-Nanclares, L., Anderson, S.A., Barrionuevo, G., Benavides-Piccione, R., Burkhalter, A., Buzsáki, G., Cauli, B., DeFelipe, J., Fairén, A., et al. (2008). Petilla terminology: nomenclature of features of GABAergic interneurons of the cerebral cortex. Nat. Rev. Neurosci. 9, 557–568.

Atallah, B.V., and Scanziani, M. (2009). Instantaneous modulation of gamma oscillation frequency by balancing excitation with inhibition. Neuron 62, 566–577.

Atallah, B.V., Bruns, W., Carandini, M., and Scanziani, M. (2012). Parvalbumin-expressing interneurons linearly transform cortical responses to visual stimuli. Neuron 73, 159–170.

Azim, E., Jabaudon, D., Fame, R.M., and Macklis, J.D. (2009). SOX6 controls dorsal progenitor identity and interneuron diversity during neocortical development. Nat. Neurosci. 12, 1238–1247.

Babij, R., and De Marco Garcia, N. (2016). Neuronal activity controls the development of interneurons in the somatosensory cortex. Front. Biol. 11, 459–470.

Bacaj, T., Wu, D., Yang, X., Morishita, W., Zhou, P., Xu, W., Malenka, R.C., and Südhof, T.C. (2013). Synaptotagmin-1 and synaptotagmin-7 trigger synchronous and asynchronous phases of neurotransmitter release. Neuron 80, 947–959.

Bagnall, M.W., Hull, C., Bushong, E.A., Ellisman, M.H., and Scanziani, M. (2011). Multiple clusters of release sites formed by individual thalamic afferents onto cortical interneurons ensure reliable transmission. Neuron 71, 180–194.

Bao, J., Wolpowitz, D., Role, L.W., and Talmage, D.A. (2003). Back signaling by the Nrg-1 intracellular domain. J. Cell Biol. 161, 1133–1141.

Bao, J., Lin, H., Ouyang, Y., Lei, D., Osman, A., Kim, T.-W., Mei, L., Dai, P., Ohlemiller, K.K., and Ambron, R.T. (2004). Activity-dependent transcription regulation of PSD-95 by neuregulin-1 and Eos. Nat. Neurosci. 7, 1250–1258.

Bartolini, G., Sánchez-Alcañiz, J.A., Osório, C., Valiente, M., García-Frigola, C., and Marín, O. (2017). Neuregulin 3 Mediates Cortical Plate Invasion and Laminar Allocation of GABAergic Interneurons. Cell Rep. 18, 1157–1170.

Basu, R., Duan, X., Taylor, M.R., Martin, E.A., Muralidhar, S., Wang, Y., Gangi-Wellman, L., Das, S.C., Yamagata, M., West, P.J., et al. (2017). Heterophilic Type II Cadherins Are Required for High-Magnitude Synaptic Potentiation in the Hippocampus. Neuron 96, 160–176.e8.

Batista, A.F.R., Martínez, J.C., and Hengst, U. (2017). Intra-axonal Synthesis of SNAP25 Is Required for the Formation of Presynaptic Terminals. Cell Rep. 20, 3085–3098.

Batista-Brito, R., and Fishell, G. (2009). The developmental integration of cortical interneurons into a functional network. Curr. Top. Dev. Biol. 87, 81–118.

Batista-Brito, R., Machold, R., Klein, C., and Fishell, G. (2008). Gene expression in cortical interneuron precursors is prescient of their mature function. Cereb. Cortex 18, 2306–2317.

Batista-Brito, R., Rossignol, E., Hjerling-Leffler, J., Denaxa, M., Wegner, M., Lefebvre, V., Pachnis, V., and Fishell, G. (2009). The cell-intrinsic requirement of Sox6 for cortical interneuron development. Neuron 63, 466–481.

Batista-Brito, R., Vinck, M., Ferguson, K.A., Chang, J.T., Laubender, D., Lur, G., Mossner, J.M., Hernandez, V.G., Ramakrishnan, C., Deisseroth, K., et al. (2017). Developmental Dysfunction of VIP Interneurons Impairs Cortical Circuits. Neuron 95, 884–895.e9.

Bemben, M.A., Shipman, S.L., Hirai, T., Herring, B.E., Li, Y., Badger, J.D., 2nd, Nicoll, R.A., Diamond, J.S., and Roche, K.W. (2014). CaMKII phosphorylation of neuroligin-1 regulates excitatory synapses. Nat. Neurosci. 17, 56–64.

Ben-Ari, Y. (2002). Excitatory actions of gaba during development: the nature of the nurture. Nat. Rev. Neurosci. 3, 728–739.

Bentley, M., and Banker, G. (2016). The cellular mechanisms that maintain neuronal polarity. Nat. Rev. Neurosci. 17, 611–622.

Bertero, A., Feyen, P.L.C., Zurita, H., and Apicella, A.J. (2019). A Non-Canonical Cortico-Amygdala Inhibitory Loop. J. Neurosci. 39, 8424–8438.

Biermann, B., Sokoll, S., Klueva, J., Missler, M., Wiegert, J.S., Sibarita, J.-B., and Heine, M. (2014). Imaging of molecular surface dynamics in brain slices using single-particle tracking. Nat. Commun. 5, 3024.

Biever, A., Donlin-Asp, P.G., and Schuman, E.M. (2019). Local translation in neuronal processes. Curr. Opin. Neurobiol. 57, 141–148.

Bloodgood, B.L., Sharma, N., Browne, H.A., Trepman, A.Z., and Greenberg, M.E. (2013). The activity-dependent transcription factor NPAS4 regulates domain-specific inhibition. Nature 503, 121–125.

Bodor, A.L., Katona, I., Nyíri, G., Mackie, K., Ledent, C., Hájos, N., and Freund, T.F. (2005). Endocannabinoid signaling in rat somatosensory cortex: laminar differences and involvement of specific interneuron types. J. Neurosci. 25, 6845–6856.

Bonifacino, J.S. (2014). Adaptor proteins involved in polarized sorting. J. Cell Biol. 204, 7–17.

Bortone, D.S., Olsen, S.R., and Scanziani, M. (2014). Translaminar inhibitory cells recruited by layer 6 corticothalamic neurons suppress visual cortex. Neuron 82, 474–485.

Boucard, A.A., Chubykin, A.A., Comoletti, D., Taylor, P., and Südhof, T.C. (2005). A splice code for trans-synaptic cell adhesion mediated by binding of neuroligin 1 to alpha- and beta-neurexins. Neuron 48, 229–236.

Boucher, A.A., Arnold, J.C., Duffy, L., Schofield, P.R., Micheau, J., and Karl, T. (2007). Heterozygous neuregulin 1 mice are more sensitive to the behavioural effects of Delta9-tetrahydrocannabinol. Psychopharmacology 192, 325–336.

Braakman, I., and Hebert, D.N. (2013). Protein folding in the endoplasmic reticulum. Cold Spring Harb. Perspect. Biol. 5, a013201.

Brigidi, G.S., and Bamji, S.X. (2011). Cadherin-catenin adhesion complexes at the synapse. Curr. Opin. Neurobiol. 21, 208–214.

Brinkmann, B.G., Agarwal, A., Sereda, M.W., Garratt, A.N., Müller, T., Wende, H., Stassart, R.M., Nawaz, S., Humml, C., Velanac, V., et al. (2008). Neuregulin-1/ErbB signaling serves distinct functions in myelination of the peripheral and central nervous system. Neuron 59, 581–595.

Buhl, E.H., Cobb, S.R., Halasy, K., and Somogyi, P. (1995). Properties of unitary IPSPs evoked by anatomically identified basket cells in the rat hippocampus. Eur. J. Neurosci. 7, 1989–2004.

Burack, M.A., Silverman, M.A., and Banker, G. (2000). The role of selective transport in neuronal protein sorting. Neuron 26, 465–472.

Burden, S., and Yarden, Y. (1997). Neuregulins and their receptors: a versatile signaling module in organogenesis and oncogenesis. Neuron 18, 847–855.

Butt, S.J.B., Fuccillo, M., Nery, S., Noctor, S., Kriegstein, A., Corbin, J.G., and Fishell, G. (2005). The temporal and spatial origins of cortical interneurons predict their physiological subtype. Neuron 48, 591–604.

Butt, S.J.B., Sousa, V.H., Fuccillo, M.V., Hjerling-Leffler, J., Miyoshi, G., Kimura, S., and Fishell, G. (2008). The requirement of Nkx2-1 in the temporal specification of cortical interneuron subtypes. Neuron 59, 722–732.

Buzsáki, G. (2002). Theta oscillations in the hippocampus. Neuron 33, 325–340.

Buzsáki, G. (2010). Neural syntax: cell assemblies, synapsembles, and readers. Neuron 68, 362–385.

Buzsáki, G., and Tingley, D. (2018). Space and Time: The Hippocampus as a Sequence Generator. Trends Cogn. Sci. 22, 853–869.

Buzsáki, G., and Wang, X.-J. (2012). Mechanisms of gamma oscillations. Annu. Rev. Neurosci. 35, 203–225.

Cajigas, I.J., Tushev, G., Will, T.J., tom Dieck, S., Fuerst, N., and Schuman, E.M. (2012). The local transcriptome in the synaptic neuropil revealed by deep sequencing and high-resolution imaging. Neuron 74, 453–466.

Cardin, J.A., Carlén, M., Meletis, K., Knoblich, U., Zhang, F., Deisseroth, K., Tsai, L.-H., and Moore, C.I. (2009). Driving fast-spiking cells induces gamma rhythm and controls sensory responses. Nature 459, 663–667.

Carraway, K.L., 3rd, Weber, J.L., Unger, M.J., Ledesma, J., Yu, N., Gassmann, M., and Lai, C. (1997). Neuregulin-2, a new ligand of ErbB3/ErbB4-receptor tyrosine kinases. Nature 387, 512–516.

Carrillo-Reid, L., Han, S., Yang, W., Akrouh, A., and Yuste, R. (2019). Controlling Visually Guided Behavior by Holographic Recalling of Cortical Ensembles. Cell 178, 447–457.e5.

Catalano, S.M., and Shatz, C.J. (1998). Activity-dependent cortical target selection by thalamic axons. Science 281, 559–562.

Cembrowski, M.S., and Spruston, N. (2019). Heterogeneity within classical cell types is the rule: lessons from hippocampal pyramidal neurons. Nat. Rev. Neurosci. 20, 193–204.

Cembrowski, M.S., Bachman, J.L., Wang, L., Sugino, K., Shields, B.C., and Spruston, N. (2016). Spatial Gene-Expression Gradients Underlie Prominent Heterogeneity of CA1 Pyramidal Neurons. Neuron 89, 351–368.

Cembrowski, M.S., Phillips, M.G., DiLisio, S.F., Shields, B.C., Winnubst, J., Chandrashekar, J., Bas, E., and Spruston, N. (2018). Dissociable Structural and Functional Hippocampal Outputs via Distinct Subiculum Cell Classes. Cell 173, 1280–1292.e18.

Chamma, I., Letellier, M., Butler, C., Tessier, B., Lim, K.-H., Gauthereau, I., Choquet, D., Sibarita, J.-B., Park, S., Sainlos, M., et al. (2016). Mapping the dynamics and nanoscale organization of synaptic adhesion proteins using monomeric streptavidin. Nat. Commun. 7, 10773.

Chang, H., Riese, D.J., 2nd, Gilbert, W., Stern, D.F., and McMahan, U.J. (1997). Ligands for ErbB-family receptors encoded by a neuregulin-like gene. Nature 387, 509–512.

Che, A., Babij, R., Iannone, A.F., Fetcho, R.N., Ferrer, M., Liston, C., Fishell, G., and De Marco García, N.V. (2018). Layer I Interneurons Sharpen Sensory Maps during Neonatal Development. Neuron 99, 98–116.e7.

Chen, L.Y., Jiang, M., Zhang, B., Gokce, O., and Südhof, T.C. (2017). Conditional Deletion of All Neurexins Defines Diversity of Essential Synaptic Organizer Functions for Neurexins. Neuron 94, 611–625.e4.

Chen, Q., Deister, C.A., Gao, X., Guo, B., Lynn-Jones, T., Chen, N., Wells, M.F., Liu, R., Goard, M.J., Dimidschstein, J., et al. (2020). Dysfunction of cortical GABAergic neurons leads to sensory hyper-reactivity in a Shank3 mouse model of ASD. Nat. Neurosci.

Chen, Y.-J., Zhang, M., Yin, D.-M., Wen, L., Ting, A., Wang, P., Lu, Y.-S., Zhu, X.-H., Li, S.-J., Wu, C.-Y., et al. (2010). ErbB4 in parvalbumin-positive interneurons is critical for neuregulin 1 regulation of long-term potentiation. Proc. Natl. Acad. Sci. U. S. A. 107, 21818–21823.

Chen, Y.-J.J., Johnson, M.A., Lieberman, M.D., Goodchild, R.E., Schobel, S., Lewandowski, N., Rosoklija, G., Liu, R.-C., Gingrich, J.A., Small, S., et al. (2008). Type III neuregulin-1 is required for normal sensorimotor gating, memory-related behaviors, and corticostriatal circuit components. J. Neurosci. 28, 6872–6883.

Cho, K.K.A., Hoch, R., Lee, A.T., Patel, T., Rubenstein, J.L.R., and Sohal, V.S. (2015). Gamma rhythms link prefrontal interneuron dysfunction with cognitive inflexibility in Dlx5/6(+/-) mice. Neuron 85, 1332–1343.

Chohan, T.W., Boucher, A.A., Spencer, J.R., Kassem, M.S., Hamdi, A.A., Karl, T., Fok, S.Y., Bennett, M.R., and Arnold, J.C. (2014). Partial genetic deletion of neuregulin 1 modulates the effects of stress on sensorimotor gating, dendritic morphology, and HPA axis activity in adolescent mice. Schizophr. Bull. 40, 1272–1284.

Chou, C.-F., and Ozaki, M. (2010). In silico analysis of neuregulin 1 evolution in vertebrates. Biosci. Rep. 30, 267–275.

Chung, D.W., Fish, K.N., and Lewis, D.A. (2016). Pathological Basis for Deficient Excitatory Drive to Cortical Parvalbumin Interneurons in Schizophrenia. Am. J. Psychiatry 173, 1131–1139.

Cioni, J.-M., Koppers, M., and Holt, C.E. (2018). Molecular control of local translation in axon development and maintenance. Curr. Opin. Neurobiol. 51, 86–94.

Cioni, J.-M., Lin, J.Q., Holtermann, A.V., Koppers, M., Jakobs, M.A.H., Azizi, A., Turner-Bridger, B., Shigeoka, T., Franze, K., Harris, W.A., et al. (2019). Late Endosomes Act as mRNA Translation Platforms and Sustain Mitochondria in Axons. Cell 176, 56–72.e15.

Citri, A., and Yarden, Y. (2006). EGF-ERBB signalling: towards the systems level. Nat. Rev. Mol. Cell Biol. 7, 505–516.

Clarke, D.J., Stuart, J., McGregor, I.S., and Arnold, J.C. (2017). Endocannabinoid dysregulation in cognitive and stress-related brain regions in the Nrg1 mouse model of schizophrenia. Prog. Neuropsychopharmacol. Biol. Psychiatry 72, 9–15.

Close, J., Xu, H., De Marco García, N.V., Batista-Brito, R., Rossignol, E., Rudy, B., and Fishell, G. (2012). Satb1 is an activity-modulated transcription factor required for the terminal differentiation and connectivity of medial ganglionic eminence-derived cortical interneurons. J. Neurosci. 32, 17690–17705.

Codeluppi, S., Borm, L.E., Zeisel, A., La Manno, G., van Lunteren, J.A., Svensson, C.I., and Linnarsson, S. (2018). Spatial organization of the somatosensory cortex revealed by osmFISH. Nat. Methods 15, 932–935.

Collins, P.Y., Patel, V., Joestl, S.S., March, D., Insel, T.R., Daar, A.S., Scientific Advisory Board and the Executive Committee of the Grand Challenges on Global Mental Health, Anderson, W., Dhansay, M.A., Phillips, A., et al. (2011). Grand challenges in global mental health. Nature 475, 27–30.

Comoletti, D., De Jaco, A., Jennings, L.L., Flynn, R.E., Gaietta, G., Tsigelny, I., Ellisman, M.H., and Taylor, P. (2004). The Arg451Cys-neuroligin-3 mutation associated with autism reveals a defect in protein processing. J. Neurosci. 24, 4889–4893.

Comoletti, D., Flynn, R.E., Boucard, A.A., Demeler, B., Schirf, V., Shi, J., Jennings, L.L., Newlin, H.R., Südhof, T.C., and Taylor, P. (2006). Gene selection, alternative splicing, and post-translational processing regulate neuroligin selectivity for beta-neurexins. Biochemistry 45, 12816–12827.

Condomitti, G., and de Wit, J. (2018). Heparan Sulfate Proteoglycans as Emerging Players in Synaptic Specificity. Front. Mol. Neurosci. 11, 14.

Condomitti, G., Wierda, K.D., Schroeder, A., Rubio, S.E., Vennekens, K.M., Orlandi, C., Martemyanov, K.A., Gounko, N.V., Savas, J.N., and de Wit, J. (2018). An Input-Specific Orphan Receptor GPR158-HSPG Interaction Organizes Hippocampal Mossy Fiber-CA3 Synapses. Neuron 100, 201–215.e9.

Corbin, J.G., Nery, S., and Fishell, G. (2001). Telencephalic cells take a tangent: non-radial migration in the mammalian forebrain. Nat. Neurosci. 4 Suppl, 1177–1182.

Corriveau, R.A., Huh, G.S., and Shatz, C.J. (1998). Regulation of class I MHC gene expression in the developing and mature CNS by neural activity. Neuron 21, 505–520.

Cossart, R., Aronov, D., and Yuste, R. (2003). Attractor dynamics of network UP states in the neocortex. Nature 423, 283–288.

Cossell, L., Iacaruso, M.F., Muir, D.R., Houlton, R., Sader, E.N., Ko, H., Hofer, S.B., and Mrsic-Flogel, T.D. (2015). Functional organization of excitatory synaptic strength in primary visual cortex. Nature 518, 399–403.

Curley, A.A., and Lewis, D.A. (2012). Cortical basket cell dysfunction in schizophrenia. J. Physiol. 590, 715–724.

Custo Greig, L.F., Woodworth, M.B., Galazo, M.J., Padmanabhan, H., and Macklis, J.D. (2013). Molecular logic of neocortical projection neuron specification, development and diversity. Nat. Rev. Neurosci. 14, 755–769.

Dai, J., Aoto, J., and Südhof, T.C. (2019). Alternative Splicing of Presynaptic Neurexins Differentially Controls Postsynaptic NMDA and AMPA Receptor Responses. Neuron.

Dávid, C., Schleicher, A., Zuschratter, W., and Staiger, J.F. (2007). The innervation of parvalbumin-containing interneurons by VIP-immunopositive interneurons in the primary somatosensory cortex of the adult rat. Eur. J. Neurosci. 25, 2329–2340.

DeFelipe, J., López-Cruz, P.L., Benavides-Piccione, R., Bielza, C., Larrañaga, P., Anderson, S., Burkhalter, A., Cauli, B., Fairén, A., Feldmeyer, D., et al. (2013). New insights into the classification and nomenclature of cortical GABAergic interneurons. Nat. Rev. Neurosci. 14, 202–216.

Dehorter, N., Ciceri, G., Bartolini, G., Lim, L., del Pino, I., and Marín, O. (2015). Tuning of fast-spiking interneuron properties by an activity-dependent transcriptional switch. Science 349, 1216–1220.

Del Pino, I., García-Frigola, C., Dehorter, N., Brotons-Mas, J.R., Alvarez-Salvado, E., Martínez de Lagrán, M., Ciceri, G., Gabaldón, M.V., Moratal, D., Dierssen, M., et al. (2013). Erbb4 deletion from fast-spiking interneurons causes schizophrenia-like phenotypes. Neuron 79, 1152–1168.

Del Pino, I., Brotons-Mas, J.R., Marques-Smith, A., Marighetto, A., Frick, A., Marín, O., and Rico, B. (2017). Abnormal wiring of CCK(+) basket cells disrupts spatial information coding. Nat. Neurosci.

Del Pino, I., Rico, B., and Marín, O. (2018). Neural circuit dysfunction in mouse models of neurodevelopmental disorders. Curr. Opin. Neurobiol. 48, 174–182.

De Marco García, N.V., Karayannis, T., and Fishell, G. (2011). Neuronal activity is required for the development of specific cortical interneuron subtypes. Nature 472, 351–355.

De Marco García, N.V., Priya, R., Tuncdemir, S.N., Fishell, G., and Karayannis, T. (2015). Sensory inputs control the integration of neurogliaform interneurons into cortical circuits. Nat. Neurosci. 18, 393–401.

DeNardo, L.A., de Wit, J., Otto-Hitt, S., and Ghosh, A. (2012). NGL-2 regulates input-specific synapse development in CA1 pyramidal neurons. Neuron 76, 762–775.

Denaxa, M., Neves, G., Rabinowitz, A., Kemlo, S., Liodis, P., Burrone, J., and Pachnis, V. (2018). Modulation of Apoptosis Controls Inhibitory Interneuron Number in the Cortex. Cell Rep. 22, 1710–1721.

Dias, C.M., and Walsh, C.A. (2020). Recent Advances in Understanding the Genetic Architecture of Autism. Annu. Rev. Genomics Hum. Genet. 21, 289–304.

tom Dieck, S., Kochen, L., Hanus, C., Heumüller, M., Bartnik, I., Nassim-Assir, B., Merk, K., Mosler, T., Garg, S., Bunse, S., et al. (2015). Direct visualization of newly synthesized target proteins in situ. Nat. Methods 12, 411–414.

Dimidschstein, J., Chen, Q., Tremblay, R., Rogers, S.L., Saldi, G.-A., Guo, L., Xu, Q., Liu, R., Lu, C., Chu, J., et al. (2016). A viral strategy for targeting and manipulating interneurons across vertebrate species. Nat. Neurosci. 19, 1743–1749.

Dittrich, L., Heiss, J.E., Warrier, D.R., Perez, X.A., Quik, M., and Kilduff, T.S. (2012). Cortical nNOS neurons co-express the NK1 receptor and are depolarized by Substance P in multiple mammalian species. Front. Neural Circuits 6, 31.

Donato, F., Rompani, S.B., and Caroni, P. (2013). Parvalbumin-expressing basket-cell network plasticity induced by experience regulates adult learning. Nature 504, 272–276.

Donato, F., Chowdhury, A., Lahr, M., and Caroni, P. (2015). Early- and late-born parvalbumin basket cell subpopulations exhibiting distinct regulation and roles in learning. Neuron 85, 770–786.

Drapeau, E., Riad, M., Kajiwara, Y., and Buxbaum, J.D. (2018). Behavioral Phenotyping of an Improved Mouse Model of Phelan-McDermid Syndrome with a Complete Deletion of the Shank3 Gene. eNeuro 5.

Duan, X., Krishnaswamy, A., De la Huerta, I., and Sanes, J.R. (2014). Type II cadherins guide assembly of a direction-selective retinal circuit. Cell 158, 793–807.

Duan, X., Krishnaswamy, A., Laboulaye, M.A., Liu, J., Peng, Y.-R., Yamagata, M., Toma, K., and Sanes, J.R. (2018). Cadherin Combinations Recruit Dendrites of Distinct Retinal Neurons to a Shared Interneuronal Scaffold. Neuron 99, 1145–1154.e6.

Duret, L., Semon, M., Piganeau, G., Mouchiroud, D., and Galtier, N. (2002). Vanishing GC-rich isochores in mammalian genomes. Genetics 162, 1837-1847.

Economo, M.N., Viswanathan, S., Tasic, B., Bas, E., Winnubst, J., Menon, V., Graybuck, L.T., Nguyen, T.N., Smith, K.A., Yao, Z., et al. (2018). Distinct descending motor cortex pathways and their roles in movement. Nature 563, 79–84.

Eggan, S.M., Hashimoto, T., and Lewis, D.A. (2008). Reduced cortical cannabinoid 1 receptor messenger RNA and protein expression in schizophrenia. Arch. Gen. Psychiatry 65, 772–784.

Elegheert, J., Kakegawa, W., Clay, J.E., Shanks, N.F., Behiels, E., Matsuda, K., Kohda, K., Miura, E., Rossmann, M., Mitakidis, N., et al. (2016). Structural basis

for integration of GluD receptors within synaptic organizer complexes. Science 353, 295–299.

Elegheert, J., Cvetkovska, V., Clayton, A.J., Heroven, C., Vennekens, K.M., Smukowski, S.N., Regan, M.C., Jia, W., Smith, A.C., Furukawa, H., et al. (2017). Structural Mechanism for Modulation of Synaptic Neuroligin-Neurexin Signaling by MDGA Proteins. Neuron 95, 896–913.e10.

von Engelhardt, J., Khrulev, S., Eliava, M., Wahlster, S., and Monyer, H. (2011). 5-HT(3A) receptor-bearing white matter interstitial GABAergic interneurons are functionally integrated into cortical and subcortical networks. J. Neurosci. 31, 16844–16854.

English, D.F., McKenzie, S., Evans, T., Kim, K., Yoon, E., and Buzsáki, G. (2017). Pyramidal Cell-Interneuron Circuit Architecture and Dynamics in Hippocampal Networks. Neuron 96, 505–520.e7.

Falls, D.L., Rosen, K.M., Corfas, G., Lane, W.S., and Fischbach, G.D. (1993). ARIA, a protein that stimulates acetylcholine receptor synthesis, is a member of the neu ligand family. Cell 72, 801–815.

Fame, R.M., MacDonald, J.L., and Macklis, J.D. (2011). Development, specification, and diversity of callosal projection neurons. Trends Neurosci. 34, 41–50.

Farías, G.G., Cuitino, L., Guo, X., Ren, X., Jarnik, M., Mattera, R., and Bonifacino, J.S. (2012). Signal-mediated, AP-1/clathrin-dependent sorting of transmembrane receptors to the somatodendritic domain of hippocampal neurons. Neuron 75, 810–823.

Farías, G.G., Guardia, C.M., Britt, D.J., Guo, X., and Bonifacino, J.S. (2015). Sorting of Dendritic and Axonal Vesicles at the Pre-axonal Exclusion Zone. Cell Rep. 13, 1221–1232.

Favuzzi, E., Marques-Smith, A., Deogracias, R., Winterflood, C.M., Sánchez-Aguilera, A., Mantoan, L., Maeso, P., Fernandes, C., Ewers, H., and Rico, B. (2017). Activity-Dependent Gating of Parvalbumin Interneuron Function by the Perineuronal Net Protein Brevican. Neuron.

Favuzzi, E., Deogracias, R., Marques-Smith, A., Maeso, P., Jezequel, J., Exposito-Alonso, D., Balia, M., Kroon, T., Hinojosa, A.J., F Maraver, E., et al. (2019). Distinct

molecular programs regulate synapse specificity in cortical inhibitory circuits. Science 363, 413–417.

Fazzari, P., Paternain, A.V., Valiente, M., Pla, R., Luján, R., Lloyd, K., Lerma, J., Marín, O., and Rico, B. (2010). Control of cortical GABA circuitry development by Nrg1 and ErbB4 signalling. Nature 464, 1376–1380.

Feldmeyer, D., Lübke, J., Silver, R.A., and Sakmann, B. (2002). Synaptic connections between layer 4 spiny neurone-layer 2/3 pyramidal cell pairs in juvenile rat barrel cortex: physiology and anatomy of interlaminar signalling within a cortical column. J. Physiol. 538, 803–822.

Feldmeyer, D., Roth, A., and Sakmann, B. (2005). Monosynaptic connections between pairs of spiny stellate cells in layer 4 and pyramidal cells in layer 5A indicate that lemniscal and paralemniscal afferent pathways converge in the infragranular somatosensory cortex. J. Neurosci. 25, 3423–3431.

Feldmeyer, D., Lübke, J., and Sakmann, B. (2006). Efficacy and connectivity of intracolumnar pairs of layer 2/3 pyramidal cells in the barrel cortex of juvenile rats. J. Physiol. 575, 583–602.

Fish, K.N., Sweet, R.A., and Lewis, D.A. (2011). Differential distribution of proteins regulating GABA synthesis and reuptake in axon boutons of subpopulations of cortical interneurons. Cereb. Cortex 21, 2450–2460.

Fishell, G., and Kepecs, A. (2019). Interneuron Types as Attractors and Controllers. Annu. Rev. Neurosci.

Flames, N., Long, J.E., Garratt, A.N., Fischer, T.M., Gassmann, M., Birchmeier, C., Lai, C., Rubenstein, J.L.R., and Marín, O. (2004). Short- and long-range attraction of cortical GABAergic interneurons by neuregulin-1. Neuron 44, 251–261.

Flames, N., Pla, R., Gelman, D.M., Rubenstein, J.L.R., Puelles, L., and Marín, O. (2007). Delineation of multiple subpallial progenitor domains by the combinatorial expression of transcriptional codes. J. Neurosci. 27, 9682–9695.

Fossati, M., Assendorp, N., Gemin, O., Colasse, S., Dingli, F., Arras, G., Loew, D., and Charrier, C. (2019). Trans-Synaptic Signaling through the Glutamate Receptor Delta-1 Mediates Inhibitory Synapse Formation in Cortical Pyramidal Neurons. Neuron 0.

Frazer, S., Prados, J., Niquille, M., Cadilhac, C., Markopoulos, F., Gomez, L., Tomasello, U., Telley, L., Holtmaat, A., Jabaudon, D., et al. (2017). Transcriptomic and anatomic parcellation of 5-HT3AR expressing cortical interneuron subtypes revealed by single-cell RNA sequencing. Nat. Commun. 8, 14219.

Freund, T.F., Maglóczky, Z., Soltész, I., and Somogyi, P. (1986). Synaptic connections, axonal and dendritic patterns of neurons immunoreactive for cholecystokinin in the visual cortex of the cat. Neuroscience 19, 1133–1159.

Fromer, M., Pocklington, A.J., Kavanagh, D.H., Williams, H.J., Dwyer, S., Gormley, P., Georgieva, L., Rees, E., Palta, P., Ruderfer, D.M., et al. (2014). De novo mutations in schizophrenia implicate synaptic networks. Nature 506, 179–184.

Früh, S., Romanos, J., Panzanelli, P., Bürgisser, D., Tyagarajan, S.K., Campbell, K.P., Santello, M., and Fritschy, J.-M. (2016). Neuronal Dystroglycan Is Necessary for Formation and Maintenance of Functional CCK-Positive Basket Cell Terminals on Pyramidal Cells. J. Neurosci. 36, 10296–10313.

Fu, Y., Kaneko, M., Tang, Y., Alvarez-Buylla, A., and Stryker, M.P. (2015). A cortical disinhibitory circuit for enhancing adult plasticity. Elife 4, e05558.

Fuccillo, M.V., Földy, C., Gökce, Ö., Rothwell, P.E., Sun, G.L., Malenka, R.C., and Südhof, T.C. (2015). Single-Cell mRNA Profiling Reveals Cell-Type-Specific Expression of Neurexin Isoforms. Neuron 87, 326–340.

Furlanis, E., Traunmüller, L., Fucile, G., and Scheiffele, P. (2019). Landscape of ribosome-engaged transcript isoforms reveals extensive neuronal-cell-class-specific alternative splicing programs. Nat. Neurosci.

Gabernet, L., Jadhav, S.P., Feldman, D.E., Carandini, M., and Scanziani, M. (2005). Somatosensory integration controlled by dynamic thalamocortical feed-forward inhibition. Neuron 48, 315–327.

Gabitto, M.I., Rasmussen, A., Wapinski, O., Allaway, K., Carriero, N., Fishell, G.J., and Bonneau, R. (2019). Characterizing the epigenetic landscape of cellular populations from bulk and single-cell ATAC-seq information.

Gao, Y., Hisey, E., Bradshaw, T.W.A., Erata, E., Brown, W.E., Courtland, J.L., Uezu, A., Xiang, Y., Diao, Y., and Soderling, S.H. (2019). Plug-and-Play Protein Modification Using Homology-Independent Universal Genome Engineering. Neuron.

Garcia-Junco-Clemente, P., Ikrar, T., Tring, E., Xu, X., Ringach, D.L., and Trachtenberg, J.T. (2017). An inhibitory pull-push circuit in frontal cortex. Nat. Neurosci. 20, 389–392.

Garrido, J.J., Fernandes, F., Giraud, P., Mouret, I., Pasqualini, E., Fache, M.P., Jullien, F., and Dargent, B. (2001). Identification of an axonal determinant in the C-terminus of the sodium channel Na(v)1.2. EMBO J. 20, 5950–5961.

Gascón, S., Paez-Gomez, J.A., Díaz-Guerra, M., Scheiffele, P., and Scholl, F.G. (2008). Dual-promoter lentiviral vectors for constitutive and regulated gene expression in neurons. J. Neurosci. Methods 168, 104–112.

Genovese, G., Fromer, M., Stahl, E.A., Ruderfer, D.M., Chambert, K., Landén, M., Moran, J.L., Purcell, S.M., Sklar, P., Sullivan, P.F., et al. (2016). Increased burden of ultra-rare protein-altering variants among 4,877 individuals with schizophrenia. Nat. Neurosci. 19, 1433–1441.

Gerashchenko, D., Wisor, J.P., Burns, D., Reh, R.K., Shiromani, P.J., Sakurai, T., de la Iglesia, H.O., and Kilduff, T.S. (2008). Identification of a population of sleep-active cerebral cortex neurons. Proc. Natl. Acad. Sci. U. S. A. 105, 10227–10232.

Ghosh, A., Antonini, A., McConnell, S.K., and Shatz, C.J. (1990). Requirement for subplate neurons in the formation of thalamocortical connections. Nature 347, 179–181.

Glantz, L.A., and Lewis, D.A. (2000). Decreased dendritic spine density on prefrontal cortical pyramidal neurons in schizophrenia. Arch. Gen. Psychiatry 57, 65–73.

Glausier, J.R., and Lewis, D.A. (2013). Dendritic spine pathology in schizophrenia. Neuroscience 251, 90–107.

Glickfeld, L.L., and Scanziani, M. (2006). Distinct timing in the activity of cannabinoid-sensitive and cannabinoid-insensitive basket cells. Nat. Neurosci. 9, 807–815.

Glock, C., Heumüller, M., and Schuman, E.M. (2017). mRNA transport & local translation in neurons. Curr. Opin. Neurobiol. 45, 169–177.

Goel, A., Cantu, D.A., Guilfoyle, J., Chaudhari, G.R., Newadkar, A., Todisco, B., de Alba, D., Kourdougli, N., Schmitt, L.M., Pedapati, E., et al. (2018). Impaired perceptual learning in a mouse model of Fragile X syndrome is mediated by parvalbumin neuron dysfunction and is reversible. Nat. Neurosci. 21, 1404–1411.

Gokce, O., and Südhof, T.C. (2013). Membrane-tethered monomeric neurexin LNS-domain triggers synapse formation. J. Neurosci. 33, 14617–14628.

Gonzalez-Burgos, G., and Lewis, D.A. (2012). NMDA receptor hypofunction, parvalbumin-positive neurons, and cortical gamma oscillations in schizophrenia. Schizophr. Bull. 38, 950–957.

Gonzalez-Burgos, G., Cho, R.Y., and Lewis, D.A. (2015). Alterations in cortical network oscillations and parvalbumin neurons in schizophrenia. Biol. Psychiatry 77, 1031–1040.

González-Burgos, G., Miyamae, T., Krimer, Y., Gulchina, Y., Pafundo, D.E., Krimer, O., Bazmi, H., Arion, D., Enwright, J.F., Fish, K.N., et al. (2019). Distinct Properties of Layer 3 Pyramidal Neurons from Prefrontal and Parietal Areas of the Monkey Neocortex. J. Neurosci. 39, 7277–7290.

Grieco, S.F., Wang, G., Mahapatra, A., Lai, C., Holmes, T.C., and Xu, X. (2020). Neuregulin and ErbB expression is regulated by development and sensory experience in mouse visual cortex. J. Comp. Neurol. 528, 419–432.

Gu, C., Jan, Y.N., and Jan, L.Y. (2003). A conserved domain in axonal targeting of Kv1 (Shaker) voltage-gated potassium channels. Science 301, 646–649.

Guardia, C.M., De Pace, R., Mattera, R., and Bonifacino, J.S. (2018). Neuronal functions of adaptor complexes involved in protein sorting. Curr. Opin. Neurobiol. 51, 103–110.

Guedes-Dias, P., Nirschl, J.J., Abreu, N., Tokito, M.K., Janke, C., Magiera, M.M., and Holzbaur, E.L.F. (2019). Kinesin-3 Responds to Local Microtubule Dynamics to Target Synaptic Cargo Delivery to the Presynapse. Curr. Biol. 29, 268–282.e8.

Gumy, L.F., and Hoogenraad, C.C. (2018). Local mechanisms regulating selective cargo entry and long-range trafficking in axons. Curr. Opin. Neurobiol. 51, 23–28.

Gumy, L.F., Katrukha, E.A., Grigoriev, I., Jaarsma, D., Kapitein, L.C., Akhmanova, A., and Hoogenraad, C.C. (2017). MAP2 Defines a Pre-axonal Filtering Zone to Regulate KIF1- versus KIF5-Dependent Cargo Transport in Sensory Neurons. Neuron 94, 347–362.e7.

Guo, N., Soden, M.E., Herber, C., Kim, M.T., Besnard, A., Lin, P., Ma, X., Cepko, C.L., Zweifel, L.S., and Sahay, A. (2018). Dentate granule cell recruitment of feedforward inhibition governs engram maintenance and remote memory generalization. Nat. Med. 24, 438–449.

Hafting, T., Fyhn, M., Molden, S., Moser, M.-B., and Moser, E.I. (2005). Microstructure of a spatial map in the entorhinal cortex. Nature 436, 801–806.

Hall, L.S., Medway, C.W., Pain, O., Pardinas, A.F., Rees, E.G., Escott-Price, V., Pocklington, A., Bray, N.J., Holmans, P.A., Walters, J.T.R., et al. (2019). A Transcriptome-Wide Association Study implicates specific pre- and post-synaptic abnormalities in Schizophrenia. Hum. Mol. Genet.

Han, K.A., Ko, J.S., Pramanik, G., Kim, J.Y., Tabuchi, K., Um, J.W., and Ko, J. (2018a). PTPσ drives excitatory presynaptic assembly via various extracellular and intracellular mechanisms. J. Neurosci.

Han, Y., Kebschull, J.M., Campbell, R.A.A., Cowan, D., Imhof, F., Zador, A.M., and Mrsic-Flogel, T.D. (2018b). The logic of single-cell projections from visual cortex. Nature.

Hancock, M.L., Canetta, S.E., Role, L.W., and Talmage, D.A. (2008). Presynaptic type III neuregulin1-ErbB signaling targets {alpha}7 nicotinic acetylcholine receptors to axons. J. Cell Biol. 181, 511–521.

Harris, K.D., and Mrsic-Flogel, T.D. (2013). Cortical connectivity and sensory coding. Nature 503, 51–58.

Harris, K.P., Zhang, Y.V., Piccioli, Z.D., Perrimon, N., and Littleton, J.T. (2016). The postsynaptic t-SNARE Syntaxin 4 controls traffic of Neuroligin 1 and Synaptotagmin 4 to regulate retrograde signaling. Elife 5.

Harrison, P.J., and Law, A.J. (2006). Neuregulin 1 and schizophrenia: genetics, gene expression, and neurobiology. Biol. Psychiatry 60, 132–140.

Hartmann, M., Parra, L.M., Ruschel, A., Lindner, C., Morrison, H., Herrlich, A., and Herrlich, P. (2015). Inside-out Regulation of Ectodomain Cleavage of Cluster-of-Differentiation-44 (CD44) and of Neuregulin-1 Requires Substrate Dimerization. J. Biol. Chem. 290, 17041–17054.

Hashimoto, T., Volk, D.W., Eggan, S.M., Mirnics, K., Pierri, J.N., Sun, Z., Sampson, A.R., and Lewis, D.A. (2003). Gene expression deficits in a subclass of GABA neurons in the prefrontal cortex of subjects with schizophrenia. J. Neurosci. 23, 6315–6326.

He, M., Tucciarone, J., Lee, S., Nigro, M.J., Kim, Y., Levine, J.M., Kelly, S.M., Krugikov, I., Wu, P., Chen, Y., et al. (2016). Strategies and Tools for Combinatorial Targeting of GABAergic Neurons in Mouse Cerebral Cortex. Neuron.

Heidenreich, M., and Zhang, F. (2016). Applications of CRISPR-Cas systems in neuroscience. Nat. Rev. Neurosci. 17, 36–44.

Hill, E.L., Gallopin, T., Férézou, I., Cauli, B., Rossier, J., Schweitzer, P., and Lambolez, B. (2007). Functional CB1 receptors are broadly expressed in neocortical GABAergic and glutamatergic neurons. J. Neurophysiol. 97, 2580–2589.

Hilscher, M.M., Leão, R.N., Edwards, S.J., Leão, K.E., and Kullander, K. (2017). Chrna2-Martinotti Cells Synchronize Layer 5 Type A Pyramidal Cells via Rebound Excitation. PLoS Biol. 15, e2001392.

Hinojosa, A.J., Deogracias, R., and Rico, B. (2018). The Microtubule Regulator NEK7 Coordinates the Wiring of Cortical Parvalbumin Interneurons. Cell Rep. 24, 1231–1242.

Hoftman, G.D., Volk, D.W., Bazmi, H.H., Li, S., Sampson, A.R., and Lewis, D.A. (2015). Altered cortical expression of GABA-related genes in schizophrenia: illness progression vs developmental disturbance. Schizophr. Bull. 41, 180–191.

Holmes, W.E., Sliwkowski, M.X., Akita, R.W., Henzel, W.J., Lee, J., Park, J.W., Yansura, D., Abadi, N., Raab, H., and Lewis, G.D. (1992). Identification of heregulin, a specific activator of p185erbB2. Science 256, 1205–1210.

Hrvatin, S., Hochbaum, D.R., Nagy, M.A., Cicconet, M., Robertson, K., Cheadle, L., Zilionis, R., Ratner, A., Borges-Monroy, R., Klein, A.M., et al. (2018). Single-cell analysis of experience-dependent transcriptomic states in the mouse visual cortex. Nat. Neurosci. 21, 120–129.

Hu, H., Gan, J., and Jonas, P. (2014). Interneurons. Fast-spiking, parvalbumin+ GABAergic interneurons: from cellular design to microcircuit function. Science 345, 1255263.

Huang, Y.Z., Won, S., Ali, D.W., Wang, Q., Tanowitz, M., Du, Q.S., Pelkey, K.A., Yang, D.J., Xiong, W.C., Salter, M.W., et al. (2000). Regulation of neuregulin signaling by PSD-95 interacting with ErbB4 at CNS synapses. Neuron 26, 443–455.

Hubel, D.H., and Wiesel, T.N. (1962). Receptive fields, binocular interaction and functional architecture in the cat's visual cortex. J. Physiol. 160, 106–154.

Huckins, L.M., Dobbyn, A., Ruderfer, D.M., Hoffman, G., Wang, W., Pardiñas, A.F., Rajagopal, V.M., Als, T.D., T Nguyen, H., Girdhar, K., et al. (2019). Gene

expression imputation across multiple brain regions provides insights into schizophrenia risk. Nat. Genet. 51, 659–674.

Iijima, T., Wu, K., Witte, H., Hanno-Iijima, Y., Glatter, T., Richard, S., and Scheiffele, P. (2011). SAM68 regulates neuronal activity-dependent alternative splicing of neurexin-1. Cell 147, 1601–1614.

Iijima, T., Iijima, Y., Witte, H., and Scheiffele, P. (2014). Neuronal cell type-specific alternative splicing is regulated by the KH domain protein SLM1. J. Cell Biol. 204, 331–342.

Insel, T.R. (2010). Rethinking schizophrenia. Nature 468, 187–193.

Ito-Ishida, A., Miyazaki, T., Miura, E., Matsuda, K., Watanabe, M., Yuzaki, M., and Okabe, S. (2012). Presynaptically released Cbln1 induces dynamic axonal structural changes by interacting with GluD2 during cerebellar synapse formation. Neuron 76, 549–564.

Jennings, J.H., Kim, C.K., Marshel, J.H., Raffiee, M., Ye, L., Quirin, S., Pak, S., Ramakrishnan, C., and Deisseroth, K. (2019). Interacting neural ensembles in orbitofrontal cortex for social and feeding behaviour. Nature 565, 645–649.

Jiang, X., Shen, S., Cadwell, C.R., Berens, P., Sinz, F., Ecker, A.S., Patel, S., and Tolias, A.S. (2015). Principles of connectivity among morphologically defined cell types in adult neocortex. Science 350, aac9462.

Kakegawa, W., Mitakidis, N., Miura, E., Abe, M., Matsuda, K., Takeo, Y.H., Kohda, K., Motohashi, J., Takahashi, A., Nagao, S., et al. (2015). Anterograde C1ql1 signaling is required in order to determine and maintain a single-winner climbing fiber in the mouse cerebellum. Neuron 85, 316–329.

Kapfer, C., Glickfeld, L.L., Atallah, B.V., and Scanziani, M. (2007). Supralinear increase of recurrent inhibition during sparse activity in the somatosensory cortex. Nat. Neurosci. 10, 743–753.

Kapitein, L.C., Schlager, M.A., Kuijpers, M., Wulf, P.S., van Spronsen, M., MacKintosh, F.C., and Hoogenraad, C.C. (2010). Mixed microtubules steer dynein-driven cargo transport into dendrites. Curr. Biol. 20, 290–299.

Kasnauskiene, J., Ciuladaite, Z., Preiksaitiene, E., Utkus, A., Peciulyte, A., and Kučinskas, V. (2013). A new single gene deletion on 2q34: ERBB4 is associated with intellectual disability. Am. J. Med. Genet. A 161A, 1487–1490.

Katona, I., Sperlágh, B., Sík, A., Käfalvi, A., Vizi, E.S., Mackie, K., and Freund, T.F. (1999). Presynaptically located CB1 cannabinoid receptors regulate GABA release from axon terminals of specific hippocampal interneurons. J. Neurosci. 19, 4544–4558.

Kepecs, A., and Fishell, G. (2014). Interneuron cell types are fit to function. Nature 505, 318–326.

Kiecker, C., and Lumsden, A. (2005). Compartments and their boundaries in vertebrate brain development. Nat. Rev. Neurosci. 6, 553–564.

Kilduff, T.S., Cauli, B., and Gerashchenko, D. (2011). Activation of cortical interneurons during sleep: an anatomical link to homeostatic sleep regulation? Trends Neurosci. 34, 10–19.

Kim, H., Ährlund-Richter, S., Wang, X., Deisseroth, K., and Carlén, M. (2016). Prefrontal Parvalbumin Neurons in Control of Attention. Cell 164, 208–218.

Kirov, G., Pocklington, A.J., Holmans, P., Ivanov, D., Ikeda, M., Ruderfer, D., Moran, J., Chambert, K., Toncheva, D., Georgieva, L., et al. (2012). De novo CNV analysis implicates specific abnormalities of postsynaptic signalling complexes in the pathogenesis of schizophrenia. Mol. Psychiatry 17, 142–153.

Kisvarday, Z.F., Martin, K.A., Friedlander, M.J., and Somogyi, P. (1987). Evidence for interlaminar inhibitory circuits in the striate cortex of the cat. J. Comp. Neurol. 260, 1–19.

Klausberger, T., and Somogyi, P. (2008). Neuronal diversity and temporal dynamics: the unity of hippocampal circuit operations. Science 321, 53–57.

Klausberger, T., Magill, P.J., Márton, L.F., Roberts, J.D.B., Cobden, P.M., Buzsáki, G., and Somogyi, P. (2003). Brain-state- and cell-type-specific firing of hippocampal interneurons in vivo. Nature 421, 844–848.

Klingler, E., De la Rossa, A., Fièvre, S., Devaraju, K., Abe, P., and Jabaudon, D. (2019). A Translaminar Genetic Logic for the Circuit Identity of Intracortically Projecting Neurons. Curr. Biol. 29, 332–339.e5.

Ko, H., Hofer, S.B., Pichler, B., Buchanan, K.A., Sjöström, P.J., and Mrsic-Flogel, T.D. (2011). Functional specificity of local synaptic connections in neocortical networks. Nature 473, 87–91.

Ko, H., Cossell, L., Baragli, C., Antolik, J., Clopath, C., Hofer, S.B., and Mrsic-Flogel, T.D. (2013). The emergence of functional microcircuits in visual cortex. Nature 496, 96–100.

Ko, J., Fuccillo, M.V., Malenka, R.C., and Südhof, T.C. (2009). LRRTM2 functions as a neurexin ligand in promoting excitatory synapse formation. Neuron 64, 791–798.

Ko, J.S., Pramanik, G., Um, J.W., Shim, J.S., Lee, D., Kim, K.H., Chung, G.-Y., Condomitti, G., Kim, H.M., Kim, H., et al. (2015). PTPσ functions as a presynaptic receptor for the glypican-4/LRRTM4 complex and is essential for excitatory synaptic transmission. Proc. Natl. Acad. Sci. U. S. A. 112, 1874–1879.

Koopmans, F., van Nierop, P., Andres-Alonso, M., Byrnes, A., Cijsouw, T., Coba, M.P., Cornelisse, L.N., Farrell, R.J., Goldschmidt, H.L., Howrigan, D.P., et al. (2019). SynGO: An Evidence-Based, Expert-Curated Knowledge Base for the Synapse. Neuron 103, 217–234.e4.

Kotzadimitriou, D., Nissen, W., Paizs, M., Newton, K., Harrison, P.J., Paulsen, O., and Lamsa, K. (2018). Neuregulin 1 Type I Overexpression Is Associated with Reduced NMDA Receptor-Mediated Synaptic Signaling in Hippocampal Interneurons Expressing PV or CCK. eNeuro 5.

Krienen, F.M., Goldman, M., Zhang, Q., del Rosario, R., Florio, M., Machold, R., Saunders, A., Levandowski, K., Zaniewski, H., Schuman, B., et al. (2019). Innovations in Primate Interneuron Repertoire.

Krivosheya, D., Tapia, L., Levinson, J.N., Huang, K., Kang, Y., Hines, R., Ting, A.K., Craig, A.M., Mei, L., Bamji, S.X., et al. (2008). ErbB4-neuregulin signaling modulates synapse development and dendritic arborization through distinct mechanisms. J. Biol. Chem. 283, 32944–32956.

Kropff, E., Carmichael, J.E., Moser, M.-B., and Moser, E.I. (2015). Speed cells in the medial entorhinal cortex. Nature 523, 419–424.

Kurshan, P.T., and Shen, K. (2019). Synaptogenic pathways. Curr. Opin. Neurobiol. 57, 156–162.

Kurshan, P.T., Merrill, S.A., Dong, Y., Ding, C., Hammarlund, M., Bai, J., Jorgensen, E.M., and Shen, K. (2018). γ-Neurexin and Frizzled Mediate Parallel Synapse Assembly Pathways Antagonized by Receptor Endocytosis. Neuron 100, 150–166.e4.

Kvitsiani, D., Ranade, S., Hangya, B., Taniguchi, H., Huang, J.Z., and Kepecs, A. (2013). Distinct behavioural and network correlates of two interneuron types in prefrontal cortex. Nature 498, 363–366.

Kwon, S.-K., Woo, J., Kim, S.-Y., Kim, H., and Kim, E. (2010). Trans-synaptic adhesions between netrin-G ligand-3 (NGL-3) and receptor tyrosine phosphatases LAR, protein-tyrosine phosphatase delta (PTPdelta), and PTPsigma via specific domains regulate excitatory synapse formation. J. Biol. Chem. 285, 13966–13978.

Lai, T., Jabaudon, D., Molyneaux, B.J., Azim, E., Arlotta, P., Menezes, J.R.L., and Macklis, J.D. (2008). SOX5 controls the sequential generation of distinct corticofugal neuron subtypes. Neuron 57, 232–247.

Lee, C.C., and Sherman, S.M. (2009). Glutamatergic inhibition in sensory neocortex. Cereb. Cortex 19, 2281–2289.

Lee, A.T., Gee, S.M., Vogt, D., Patel, T., Rubenstein, J.L., and Sohal, V.S. (2014). Pyramidal Neurons in Prefrontal Cortex Receive Subtype-Specific Forms of Excitation and Inhibition. Neuron 81, 61–68.

Lee, S., Hjerling-Leffler, J., Zagha, E., Fishell, G., and Rudy, B. (2010a). The largest group of superficial neocortical GABAergic interneurons expresses ionotropic serotonin receptors. J. Neurosci. 30, 16796–16808.

Lee, S., Kruglikov, I., Huang, Z.J., Fishell, G., and Rudy, B. (2013). A disinhibitory circuit mediates motor integration in the somatosensory cortex. Nat. Neurosci. 16, 1662–1670.

Lee, S.-H., Földy, C., and Soltesz, I. (2010b). Distinct endocannabinoid control of GABA release at perisomatic and dendritic synapses in the hippocampus. J. Neurosci. 30, 7993–8000.

Lee, S.-H., Kwan, A.C., Zhang, S., Phoumthipphavong, V., Flannery, J.G., Masmanidis, S.C., Taniguchi, H., Huang, Z.J., Zhang, F., Boyden, E.S., et al. (2012). Activation of specific interneurons improves V1 feature selectivity and visual perception. Nature 488, 379–383.

Lee, S.-J., Wei, M., Zhang, C., Maxeiner, S., Pak, C., Calado Botelho, S., Trotter, J., Sterky, F.H., and Südhof, T.C. (2017). Presynaptic Neuronal Pentraxin Receptor Organizes Excitatory and Inhibitory Synapses. J. Neurosci. 37, 1062–1080.

Lemke, G. (1996). Neuregulins in development. Mol. Cell. Neurosci. 7, 247–262.

Lewis, D.A. (2014). Inhibitory neurons in human cortical circuits: substrate for cognitive dysfunction in schizophrenia. Curr. Opin. Neurobiol. 26, 22–26.

Lewis, D.A., Hashimoto, T., and Volk, D.W. (2005). Cortical inhibitory neurons and schizophrenia. Nat. Rev. Neurosci. 6, 312–324.

Lewis, D.A., Fish, K.N., Arion, D., and Gonzalez-Burgos, G. (2011). Perisomatic inhibition and cortical circuit dysfunction in schizophrenia. Curr. Opin. Neurobiol. 21, 866–872.

Li, B., Woo, R.-S., Mei, L., and Malinow, R. (2007). The neuregulin-1 receptor erbB4 controls glutamatergic synapse maturation and plasticity. Neuron 54, 583–597.

Li, J., Shalev-Benami, M., Sando, R., Jiang, X., Kibrom, A., Wang, J., Leon, K., Katanski, C., Nazarko, O., Lu, Y.C., et al. (2018). Structural Basis for Teneurin Function in Circuit-Wiring: A Toxin Motif at the Synapse. Cell 173, 735–748.e15.

Li, K.-X., Lu, Y.-M., Xu, Z.-H., Zhang, J., Zhu, J.-M., Zhang, J.-M., Cao, S.-X., Chen, X.-J., Chen, Z., Luo, J.-H., et al. (2011). Neuregulin 1 regulates excitability of fast-spiking neurons through Kv1.1 and acts in epilepsy. Nat. Neurosci. 15, 267–273.

Li, P., Merrill, S.A., Jorgensen, E.M., and Shen, K. (2016). Two Clathrin Adaptor Protein Complexes Instruct Axon-Dendrite Polarity. Neuron 90, 564–580.

Lien, A.D., and Scanziani, M. (2013). Tuned thalamic excitation is amplified by visual cortical circuits. Nat. Neurosci. 16, 1315–1323.

Lien, A.D., and Scanziani, M. (2018). Cortical direction selectivity emerges at convergence of thalamic synapses. Nature 558, 80–86.

Lim, L., Mi, D., Llorca, A., and Marín, O. (2018a). Development and Functional Diversification of Cortical Interneurons. Neuron 100, 294–313.

Lim, L., Pakan, J.M.P., Selten, M.M., Marques-Smith, A., Llorca, A., Bae, S.E., Rochefort, N.L., and Marín, O. (2018b). Optimization of interneuron function by direct coupling of cell migration and axonal targeting. Nat. Neurosci. 21, 920–931.

Linhoff, M.W., Laurén, J., Cassidy, R.M., Dobie, F.A., Takahashi, H., Nygaard, H.B., Airaksinen, M.S., Strittmatter, S.M., and Craig, A.M. (2009). An Unbiased Expression Screen for Synaptogenic Proteins Identifies the LRRTM Protein Family as Synaptic Organizers. Neuron 61, 734–749.

Liodis, P., Denaxa, M., Grigoriou, M., Akufo-Addo, C., Yanagawa, Y., and Pachnis, V. (2007). Lhx6 activity is required for the normal migration and specification of cortical interneuron subtypes. J. Neurosci. 27, 3078–3089.

Liu, X., Hwang, H., Cao, L., Wen, D., Liu, N., Graham, R.M., and Zhou, M. (1998). Release of the neuregulin functional polypeptide requires its cytoplasmic tail. J. Biol. Chem. 273, 34335–34340.

Lodato, S., Rouaux, C., Quast, K.B., Jantrachotechatchawan, C., Studer, M., Hensch, T.K., and Arlotta, P. (2011). Excitatory projection neuron subtypes control the distribution of local inhibitory interneurons in the cerebral cortex. Neuron 69, 763–779.

Lodato, S., Molyneaux, B.J., Zuccaro, E., Goff, L.A., Chen, H.-H., Yuan, W., Meleski, A., Takahashi, E., Mahony, S., Rinn, J.L., et al. (2014). Gene co-regulation by Fezf2 selects neurotransmitter identity and connectivity of corticospinal neurons. Nat. Neurosci. 17, 1046–1054.

Lodato, S., Shetty, A.S., and Arlotta, P. (2015). Cerebral cortex assembly: generating and reprogramming projection neuron diversity. Trends Neurosci. 38, 117–125.

Loh, K.H., Stawski, P.S., Draycott, A.S., Udeshi, N.D., Lehrman, E.K., Wilton, D.K., Svinkina, T., Deerinck, T.J., Ellisman, M.H., Stevens, B., et al. (2016). Proteomic Analysis of Unbounded Cellular Compartments: Synaptic Clefts. Cell 166, 1295–1307.e21.

Longart, M., Liu, Y., Karavanova, I., and Buonanno, A. (2004). Neuregulin-2 is developmentally regulated and targeted to dendrites of central neurons. J. Comp. Neurol. 472, 156–172.

Lu, J., Tucciarone, J., Padilla-Coreano, N., He, M., Gordon, J.A., and Huang, Z.J. (2017). Selective inhibitory control of pyramidal neuron ensembles and cortical subnetworks by chandelier cells. Nat. Neurosci. 20, 1377–1383.

Lu, Y.C., Nazarko, O.V., Sando, R., 3rd, Salzman, G.S., Li, N.-S., Südhof, T.C., and Araç, D. (2015). Structural Basis of Latrophilin-FLRT-UNC5 Interaction in Cell Adhesion. Structure 23, 1678–1691.

Lübke, J., Egger, V., Sakmann, B., and Feldmeyer, D. (2000). Columnar organization of dendrites and axons of single and synaptically coupled excitatory spiny neurons in layer 4 of the rat barrel cortex. J. Neurosci. 20, 5300–5311.

Lübke, J., Roth, A., Feldmeyer, D., and Sakmann, B. (2003). Morphometric analysis of the columnar innervation domain of neurons connecting layer 4 and layer 2/3 of juvenile rat barrel cortex. Cereb. Cortex 13, 1051–1063.

Luo, F., and Südhof, T.C. (2017). Synaptotagmin-7-Mediated Asynchronous Release Boosts High-Fidelity Synchronous Transmission at a Central Synapse. Neuron 94, 826–839.e3.

Luo, C., Keown, C.L., Kurihara, L., Zhou, J., He, Y., Li, J., Castanon, R., Lucero, J., Nery, J.R., Sandoval, J.P., et al. (2017). Single-cell methylomes identify neuronal subtypes and regulatory elements in mammalian cortex. Science 357, 600–604.

Ma, Y., Hu, H., Berrebi, A.S., Mathers, P.H., and Agmon, A. (2006). Distinct subtypes of somatostatin-containing neocortical interneurons revealed in transgenic mice. J. Neurosci. 26, 5069–5082.

Madisen, L., Zwingman, T.A., Sunkin, S.M., Oh, S.W., Zariwala, H.A., Gu, H., Ng, L.L., Palmiter, R.D., Hawrylycz, M.J., Jones, A.R., et al. (2010). A robust and high-throughput Cre reporting and characterization system for the whole mouse brain. Nat. Neurosci. 13, 133–140.

Marchionni, M.A., Goodearl, A.D., Chen, M.S., Bermingham-McDonogh, O., Kirk, C., Hendricks, M., Danehy, F., Misumi, D., Sudhalter, J., and Kobayashi, K. (1993). Glial growth factors are alternatively spliced erbB2 ligands expressed in the nervous system. Nature 362, 312–318.

Mardones, G.A., Burgos, P.V., Lin, Y., Kloer, D.P., Magadán, J.G., Hurley, J.H., and Bonifacino, J.S. (2013). Structural basis for the recognition of tyrosine-based sorting signals by the μ3A subunit of the AP-3 adaptor complex. J. Biol. Chem. 288, 9563–9571.

Marín, O. (2012). Interneuron dysfunction in psychiatric disorders. Nat. Rev. Neurosci. 13, 107–120.

Marín, O. (2013). Cellular and molecular mechanisms controlling the migration of neocortical interneurons. Eur. J. Neurosci. 38, 2019–2029.

Marín, O. (2016). Developmental timing and critical windows for the treatment of psychiatric disorders. Nat. Med.

Marín, O., and Rubenstein, J.L. (2001). A long, remarkable journey: tangential migration in the telencephalon. Nat. Rev. Neurosci. 2, 780–790.

Markram, H., Lübke, J., Frotscher, M., Roth, A., and Sakmann, B. (1997). Physiology and anatomy of synaptic connections between thick tufted pyramidal neurones in the developing rat neocortex. J. Physiol. 500 (Pt 2), 409–440.

Marques-Smith, A., Lyngholm, D., Kaufmann, A.-K., Stacey, J.A., Hoerder-Suabedissen, A., Becker, E.B.E., Wilson, M.C., Molnár, Z., and Butt, S.J.B. (2016). A Transient Translaminar GABAergic Interneuron Circuit Connects Thalamocortical Recipient Layers in Neonatal Somatosensory Cortex. Neuron 89, 536–549.

Marro, S.G., Chanda, S., Yang, N., Janas, J.A., Valperga, G., Trotter, J., Zhou, B., Merrill, S., Yousif, I., Shelby, H., et al. (2019). Neuroligin-4 Regulates Excitatory Synaptic Transmission in Human Neurons. Neuron.

Martin, E.A., Muralidhar, S., Wang, Z., Cervantes, D.C., Basu, R., Taylor, M.R., Hunter, J., Cutforth, T., Wilke, S.A., Ghosh, A., et al. (2015). The intellectual disability gene Kirrel3 regulates target-specific mossy fiber synapse development in the hippocampus. Elife 4, e09395.

Martinelli, D.C., Chew, K.S., Rohlmann, A., Lum, M.Y., Ressl, S., Hattar, S., Brunger, A.T., Missler, M., and Südhof, T.C. (2016). Expression of C1ql3 in Discrete Neuronal Populations Controls Efferent Synapse Numbers and Diverse Behaviors. Neuron 91, 1034–1051.

Matsuda, K., Miura, E., Miyazaki, T., Kakegawa, W., Emi, K., Narumi, S., Fukazawa, Y., Ito-Ishida, A., Kondo, T., Shigemoto, R., et al. (2010). Cbln1 is a ligand for an orphan glutamate receptor delta2, a bidirectional synapse organizer. Science 328, 363–368.

Matsuda, K., Budisantoso, T., Mitakidis, N., Sugaya, Y., Miura, E., Kakegawa, W., Yamasaki, M., Konno, K., Uchigashima, M., Abe, M., et al. (2016). Transsynaptic Modulation of Kainate Receptor Functions by C1q-like Proteins. Neuron 90, 752–767.

Matsuda, S., Miura, E., Matsuda, K., Kakegawa, W., Kohda, K., Watanabe, M., and Yuzaki, M. (2008). Accumulation of AMPA receptors in autophagosomes in neuronal axons lacking adaptor protein AP-4. Neuron 57, 730–745.

Mattera, R., Boehm, M., Chaudhuri, R., Prabhu, Y., and Bonifacino, J.S. (2011). Conservation and diversification of dileucine signal recognition by adaptor protein (AP) complex variants. J. Biol. Chem. 286, 2022–2030.

Mayer, C., Hafemeister, C., Bandler, R.C., Machold, R., Brito, R.B., Jaglin, X., Allaway, K., Butler, A., Fishell, G., and Satija, R. (2018). Developmental diversification of cortical inhibitory interneurons. Nature.

McConnell, S.K., Ghosh, A., and Shatz, C.J. (1989). Subplate neurons pioneer the first axon pathway from the cerebral cortex. Science 245, 978–982.

McGarry, L.M., Packer, A.M., Fino, E., Nikolenko, V., Sippy, T., and Yuste, R. (2010). Quantitative classification of somatostatin-positive neocortical interneurons identifies three interneuron subtypes. Front. Neural Circuits 4, 12.

Mei, L., and Nave, K.-A. (2014). Neuregulin-ERBB signaling in the nervous system and neuropsychiatric diseases. Neuron 83, 27–49.

Mei, L., and Xiong, W.-C. (2008). Neuregulin 1 in neural development, synaptic plasticity and schizophrenia. Nat. Rev. Neurosci. 9, 437–452.

Meyer, D., and Birchmeier, C. (1995). Multiple essential functions of neuregulin in development. Nature 378, 386–390.

Meyer, H.S., Wimmer, V.C., Hemberger, M., Bruno, R.M., de Kock, C.P.J., Frick, A., Sakmann, B., and Helmstaedter, M. (2010). Cell type-specific thalamic innervation in a column of rat vibrissal cortex. Cereb. Cortex 20, 2287–2303.

Mi, D., Li, Z., Lim, L., Li, M., Moissidis, M., Yang, Y., Gao, T., Hu, T.X., Pratt, T., Price, D.J., et al. (2018). Early emergence of cortical interneuron diversity in the mouse embryo. Science.

Mikuni, T., Nishiyama, J., Sun, Y., Kamasawa, N., and Yasuda, R. (2016). High-Throughput, High-Resolution Mapping of Protein Localization in Mammalian Brain by In Vivo Genome Editing. Cell 165, 1803–1817.

Millan, M.J., Andrieux, A., Bartzokis, G., Cadenhead, K., Dazzan, P., Fusar-Poli, P., Gallinat, J., Giedd, J., Grayson, D.R., Heinrichs, M., et al. (2016). Altering the course of schizophrenia: progress and perspectives. Nat. Rev. Drug Discov.

Miller, J.-E.K., Ayzenshtat, I., Carrillo-Reid, L., and Yuste, R. (2014). Visual stimuli recruit intrinsically generated cortical ensembles. Proc. Natl. Acad. Sci. U. S. A. 111, E4053–E4061.

Miura, P., Shenker, S., Andreu-Agullo, C., Westholm, J.O., and Lai, E.C. (2013). Widespread and extensive lengthening of 3’ UTRs in the mammalian brain. Genome Res. 23, 812–825.

Miyoshi, G., Hjerling-Leffler, J., Karayannis, T., Sousa, V.H., Butt, S.J.B., Battiste, J., Johnson, J.E., Machold, R.P., and Fishell, G. (2010). Genetic fate mapping reveals that the caudal ganglionic eminence produces a large and diverse population of superficial cortical interneurons. J. Neurosci. 30, 1582–1594.

Miyoshi, G., Young, A., Petros, T., Karayannis, T., McKenzie Chang, M., Lavado, A., Iwano, T., Nakajima, M., Taniguchi, H., Huang, Z.J., et al. (2015). Prox1 Regulates the Subtype-Specific Development of Caudal Ganglionic Eminence-Derived GABAergic Cortical Interneurons. J. Neurosci. 35, 12869–12889.

Molyneaux, B.J., Arlotta, P., Hirata, T., Hibi, M., and Macklis, J.D. (2005). Fezl is required for the birth and specification of corticospinal motor neurons. Neuron 47, 817–831.

Molyneaux, B.J., Arlotta, P., Menezes, J.R.L., and Macklis, J.D. (2007). Neuronal subtype specification in the cerebral cortex. Nat. Rev. Neurosci. 8, 427–437.

Molyneaux, B.J., Arlotta, P., Fame, R.M., MacDonald, J.L., MacQuarrie, K.L., and Macklis, J.D. (2009). Novel subtype-specific genes identify distinct subpopulations of callosal projection neurons. J. Neurosci. 29, 12343–12354.

Molyneaux, B.J., Goff, L.A., Brettler, A.C., Chen, H.-H., Brown, J.R., Hrvatin, S., Rinn, J.L., and Arlotta, P. (2015). DeCoN: genome-wide analysis of in vivo transcriptional dynamics during pyramidal neuron fate selection in neocortex. Neuron 85, 275–288.

Mukai, J., Tamura, M., Fénelon, K., Rosen, A.M., Spellman, T.J., Kang, R., MacDermott, A.B., Karayiorgou, M., Gordon, J.A., and Gogos, J.A. (2015). Molecular substrates of altered axonal growth and brain connectivity in a mouse model of schizophrenia. Neuron 86, 680–695.

Mukherjee, A., Carvalho, F., Eliez, S., and Caroni, P. (2019). Long-Lasting Rescue of Network and Cognitive Dysfunction in a Genetic Schizophrenia Model. Cell.

Müller, T., Braud, S., Jüttner, R., Voigt, B.C., Paulick, K., Sheean, M.E., Klisch, C., Gueneykaya, D., Rathjen, F.G., Geiger, J.R., et al. (2018). Neuregulin 3 promotes excitatory synapse formation on hippocampal interneurons. EMBO J.

Murayama, M., Pérez-Garci, E., Nevian, T., Bock, T., Senn, W., and Larkum, M.E. (2009). Dendritic encoding of sensory stimuli controlled by deep cortical interneurons. Nature 457, 1137–1141.

Murray, R.M., and Lewis, S.W. (1988). Is schizophrenia a neurodevelopmental disorder? Br. Med. J. 296, 63.

Namba, T., Nakamuta, S., Funahashi, Y., and Kaibuchi, K. (2011). The role of selective transport in neuronal polarization. Dev. Neurobiol. 71, 445–457.

Neupert, C., Schneider, R., Klatt, O., Reissner, C., Repetto, D., Biermann, B., Niesmann, K., Missler, M., and Heine, M. (2015). Regulated Dynamic Trafficking of Neurexins Inside and Outside of Synaptic Terminals. J. Neurosci. 35, 13629–13647.

Nguyen, Q.-A., Horn, M.E., and Nicoll, R.A. (2016a). Distinct roles for extracellular and intracellular domains in neuroligin function at inhibitory synapses. Elife 5.

Nguyen, R., Venkatesan, S., Binko, M., Bang, J.Y., Cajanding, J.D., Briggs, C., Sargin, D., Imayoshi, I., Lambe, E.K., and Kim, J.C. (2020). Cholecystokinin-Expressing Interneurons of the Medial Prefrontal Cortex Mediate Working Memory Retrieval. J. Neurosci. 40, 2314–2331.

Nguyen, T.-M., Schreiner, D., Xiao, L., Traunmüller, L., Bornmann, C., and Scheiffele, P. (2016b). An alternative splicing switch shapes neurexin repertoires in principal neurons versus interneurons in the mouse hippocampus. Elife 5.

Nigro, M.J., Hashikawa-Yamasaki, Y., and Rudy, B. (2018). Diversity and Connectivity of Layer 5 Somatostatin-Expressing Interneurons in the Mouse Barrel Cortex. J. Neurosci. 38, 1622–1633.

Nishiyama, J., Mikuni, T., and Yasuda, R. (2017). Virus-Mediated Genome Editing via Homology-Directed Repair in Mitotic and Postmitotic Cells in Mammalian Brain. Neuron 96, 755–768.e5.

Norton, N., Moskvina, V., Morris, D.W., Bray, N.J., Zammit, S., Williams, N.M., Williams, H.J., Preece, A.C., Dwyer, S., Wilkinson, J.C., et al. (2006a). Evidence that interaction between neuregulin 1 and its receptor erbB4 increases susceptibility to schizophrenia. Am. J. Med. Genet. B Neuropsychiatr. Genet. 141B, 96–101.

Norton, N., Williams, H.J., and Owen, M.J. (2006b). An update on the genetics of schizophrenia. Curr. Opin. Psychiatry 19, 158–164.

Nunzi, M.G., Gorio, A., Milan, F., Freund, T.F., Somogyi, P., and Smith, A.D. (1985). Cholecystokinin-immunoreactive cells form symmetrical synaptic contacts

with pyramidal and nonpyramidal neurons in the hippocampus. J. Comp. Neurol. 237, 485–505.

Oláh, S., Komlósi, G., Szabadics, J., Varga, C., Tóth, E., Barzó, P., and Tamás, G. (2007). Output of neurogliaform cells to various neuron types in the human and rat cerebral cortex. Front. Neural Circuits 1, 4.

Oláh, S., Füle, M., Komlósi, G., Varga, C., Báldi, R., Barzó, P., and Tamás, G. (2009). Regulation of cortical microcircuits by unitary GABA-mediated volume transmission. Nature 461, 1278–1281.

Olsen, S.R., Bortone, D.S., Adesnik, H., and Scanziani, M. (2012). Gain control by layer six in cortical circuits of vision. Nature 483, 47–52.

Omiya, Y., Uchigashima, M., Konno, K., Yamasaki, M., Miyazaki, T., Yoshida, T., Kusumi, I., and Watanabe, M. (2015). VGluT3-expressing CCK-positive basket cells construct invaginating synapses enriched with endocannabinoid signaling proteins in particular cortical and cortex-like amygdaloid regions of mouse brains. J. Neurosci. 35, 4215–4228.

Owen, M.J., and O'Donovan, M.C. (2017). Schizophrenia and the neurodevelopmental continuum:evidence from genomics. World Psychiatry 16, 227–235.

Pan-Vazquez, A., Wefelmeyer, W., Sabater, V.G., and Burrone, J. (2018). Homeostatic plasticity rules control the wiring of axo-axonic synapses at the axon initial segment.

Paramo, B., Wyatt, S., and Davies, A.M. (2018). An essential role for neuregulin-4 in the growth and elaboration of developing neocortical pyramidal dendrites. Exp. Neurol. 302, 85–92.

Pardiñas, A.F., Holmans, P., Pocklington, A.J., Escott-Price, V., Ripke, S., Carrera, N., Legge, S.E., Bishop, S., Cameron, D., Hamshere, M.L., et al. (2018). Common schizophrenia alleles are enriched in mutation-intolerant genes and in regions under strong background selection. Nat. Genet. 50, 381–389.

Parra, L.M., Hartmann, M., Schubach, S., Li, Y., Herrlich, P., and Herrlich, A. (2015). Distinct Intracellular Domain Substrate Modifications Selectively Regulate Ectodomain Cleavage of NRG1 or CD44. Mol. Cell. Biol. 35, 3381–3395.

Parra, P., Gulyás, A.I., and Miles, R. (1998). How many subtypes of inhibitory cells in the hippocampus? Neuron 20, 983–993.

Paul, A., Crow, M., Raudales, R., He, M., Gillis, J., and Huang, Z.J. (2017). Transcriptional Architecture of Synaptic Communication Delineates GABAergic Neuron Identity. Cell.

Peixoto, R.T., Kunz, P.A., Kwon, H., Mabb, A.M., Sabatini, B.L., Philpot, B.D., and Ehlers, M.D. (2012). Transsynaptic signaling by activity-dependent cleavage of neuroligin-1. Neuron 76, 396–409.

Peixoto, R.T., Wang, W., Croney, D.M., Kozorovitskiy, Y., and Sabatini, B.L. (2016). Early hyperactivity and precocious maturation of corticostriatal circuits in Shank3B(-/-) mice. Nat. Neurosci. 19, 716–724.

Peles, E., Bacus, S.S., Koski, R.A., Lu, H.S., Wen, D., Ogden, S.G., Levy, R.B., and Yarden, Y. (1992). Isolation of the neu/HER-2 stimulatory ligand: a 44 kd glycoprotein that induces differentiation of mammary tumor cells. Cell 69, 205–216.

Pelkey, K.A., Barksdale, E., Craig, M.T., Yuan, X., Sukumaran, M., Vargish, G.A., Mitchell, R.M., Wyeth, M.S., Petralia, R.S., Chittajallu, R., et al. (2016). Pentraxins Coordinate Excitatory Synapse Maturation and Circuit Integration of Parvalbumin Interneurons. Neuron 90, 661.

Peng, J., Santiago, I.J., Ahn, C., Gur, B., Tsui, C.K., Su, Z., Xu, C., Karakhanyan, A., Silies, M., and Pecot, M.Y. (2018). Drosophila Fezf coordinates laminar-specific connectivity through cell-intrinsic and cell-extrinsic mechanisms. Elife 7.

Peng, Y.-R., James, R.E., Yan, W., Kay, J.N., Kolodkin, A.L., and Sanes, J.R. (2019). Binary Fate Choice between Closely Related Interneuronal Types Is Determined by a Fezf1-Dependent Postmitotic Transcriptional Switch. Neuron.

Pettem, K.L., Yokomaku, D., Luo, L., Linhoff, M.W., Prasad, T., Connor, S.A., Siddiqui, T.J., Kawabe, H., Chen, F., Zhang, L., et al. (2013). The specific α-neurexin interactor calsyntenin-3 promotes excitatory and inhibitory synapse development. Neuron 80, 113–128.

Pfeffer, C.K., Xue, M., He, M., Huang, Z.J., and Scanziani, M. (2013). Inhibition of inhibition in visual cortex: the logic of connections between molecularly distinct interneurons. Nat. Neurosci. 16, 1068–1076.

Pi, H.-J., Hangya, B., Kvitsiani, D., Sanders, J.I., Huang, Z.J., and Kepecs, A. (2013). Cortical interneurons that specialize in disinhibitory control. Nature 503, 521–524.

Pocklington, A.J., Rees, E., Walters, J.T.R., Han, J., Kavanagh, D.H., Chambert, K.D., Holmans, P., Moran, J.L., McCarroll, S.A., Kirov, G., et al. (2015). Novel Findings from CNVs Implicate Inhibitory and Excitatory Signaling Complexes in Schizophrenia. Neuron 86, 1203–1214.

Polepalli, J.S., Wu, H., Goswami, D., Halpern, C.H., Südhof, T.C., and Malenka, R.C. (2017). Modulation of excitation on parvalbumin interneurons by neuroligin-3 regulates the hippocampal network. Nat. Neurosci.

Polioudakis, D., de la Torre-Ubieta, L., Langerman, J., Elkins, A.G., Shi, X., Stein, J.L., Vuong, C.K., Nichterwitz, S., Gevorgian, M., Opland, C.K., et al. (2019). A Single-Cell Transcriptomic Atlas of Human Neocortical Development during Mid-gestation. Neuron.

Pouille, F., and Scanziani, M. (2001). Enforcement of temporal fidelity in pyramidal cells by somatic feed-forward inhibition. Science 293, 1159–1163.

Priya, R., Paredes, M.F., Karayannis, T., Yusuf, N., Liu, X., Jaglin, X., Graef, I., Alvarez-Buylla, A., and Fishell, G. (2018). Activity Regulates Cell Death within Cortical Interneurons through a Calcineurin-Dependent Mechanism. Cell Rep. 22, 1695–1709.

Prönneke, A., Scheuer, B., Wagener, R.J., Möck, M., Witte, M., and Staiger, J.F. (2015). Characterizing VIP Neurons in the Barrel Cortex of VIPcre/tdTomato Mice Reveals Layer-Specific Differences. Cereb. Cortex 25, 4854–4868.

Purcell, S.M., Moran, J.L., Fromer, M., Ruderfer, D., Solovieff, N., Roussos, P., O'Dushlaine, C., Chambert, K., Bergen, S.E., Kähler, A., et al. (2014). A polygenic burden of rare disruptive mutations in schizophrenia. Nature 506, 185–190.

Quadrato, G., Brown, J., and Arlotta, P. (2016). The promises and challenges of human brain organoids as models of neuropsychiatric disease. Nat. Med. 22, 1220–1228.

Rahman, A., Weber, J., Labin, E., Lai, C., and Prieto, A.L. (2018). Developmental Expression of Neuregulin-3 in the Rat Central Nervous System. J. Comp. Neurol.

Ran, F.A., Hsu, P.D., Wright, J., Agarwala, V., Scott, D.A., and Zhang, F. (2013). Genome engineering using the CRISPR-Cas9 system. Nat. Protoc. 8, 2281–2308.

Ren, X., Farías, G.G., Canagarajah, B.J., Bonifacino, J.S., and Hurley, J.H. (2013). Structural basis for recruitment and activation of the AP-1 clathrin adaptor complex by Arf1. Cell 152, 755–767.

Ribeiro, L.F., Verpoort, B., and de Wit, J. (2018). Trafficking mechanisms of synaptogenic cell adhesion molecules. Mol. Cell. Neurosci.

Ribeiro, L.F., Verpoort, B., Nys, J., Vennekens, K.M., Wierda, K.D., and de Wit, J. (2019). SorCS1-mediated sorting in dendrites maintains neurexin axonal surface polarization required for synaptic function. PLoS Biol. 17, e3000466.

Rico, B., and Marín, O. (2011). Neuregulin signaling, cortical circuitry development and schizophrenia. Curr. Opin. Genet. Dev. 21, 262–270.

Rio, C., Rieff, H.I., Qi, P., Khurana, T.S., and Corfas, G. (1997). Neuregulin and erbB receptors play a critical role in neuronal migration. Neuron 19, 39–50.

Rivera, J.F., Ahmad, S., Quick, M.W., Liman, E.R., and Arnold, D.B. (2003). An evolutionarily conserved dileucine motif in Shal K+ channels mediates dendritic targeting. Nat. Neurosci. 6, 243–250.

Rivera, J.F., Chu, P.-J., and Arnold, D.B. (2005). The T1 domain of Kv1.3 mediates intracellular targeting to axons. Eur. J. Neurosci. 22, 1853–1862.

Robinson, M.S., and Bonifacino, J.S. (2001). Adaptor-related proteins. Curr. Opin. Cell Biol. 13, 444–453.

Rocco, B.R., Lewis, D.A., and Fish, K.N. (2016). Markedly Lower Glutamic Acid Decarboxylase 67 Protein Levels in a Subset of Boutons in Schizophrenia. Biol. Psychiatry 79, 1006–1015.

Rocco, B.R., DeDionisio, A.M., Lewis, D.A., and Fish, K.N. (2017). Alterations in a Unique Class of Cortical Chandelier Cell Axon Cartridges in Schizophrenia. Biol. Psychiatry 82, 40–48.

Rogers, K.W., and Schier, A.F. (2011). Morphogen gradients: from generation to interpretation. Annu. Rev. Cell Dev. Biol. 27, 377–407.

Romiguier, J., Ranwez, V., Douzery, E.J., and Galtier, N. (2010). Contrasting GC-content dynamics across 33 mammalian genomes: relationship with life-history traits and chromosomes sizes. Genome Res. 20, 1001-1009.

Rosales, C.R., Osborne, K.D., Zuccarino, G.V., Scheiffele, P., and Silverman, M.A. (2005). A cytoplasmic motif targets neuroligin-1 exclusively to dendrites of cultured hippocampal neurons. Eur. J. Neurosci. 22, 2381–2386.

Rouaux, C., and Arlotta, P. (2010). Fezf2 directs the differentiation of corticofugal neurons from striatal progenitors in vivo. Nat. Neurosci. 13, 1345–1347.

Rouaux, C., and Arlotta, P. (2013). Direct lineage reprogramming of post-mitotic callosal neurons into corticofugal neurons in vivo. Nat. Cell Biol. 15, 214–221.

Rubenstein, J.L., Martinez, S., Shimamura, K., and Puelles, L. (1994). The embryonic vertebrate forebrain: the prosomeric model. Science 266, 578–580.

Rudy, B., Fishell, G., Lee, S., and Hjerling-Leffler, J. (2011). Three groups of interneurons account for nearly 100% of neocortical GABAergic neurons. Dev. Neurobiol. 71, 45–61.

Sakata, S., and Harris, K.D. (2009). Laminar structure of spontaneous and sensory-evoked population activity in auditory cortex. Neuron 64, 404–418.

Sampo, B., Kaech, S., Kunz, S., and Banker, G. (2003). Two distinct mechanisms target membrane proteins to the axonal surface. Neuron 37, 611–624.

Sando, R., Jiang, X., and Südhof, T.C. (2019). Latrophilin GPCRs direct synapse specificity by coincident binding of FLRTs and teneurins. Science 363.

SantaLucia, Jr. J., and Hicks, D. (2004). The thermodynamics of DNA structural motifs. Annu. Rev. Biophys. Biomol. Struct. 33, 415-440.

Sanz, E., Yang, L., Su, T., Morris, D.R., McKnight, G.S., and Amieux, P.S. (2009). Cell-type-specific isolation of ribosome-associated mRNA from complex tissues. Proc. Natl. Acad. Sci. U. S. A. 106, 13939–13944.

Sanz, E., Bean, J.C., Carey, D.P., Quintana, A., and McKnight, G.S. (2019). RiboTag: Ribosomal Tagging Strategy to Analyze Cell-Type-Specific mRNA Expression In Vivo. Curr. Protoc. Neurosci. 88, e77.

Sardi, S.P., Murtie, J., Koirala, S., Patten, B.A., and Corfas, G. (2006). Presenilin-dependent ErbB4 nuclear signaling regulates the timing of astrogenesis in the developing brain. Cell 127, 185–197.

Satterstrom, F.K., Kosmicki, J.A., Wang, J., Breen, M.S., De Rubeis, S., An, J.-Y., Peng, M., Collins, R., Grove, J., Klei, L., et al. (2020). Large-Scale Exome Sequencing Study Implicates Both Developmental and Functional Changes in the Neurobiology of Autism. Cell 180, 568–584.e23.

Saunders, A., Macosko, E.Z., Wysoker, A., Goldman, M., Krienen, F.M., de Rivera, H., Bien, E., Baum, M., Bortolin, L., Wang, S., et al. (2018). Molecular Diversity and Specializations among the Cells of the Adult Mouse Brain. Cell 174, 1015–1030.e16.

Savas, J.N., Ribeiro, L.F., Wierda, K.D., Wright, R., DeNardo-Wilke, L.A., Rice, H.C., Chamma, I., Wang, Y.-Z., Zemla, R., Lavallée-Adam, M., et al. (2015). The Sorting Receptor SorCS1 Regulates Trafficking of Neurexin and AMPA Receptors. Neuron 87, 764–780.

Scala, F., Kobak, D., Shan, S., Bernaerts, Y., Laturnus, S., Cadwell, C.R., Hartmanis, L., Froudarakis, E., Castro, J., Tan, Z.H., et al. (2019). Neocortical layer 4 in adult mouse differs in major cell types and circuit organization between primary sensory areas.

Scala, F., Kobak, D., Bernabucci, M., Bernaerts, Y., Cadwell, C.R., Castro, J.R., Hartmanis, L., Jiang, X., Laturnus, S., Miranda, E., et al. (2020). Phenotypic variation of transcriptomic cell types in mouse motor cortex. Nature.

Scheiffele, P., Fan, J., Choih, J., Fetter, R., and Serafini, T. (2000). Neuroligin expressed in nonneuronal cells triggers presynaptic development in contacting axons. Cell 101, 657–669.

Schizophrenia Working Group of the Psychiatric Genomics Consortium (2014). Biological insights from 108 schizophrenia-associated genetic loci. Nature 511, 421–427.

Schreiner, D., Nguyen, T.-M., Russo, G., Heber, S., Patrignani, A., Ahrné, E., and Scheiffele, P. (2014). Targeted combinatorial alternative splicing generates brain region-specific repertoires of neurexins. Neuron 84, 386–398.

Schreiner, D., Savas, J.N., Herzog, E., Brose, N., and de Wit, J. (2017). Synapse biology in the “circuit-age”-paths toward molecular connectomics. Curr. Opin. Neurobiol. 42, 102–110.

Schroeder, A., Vanderlinden, J., Vints, K., Ribeiro, L.F., Vennekens, K.M., Gounko, N.V., Wierda, K.D., and de Wit, J. (2018). A Modular Organization of LRR Protein-Mediated Synaptic Adhesion Defines Synapse Identity. Neuron 99, 329–344.e7.

Schuman, B., Machold, R., Hashikawa, Y., Fuzik, J., Fishell, G., and Rudy, B. (2019). Four unique interneuron populations reside in neocortical layer 1. J. Neurosci.

Seigneur, E., and Südhof, T.C. (2017). Cerebellins are differentially expressed in selective subsets of neurons throughout the brain. J. Comp. Neurol.

Seigneur, E., and Südhof, T.C. (2018). Genetic Ablation of All Cerebellins Reveals Synapse Organizer Functions in Multiple Regions Throughout the Brain. J. Neurosci. 38, 4774–4790.

Shatz, C.J., and Stryker, M.P. (1988). Prenatal tetrodotoxin infusion blocks segregation of retinogeniculate afferents. Science 242, 87–89.

Siddiqui, T.J., Pancaroglu, R., Kang, Y., Rooyakkers, A., and Craig, A.M. (2010). LRRTMs and Neuroligins Bind Neurexins with a Differential Code to Cooperate in Glutamate Synapse Development. J. Neurosci. 30, 7495.

Siddiqui, T.J., Tari, P.K., Connor, S.A., Zhang, P., Dobie, F.A., She, K., Kawabe, H., Wang, Y.T., Brose, N., and Craig, A.M. (2013). An LRRTM4-HSPG complex mediates excitatory synapse development on dentate gyrus granule cells. Neuron 79, 680–695.

Sigoillot, S.M., Iyer, K., Binda, F., González-Calvo, I., Talleur, M., Vodjdani, G., Isope, P., and Selimi, F. (2015). The Secreted Protein C1QL1 and Its Receptor BAI3 Control the Synaptic Connectivity of Excitatory Inputs Converging on Cerebellar Purkinje Cells. Cell Rep.

Silberberg, G., and Markram, H. (2007). Disynaptic inhibition between neocortical pyramidal cells mediated by Martinotti cells. Neuron 53, 735–746.

Sohal, V.S., Zhang, F., Yizhar, O., and Deisseroth, K. (2009). Parvalbumin neurons and gamma rhythms enhance cortical circuit performance. Nature 459, 698–702.

Sohur, U.S., Padmanabhan, H.K., Kotchetkov, I.S., Menezes, J.R.L., and Macklis, J.D. (2014). Anatomic and molecular development of corticostriatal projection neurons in mice. Cereb. Cortex 24, 293–303.

Solstad, T., Boccara, C.N., Kropff, E., Moser, M.-B., and Moser, E.I. (2008). Representation of geometric borders in the entorhinal cortex. Science 322, 1865–1868.

Sommeijer, J.-P., and Levelt, C.N. (2012). Synaptotagmin-2 is a reliable marker for parvalbumin positive inhibitory boutons in the mouse visual cortex. PLoS One 7, e35323.

Somogyi, P. (1977). A specific “axo-axonal” interneuron in the visual cortex of the rat. Brain Res. 136, 345–350.

Somogyi, J., Baude, A., Omori, Y., Shimizu, H., El Mestikawy, S., Fukaya, M., Shigemoto, R., Watanabe, M., and Somogyi, P. (2004). GABAergic basket cells expressing cholecystokinin contain vesicular glutamate transporter type 3 (VGLUT3) in their synaptic terminals in hippocampus and isocortex of the rat. Eur. J. Neurosci. 19, 552–569.

Somogyi, P., Hodgson, A.J., Smith, A.D., Nunzi, M.G., Gorio, A., and Wu, J.Y. (1984). Different populations of GABAergic neurons in the visual cortex and hippocampus of cat contain somatostatin- or cholecystokinin-immunoreactive material. J. Neurosci. 4, 2590–2603.

Somogyi, P., Freund, T.F., Hodgson, A.J., Somogyi, J., Beroukas, D., and Chubb, I.W. (1985). Identified axo-axonic cells are immunoreactive for GABA in the hippocampus and visual cortex of the cat. Brain Res. 332, 143–149.

Song, A.-H., Wang, D., Chen, G., Li, Y., Luo, J., Duan, S., and Poo, M.-M. (2009). A selective filter for cytoplasmic transport at the axon initial segment. Cell 136, 1148–1160.

Soo Hoo, L., Banna, C.D., Radeke, C.M., Sharma, N., Albertolle, M.E., Low, S.H., Weimbs, T., and Vandenberg, C.A. (2016). The SNARE Protein Syntaxin 3 Confers Specificity for Polarized Axonal Trafficking in Neurons. PLoS One 11, e0163671.

Southwell, D.G., Paredes, M.F., Galvao, R.P., Jones, D.L., Froemke, R.C., Sebe, J.Y., Alfaro-Cervello, C., Tang, Y., Garcia-Verdugo, J.M., Rubenstein, J.L., et al. (2012). Intrinsically determined cell death of developing cortical interneurons. Nature 491, 109–113.

Spellman, T.J., and Gordon, J.A. (2015). Synchrony in schizophrenia: a window into circuit-level pathophysiology. Curr. Opin. Neurobiol. 30, 17–23.

Sretavan, D., and Shatz, C.J. (1984). Prenatal development of individual retinogeniculate axons during the period of segregation. Nature 308, 845–848.

Stachniak, T.J., Kastli, R., Hanley, O., Argunsah, A.Ö., and Karayannis, T. (2020). Post-mitotic Prox1 expression controls the final specification of cortical VIP interneuron subtypes.

Staiger, J.F., Flagmeyer, I., Schubert, D., Zilles, K., Kötter, R., and Luhmann, H.J. (2004). Functional diversity of layer IV spiny neurons in rat somatosensory cortex:

quantitative morphology of electrophysiologically characterized and biocytin labeled cells. Cereb. Cortex 14, 690–701.

Stanley, G., Gokce, O., Malenka, R.C., Südhof, T.C., and Quake, S.R. (2019). Continuous and Discrete Neuron Types of the Adult Murine Striatum. Neuron.

Stark, E., Roux, L., Eichler, R., Senzai, Y., Royer, S., and Buzsáki, G. (2014). Pyramidal cell-interneuron interactions underlie hippocampal ripple oscillations. Neuron 83, 467–480.

Steinecke, A., Hozhabri, E., Tapanes, S., Ishino, Y., Zeng, H., Kamasawa, N., and Taniguchi, H. (2017). Neocortical Chandelier Cells Developmentally Shape Axonal Arbors through Reorganization but Establish Subcellular Synapse Specificity without Refinement. eNeuro 4.

Steward, O., and Schuman, E.M. (2001). Protein synthesis at synaptic sites on dendrites. Annu. Rev. Neurosci. 24, 299–325.

Stroud, H., Yang, M.G., Tsitohay, Y.N., Davis, C.P., Sherman, M.A., Hrvatin, S., Ling, E., and Greenberg, M.E. (2020). An Activity-Mediated Transition in Transcription in Early Postnatal Neurons. Neuron.

Südhof, T.C. (2017). Synaptic Neurexin Complexes: A Molecular Code for the Logic of Neural Circuits. Cell 171, 745–769.

Sullivan, P.F., Daly, M.J., and O'Donovan, M. (2012). Genetic architectures of psychiatric disorders: the emerging picture and its implications. Nat. Rev. Genet. 13, 537–551.

Sun, Y., Ikrar, T., Davis, M.F., Gong, N., Zheng, X., Luo, Z.D., Lai, C., Mei, L., Holmes, T.C., Gandhi, S.P., et al. (2016). Neuregulin-1/ErbB4 Signaling Regulates Visual Cortical Plasticity. Neuron 92, 160–173.

Sussel, L., Marin, O., Kimura, S., and Rubenstein, J.L. (1999). Loss of Nkx2.1 homeobox gene function results in a ventral to dorsal molecular respecification within the basal telencephalon: evidence for a transformation of the pallidum into the striatum. Development 126, 3359–3370.

Sutton, M.A., and Schuman, E.M. (2006). Dendritic protein synthesis, synaptic plasticity, and memory. Cell 127, 49–58.

Suzuki, K., Hayashi, Y., Nakahara, S., Kumazaki, H., Prox, J., Horiuchi, K., Zeng, M., Tanimura, S., Nishiyama, Y., Osawa, S., et al. (2012). Activity-dependent proteolytic cleavage of neuroligin-1. Neuron 76, 410–422.

Suzuki, K., Tsunekawa, Y., Hernandez-Benitez, R., Wu, J., Zhu, J., Kim, E.J., Hatanaka, F., Yamamoto, M., Araoka, T., Li, Z., et al. (2016). In vivo genome editing via CRISPR/Cas9 mediated homology-independent targeted integration. Nature 540, 144–149.

Syken, J., Grandpre, T., Kanold, P.O., and Shatz, C.J. (2006). PirB restricts ocular-dominance plasticity in visual cortex. Science 313, 1795–1800.

Tabuchi, K., and Südhof, T.C. (2002). Structure and evolution of neurexin genes: insight into the mechanism of alternative splicing. Genomics 79, 849–859.

Tai, Y., Janas, J.A., Wang, C.-L., and Van Aelst, L. (2014). Regulation of chandelier cell cartridge and bouton development via DOCK7-mediated ErbB4 activation. Cell Rep. 6, 254–263.

Tai, Y., Gallo, N.B., Wang, M., Yu, J.-R., and Van Aelst, L. (2019). Axo-axonic Innervation of Neocortical Pyramidal Neurons by GABAergic Chandelier Cells Requires AnkyrinG-Associated L1CAM. Neuron 0.

Takahashi, H., and Craig, A.M. (2013). Protein tyrosine phosphatases PTPδ, PTPσ, and LAR: presynaptic hubs for synapse organization. Trends Neurosci. 36, 522–534.

Takahashi, H., Arstikaitis, P., Prasad, T., Bartlett, T.E., Wang, Y.T., Murphy, T.H., and Craig, A.M. (2011). Postsynaptic TrkC and presynaptic PTPσ function as a bidirectional excitatory synaptic organizing complex. Neuron 69, 287–303.

Takahashi, H., Katayama, K.-I., Sohya, K., Miyamoto, H., Prasad, T., Matsumoto, Y., Ota, M., Yasuda, H., Tsumoto, T., Aruga, J., et al. (2012). Selective control of inhibitory synapse development by Slitrk3-PTPδ trans-synaptic interaction. Nat. Neurosci. 15, 389–398, S1–S2.

Tamás, G., Lorincz, A., Simon, A., and Szabadics, J. (2003). Identified sources and targets of slow inhibition in the neocortex. Science 299, 1902–1905.

Tan, G.-H., Liu, Y.-Y., Hu, X.-L., Yin, D.-M., Mei, L., and Xiong, Z.-Q. (2011). Neuregulin 1 represses limbic epileptogenesis through ErbB4 in parvalbumin-expressing interneurons. Nat. Neurosci. 15, 258–266.

Tanabe, Y., Naito, Y., Vasuta, C., Lee, A.K., Soumounou, Y., Linhoff, M.W., and Takahashi, H. (2017). IgSF21 promotes differentiation of inhibitory synapses via binding to neurexin2α. Nat. Commun. 8, 408.

Taniguchi, H., He, M., Wu, P., Kim, S., Paik, R., Sugino, K., Kvitsiani, D., Kvitsani, D., Fu, Y., Lu, J., et al. (2011). A resource of Cre driver lines for genetic targeting of GABAergic neurons in cerebral cortex. Neuron 71, 995–1013.

Taniguchi, H., Lu, J., and Huang, Z.J. (2013). The spatial and temporal origin of chandelier cells in mouse neocortex. Science 339, 70–74.

Tasic, B., Yao, Z., Graybuck, L.T., Smith, K.A., Nguyen, T.N., Bertagnolli, D., Goldy, J., Garren, E., Economo, M.N., Viswanathan, S., et al. (2018). Shared and distinct transcriptomic cell types across neocortical areas. Nature 563, 72–78.

Taveggia, C., Thaker, P., Petrylak, A., Caporaso, G.L., Toews, A., Falls, D.L., Einheber, S., and Salzer, J.L. (2008). Type III neuregulin-1 promotes oligodendrocyte myelination. Glia 56, 284–293.

Tian, B., and Manley, J.L. (2017). Alternative polyadenylation of mRNA precursors. Nat. Rev. Mol. Cell Biol. 18, 18–30.

Ting, A.K., Chen, Y., Wen, L., Yin, D.-M., Shen, C., Tao, Y., Liu, X., Xiong, W.-C., and Mei, L. (2011). Neuregulin 1 promotes excitatory synapse development and function in GABAergic interneurons. J. Neurosci. 31, 15–25.

Tosches, M.A., Yamawaki, T.M., Naumann, R.K., Jacobi, A.A., Tushev, G., and Laurent, G. (2018). Evolution of pallium, hippocampus, and cortical cell types revealed by single-cell transcriptomics in reptiles. Science 360, 881–888.

Tranchevent, L.-C., Ardeshirdavani, A., ElShal, S., Alcaide, D., Aerts, J., Auboeuf, D., and Moreau, Y. (2016). Candidate gene prioritization with Endeavour. Nucleic Acids Res. 44, W117–W121.

Traunmüller, L., Gomez, A.M., Nguyen, T.-M., and Scheiffele, P. (2016). Control of neuronal synapse specification by a highly dedicated alternative splicing program. Science 352, 982–986.

Trettel, J., and Levine, E.S. (2002). Cannabinoids depress inhibitory synaptic inputs received by layer 2/3 pyramidal neurons of the neocortex. J. Neurophysiol. 88, 534–539.

Treutlein, B., Gokce, O., Quake, S.R., and Südhof, T.C. (2014). Cartography of neurexin alternative splicing mapped by single-molecule long-read mRNA sequencing. Proc. Natl. Acad. Sci. U. S. A. 111, E1291–E1299.

Tuncdemir, S.N., Wamsley, B., Stam, F.J., Osakada, F., Goulding, M., Callaway, E.M., Rudy, B., and Fishell, G. (2016). Early Somatostatin Interneuron Connectivity Mediates the Maturation of Deep Layer Cortical Circuits. Neuron 89, 521–535.

Tushev, G., Glock, C., Heumüller, M., Biever, A., Jovanovic, M., and Schuman, E.M. (2018). Alternative 3′ UTRs Modify the Localization, Regulatory Potential, Stability, and Plasticity of mRNAs in Neuronal Compartments. Neuron 98, 495–511.e6.

Uemura, T., Lee, S.-J., Yasumura, M., Takeuchi, T., Yoshida, T., Ra, M., Taguchi, R., Sakimura, K., and Mishina, M. (2010). Trans-synaptic interaction of GluRdelta2 and Neurexin through Cbln1 mediates synapse formation in the cerebellum. Cell 141, 1068–1079.

Uhlhaas, P.J., and Singer, W. (2010). Abnormal neural oscillations and synchrony in schizophrenia. Nat. Rev. Neurosci. 11, 100–113.

Ule, J., and Darnell, R.B. (2006). RNA binding proteins and the regulation of neuronal synaptic plasticity. Curr. Opin. Neurobiol. 16, 102–110.

Ullrich, B., Ushkaryov, Y.A., and Südhof, T.C. (1995). Cartography of neurexins: more than 1000 isoforms generated by alternative splicing and expressed in distinct subsets of neurons. Neuron 14, 497–507.

Urwyler, O., Izadifar, A., Vandenbogaerde, S., Sachse, S., Misbaer, A., and Schmucker, D. (2019). Branch-restricted localization of phosphatase Prl-1 specifies axonal synaptogenesis domains. Science 364.

Vagnoni, C., Baruchin, L.J., Ghezzi, F., Ratti, S., Molnár, Z., and Butt, S.J.B. (2020). Ontogeny of the VIP+ interneuron sensory-motor circuit prior to active whisking.

Viney, T.J., Lasztoczi, B., Katona, L., Crump, M.G., Tukker, J.J., Klausberger, T., and Somogyi, P. (2013). Network state-dependent inhibition of identified hippocampal CA3 axo-axonic cells in vivo. Nat. Neurosci. 16, 1802–1811.

Vormstein-Schneider, D.C., Lin, J.D., Pelkey, K.A., Chittajallu, R., Guo, B., Arias Garcia, M., Sakopoulos, S., Stevenson, O., Schneider, G., Zhang, Q., et al. (2019). Viral manipulation of functionally distinct neurons from mice to humans.

Vucurovic, K., Gallopin, T., Ferezou, I., Rancillac, A., Chameau, P., van Hooft, J.A., Geoffroy, H., Monyer, H., Rossier, J., and Vitalis, T. (2010). Serotonin 3A receptor subtype as an early and protracted marker of cortical interneuron subpopulations. Cereb. Cortex 20, 2333–2347.

Vullhorst, D., Neddens, J., Karavanova, I., Tricoire, L., Petralia, R.S., McBain, C.J., and Buonanno, A. (2009). Selective expression of ErbB4 in interneurons, but not pyramidal cells, of the rodent hippocampus. J. Neurosci. 29, 12255–12264.

Vullhorst, D., Ahmad, T., Karavanova, I., Keating, C., and Buonanno, A. (2017). Structural Similarities between Neuregulin 1-3 Isoforms Determine Their Subcellular Distribution and Signaling Mode in Central Neurons. J. Neurosci. 37, 5232–5249.

Waddington, C.H. (1957). THE STRATEGY OF THE GENES (George Allen & Unwin, London).

Walker, F., Möck, M., Feyerabend, M., Guy, J., Wagener, R.J., Schubert, D., Staiger, J.F., and Witte, M. (2016). Parvalbumin- and vasoactive intestinal polypeptide-expressing neocortical interneurons impose differential inhibition on Martinotti cells. Nat. Commun. 7, 13664.

Walsh, T., McClellan, J.M., McCarthy, S.E., Addington, A.M., Pierce, S.B., Cooper, G.M., Nord, A.S., Kusenda, M., Malhotra, D., Bhandari, A., et al. (2008). Rare structural variants disrupt multiple genes in neurodevelopmental pathways in schizophrenia. Science 320, 539–543.

Wamsley, B., Jaglin, X.H., Favuzzi, E., Quattrocolo, G., Nigro, M.J., Yusuf, N., Khodadadi-Jamayran, A., Rudy, B., and Fishell, G. (2018). Rbfox1 Mediates Cell-type-Specific Splicing in Cortical Interneurons. Neuron 0.

Wang, J., Song, F., and Loeb, J.A. (2017). Neuregulin1 fine-tunes pre-, post-, and perisynaptic neuromuscular junction development. Dev. Dyn. 246, 368–380.

Wang, J.Y., Miller, S.J., and Falls, D.L. (2001). The N-terminal region of neuregulin isoforms determines the accumulation of cell surface and released neuregulin ectodomain. J. Biol. Chem. 276, 2841–2851.

Wang, X., Allen, W.E., Wright, M.A., Sylwestrak, E.L., Samusik, N., Vesuna, S., Evans, K., Liu, C., Ramakrishnan, C., Liu, J., et al. (2018a). Three-dimensional intact-tissue sequencing of single-cell transcriptional states. Science.

Wang, Y., Toledo-Rodriguez, M., Gupta, A., Wu, C., Silberberg, G., Luo, J., and Markram, H. (2004). Anatomical, physiological and molecular properties of Martinotti cells in the somatosensory cortex of the juvenile rat. J. Physiol. 561, 65–90.

Wang, Y., Dye, C.A., Sohal, V., Long, J.E., Estrada, R.C., Roztocil, T., Lufkin, T., Deisseroth, K., Baraban, S.C., and Rubenstein, J.L.R. (2010). Dlx5 and Dlx6 regulate the development of parvalbumin-expressing cortical interneurons. J. Neurosci. 30, 5334–5345.

Wang, Y.-N., Figueiredo, D., Sun, X.-D., Dong, Z.-Q., Chen, W.-B., Cui, W.-P., Liu, F., Wang, H.-S., Li, H.-W., Robinson, H., et al. (2018b). Controlling of glutamate release by neuregulin3 via inhibiting the assembly of the SNARE complex. Proc. Natl. Acad. Sci. U. S. A.

Weinberger, D.R. (1987). Implications of normal brain development for the pathogenesis of schizophrenia. Arch. Gen. Psychiatry 44, 660–669.

Wen, D., Peles, E., Cupples, R., Suggs, S.V., Bacus, S.S., Luo, Y., Trail, G., Hu, S., Silbiger, S.M., and Levy, R.B. (1992). Neu differentiation factor: a transmembrane glycoprotein containing an EGF domain and an immunoglobulin homology unit. Cell 69, 559–572.

Whissell, P.D., Cajanding, J.D., Fogel, N., and Kim, J.C. (2015). Comparative density of CCK- and PV-GABA cells within the cortex and hippocampus. Front. Neuroanat. 9, 124.

Willems, J., de Jong, A.P.H., Scheefhals, N., and MacGillavry, H.D. (2019). ORANGE: A CRISPR/Cas9-based genome editing toolbox for epitope tagging of endogenous proteins in neurons.

Williams, M.E., Wilke, S.A., Daggett, A., Davis, E., Otto, S., Ravi, D., Ripley, B., Bushong, E.A., Ellisman, M.H., Klein, G., et al. (2011). Cadherin-9 regulates synapse-specific differentiation in the developing hippocampus. Neuron 71, 640–655.

Williams, R.H., Vazquez-DeRose, J., Thomas, A.M., Piquet, J., Cauli, B., and Kilduff, T.S. (2018). Cortical nNOS/NK1 Receptor Neurons are Regulated by Cholinergic Projections From the Basal Forebrain. Cereb. Cortex 28, 1959–1979.

Willsey, A.J., Sanders, S.J., Li, M., Dong, S., Tebbenkamp, A.T., Muhle, R.A., Reilly, S.K., Lin, L., Fertuzinhos, S., Miller, J.A., et al. (2013). Coexpression

networks implicate human midfetal deep cortical projection neurons in the pathogenesis of autism. Cell 155, 997–1007.

Wilson, N.R., Runyan, C.A., Wang, F.L., and Sur, M. (2012). Division and subtraction by distinct cortical inhibitory networks in vivo. Nature 488, 343–348.

Wilson, R.I., Kunos, G., and Nicoll, R.A. (2001). Presynaptic specificity of endocannabinoid signaling in the hippocampus. Neuron 31, 453–462.

Wisco, D., Anderson, E.D., Chang, M.C., Norden, C., Boiko, T., Fölsch, H., and Winckler, B. (2003). Uncovering multiple axonal targeting pathways in hippocampal neurons. J. Cell Biol. 162, 1317–1328.

de Wit, J., and Ghosh, A. (2016). Specification of synaptic connectivity by cell surface interactions. Nat. Rev. Neurosci. 17, 22–35.

de Wit, J., Sylwestrak, E., O'Sullivan, M.L., Otto, S., Tiglio, K., Savas, J.N., Yates, J.R., 3rd, Comoletti, D., Taylor, P., and Ghosh, A. (2009). LRRTM2 interacts with Neurexin1 and regulates excitatory synapse formation. Neuron 64, 799–806.

de Wit, J., O'Sullivan, M.L., Savas, J.N., Condomitti, G., Caccese, M.C., Vennekens, K.M., Yates, J.R., 3rd, and Ghosh, A. (2013). Unbiased discovery of glypican as a receptor for LRRTM4 in regulating excitatory synapse development. Neuron 79, 696–711.

Wolpowitz, D., Mason, T.B., Dietrich, P., Mendelsohn, M., Talmage, D.A., and Role, L.W. (2000). Cysteine-rich domain isoforms of the neuregulin-1 gene are required for maintenance of peripheral synapses. Neuron 25, 79–91.

Wong, F.K., Bercsenyi, K., Sreenivasan, V., Portalés, A., Fernández-Otero, M., and Marín, O. (2018). Pyramidal cell regulation of interneuron survival sculpts cortical networks. Nature 557, 668–673.

Wong, H.H.-W., Lin, J.Q., Ströhl, F., Roque, C.G., Cioni, J.-M., Cagnetta, R., Turner-Bridger, B., Laine, R.F., Harris, W.A., Kaminski, C.F., et al. (2017). RNA Docking and Local Translation Regulate Site-Specific Axon Remodeling In Vivo. Neuron 95, 852–868.e8.

Woo, J., Kwon, S.-K., Choi, S., Kim, S., Lee, J.-R., Dunah, A.W., Sheng, M., and Kim, E. (2009). Trans-synaptic adhesion between NGL-3 and LAR regulates the formation of excitatory synapses. Nat. Neurosci. 12, 428–437.

Woo, J., Kwon, S.-K., Nam, J., Choi, S., Takahashi, H., Krueger, D., Park, J., Lee, Y., Bae, J.Y., Lee, D., et al. (2013). The adhesion protein IgSF9b is coupled to neuroligin 2 via S-SCAM to promote inhibitory synapse development. J. Cell Biol. 201, 929–944.

Woo, R.-S., Li, X.-M., Tao, Y., Carpenter-Hyland, E., Huang, Y.Z., Weber, J., Neiswender, H., Dong, X.-P., Wu, J., Gassmann, M., et al. (2007). Neuregulin-1 enhances depolarization-induced GABA release. Neuron 54, 599–610.

Woo, T.U., Whitehead, R.E., Melchitzky, D.S., and Lewis, D.A. (1998). A subclass of prefrontal gamma-aminobutyric acid axon terminals are selectively altered in schizophrenia. Proc. Natl. Acad. Sci. U. S. A. 95, 5341–5346.

Woodworth, M.B., Greig, L.C., Liu, K.X., Ippolito, G.C., Tucker, H.O., and Macklis, J.D. (2016). Ctip1 Regulates the Balance between Specification of Distinct Projection Neuron Subtypes in Deep Cortical Layers. Cell Rep. 15, 999–1012.

Wu, X., Morishita, W.K., Riley, A.M., Hale, W.D., Südhof, T.C., and Malenka, R.C. (2019). Neuroligin-1 Signaling Controls LTP and NMDA Receptors by Distinct Molecular Pathways. Neuron 102, 621–635.e3.

Xu, H., Jeong, H.-Y., Tremblay, R., and Rudy, B. (2013). Neocortical somatostatin-expressing GABAergic interneurons disinhibit the thalamorecipient layer 4. Neuron 77, 155–167.

Xu, J., Mashimo, T., and Südhof, T.C. (2007). Synaptotagmin-1, -2, and -9: Ca(2+) sensors for fast release that specify distinct presynaptic properties in subsets of neurons. Neuron 54, 567–581.

Xu, X., Roby, K.D., and Callaway, E.M. (2006). Mouse cortical inhibitory neuron type that coexpresses somatostatin and calretinin. J. Comp. Neurol. 499, 144–160.

Xue, M., Atallah, B.V., and Scanziani, M. (2014). Equalizing excitation-inhibition ratios across visual cortical neurons. Nature 511, 596–600.

Yamagata, M., and Sanes, J.R. (2018). Expression and Roles of the Immunoglobulin Superfamily Recognition Molecule Sidekick1 in Mouse Retina. Front. Mol. Neurosci. 11, 485.

Yamagata, A., Sato, Y., Goto-Ito, S., Uemura, T., Maeda, A., Shiroshima, T., Yoshida, T., and Fukai, S. (2015a). Structure of Slitrk2-PTPδ complex reveals mechanisms for splicing-dependent trans-synaptic adhesion. Sci. Rep. 5, 9686.

Yamagata, A., Yoshida, T., Sato, Y., Goto-Ito, S., Uemura, T., Maeda, A., Shiroshima, T., Iwasawa-Okamoto, S., Mori, H., Mishina, M., et al. (2015b). Mechanisms of splicing-dependent trans-synaptic adhesion by PTPδ-IL1RAPL1/IL-1RAcP for synaptic differentiation. Nat. Commun. 6, 6926.

Yang, J.-M., Zhang, J., Chen, X.-J., Geng, H.-Y., Ye, M., Spitzer, N.C., Luo, J.-H., Duan, S.-M., and Li, X.-M. (2013). Development of GABA circuitry of fast-spiking basket interneurons in the medial prefrontal cortex of erbb4-mutant mice. J. Neurosci. 33, 19724–19733.

Yang, X., Arber, S., William, C., Li, L., Tanabe, Y., Jessell, T.M., Birchmeier, C., and Burden, S.J. (2001). Patterning of muscle acetylcholine receptor gene expression in the absence of motor innervation. Neuron 30, 399–410.

Yap, C.C., Nokes, R.L., Wisco, D., Anderson, E., Fölsch, H., and Winckler, B. (2008). Pathway selection to the axon depends on multiple targeting signals in NgCAM. J. Cell Sci. 121, 1514–1525.

Ye, L., Allen, W.E., Thompson, K.R., Tian, Q., Hsueh, B., Ramakrishnan, C., Wang, A.-C., Jennings, J.H., Adhikari, A., Halpern, C.H., et al. (2016). Wiring and Molecular Features of Prefrontal Ensembles Representing Distinct Experiences. Cell 165, 1776–1788.

Ye, Z., Mostajo-Radji, M.A., Brown, J.R., Rouaux, C., Tomassy, G.S., Hensch, T.K., and Arlotta, P. (2015). Instructing Perisomatic Inhibition by Direct Lineage Reprogramming of Neocortical Projection Neurons. Neuron 88, 475–483.

Yi, F., Danko, T., Botelho, S.C., Patzke, C., Pak, C., Wernig, M., and Südhof, T.C. (2016). Autism-associated SHANK3 haploinsufficiency causes Ih channelopathy in human neurons. Science 352, aaf2669.

Yoshida, T., Yasumura, M., Uemura, T., Lee, S.-J., Ra, M., Taguchi, R., Iwakura, Y., and Mishina, M. (2011). IL-1 receptor accessory protein-like 1 associated with mental retardation and autism mediates synapse formation by trans-synaptic interaction with protein tyrosine phosphatase δ. J. Neurosci. 31, 13485–13499.

Yoshida, T., Shiroshima, T., Lee, S.-J., Yasumura, M., Uemura, T., Chen, X., Iwakura, Y., and Mishina, M. (2012). Interleukin-1 receptor accessory protein organizes neuronal synaptogenesis as a cell adhesion molecule. J. Neurosci. 32, 2588–2600.

Yuste, R., Peinado, A., and Katz, L.C. (1992). Neuronal domains in developing neocortex. Science 257, 665–669.

Yuzaki, M. (2017). The C1q complement family of synaptic organizers: not just complementary. Curr. Opin. Neurobiol. 45, 9–15.

Zeisel, A., Muñoz-Manchado, A.B., Codeluppi, S., Lönnerberg, P., La Manno, G., Juréus, A., Marques, S., Munguba, H., He, L., Betsholtz, C., et al. (2015). Cell types in the mouse cortex and hippocampus revealed by single-cell RNA-seq. Science 347, 1138–1142.

Zeisel, A., Hochgerner, H., Lönnerberg, P., Johnsson, A., Memic, F., van der Zwan, J., Häring, M., Braun, E., Borm, L.E., La Manno, G., et al. (2018). Molecular Architecture of the Mouse Nervous System. Cell 174, 999–1014.e22.

Zeng, H., and Sanes, J.R. (2017). Neuronal cell-type classification: challenges, opportunities and the path forward. Nat. Rev. Neurosci. 18, 530–546.

Zhang, B., Chen, L.Y., Liu, X., Maxeiner, S., Lee, S.-J., Gokce, O., and Südhof, T.C. (2015). Neuroligins Sculpt Cerebellar Purkinje-Cell Circuits by Differential Control of Distinct Classes of Synapses. Neuron 87, 781–796.

Zhang, D., Sliwkowski, M.X., Mark, M., Frantz, G., Akita, R., Sun, Y., Hillan, K., Crowley, C., Brush, J., and Godowski, P.J. (1997). Neuregulin-3 (NRG3): a novel neural tissue-enriched protein that binds and activates ErbB4. Proc. Natl. Acad. Sci. U. S. A. 94, 9562–9567.

Zhang, P., Lu, H., Peixoto, R.T., Pines, M.K., Ge, Y., Oku, S., Siddiqui, T.J., Xie, Y., Wu, W., Archer-Hartmann, S., et al. (2018). Heparan Sulfate Organizes Neuronal Synapses through Neurexin Partnerships. Cell.

Zhang, X., Gureasko, J., Shen, K., Cole, P.A., and Kuriyan, J. (2006). An allosteric mechanism for activation of the kinase domain of epidermal growth factor receptor. Cell 125, 1137–1149.

Zhang, Y., Pak, C., Han, Y., Ahlenius, H., Zhang, Z., Chanda, S., Marro, S., Patzke, C., Acuna, C., Covy, J., et al. (2013). Rapid single-step induction of functional neurons from human pluripotent stem cells. Neuron 78, 785–798.

Zhou, X., Rickmann, M., Hafner, G., and Staiger, J.F. (2017). Subcellular Targeting of VIP Boutons in Mouse Barrel Cortex is Layer-Dependent and not Restricted to Interneurons. Cereb. Cortex 27, 5353–5368.